INTESTINE OF ZEBRAFISH: REGIONALIZATION, CHARACTERIZATION AND STEM CELLS

WANG ZHENGYUAN
(M.Sci., NUS)
(B.Eng., NPU)

A THESIS SUBMITTED FOR THE DEGREE OF DOCTOR OF PHILOSOPHY IN COMPUTATION AND SYSTEMS BIOLOGY (CSB) SINGAPORE-MIT ALLIANCE NATIONAL UNIVERSITY OF SINGAPORE

2010

Acknowledgements

I want to thank my supervisors, professor Matsudaira Paul and professor Gong Zhiyuan, whose time, knowledge and wise guidance has constituted a key component ensuring the continual progression of my research work.

I want to thank my thesis committee members, professor Lodish Harvey and assistant professor Bhowmic Sourav, for following my progress, evaluating and steering my work.

Thanks also go to professor Rajagopal Gunaretnam, who initiated the project and helped much to get the project started several years ago.

This study was supported by funding and a graduate fellowship from the Singapore-MIT Alliance.

Special thanks to my labmates, Zhan Huiqing, Wu Yilian, Du Jianguo, Tavakoli Sahar, Li Zhen, Zheng Weiling, Tina Sim Huey Fen, Liang Bing, Ung Choon Yong, Lam Siew Hong, Yin Ao, Mintzu, Li Caixia, Grace Ng, Sun Lili, Cecilia, Lana and others. Four years of doctoral study in the laboratory would by no means be joyful and fun-filled without the company of them.

Last but not least, thanks go to my family members, including my parents, sisters, wife and son for their full support during my doctoral study. Time spent in the laboratory could not be spent with my family. Thank them for

bearing with me during the years of scientific training. Thank my son, the little lovely creature, for bringing oceans of joy to me.

Contents

Abstract

Unlike the mammalian digestive tract that has been developed into distinct regions for different functions, fish have a relatively simple intestine and many fishes have no recognizable stomach. We used the zebrafish microarray approach to characterize its intestine. By dividing the zebrafish intestine into seven segments along its length, we found that the first five segments resemble the mammalian small intestine and the last two segments resemble the mammalian large intestine. We then investigated the role of Notch signaling and found that a specific group of glycogen-rich fibroblasts were involved in the Notch-mediated cell fate decision process. Further, we studied the effects of radiation and found an interesting pattern of regeneration in the intestine. Moreover, the number of intestinal stem cells was investigated through a novel computational model, which was applicable not only to zebrafish, but also to mammalian intestinal tracts.

Summary

A systemic study of adult zebrafish intestine has been carried out in this thesis project integrating morphological, histological, molecular and computational approaches.

Morphologically, the zebrafish intestine is organized as an inverted Z shape *in vivo*. Dilation of the intestinal tube at its anterior is frequently seen containing ingested food, especially after feeding; while compaction of stools is often observed in its posterior region. Histologically, villi are present almost along the whole intestine with expcetion in the very posterior region (segment S7). Interestingly, crypts are absent along the whole intestine. Our transcriptomic analysis has shown that the zebrafish mucosa only resembles the mouse villi but not the crypts, supporting the absence of crypts in zebrafish.

cDNA microarray has been performed to profile the region-specific transcriptomes along the anterior-posterior axis. Transcriptomic analysis shows segments S1-S5 are very similar to each other, while S6 and S7 shows major difference. This is consisten with our qRT-PCR results and *in situ* hybridization results. Expression of *fabp2*, the well known marker gene of the small intestine, is switched off in the proximal region of S5. Similar results are seen for villin, another marker gene of the small intestine.

Based on our results, we like to propose that the zebrafish intestine regionalizes into the small intestine and the large intestine. The small intestine connects to the large intestine through a transitional region, while the large intestine further regionalizes into a proximal part and a distal part. There is no stomach or cecum found. The pepsin gene locus, conserved in most vertebrate species, seems evolutionarily lost in zebrafish genome. In the mean time, trypsin and chymotrypsin are synthesized by the intestinal cells.

Perturbation to Notch signaling shows that Notch influences the fate determination of the bipotent precursor cells toward an absorptive or secretory lineage. Inhibition of Notch signaling has led to precocious differentiation of the precursor cells along the secretory lineage with involvement of a glycogen-rich intestinal subepithelial myofibroblasts.

Gamma-radiation has allowed us to study the regenerative process of zebrafish intestine. Despite degeneration of villi after radiation, regeneration are observed and the intestinal functions are sustained, which partially explains the survival of fish after radiation. Our discovery that zebrafish intestine experiences multiple waves of tissue regeneration has shed new light on our current unserstanding of the nature of the intestinal organ with potential therapeutic values.

Computational analysis suggests that the number of stem cells is about 2 to 4 per section of an inter-villi pocket in the small intestine of zebrafish. Interestingly, this number seems to remain similar in the small intestines of other species including mouse and human, despite the vast difference in their villous size. Transient responses during restitution of the intestinal epithelium, however, appear to be following different strategies in different species.

List of Figures

List of Tables

Chapter 1

Introduction

1.1 Introduction to the digestive system

The digestive tract, also known as the alimentary canal, is present in all multicellular organisms. It takes in food, digests it to extract energy and nutrients, and expels the remaining waste [1, 2]. The digestive tract differs substantially from organism to organism. In its simplest form, it is a more or less uniform tube from mouth to anus opening. In human, it consists of mouth, pharynx, esophagus, stomach, small intestine, large intestine, rectum and anus (Fig.1.1A). The small intestine is further divided into duodenum, jejunum and ileum, while the large intestine is further divided into ascending colon, transverse colon and descending colon.

Apart from the digestive tract, several other organs also form part of the digestive system, including the liver, pancreas and gall bladder [1]. These organs, together with the digestive tract and several auxiliary parts such as the saliva glands and the tongue, form one of the largest systems in the human body.

The human digestive system is amazing in many aspects. In a normal human adult, the digestive tract is approximately 7-9 meters long [3] and the large intestine is about 1.5 meters long [4]. It processes about 500 kilogram of food each year. In one square inch of human small intestine, there are about

20,000 units of epithelial projections termed villi and ten billion microvilli [5]. The epithelium lining the inner surface of the intestine is constantly under abrasion and in the mean time, is constantly being renewed. The epithelium lining will be renewed following a cycle of 2 to 7 days. In other words, the intestinal epithelium will go through several thousand rounds of renewal during the human lifespan, representing the most rapidly renewing tissue in the human body [6].

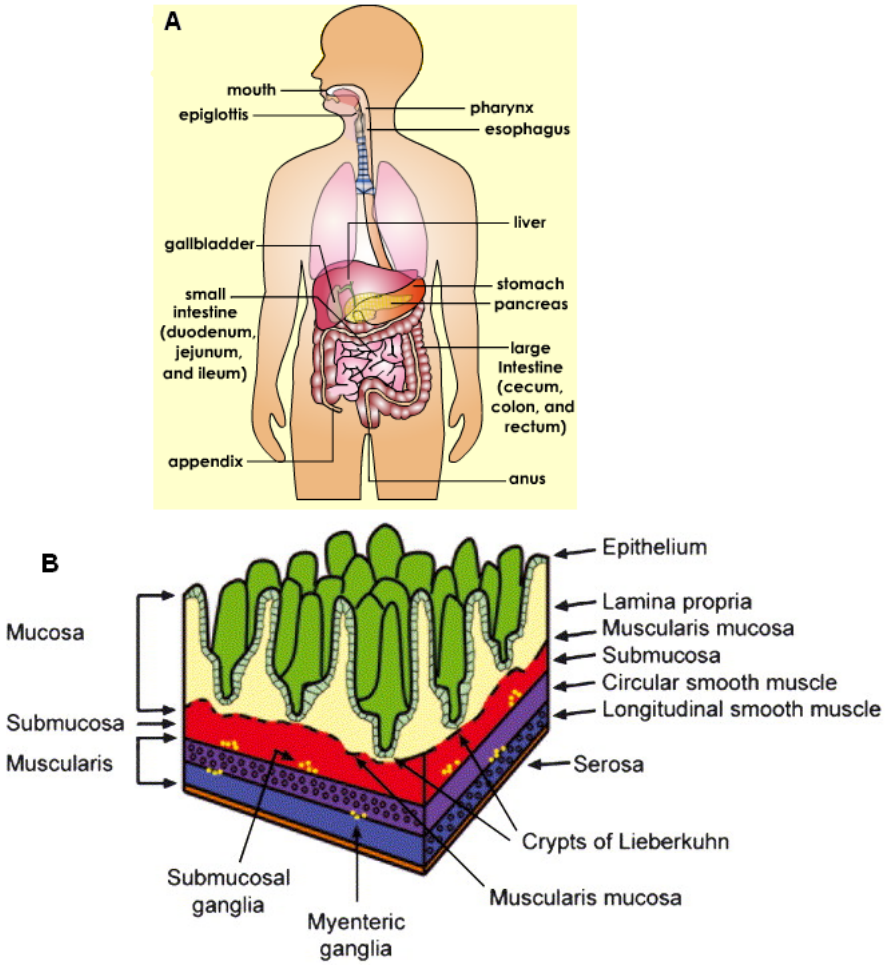

Figure 1.1: Human digestive system and intestinal architecture
(A) The human digestive system. It consists of the liver, pancreas, gall ladder and the digestive tract running from mouth, pharynx, esophagus, stomach, small intestine, large intestine to anus opening. Panel A is from http://kidshealth.org/misc/movie/bodybasics/digestive-system.html and panel B from ref. [7] (top to bottom). (B) Architecture of the small intestine. From innermost to outermost, it includes mucosa, submucosa, mascularis and serosa.

1.2 Tissue architecture and cell types of the intestinal epithelium

The intestinal epithelium has been best characterized in mammals. Architecturally, several layers are observable in a cross-section of the small intestine, including mucosa, submucosa, muscularis and serosa (from innermost to outermost). The muscularis further consists of two layers: circular smooth muscle and longitudinal smooth muscle (Fig.1.1 B).

In the small intestine, the epithelial lining invaginates to form numerous crypts and larger, finger-shaped projections called villi. In the colon, there are again numerous villi, with regional variations in size. The intestinal epithelium harbors four major types of epithelial cells, including columnar cells, mucin-secreting cells, endocrine cells, and, in the small intestine, Paneth cells [8, 9]. Other less common cell lineages are also present, such as caveolated cells and M (membranous or microfold) cells, but are less well characterized [10, 11].

Columnar cells represent the most abundant epithelial cells with microvilli structures along the apical membrane. They are called enterocytes in the small intestine and colonocytes in the large intestine. Mucin-secreting cells, or goblet cells, are named due to their goblet shape and presence of mucus

granules to produce a swollen theca. Endocrine, also called neuroendocrine or enteroendocrine, cells represent a minor cell population distributed throughout the intestinal epithelium. They secrete peptide hormones in an endocrine or paracrine manner from the neurosecretory granules. Paneth cells are located almost exclusively at the crypt base of the small intestine and ascending colon. Paneth cells contain large apical secretory granules and express a number of proteins, including lysozyme, tumor necrosis factor, and the antibacterial cryptins [11].

1.3 Turnover of the intestinal epithelium

The intestinal epithelium represents one of the most rapidly renewing tissues of the human body [6]. The epithelial cells of the intestine undergo apoptosis at the tips of villi, and the sloughed cells are replaced by neighboring cells migrating upward. In the crypts, new cells are generated by stem/progenitor cells to maintain the epithelial homeostasis. Turnover of the epithelial cell lineages within the gastrointestinal tract is a constant process, occurring every 2-7 days in normal homeostasis and increasing after damage [10]. Renewal of epithelium maintains tissue homeostasis and may also serve functions like expulsion of intestinal parasites [12]. Rapid renewal of the epithelium tissue over

the whole lifespan of the host organism, however, has aroused wide scientific interests in regulation of cell differentiation, tissue homeostasis, the maintenance of genome integrity, gene mutations and development of cancer, which will be further discussed below.

1.4 Significance of the study of the digestive system

Dysfunction of the digestive system may yield a wide range of digestive, nutritional or metabolic problems. The digestive system itself may be vulnerable to diseases such as gastroenteritis, inflammation, infection, ulcer and even formation of cancer.

According to recent surveys on human cancers, both gastric and colorectal cancers are among the leading cancers in modern societies, with 21,500 new cases for gastric cancer and 148,810 new cases for colorectal cancer as estimated for the United States in 2008 [13]. According to statistic data released by the National Cancer Institute (Bethesda, US), colorectal cancer has been one of the most frequent human cancers, with an incidence much higher than that in many other organs including the stomach and it has a mortality of 30-50%

in five years after diagnosis [14]. According to a survey released in Singapore, colorectal cancer has been ranked the most frequent cancer (gastric cancer in the third place), which has hit 4899 patients from 1993-1997, with 2621 deaths during the same period [15]. Thus, efforts toward a better understanding of the digestive tract and cancer formation have great significance in both research and clinical applications.

1.5 Intestinal stem cells

The intestine has been a fascinating organ for biologists due to the spatial organization of the sequential cellular events including proliferation, differentiation and apoptosis. In the mouse, proliferation of the intestinal epithelium is restricted to the crypts and apoptosis is restricted to the tips of villi. Loss of cells are thus being constantly replenished by newly generated cells from the lower region of crypts [16, 9, 17].

Leblond and Cheng (1974) proposed a unitarian hypothesis, stating that all the cell types of the intestinal epithelium, including absorptive enterocytes, goblet cells, enteroendocrine cells and Paneth cells, arise from the same source of stem cells [18]. Following that, increasing attention has been drawn to this field of research due to the potential medical importance [19]. Evidence

in support of the existence of intestinal stem cells and their multipotency has been ever growing.

1.5.1 Location of intestinal stem cells

Historically, there have been two schools of thought regarding the location of intestinal stem cells. One school believes that the stem cells are located at the so-called +4 position, just sitting above the Paneth cells. In this school of thought, the finding of cells with long-term retention of tritiated thymidine or BrdU labelling [20, 21, 22] led to the hypothesis that stem cells in the intestine, as well as in epidermis or hair follicle, protect their genome against DNA-replication-induced errors through selective DNA strand segregation by retaining an immortal DNA strand [23, 24, 25]. It was found that these label-retaining cells often appeared at the position +4 from the very bottom of the crypt, sitting above the differentiated Paneth cells, thus this position was proposed to be the location of intestinal stem cells [26, 27]. This view seems to be supported by the recent report that Bmi1 expression specifically marks the cells at the +4 position of the crypt and these cells are able to generate the four major epithelial cell types (columnar cells, goblet cells, enteroendocrine cells and Paneth cells) in mouse small intestine [28].

The second school believes that the stem cells are sandwiched between the post-mitotic Paneth cells near the bottom of the crypts based on the identification of crypt base columnar (CBC) cells, which are small, undifferentiated, cycling cells hidden between the Paneth cells [18, 29, 30, 31, 32]. Originally based on morphological considerations, but more recently also based on clonal analysis through N-nitroso-N-ethylurea(NEU)-induced mutations in the *Dlb-1* gene [31, 33], these CBC cells are believed to represent the true stem cells. This seems to be supported by the recent reports that both *Lgr5* and *Ascl2* mRNAs mark the CBC cells in the crypt, which are able to generate the four major epithelial cell types in mouse intestine [34, 35, 36].

Proof of pluripotency of the intestinal stem cells based on lineage tracing in genetically modified mice has been equally successful in support of either school of thoughts [28, 37, 34, 36]. Current results, therefore, appear to support the presence of two populations of intestinal stem cells, which differ in their location, cell number and molecular profiles. In view of their apparently equal power of regeneration, questions arise regarding the necessity of maintaining two populations of stem cells, their potential interactions and the roles they play during tissue homeostasis. Is it possible that one population of stem cells are descendants of the other population? Or are all of them derived from a

single stem cell at different phases? Unfortunately, the answers remain unclear today. Insights that we may gain from studies in other species like zebrafish would definitely be a plus to further our understanding of the nature of the intestinal biology.

1.5.2 Intestinal stem cell number

The number of intestinal stem cells is under tight regulation under normal physiology. Excessive stem cells are believed to cause crypt division or fission, thereby maintaining the desired number of stem cells within each crypt. Stem cells are sensitive to irradiation and irradiation-induced DNA damage will cause the stem cells to undergo apoptosis in an altruistic manner to prevent passing the DNA damage to their daughter cells. Loss of stem cells will be compensated by expansion of the remaining stem cells or their immediate daughter cells that still possess stemness property or with colonogenic potential. Due to unavailability of molecular makers, the number of stem cells has not been verified for a long time, though it is estimated to be 4-6 in each crypt of mouse small intestine [38, 39, 16].

1.5.3 Intestinal stem cell marker

It has been one of the major goals to identify specific molecular markers for intestinal stem cells. At the time when the thesis project was initiated in 2005, there were no gene markers identified for intestinal stem cells. Several gene markers were proposed in literature, including Msi-1 [40, 41], BMPR1a [42], phospho-PTEN [42], DCAMKL1 [43], Eph receptors and integrins [44]. However, no convincing data are available to prove the pluripotnecy of these cells. Recently, a few other markers, including Lgr5 [34, 45], Ascl2 [36], Bmi1 [28, 46] and Prominin1 [47], have been published with rigorous proof of the pluripotency of the identified stem cells.

The recent identification of intestinal stem cell gene markers has led to a sudden flourish in this field of research. For example, Lgr5 not only marks stem cells in the small intestine, but also marks stem cells in the hair follicle [48]. It is also suggested to mark stem cells in the stomach and mammary gland [34, 45]. Like Lgr5, Ascl2 has also been identified to mark intestinal stem cells in a more specific manner [36]. Transcriptome of intestinal stem cells have been probed by microarray [36] and culture of the stem cells has been reported to be able to grow villus-like structures even without support of mesenchymal cells [37].

1.6 Intestines of different vertebrate models

1.6.1 Mouse intestine

The digestive tract of mouse traverses from mouth to pharynx, esophagus, stomach, small intestine, large intestine till anus opening. Due to its similarity to human intestine, the mouse intestine has been a popular model for studying human intestine.

Development of mouse intestines has been described previously [49]. About 12 days after fertilization, the duodenum shows the epithelium, with its round or slightly elliptical internal and external contours. The epithelium is 1-2 cells thick and surrounded by a loose mesenchymal layer. One day later, the outer profile of the epithelium is still elliptical. The lumen has a slit-like appearance or sometimes a triangular shape. Along with development, the epithelium forms elevations projecting into the lumen, but there are no indications of the presence of previllous ridges as described for the chick (see below). Around 14 dpf, degenerating cells appear at the top of the epithelial elevations. These cells become rounded and are extruded into the lumen.

Adult mouse features presence of crypts and villi in the small intestine, but only crypts in the large intestine [34]. Each crypt contains a monoclonal popu-

lation of cells [50, 51] derived from multipotent stem cells [52]. After a phase of rapid amplification, the clonal descendants undergo terminal differentiation to four principal cell types during a bipolar migration [52]: columnar and goblet cells arise as they are rapidly translocated in vertical coherent bands to the apical extrusion zone [53]. Paneth cells differentiate as they descend to the crypt base, while enteroendocrine cells arise as they migrate out of the proliferative zone. Of these cell types, the columnar cells are most abundant (about 80% of the whole epithelial population), followed by the goblet cells (about 10-15% in the small intestine, often in the crypts; the population is bigger in the large intestine). The Paneth cells fall into minority and the enteroendocrine cells are rare. Organization of the cellular events in well demarcated anatomic units provides a unique opportunity for us to infer the biological properties of stem cells [54] and investigate the regulatory mechanisms of cell proliferation, commitment and differentiation.

1.6.2 Chicken intestine

The digestive tract of chicken runs from mouth/beak through esophagus, crop, proventriculus (glandular stomach), gizzard, small intestine, ceca, large intestine, cloaca to the vent [55, 56, 57]. The most prominent feature is the presence

of the gizzard, which temporarily stores food intake and mechanically breaks the food particles into smaller sizes to make the work of the enzymes easier. The crop buffers the food passage and moistens it before it traverses into the proventriculus. Chicken also possesses two ceca that are essentially nonfunctional, proximal to its cloaca that functions as a common chamber for the gastrointestinal tract and the urinary tract.

Development of chicken intestine demonstrates some interesting features. During early embryonic development, the epithelium of chicken intestine undergoes three stages, including the circle, ellipse and triangle stages, to establish the first three previllous ridges [58, 59]. Following that, new previllous ridges will form in the location occupied by the valley between two established ridges. After this period, ridge formation becomes more irregular. There will be about eight previllous ridges by eleven days and sixteen by thirteen days. Epithelium proliferation in the chicken intestine, however, occurs both in the crypts and along the villus [60], which differs from that in mouse intestine where proliferation is restricted to the crypts only [9].

Similar to mouse, adult chicken also features presence of crypts and villi in the small intestine, but only crypts in the large intestine [61]. Vacuolated columnar cells, mucin-secreting goblet cells and peptide-synthesizing enteren-

docrine cells are present along the villus axis [62, 60, 63, 64, 65]. But the presence of the Paneth cells has not been reported in chicken intestine [66].

1.6.3 Frog intestine

The digestive tract of frog proceeds from mouth to esophagus, stomach, small intestine, large intestine and anus opening. The frog is prominently featured by its metamorphosis during development, where significant changes occur to its organs, including its intestine [67]. During metamorphosis, undifferentiated cells appear at stage 60 (the start of metamorphic climax) as small islets between the larval epithelium and connective tissue. They actively proliferate and finally differentiate into the secondary or adult epithelium. In the mean time, all of the larval epithelial cells undergo apoptosis on and after stage 60 and are gradually replaced by the adult epithelial cells. An interesting difference between frog and most other vertebrate species, however, is the absence of villous structures in frog intestine till the metamorphic stage [67, 68].

Following the metamorphosis, adult frog intestine features presence of both villi and crypts (also called crests and troughs, respectively). The intestinal epithelium contains columnar cells, goblet cells and enteroendocrine cells [69, 70]. The columnar cells are most abundant and the goblet cells take up about

10% of the epithelial population [70]. But the presence of the Paneth cells has not been reported in frog intestine.

1.6.4 Zebrafish intestine

The digestive tract of zebrafish starts with mouth and proceeds to pharynx, esophagus, intestine and ends with the anus opening. During development, the time period between 26 hpf and 76 hpf represents a critical period where the entire intestinal endoderm remains highly proliferative [71, 7]. At 26-30 hpf, the cells give rise to the primitive gut comprising a continuous thin layer of endoderm just above the dorsal surface of the yolk at the midline of the embryo. The endoderm cells then adopt a bilayer configuration and form small cavities to make an intestinal lumen. Later the endoderm cells polarize and differentiate into distinct cell lineages. Enteroendocrine cells are identifiable first at 52 hpf in the caudal region of the intestine. By 74-76 hpf, the entire digestive tract is a hollow tube. The mouth has opened and a single continuous lumen from mouth to anus is formed, but the anus remains closed till a day later. The differentiation of mucin-containing goblet cells is first evident at 100 hpf and is restricted to the middle segment of the intestine, where enterocytes with large supranuclear vacuoles are also present. Meanwhile, expansion of

the lumen in the rostral intestine forms the intestinal bulb. The epithelium elaborates folds and proliferating cells become progressively restricted to a basal compartment analogous to the crypts of Lieberkühn in mammals.

Similar to its mammalian counterparts, the epithelium of zebrafish intestine contains columnar cells, goblet cells and enteroendocrine cells [71]. But zebrafish intestine has demonstrated some differences from their mammalian counterparts. Previous studies have suggested the absence of a stomach based on gross morphological observations in cyprinids [72], though this is not well grounded at the molecular level. The absence of crypts and the Paneth cells has also been reported in larval zebrafish intestine [71]. These differences between species have triggered interests into questions like how the gastric functions may be carried out in the intestine and how the zebrafish intestine may be regionalized to carry out different functions like mammalian small/large intestines.

1.7 Establishing zebrafish as a vertebrate model for study on intestine

Since its introduction to the scientific research community in the early 1970's by Professor George Streisinger of University of Oregon, the zebrafish has been widely employed as a vertebrate model in a broad range of studies including developmental studies, genetic studies, modeling of human diseases and drug screening [73, 74]. Nowadays, zebrafish has become one of the most popular animal models for molecular research and the zebrafish community has been growing.

In recent years, the zebrafish has become an increasingly popular experimental model with its own advantages. It is a vertebrate model with rapid development. *Ex utero* development and optical transparency of its embryos greatly facilitate developmental analysis and imaging. Its genome data is now publicly accessible.

Due to the advantages of zebrafish as a model for molecular research, it has begun to be used for studies on intestinal biology. To characterize zebrafish intestine, several pioneer reports have probed the developmental process of zebrafish intestine. From morphology, cell type and tissue renewal, zebrafish in-

testine demonstrates similarity to mammalian intestines [71, 75, 76]. To model human intestinal cancer, pioneering work has been done to produce tumors in zebrafish intestine by manipulating the Wnt/beta-catenin pathway [77, 78].

However our current understanding of zebrafish intestine generally remains fragmented. For example, the molecular and functional difference along the anterior-posterior axis of zebrafish intestine remains unclear. Its similarity to human intestines is also unclear. Current work aims to unravel the general characteristics of adult zebrafish intestine from morphological, histological and molecular aspects. Features of small intestine and large intestine will be explored and molecular similarity between regions of zebrafish intestine and their mammalian counterparts will be investigated. Research goals of the thesis work are briefly outlined in the next section.

1.8 Research goals of the current work

The current thesis work aims to have a better understanding of the regionalization and characteristics of adult zebrafish intestine. We have integrated morphological, histological and molecular approaches toward this end.

1.8.1 Morphological and histological features of zebrafish intestine

Previous work on zebrafish has been largely carried out in larval fish where the intestinal organ is still developing. Mature zebrafish intestine distinguishes itself from the developing intestine in morphology, histology as well as functional specialization. These characteristics of adult intestine have not been adequately studied so far. Here we want to address these aspects starting with morphology and histology.

1.8.2 Characterization of regionalization of zebrafish intestine through genome-wide gene expression analysis

Functional specialization and regionalization of adult zebrafish intestine remain poorly understood today. There is no definitive morphological, histological or architectural demarcation to help us identify the functional transition along the intestinal tract. Thus gene expression features may become necessary for this purpose. In this project, genome-wide gene expression profiles will be probed in a region-specific manner along the adult fish intestine. Any analogy between

zebrafish intestine and the mammalian intestines will thus be determined by analysis using these gene expression profiles.

1.8.3 Study of the cell fate decision in zebrafish intestine

Several signaling pathways serve important roles in the cell fate decision process in the intestines and one of them is the Notch pathway. Though it has been shown to influence the cell fate specification in larval or juvenile zebrafish intestine [79], we want to examine its role in adult intestine and to further understand its relationships with other signaling pathways that are also known to be important in the intestine, such as Wnt signaling, BMP signaling, GATA transcription factors as well as mesenchymal cell activities.

1.8.4 Responsive nature of intestine during regeneration

The responsive nature of the intestine upon perturbation is yet to be further explored. As the intestinal stem cells are known to be very sensitive to radiation [80], we expect to see drastic changes taking place in the intestine upon high dose radiation. So we will use high dose whole body radiation to investi-

gate the responsive dynamics of intestine during tissue regeneration and find out how events of cell proliferation, apoptosis and renewal are orchestrated to re-establish homeostasis.

1.8.5 Computational analysis of intestinal stem cells and their adaptive changes

Due to absence of specific molecular markers for intestinal stem cells in zebrafish, we aim to investigate the number of pluripotent intestinal stem cells present in each inter-villi pocket and their adaptive changes through computational analysis. A generalized mathematical model will be developed to investigate the number of stem cells and their adaptive kinetics during pathological conditions.

Chapter 2

Functional organization along the rostrocaudal axis of the intestine

2.1 Background

The surface of the intestine epithelium is the site where nutrients are absorbed into the body. This absorption function is aided by expanding the surface area of the gut into villi at the tissue level and microvilli at the cellular level. Consequently, the mouse and human intestine has become a model for studying how this large surface develops during embryogenesis, the role of stem cells in the renewal of the epithelium, and development of colorectal cancer [81, 9, 82]. However, these complex problems can be studied in a simpler system, the zebrafish (*Danio rerio*), which has emerged as an important vertebrate model for study of not only human development but also disease [73, 83, 78, 84, 85]. In comparison with the mouse or human intestine, the zebrafish intestine shares structural and functional similarity at the tissue level but is structurally simple and develops rapidly [7, 86, 71].

So far, morphological development of zebrafish intestine has been relatively well characterized in embryos and larvae [7, 71]. However, the organization and physiology of digestive tract has not been specifically documented for adult zebrafish although several books are available for description of general fish intestine anatomy [72]. Zebrafish, like many fish, lacks a morphologically and functionally distinct stomach and does not express genes that encode specific

gastric functions [78, 87, 88, 79]. Sections of intact zebrafish embryos and juveniles and microCT tomography reveal the digestive tract from pharynx and esophagus to the three sections of the folded intestine and anus. Previous studies have described the zebrafish intestine as a tapered tube that begins at the esophageal junction and is folded into three sections, the large diameter rostral intestinal bulb, the mid-intestine, and the small diameter caudal intestine. However, it is not known whether these regions are functionally distinct or whether their functions correspond to the mammalian stomach, small intestine or large intestine. In this study, we characterized the anterior-posterior axis of adult zebrafish intestine at tissue, cellular and molecular levels. By comparing the morphological and molecular characteristics, we identified structurally and functionally distinct areas that correspond to the small intestine and large intestine but not stomach.

2.2 Materials and Methods

2.2.1 Maintenance of zebrafish and dissection of zebrafish intestine

Danio rerio of about one year old were maintained following established protocols [89] and in compliance with Institutional Animal Care and Use Committee (IACUC) guidelines. Zebrafish were euthanized by 0.1% 2-phenoxyethanol and their intestines were isolated and cut into seven segments along the anterior and posterior axis, as shown in Fig.2.1B. The seven segments were labeled S1, S2, S3, S4, S5, S6 and S7, respectively.

2.2.2 Paraffin sectioning of zebrafish intestine

Intestinal segments were fixed in 4% paraformaldehyde in phosphate buffered saline at room temperature overnight. Then the intestine samples were dehydrated in 70% ethanol overnight and further dehydrated in ethanol with increasing gradients (75%, 90%, 95% and 100%). The samples were cleared in 100% Histoclear II (National Diagnostics, US) for 30 min twice, embedded in liquid paraffin at 58^oC for 30 min, then changed into fresh paraffin for final embedding at 58^oC overnight. Finally, the samples were sectioned at 7 μm on

a Reichert-Jung 2030 microtome (Leica, Germany) and collected onto Fisher SuperFrost slides. The slides were left on a heating block at 42^oC overnight before further assays were conducted.

2.2.3 Hematoxylin and eosin and alcian blue staining

Tissue sections were stained by Meyer's hematoxylin for 10 min, rinsed in tap water, stained by eosin for 1 min, followed by dips in acidic ethanol and rinse in tap water. They were stained by alcian blue (Biogenex, US) for 10 min and rinsed in tap water. Finally, the slides were dehydrated in ethanol of increasing gradients (75%, 90%, 95% and 100%), cleared by HistoClear II (National Diagnostics, US), mounted with DePeX (EMS, US) mounting medium and covered by cover slips. Images were taken using a Zeiss Axiovert imaging system.

2.2.4 Quantitative real-time PCR (qRT-PCR)

Quantitative real-time PCR was carried out in 96-well plates on a LightCycler 480 system (Roche, Swiss). The PCR reaction was set up according to the manufacturer's protocol with optimization of primer-specific annealing temperature and extension time. PCR products were labeled by SYBR Green

dye. All gene expression levels were measured and normalized against the level of house-keeping gene actin beta 2 expression.

2.2.5 Microarray experiments

Intestines were isolated from male adult zebrafish, quickly rinsed in 1x phosphate buffered saline/diethylpyrocarbonate, and cut into seven segments according to Fig.2.1B. To maintain a more homogeneous molecular background, only male fish were used for microarray analyses. The same segments from every 10 fish were pooled as one biological replicate and they were kept in liquid nitrogen till extraction of RNA. Two rounds of extraction of RNA were performed using Trizol (Invitrogen, USA). A total of five replicates were prepared for each segment. For each replicate, 10 μg RNA was reverse-transcribed into cDNA with incorporation of aminoallyl-dUTPs. Later the samples were hybridized onto in-house spotted microarray chips with labeling by Cy5 as described previously [90]. RNAs from whole fish were used as reference for all experiments and labeled by Cy3. After hybridization, the microarray chips were scanned and graded, and raw data were normalized using LOWESS method implemented in Gene Cluster 3.0 during the pre-processing stage.

2.2.6 Identification of differentially expressed genes from the microarray data

Pre-processed microarray data were visualized and subjected to one-way ANOVA test using MeV MultiExperiment Viewer software [91]. One-way ANOVA test was performed using a critical p-value of 0.1 with standard Bonferroni correction for all seven intestinal segments. The selected genes were used for clustering and expression pattern analysis to compare the similarity and differences in the seven segments.

2.2.7 Gene ontology (GO) analysis by GO Tree Machine

Up-regulated genes were selected for each individual segment based on the fold changes of their expression levels (at least two told up against the RNA of pooled adult zebrafish and FDR adjusted p-value ≤ 0.05). Gene ontology was carried out using GO Tree Machine, which is a web-based tool developed by the Vanderbilt University to analyze gene ontology for a given set of genes [92]. It compares the distribution of genes in the gene set of interest in each GO category to those in the reference gene set, i.e. the transcriptome of zebrafish in our case. Gene information was retrieved from GeneKeyDB, a database that integrates gene information from Ensembl, Swiss-Prot, HomoloGene, Unigene,

Gene Ontology Consortium and Affymetrix etc. Statistical tests were used for the assessment of enrichment of each gene category.

2.2.8 Pathway analysis using WebGestalt

WebGestalt is web-based software package developed by the Vanderbilt University, including gene ontology analysis, KEGG (Kyoto Encyclopedia of Genes and Genomes) pathway analysis, intersection of gene sets and so on [93]. In this work, the KEGG pathway analysis was used and the program took a set of genes of interest as input, retrieved information about pathways and their associated genes from the GeneKeyDB. The gene set of interest was compared to a reference gene set for the proportion of genes in the pathway. Hypergeometric test or Fishe's exact test was used to assess the statistical significance. Since the pathway database only accepted mouse and human genes, thus zebrafish genes were first mapped to their mouse homologs prior to pathway analysis. Zebrafish genes were mapped to their mouse homologs using the web-based tool developed by the Genome Institute of Singapore using DR build #115-63 (http://giscompute.gis.a-star.edu.sg/∼govind/unigene_db/).

2.2.9 Gene Set Enrichment Analysis

GSEA is a computational method that determines whether a priori defined set of genes shows statistically significant, concordant differences between two biological samples; it calculates an enrichment score using a running-sum statistic through a ranked list of gene expression data set [94]. In this work, the software GSEA2.0 developed by the Broad Institute [94] was used. The statistical significance of the enrichment score was estimated by using an empirical phenotype-based permutation test procedure. A false discovery rate was provided by introducing adjustment of multiple hypothesis testing.

2.3 Results

2.3.1 Architectural differences along the zebrafish intestinal tract

The anterior-posterior axis of the embryonic, juvenile, and adult zebrafish digestive tract has been described in several atlases [95, 96, 97]. In summary, the adult digestive tract consists of the mouth, pharynx, esophagus, intestine, and anus (Additional file 1). However, the zebrafish belongs to the group of stomach-less fishes in which the intestine transits directly from esophagus. In

adult fish, it is folded into three sections: the rostral intestinal bulb, mid-intestine and caudal intestine (Fig.2.1A). When dissected from the animal and freed of the surrounding mesentery, the intestine remains folded by two turns into three straight regions that correspond anatomically to the three portions as observed *in vivo* (Fig.2.1B). Their diameters decrease along the anterior-posterior axis (Fig.2.1B).

To characterize intestinal function, we subdivided the intestinal bulb, mid-intestine, and caudal sections into seven segments, S1-S7 (Fig.2.1B) and examined their architecture under a light microscope. We observe that the zebrafish intestine surface in segments S1-S6 is covered by ridges that are oriented circumferentially across the intestine axis (Fig.2.1C-I). The ridges are densely packed and highly branched. In segment S6 the ridges are shorter and broader than the anterior segments. Segment S7 is morphologically distinguished from the other six segments by a smooth surface devoid of any folds or villus-type structures (Fig.2.1I).

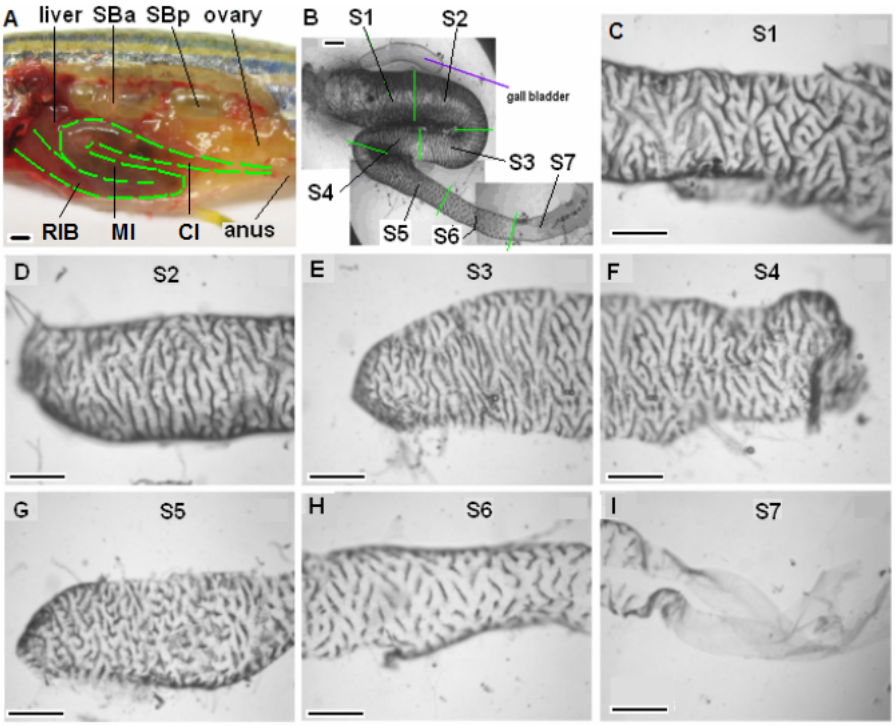

Figure 2.1: Morphology of adult zebrafish intestine
(A) A partially dissected 6-month-old zebrafish shows the anterior, medial, and posterior portions of the intestine (green-outlined). RIB: rostral intestinal bulb; MI: mid-intestine; CI: caudal intestine. (B) Division of a dissected zebrafish intestine into seven equal-length segments (green lines), S1 to S7, along the anterior-posterior axis. (C-I) Surface views of segments S1-S7 showing the folding of the mucosal surface into ridges. Scale bars, 500 μm.

Cross-sections of the intestinal segments reveal a simple architecture for the zebrafish digestive tract of a mucosa, muscularis externa and serosa layer (Fig.2.2). The intestinal mucosa consists of a simple epithelium of enterocytes and mucous-secreting goblet cells and an underlying lamina propria containing blood capillaries, lymphatic vessels, muscle fibres and mesenchymal cells [7]. The mucosal layer is directly ensheathed by circular and longitudinal smooth muscle tiers of the muscularis externa within which are embedded the plexus of myenteric neurons as reported previously [7, 71]. In the mammalian duodenum, a typical submucosal layer contain Brunner's glands, the branched tubular or branched tubuloalveolar glands that produce alkaline secretions to neutralize the acidic chime entering the duodenum [98]. However, in the zebrafish intestine the submucosa layer and Brunner's glands are absent (Fig.2.2).

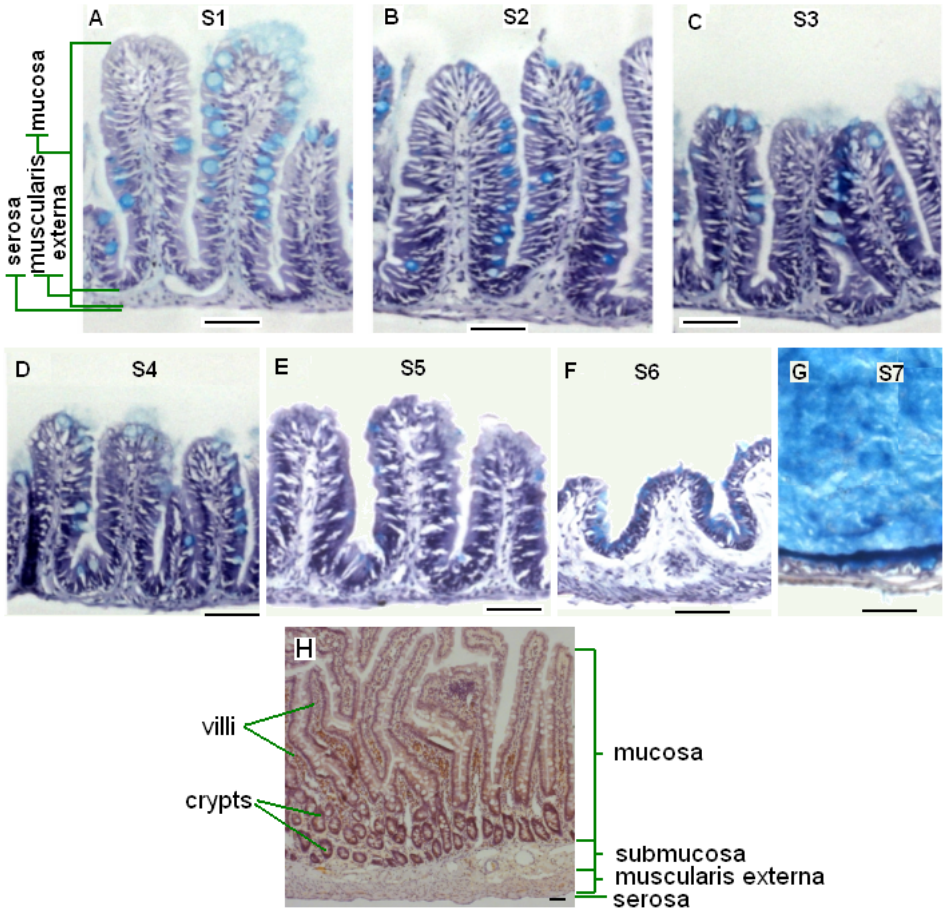

Figure 2.2: Cross-section views of zebrafish intestine segments Hematoxylin/Eosin/alcian blue-stained views of segments S1-S7 in cross section. Segments S1-S6 contain three tissue layers: mucosa, muscularis externa and serosa, while S7 has a simple epithelium directly adjacent to the muscularis externa. Goblet cells (stained blue) are interspersed among the absorptive cells. Panel H shows a section of a mammalian rat small intestine, for comparison purpose. Scale bars: $50\mu m$

Consistent with our earlier observations of intestinal ridges in segments S1 to S6 and absence of ridges in S7, these ridges in cross-section resemble the spatially separate villi in the mouse or human small intestine (Fig.2.2). The villar ridges are comparable in height from segments S1 to S5 (Fig.2.2A-E), shorten and broaden in segment S6 (Fig.2.2F), and absent in segment S7 (Fig.2.2G). Segments S5 and S7 often contain compact excretions that are ensheathed by a mucous layer (stained blue by Alcian Blue in (Fig.2.2G). In addition to the absence of villi, segment S7 is distinguished by its lining of abundant goblet cells that are interspersed by absorptive epithelial cells (Fig.2.2G). The muscularis externa is apparent, but the mucosa layer, in general, appears very thin compared with other segments of the intestine. Thus, based on histology and architecture, the intestinal lining is divided into three morphologically distinct regions, segments S1-5, S6, and S7.

2.3.2 Distinct molecular signatures along the zebrafish intestinal tract

Based on gross morphology, segments S1-S5 are similar while segments S6 and S7 are different. These differences in structure suggest that there should be inherent differences in function. To test this idea, we examined and compared the

molecular signatures of each segment by profiling their transcriptional activity. Using a standard Bonferroni corrected p-value ≤ 0.1 (adjusted for false discovery) applied to results from a one-way ANOVA analysis, we identified 2,558 genes that were differentially expressed in at least one of the seven segments and organized the genes by hierarchical clustering analysis [91] (Fig.2.3A) for similarities in patterns of gene expression. This analysis sorted the seven segments in their anatomical sequence, S1-S7 with S1-S5 more similar to each other than to segments, S6 and S7.

To understand the significance of the clusters, we then applied a threshold of 2.0 fold against pooled RNA extracted from whole adult zebrafish to the set of 2,558 genes from the ANOVA analysis. This analysis shows the numbers of genes that are abundantly expressed in each individual segment are: 830 (S1), 801 (S2), 820 (S3), 818 (S4), 825 (S5), 950 (S6) and 1023 (S7). To determine the extent to which genes are commonly expressed along the intestinal tract, we determined the overlap in gene sets between pairs of adjacent segments (Fig.2.3B). Consistent with the clustering results in Fig.2.3A, significant intersection was found between segments S1-S5 [more than 700 genes (or $\geq$89.9%) for each overlap, Fig.2.3B]. However, segments S6 and S7 express quite different sets of genes than the anterior segments. S5 and S6 overlap in 12.3%

genes while S6 and S7 share only 45.2% genes in common. Full lists of genes are shown in the Appendix section (Genes commonly enriched in S1-S5 are shown in table 1; The rest of genes enriched in S1, S2, S3, S4, S5 are shown in table 2, table 3, table 4, table 5, table 6, respectively; Genes enriched in S6 are shown in table 7; Genes enriched in S7 are shown in table 8). Similar results were also observed from analysis of down-regulated genes (data not shown).

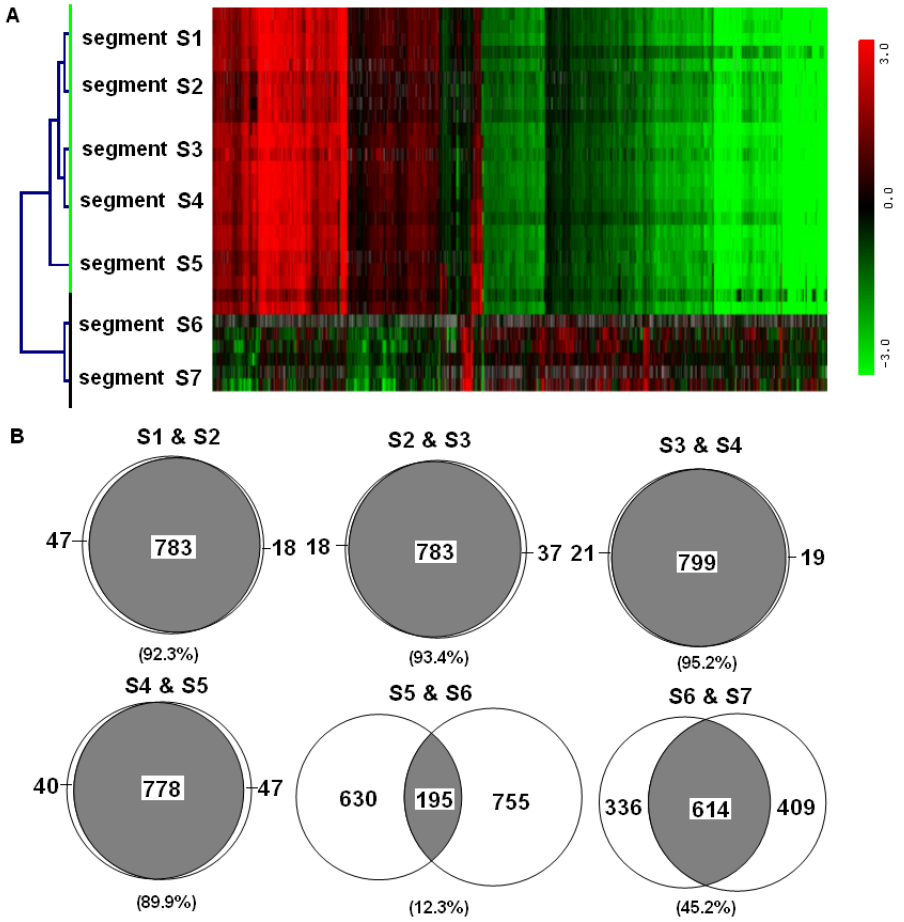

Figure 2.3: Identification of genes differentially expressed along the anterior-posterior intestine
(A) Hierarchical clustering of segments S1-7 by differentially expressed genes selected by ANOVA analysis. Segments S1 to S5 are clustered as one group; segments S6 and S7 are clustered as another group. (B) Overlap analysis of up-regulated genes in adjacent segments. The number and percentage of overlapping genes are indicated within and below the intersection respectively.

To confirm these patterns of overlap, we identified a number of genes that were either highly expressed in segments S1-S5 (e.g. *gdpd1*, *chchd7*, *zgc:11410*, *hbl3*, etc) or in segments S6 and S7 (e.g. *trp*, *ctsl1*, *ctsc*, *gnb3*, *gsbp1*, *ppp2r2d*, etc), suggesting a comprehensive functional transition along the zebrafish intestine (Fig.2.4A). The expression patterns of *vil1l* (Fig.2.4B), *fabp2* (Fig.2.4C), *apoa1* (Fig.2.4D), *apoa4* (Fig.2.4E), *cfl1* (Fig.2.4F), *zgc:110410* (Fig.2.4G), *typ* (Fig.2.4H) and *ctsl1* (Fig.2.4I) were confirmed by real time RT-PCR. Thus, based on the molecular analyses, the zebrafish intestine can be divided into three molecularly distinct regions as represented by segments S1-S5, S6, S7, respectively.

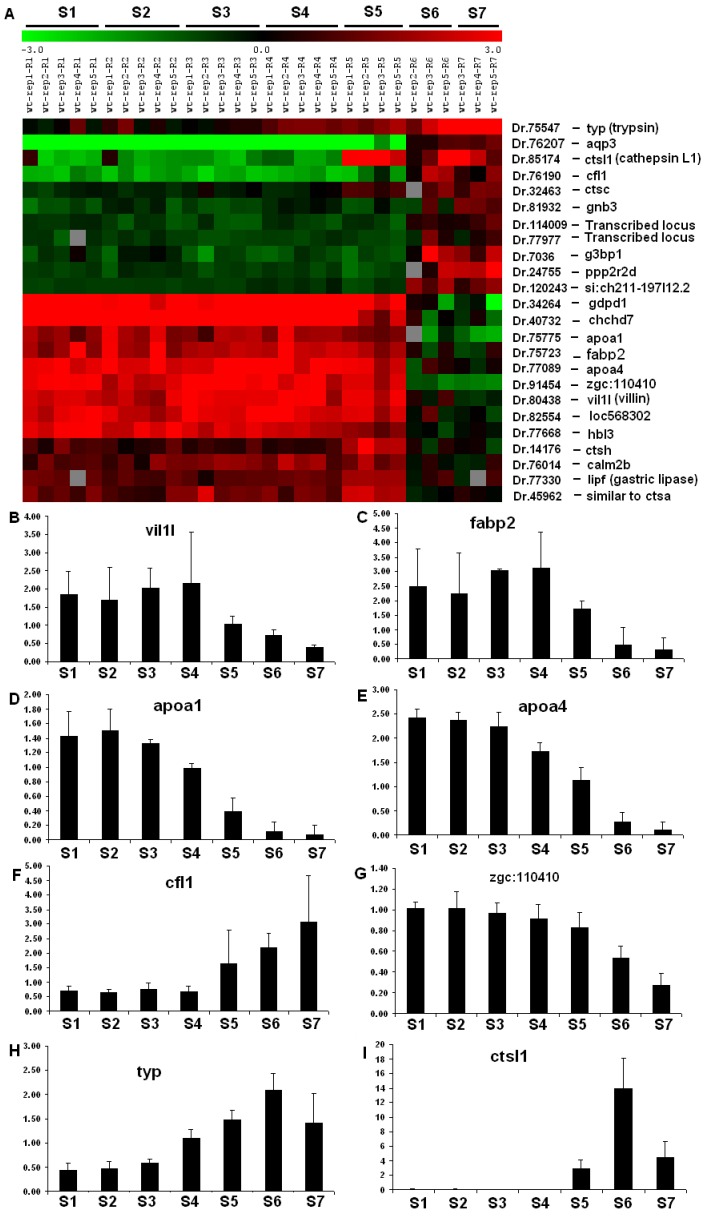

Figure 2.4: Expression patterns of selected intestinal genes
(A) Expression patterns of selected genes based on microarray data. The genes were selected based on their known function in the digestive tract and/or from their expression profiles. (B-I) qRT-PCR validated expression pattern of selected genes. The histograms show the relative changes of the gene expression levels compared with their respective levels of the housekeeping gene bactin2. Gene names are indicated in each panel.

2.3.3 Molecular features of the small and large intestine-like functions

Having shown the intestine can be subdivided into three regions, S1-S5, S6, and S7, based on similarities in expressed genes, we investigated whether the identity of the genes gives insight into intestine function and thus we selected several markers for more detailed analysis.

The functions of the mouse and human small intestine have been characterized by well known molecular markers including *fabp2* [99], *vil1l* [100, 101, 102], *apoa1* and *apoa4* [103, 104, 105]. All of these genes were detected in S1-S5 in our microarray analyses by their higher levels of expression compared with total RNAs from whole fish (Fig.2.4A) and confirmed by real time RT-PCR analyses (Fig.2.4B-E). Intestinal *fabp2* gene encodes a fatty acid binding protein that is specifically involved in the intracellular transport of fatty acids in the small intestine [99, 106, 107]. This gene is highly conserved in teleosts, amphibians, avians and mammals [108]. Previously, a RFP transgenic zebrafish line under the intestinal *fabp2* promoter, *Tg(fabp2:RFP)*, has been generated and RFP reporter gene is specifically expressed in the intestine [109]. To further verify the expression of intestinal *fabp2*, we isolated an intestine from a 3-month-old *Tg(fabp2:RFP)* transgenic zebrafish and found that RFP fluores-

cence was high in segments S1-S4, but quickly diminished around the second turn of the intestine (Fig.2.5A). This expression pattern was also confirmed by direct detection of endogenous *fabp2* mRNA expression by *in situ* hybridization (Fig.2.5C). Closely resembling the pattern of *fabp2* expression, *vil1l* expression is also restricted to the mammalian gastrointestinal tracts where it is highly expressed in the small intestine [101]. Our microarray data show that zebrafish villin gene (*vil1l*) is highly expressed in segments S1-S5 and its expression is reduced in segments S6 and S7. This finding is further validated by real time RT-PCR (Fig.2.4C), where the expression of *vil1l* decreases in segment S5 and to a negligible level in segments S6 and S7. In further support that segments S1-S4 possess features of a small intestine, another two conserved markers, *apoa1* and *apoa4*, also showed similar expression pattern to *fabp2* and *vil1l* genes along the anterior-posterior axis of zebrafish intestine. These two genes can also be considered to be reliable molecular markers for small intestine because in 36 human tissues and 45 mouse tissues examined, expression of mammalian *Apoa1* and *Apoa4* are highly restricted to the digestive organs including small intestine and liver (GSE2361 and GDS182, GEO database, NCBI). These patterns of small intestine markers together with the transcriptome data suggest that the small intestine comprises segments S1-S4

and transitions into a different function in segment S5.

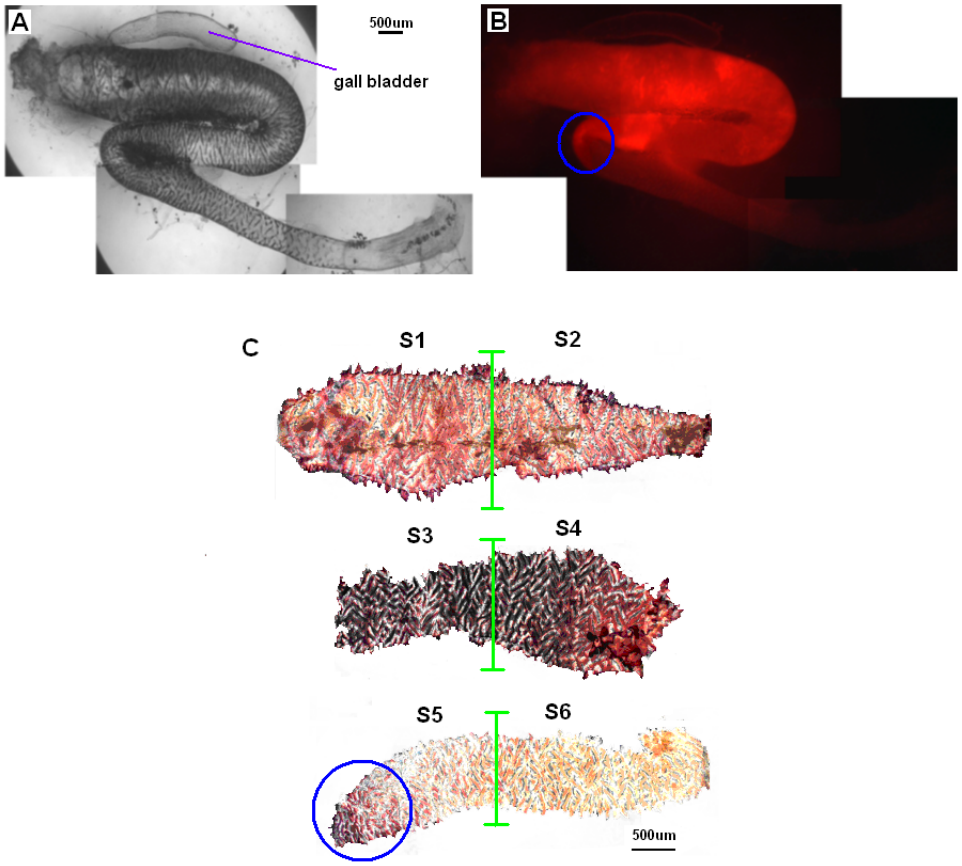

Figure 2.5: Identifying the boundary site between the small and the large intestine
(A) Bright-field image of an intestine isolated from the transgenic line Tg(fabp2:RFP). (B) Examination of fabp2 gene expression in the same intestine, where expression of RPF reporter was driven by the *fabp2* gene promoter. The circle indicates the site where transgenic *fabp2* expression is switched off. (C) *In situ* hybridization of *fabp2* gene in zebrafish intestine. Endogenous expression of *fabp2* was evident in segments S1, S2, S3, S4, but it quickly diminished to negligible level in the proximal site of segment S5.

If segments S1-S4 are small intestine-like, then we investigated whether S5-S7 expresses gene markers for the large intestine. Two genes, *cfl1* (cofilin1) and *aqp3* (aquaporin 3), distinguish segments S5-S7 from S1-S4. *Cfl1* belongs to a family of actin-binding proteins and mediates dynamic stabilization of actin filaments [110]. Our microarray and real time RT-PCR data (Fig.2.4A and F) indicate that *cfl1* is primarily expressed in segments S5-S7, but down-regulated in the first four segments. Analysis of rat EST database suggests that *Cfl1* is expressed in the large intestine but not in the small intestine (Unigene's EST profile viewer, Unigene Rn.11675, NCBI). Similarly, our microarray data indicated increased expression of *Aqp3*, an osomoregulatory channel protein on membrane of epithelial cells [111] and mucus cells of the posterior intestine of teleost eel [112], in segments S6 and S7 (Fig.2.4A, Dr.76207). Aquaporins are water channel proteins that facilitate water movement, hence increase water permeability, across cell membrane and the increase expression of Aqp3 is therefore important for absorption of water in the intestine, in particular, for the fecal dehydration in the large intestine. In line with this, the mammalian aquaporin 3 is expressed along the gastrointestinal tract, with its highest expression in the colon [111]. Thus, while segments S1-S5 possess molecular features of small intestine, segments S6 and S7 have molecular features of

large intestine with segment S5 as a transitional region.

2.3.4 Analysis of gene ontology along the anterior-posterior axis

To infer the functions of the intestinal segments, we pooled the data sets of genes that showed up-regulated expression in each segment into three groups, S1-S5 (891 genes), S6 (1147 genes), and S7 (1107 genes), and identified ontologies that were revealed [92]. The significantly enriched (p-value ≤ 0.01) categories based on GO analysis are shown in Table 2.1.

As expected from a major metabolic organ, the intestine of zebrafish harbors a rich collection of genes involved in metabolism, molecular transport and localization, catalytic activities among others. However, major differences were found between the three groups of S1-S5, S6 and S7. There are 56 categories that were statistically enriched in S1-S5, but only 6 categories in S6 and 8 categories in S7. Among these enriched categories, up-regulated genes in S1-S5 are involved in a wide range of metabolic processes, including metabolism of fatty acid, organic acid, lipid, vitamin, heme, alcohol, glucose, hexose, monosaccharide, carbohydrate, etc. (Table 2.1). They also play important roles in energy generation and homeostasis of ion, iron and cations. Notably, a group

of genes are associated with catalytic activities such as hydrolase activity and transferase activity, which are important for the absorptive function of the small intestine. The variety of GO categories in the S1-S5 group supports the multiple functions of this part of zebrafish intestine with features of the small intestine (to be discussed below).

The S6 and S7 groups, on the other hand, only show a few statistically enriched categories. For example, genes from S6 are involved in oxidoreductase activities while genes from S7 are enriched in biosynthesis of vitamin and pyridine nucleotide (Table 2.1). They are also involved in intracellular signaling and pentosyl/phosphoribosyl transferase activity. These results suggest that segments S6 and S7 represent two regions of zebrafish intestine that perform tasks apparently different from those of S1-S5.

Table 2.1: Enriched gene ontologies in zebrafish intestine. O: observed; E: expected; R: ratio of observed over expected; P: p-value

segments S1-S5				
In biologicial process	O	E	R	P
vitamin biosynthesis	3	0.08	37.5	1.55E-05
water-soluble vitamin biosynthesis	3	0.08	37.5	1.55E-05
alcohol metabolism	7	1.28	5.47	2.42E-04
gluconeogenesis	3	0.15	20.0	2.92E-04
alcohol biosynthesis	3	0.18	16.67	5.02E-04
hexose biosynthesis	3	0.18	16.67	5.02E-04
monosaccharide biosynthesis	3	0.18	16.67	5.02E-04
pyruvate metabolism	3	0.18	16.67	5.02E-04
heme biosynthesis	6	1.08	5.56	6.26E-04
heme metabolism	6	1.08	5.56	6.26E-04
monosaccharide metabolism	6	1.08	5.56	6.26E-04
pigment biosynthesis	6	1.08	5.56	6.26E-04
pigment metabolism	6	1.08	5.56	6.26E-04
pyridine nucleotide biosynthesis	2	0.05	40	6.31E-04
vascular endothelial growth factor receptor signaling pathway	2	0.05	40	6.31E-04
heterocycle metabolism	7	1.51	4.64	6.70E-04
iron ion transport	7	1.51	4.64	6.70E-04
iron ion homeostasis	7	1.53	4.58	7.41E-04
transition metal ion homeostasis	7	1.53	4.58	7.41E-04
water-soluble vitamin metabolism	3	0.2	15	7.88E-04
secondary metabolism	6	1.13	5.31	8.03E-04
di-, tri-valent inorganic cation homeostasis	7	1.58	4.43	9.02E-04
metal ion homeostasis	7	1.58	4.43	9.02E-04
porphyrin biosynthesis	6	1.16	5.17	9.04E-04
porphyrin metabolism	6	1.16	5.17	9.04E-04
generation of precursor metabolites and energy	12	4.37	2.75	1.23E-03
carboxylic acid metabolism	8	2.16	3.7	1.28E-03

organic acid metabolism	8	2.16	3.7	1.28E-03
cofactor metabolism	9	2.69	3.35	1.31E-03
cation homeostasis	7	1.71	4.09	1.43E-03
cell ion homeostasis	7	1.73	4.05	1.55E-03
cofactor biosynthesis	8	2.24	3.57	1.60E-03
ion homeostasis	7	1.78	3.93	1.84E-03
glucose metabolism	5	0.9	5.56	1.85E-03
cell homeostasis	7	2.01	3.48	3.65E-03
vitamin metabolism	3	0.33	9.09	3.67E-03
hexose metabolism	5	1.08	4.63	4.11E-03
homeostasis	7	2.06	3.4	4.20E-03
main pathways of carbohydrate metabolism	5	1.16	4.31	5.51E-03
carbohydrate biosynthesis	3	0.38	7.89	5.63E-03
energy derivation by oxidation of organic compounds	5	1.18	4.24	6.04E-03
In molecular function				
fatty acid binding	4	0.15	26.67	4.79E-06
iron ion binding	9	2.19	4.11	2.92E-04
nicotinate phosphoribosyltransferase activity	2	0.02	100	3.03E-04
lipid binding	6	1.12	5.36	7.67E-04
catalytic activity	46	32.34	1.42	3.20E-03
acyl-CoA binding	2	0.1	20	3.41E-03
tetrapyrrole binding	5	1.05	4.76	3.59E-03
heme binding	5	1.05	4.76	3.59E-03
ligand-dependent nuclear receptor activity	4	0.78	5.13	7.06E-03
steroid hormone receptor activity	4	0.78	5.13	7.06E-03
cytoskeletal protein binding	4	0.8	5	7.88E-03
hydrolase activity, acting on carbon-nitrogen (but not peptide) bonds, in linear amides	2	0.15	13.33	8.26E-03
In cellular component				
heterotrimeric G-protein complex	2	0.15	13.33	8.83E-03
plasma membrane part	6	1.81	3.31	8.98E-03

segment S6

In biologicial process	O	E	R	P

one-carbon compound metabolism	5	0.99	5.05	2.48E-03
In molecular function				
oxidoreductase activity, acting on the aldehyde or oxo group of donors, NAD or NADP as acceptor	3	0.23	13.04	8.81E-04
catalase activity	2	0.05	40	1.11E-03
oxidoreductase activity, acting on the aldehyde or oxo group of donors	3	0.37	8.11	4.45E-03
In cellular component				
contractile fiber	2	0.04	50	9.09E-04
contractile fiber part	2	0.04	50	9.09E-04

segment S7

In biologicial process	O	E	R	P
pyridine nucleotide biosynthesis	2	0.08	25	1.78E-03
intracellular signaling cascade	16	7.6	2.11	3.44E-03
vitamin biosynthesis	2	0.13	15.38	5.11E-03
water-soluble vitamin biosynthesis	2	0.13	15.38	5.11E-03
neuropeptide signaling pathway	3	0.42	7.14	7.01E-03
membrane organization and biogenesis	2	0.17	11.76	9.94E-03
In molecular function				
transferase activity transferring pentosyl groups	3	0.44	6.82	8.38E-03
nicotinate phosphoribosyltransferase activity	2	0.04	50	8.54E-04
In cellular component				
nil	-	-	-	-

2.3.5 Cross-species Gene Set Enrichment Analysis (GSEA) indicates the segments S1-S5 to be multi-functional

An independent approach to confirm the identity of the intestine sections as small and large intestine is by taking the three gene set pools from S1-S5, S6, and S7 and comparing them by GSEA analysis against the whole transcriptomes of the mouse and human stomach, small intestine and large intestine (GDS182 and GSE2361, GEO database, NCBI). Results, summarized in Table 2.2, show segments S1-S5 closely resemble the small intestines of mouse and human with highly significant FDR values (less than 0.001). Segments S1-S5 show little resemblance to stomach (mouse FDR = 0.06; human FDR = 0.68) and no resemblance to the human cecum. Gene ontology analysis shows that majority of the genes corresponding to the leading edge of the GSEA curve are involved in the metabolism of lipid, fatty acid, cholesterol and glycerolipid, or involved in peptidase, oxidoreductase activity, reminiscent of the activities of the mammalian small intestine (data not shown). In addition, segments S1-S5 also produced significant FDR values for human colon and rectum, indicating that these segments are multi-functional.

Table 2.2: Comparison of transcriptome similarity of zebrafish intestinal segments and human/mouse intestines by GSEA analyses. FDR: false discovery rate ***highly significant; **significant; *marginally significant

Human/mouse intestines	S1-S5	S6	S7	GEO accession
Mouse stomach	0.06*	1.00	0.94	GDS182
Human stomach	0.68	0.63	0.55	GSE2361
Mouse small int.	≤0.001***	0.34	0.40	GDS182
Human small int.	≤0.001***	0.21*	0.86	GSE2361
Mouse cecum	0.17*	0.28*	0.21*	GDS182
Human cecum	1.00	≤0.001***	0.016**	GSE9254
Human colon	≤0.001***	1.00	0.90	GSE2361
Human sigmoid colon	≤0.001***	0.015**	0.038**	GSE9254
Human rectum	≤0.001***	≤0.001***	0.003***	GSE9254

In contrast to segments S1-S5, segment S6 closely resembles the cecum and rectum of the human large intestine (FDR ≤ 0.001), while segment S7 resembles human rectum only (FDR $= 0.003$). Gene ontology analysis shows that S6 resembles human cecum in glycolysis, oxidoreductase activity, metabolism of amino acid, amine derivative, organic acid, carboxylic acid and alcohol. While in S7, metabolism of membrane lipid was found to be enriched. Water retention is a commonly found function in mammalian large intestine and we found it also enriched in S6/S7 of zebrafish, where several aquaporin genes are highly expressed including aquaporins 1, 3 and 10. In particular, the aquaporin 3 has been known to be a key component of faecal dehydration in mammalian colon [111]. Interestingly, significant results are also found between S1-S5 and the human sigmoid colon and rectum, suggesting that the zebrafish segments S1-S5 may have broad functions.

In summary, GSEA analysis supports that segments S1-S5 of zebrafish intestine possess features of a mammalian small intestine, while segments S6 and S7 possess features of a mammalian large intestine (with S7 resembling rectum in particular).

2.3.6 Stomach-like functions of the intestine

A striking feature of the zebrafish anatomy is the absence of stomach [72, 113]. To understand whether the gut carries out a cryptic gastric function, we examined the zebrafish genes encoding enzymes including pepsin and some digestive proteases with implications of functions of a stomach. Mammalian pepsinogens are classified into three major groups and two minor groups [114, 115], however, a pepsinogen gene in zebrafish has never been reported. We searched for potential pepsinogen sequences in the zebrafish genome. First, we conducted a BLAST search against the Ensembl genome database (www.ensembl.org) using sequences of human PGC (PEPSINOGEN C) and PGA (PEPSINOGEN A) but did not detect any significant hits relevant to the pepsinogen gene. Then in a more specific TBLASTN search [116] using the pfam00026 domain that is well conserved across all aspartic proteases in vertebrates, we identified pepsinogen genes as well as some aspartic protease genes in human, mouse, Xenopus and Fugu fish, together with a few zebrafish aspartic protease genes and a putative gene sequence encoding a hypothetical protein NP956325.1. To determine whether these zebrafish sequences could represent a pepsinogen gene, relevant amino acid sequences were aligned, a phylogenetic tree was constructed using quartet puzzling algorithm implemented in the Tree-Puzzle

program [117], and the result was visualized by TreeViewX [118]. Our analysis suggests that the zebrafish has genes coding for rennin, nothepsin and several members of cathepsins (Fig.2.6). However, none of these zebrafish genes resemble the mammalian pepsinogen genes. The genome search results and phylogeny analysis results together suggest that the pepsinogen gene locus is not present in the zebrafish genome.

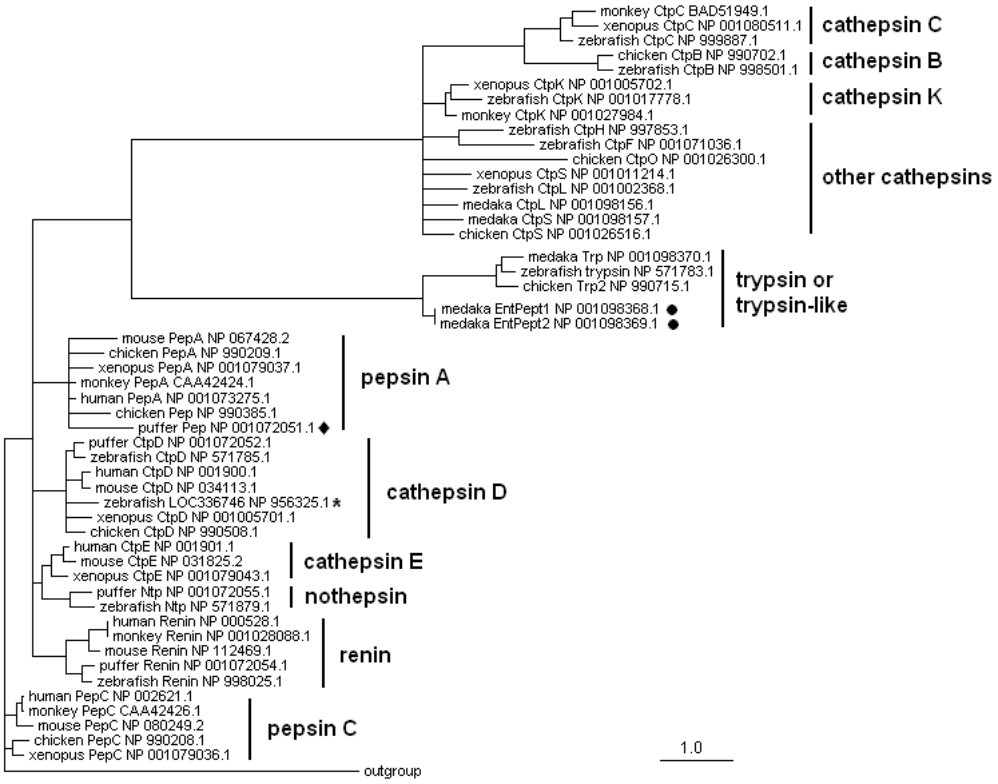

Figure 2.6: Phylogeny analysis of zebrafish genes encoding aspartic proteases The amino acid sequences of zebrafish digestive proteases were compared with those from other species, including mammals, amphibians and fishes. The parasite aspartic protease (Haemonchus contortus), CAA96571, is used as the outgroup. $\star$ indicates a candidate hypothetical protein product.

Whereas pepsinogen is not encoded in the zebrafish genome, other stomach markers may be expressed by the intestine. For example, *lipf* is a gastric lipase gene encoding an acidophilic lipase known to be secreted by mammalian gastric chief cells [119, 120]. Its expression in human is restricted to esophagus, stomach and several other tissues, but not in the intestine (Unigene's EST profile viewer, UniGene Hs.523130, NCBI database). In contrast, *lipf* is expressed in all seven segments of the zebrafish intestine and not restricted to any particular segment (Fig.2.4A).

2.3.7 Pathway analysis for zebrafish intestine

Genes up-regulated in different segments of zebrafish intestine are selected in the same way as previously described. Based on similarity of their transcriptomes, they are grouped into three groups, representing segments S1-S5, S6 and S7, respectively. Pathway analysis was done using the WebGestalt toolkit [93], with a cut-off p value of 0.01 and requirement that the number of observed genes is not less than 5.

Pathways that are significantly enriched in segments S1-S5 are shown in Fig.2.7. In total, there are 26 pathways found to be enriched with p value less than 0.01 and the number of observed genes not less than 5. One group of

pathways are involved in cellular signaling, including PPAR signaling, adipocytokine signaling, insulin signaling, VEGF signaling, GnRH signaling and so on. A second group of pathways are involved in metabolic processes, including metabolism of fatty acid, citrate, ether lipid, arachidonic acid, pyruvate and so on. A third group of pathways are involved in cell migration and proliferation, including tight junction, adherens junction, Wnt signaling, cell cycles and so on.

Enrichment of Wnt signaling is consistent with our current knowledge that Wnt signaling is a major pathway mediating the proliferation of intestinal epithelium [121, 122]. In line with this, cell cycle pathway is also enriched as the small intestinal epithelium are well known to be renewing at a fast pace [6, 123]. The enrichment of multiple metabolic pathways evidences the metabolic activities in the small intestine. While the enrichment of tight junction and adherens junction indicates the barrier function of the epithelial cells.

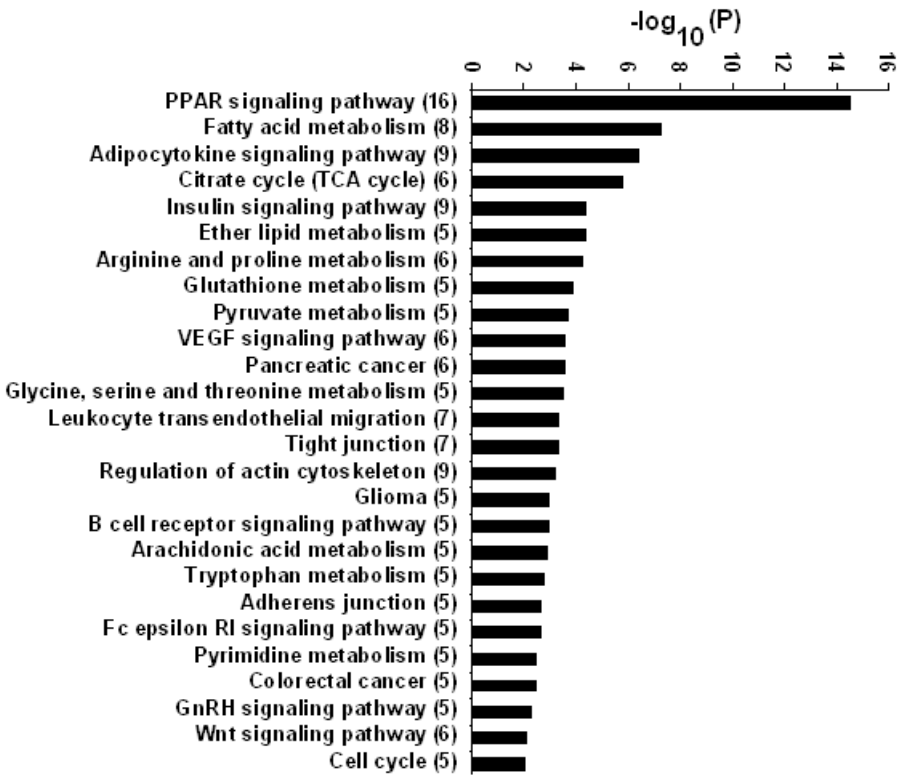

Figure 2.7: Enriched pathways in segments S1-S5 of zebrafish intestine. Pathway analysis was performed using the WebGestalt program. The significance was tested by a critical p value of 0.01 and requirement of at least 5 gene observed to be present in one pathway. Numbers in brackets indicate the number of genes that are observed to be present in each pathway. In total, there are 26 pathways found to be enriched in segments S1-S5 of zebrafish intestine. See the text for more information about the pathways.

Using the same settings as mentioned earlier, pathways that are significantly enriched in segment S6 are shown in Fig.2.8. In total, there are 22 pathways found to be enriched here. 14 of these pathways are enriched in S6, but not in S1-S5, including focal adhesion, long-term depression, long-term potentiation, apoptosis, axon guidance and so on. These differences are consistent with our previous gene overlapping analysis of their transcriptomes.

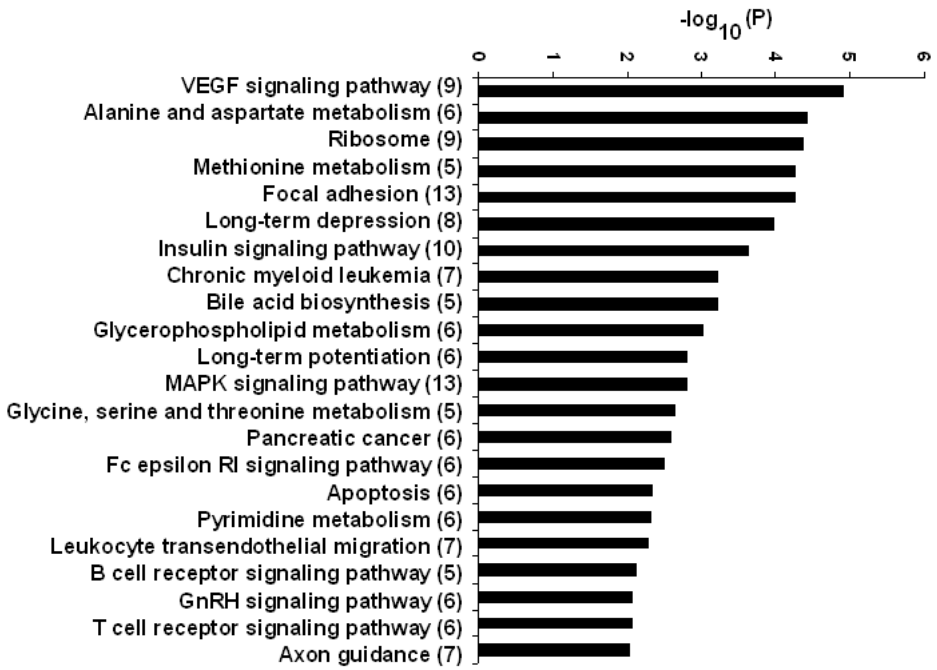

Figure 2.8: Statistically enriched pathways in segment S6 of zebrafish intestine. Pathway analysis was performed using the WebGestalt program. The significance was tested by a critical p value of 0.01 and requirement of at least 5 gene observed to be present in one pathway. Numbers in brackets indicate the number of genes that are observed to be present in each pathway. In total, there are 22 pathways found to be enriched in segment S6 of zebrafish intestine. See the text for more information about the pathways.

Similarly, 14 pathways are found to be enriched in segment S7 of zebrafish intestine. Results are shown in Fig.2.9. 10 of these pathways have been found to be also enriched in S6, including focal adhesion, apoptosis, axon guidance, longterm potentiation, GnRH signaling and so on. The newly emerged pathways in S7, compared with S6, include: Wnt signaling, regulation of actin cytoskeleton, tight junction and PPAR signaling. Thus the distal large intestine shows some functional difference from the proximal large intestine, though they share some similarity. The enriched pathways in S7 implicate an active process of cell renewal. On the one hand, MAPK signaling and Wnt signaling promote cell survival and proliferation; On the other hand, GnRH signaling counter-mediate cell proliferation and undesired cells may be removed through apoptosis.

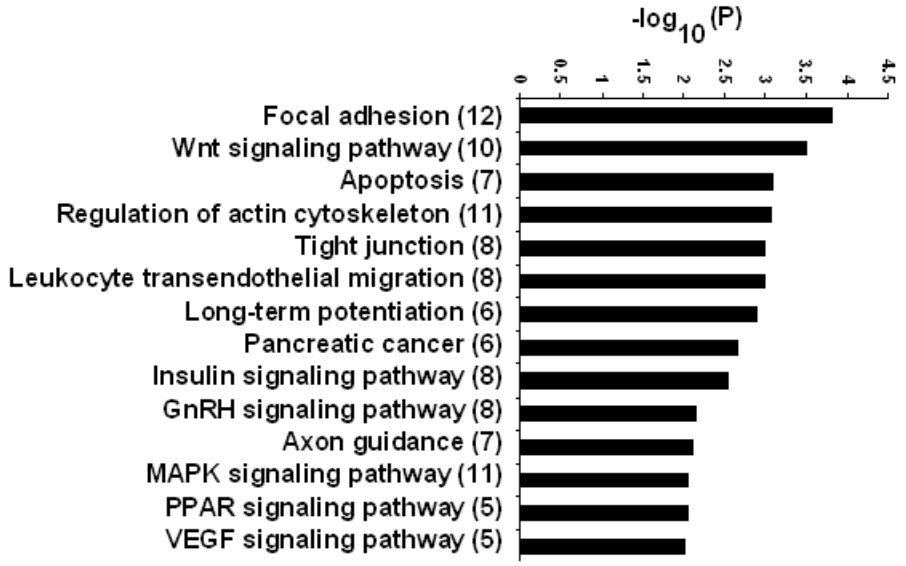

Figure 2.9: Statistically enriched pathways in segments S7 of zebrafish intestine.
Pathway analysis was performed using the WebGestalt program. The significance was tested by a critical p value of 0.01 and requirement of at least 5 gene observed to be present in one pathway. Numbers in brackets indicate the number of genes that are observed to be present in each pathway. In total, there are 14 pathways found to be enriched in segment S7 of zebrafish intestine. See the text for more information about the pathways.

2.3.8 Discussion

The results in this study document that the zebrafish intestine is regionally segmented into a small intestine and large intestine. This conclusion is supported by three lines of independent analysis of gene expression profiles from seven segments of the intestine. Clustering analysis reveals a general similarity between S1-S5 and differences between S6 and S7 and the degree of similarity is measured by the degree of overlap in gene sets expressed in neighboring segments. Second, we showed that well-known markers of the mammalian small and large intestine such as villin, intestinal fatty acid binding protein, and cofilin 1 are differentially expressed along the anterior-posterior axis. Finally by ontologies of genes expressed in the segments are consistent with small and large intestine function and confirmed by whole transcriptome comparisons with human and mouse small and large intestine gene sets. Based on these results, we suggest that the intestinal bulb, mid-intestine, and the anterior third of the caudal intestine corresponds to the small intestine of the mammalian gut while the remaining posterior portion of the caudal intestine corresponds to the large intestine terminating with the rectum.

In comparison with the mammalian intestine, the zebrafish intestine has a simple architecture with the intestinal lining folded into villar ridges rather

than distinct finger-shaped villi of the mammalian small intestine. In cross section, a ridge appears identical to a villus and thus may be an evolutionary precursor to discrete villi. In support of this idea, an intermediate stage (from D8-D8.5) in the morphogenesis of the chick intestine includes the initial formation of longitudinally oriented previllous ridges that buckle into a zig-zag pattern and eventually form villi in adult intestine. Thus, in birds, ridges are embryological precursors to villi [58].

In addition to the lack of well-defined villi, the zebrafish intestine lacks well-defined crypts [7, 71], infoldings of the intestinal surface where stem cells and proliferating cells are located. Intestinal crypts are normally found at the base of the villus or lining the colon of the large intestine. In the zebrafish intestine, mitosis is restricted to the base of the villar ridges ([79] and our unpublished data), suggesting that the crypts of Lieberkuhn are specializations of the mammalian intestine. This arrangement also raises questions about the dynamics of epithelial renewal because cell proliferation in the intestine is balanced by apoptosis at the villus tips. Location of apoptosis in the adult zebrafish intestine is rarely reported but we find most cell death occurs in the distal portion of the villar ridges and apoptosis is much more active when compared with mammalian intestines (our unpublished data). In contrast,

apoptosis in the embryonic and larval zebrafish intestine goes undetectable till morphogenesis completes [7, 71], while apoptosis occurs throughout the development of the mouse duodenum [124] but is reduced to a few cells per villus during adulthood [121].

Like many other fish including cyprinids and others [113], the zebrafish has evolved into a stomachless fish. The absence of a functional pepsinogen gene from the digestive tract is not unique to zebrafish but also occurs in medaka fish (*Oryzias latipes*) and other stomach-less fishes. Interestingly, the expression of pepsinogen gene in another stomchless fish, the puffer fish (*Takifugu rubipes*), is restricted to its skin tissue, adopting different functions [113]. Without a stomach, digestion and absorption must begin as early as possible in the limited length of the zebrafish digestive tract. Ingested food is temporarily stored in the rostral intestinal bulb that bulges like an elastic sac, where food starts to be broken down in the absence of a stomach [72] and the entire length of the intestine may serve to degrade food.

Based on analysis in larval zebrafish and other cyprinids, previous reports raised that the posterior zebrafish intestine may be analogous to the mammalian colon [48,49]. This has also been proposed in a recent study based on histological data and molecular markers [7]. Here our transcriptome data pro-

vide more solid evidence that this part of intestine in adult zebrafish resembles mammalian colon and rectum and moreover, segments S6 and S7 distinguish themselves from each other.

2.3.9 Conclusions

In the present study, the entire intestine of adult zebrafish was systematically examined at the levels of anatomy, histology and transcriptome. Despite the lack of crypts and evident structural distinction throughout most of the length of intestine, our genome-wide gene expression data have shown that the rostral, mid, and caudal portions of the zebrafish intestine have distinct functions analogous to the mammalian small and large intestine, respectively. Organization of ridge structures represents a unique feature of zebrafish intestine, though they produce similar cross sections to mammalian intestines. Evolutionary lack of stomach, crypts, Paneth cells and submucosal glands has shaped the zebrafish intestine into a simpler but unique organ in vertebrate intestinal biology. This scenario may represent an evolutionary primitive feature of the digestive tract, where functional regionalization precedes morphological regionalization in a low vertebrate.

Chapter 3

Regulation of cell fate and composition of the intestinal epithelium

3.1 Background

Notch signaling is one of the major regulators of epithelium proliferation in the intestine [79, 125, 126]. Notch signal is usually restricted to the basal region of crypts where epithelium proliferation is active. As the cells migrate out of the basal region, they lose the Notch signal and differentiation is initiated. The role of Notch, however, goes beyond regulation of proliferation. When Notch signaling is inhibited in mouse intestine, precursor cells are induced to differentiate precociously along with a shift in epithelium composition in favor of the secretory lineage [125, 126]. Here we would like to investigate whether similar roles of Notch are also played in zebrafish intestine, and further, what specific mesenchymal cells are responsible for this process in view of the close interaction between epithelial and mesenchymal cells. By inhibiting Notch signaling through a potent γ-secretase inhibitor, N-[N-(3,5-Difluorophenacetyl-L-alanyl)]-S-phenylglycine t-butyl ester (DAPT), we found a reduction in epithelium proliferation, accompanied by a cellular compositional shift toward the secretory lineage in zebrafish intestine. Histological analysis indicated a reduction in a distinct cohort of glycogen-rich intestinal subepithelial myofibroblasts (ISEMFs) along the villus axis in response to this compositional shift. In the mean time, BMP4 signaling, which is usually antagonized near basal region

of crypts [127], and the activity of GATA6, one of the master regulators of endodermal gene expression [128], were enhanced.

3.2 Materials and Methods

The Materials and Methods partially overlap with those in Chapter 2, including maintenance of zebrafish, tissue sectioning of zebrafish intestine and quantitative real-time PCR, which have been described in section 2.2 of Chapter 2. Here only the part of the Materials and Methods specific to Chapter 3 are described.

3.2.1 DAPT treatment of zebrafish

Adult male wild-type zebrafish were raised to about six months old according to established protocols [129], till treatment by DAPT (N-[N-(3,5-Difluorophenacetyl-l-alanyl]-S-phenylglycine-t-butyl ester; Sigma-Aldrich, USA). DAPT was prepared at 100 μM in 0.1% DMSO. The concentration was optimized from treatment at 50 and 100 μM, respectively, and the 100 μM produced more goblet cells than 50 μM. Control fish were incubated in 0.1% DMSO. They were euthanized after treatment for 24 hours for RNA analysis or 72 hours for histological analysis. BrdU was orally administered 20 min before euthanasia if

proliferation assay was to be carried out. The Tg(nkx2.2a-GFP) transgenic zebrafish is a kind gift from Dr. Joan K Heath's laboratory, Ludwig Institute for Cancer Research, Australia.

3.2.2 Alcian blue and Periodic Acid in Schiff's reagent staining

The paraformaldehyde-fixed, paraffin-embedded tissue sections were stained according to the manufacturer's protocol coming with the kit (cat# ss020, BioGenex, San Ramon, USA). Briefly, the slides were dewaxed in HistoClearII for 5 min twice, rinsed in phosphate-buffered saline and incubated in Alcian blue solution for 20 min. They were rinsed in tap water before they were incubated in periodic acid and Schiff's reagent for 5 min each, then subjected to the reducing reagent for another 5 min, rinsed between these steps. They were counterstained by Mayer's hematoxylin for 1 min and rinsed in running tap water for 5 min. The slides were then dehydrated in 75%, 95%, 100% ethanol, respectively, cleared in HistoClearII and finally mounted in DePex mounting medium with cover slips for microscopy on an Zeiss Axiovert system.

3.2.3 Whole mount *in situ* hybridization

Whole-mount in situ hybridization using digoxigenin (DIG)-labeled riboprobes was carried out as previously described [130]. Briefly, the cDNA clones were linearized with a selected restriction enzyme, followed by in vitro transcription for the antisense RNA probe. The samples were fixed with 4% paraformaldehyde/ phosphate-buffered saline, hybridized with a DIG labeled RNA probe in a hybridization buffer (50% formamide, 5XSSC, 50 μg/ml tRNA and 0.1% Tween 20) at 70^oC, followed by incubation with anti-DIG antibody conjugated with alkaline phosphatase and by staining with the substrates, NBT (nitro blue tetrazolium) and BCIP (5-bromo, 4-chloro, 3-indolil phosphate), to produce purple, insoluble precipitates.

3.2.4 Cryosection of zebrafish intestine

The samples after whole mount *in situ* hybridization were placed on the frozen surface of a layer of tissue freezing medium (Reichert-Jung, Germany) on the pre-chilled tissue holder, and coated with a drop of cryostat freezing medium and then immersed in liquid nitrogen until thoroughly chilled. The frozen block was placed in the cryostat chamber (Reichert-Jung, Germany) for 30 min to 1 hour to equilibrate with chamber temperature of -30^oC. Samples were

sectioned at 20 μm thickness and collected onto Superfrost plus slides (Fisher, USA). The slides were completely dried on a 42^oC heating block overnight. The sections were embedded in several drops of glycerol/phosphate-buffered saline (1:1) for photo-taking on a Zeiss Axiovert imaging system (Zeiss, Germnay).

3.2.5 Immunohistochemistry

BrdU assay was carried out according to the manufacturer's protocol coming with the kit (cat# 2760, Chemicon International, USA). Briefly, the paraformaldehyde-fixed, paraffin-embedded tissue sections were dewaxed in HistoClearII 5 min for twice, rehydrated in 100%, 90%, 80% and 70% ethanol, respectively. They were quenched in 3% hydrogen peroxide, incubated in 1X trypsin solution, then incubated in Denaturing solution. Next they were blocked in Blocking solution before they were incubated in Detector antibody and Streptavidin-horse radish peroxidase Conjugate, respectively. Diaminobenzidine substrate mixed in Substrate Reaction Buffer was added to the slides to produce the dark brown color before the slides were counterstained by hematoxylin. Finally, the slides were dehydrated and mounted in DePex mounting medium with cover slips for microsopcy on a Zeiss Axiovert imaging system (Zeiss, Germany).

3.3 Results

3.3.1 Inhibition of Notch signaling in larval zebrafish intestine

Effect of inhibition of Notch signaling by DAPT in larval zebrafish was investigated by utilizing Tg(nkx2.2a-GFP) zebrafish, where specific expression of nkx2.2a in enteroendocrine cells was indicated by GFP fluorescence. 14 dpf Tg(nkx2.2a-GFP) larval fish were incubated in aquarial water containing 100 μM DAPT for 24 hours (the duration of treatment was similar to previous studies using DAPT for zebrafish larvae [131]). The larvae were immobilized by 2-phenoxyethanol for imaging on a Zeiss Aviovert system. As shown in Fig.3.1A and B, the population of nkx2.2a-expressing enteroendocrine cells in larval fish intestine increased after treatment, consistent with previous reports of an increase in the pan-secretory cell lineages after inhibition of Notch signaling [125, 126]. Thus the DAPT treatment of zebrafish proves to be effective in perturbing Notch signaling in larval intestine.

3.3.2 Verification of inhibition of Notch signaling in adult zebrafish intestine

Adult zebrafish (6-month-old) were immersed in aquarium water containing 100 μM DAPT for 24 hours and then euthanized for assays. To verify the effect of inhibition of Notch signaling, RNA was extracted from the zebrafish intestines and quantitative RT-PCR on several indicator genes was conducted. Zebrafish atonal homolog gene *zath1* (orthologous to *Math1* in mouse and *HATH1* in human), the expression of which is normally suppressed by Notch signaling [126], were found to be up-regulated upon inhibition of Notch signaling (Fig.3.1 C). Another bHLH transcription factor, *hes1*, which has been known to be a target gene of Notch signaling [126], was down-regulated as expected (Fig.3.1 D). These results proved the effectiveness of inhibition of Notch signaling in adult zebrafish intestine. In addition, we noticed that the downstream effector of Wnt signaling, *tcf4*, was also down-regulated (Fig.3.1E), consistent with the reduction of the progenitor cells as observed below.

3.3.3 Reduction in the pool of intestinal progenitor cells upon inhibition of Notch

BrdU was orally administered 15 min before euthanasia of the fish and the intestines were isolated for paraffin sectioning. Immunohistochemistry with antibody against BrdU showed a significant reduction in the population of intestinal progenitor cells upon inhibition of Notch signaling (Fig.3.2A-C). By measurement of over 600 villi, we found that the number of BrdU+ progenitor cells in the intestinal epithelium after Notch inhibition is about one third of those in the control (Fig.3.2C). The expression of the cell cycle check point gene *p21WAF1/cip1* [132, 133] was also up-regulated upon inactivation of Notch in zebrafish intestine (Fig.3.2D). This explains the reduction in the pool of proliferative progenitor cells as more cells are arrested in cell division. This is also consistent with previous reports that CDK inhibitors p27Kip1 and p57Kip2 are derepressed upon inactivation of Notch in larval zebrafish [134],

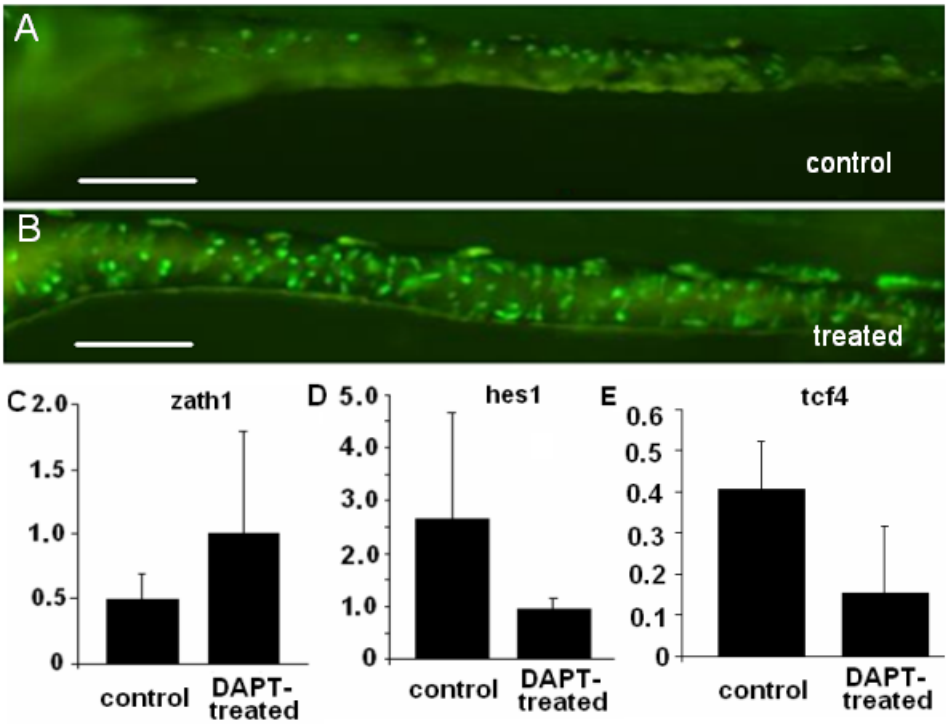

Figure 3.1: Pharmocological inhibition of Notch signaling by DAPT treatment (A and B) Fluorescent imaging of the intestines of the 14 dpf Tg(nkx2.2a:GFP) larval fish. The *nkx2.2a*-expressing enteroendocrine cells are dispersed along the intestine in the control fish (A), and their population is increased after pharmocological inhibition of Notch signaling by DAPT-treatment (B). (C-E) qRT-PCR results for expression of *zath1*, *hes1* and *tcf4*, respectively. mRNAs were extracted from the adult intestines using trizol (Sigma, USA). Suppression of *zath1* expression by Notch is relieved after DAPT-treatment (C); while expression of *hes1* is up-regulated (D). In the mean time, expression of *tcf4* is down-regulated after DAPT-treatment. Scale bar: 100 μm

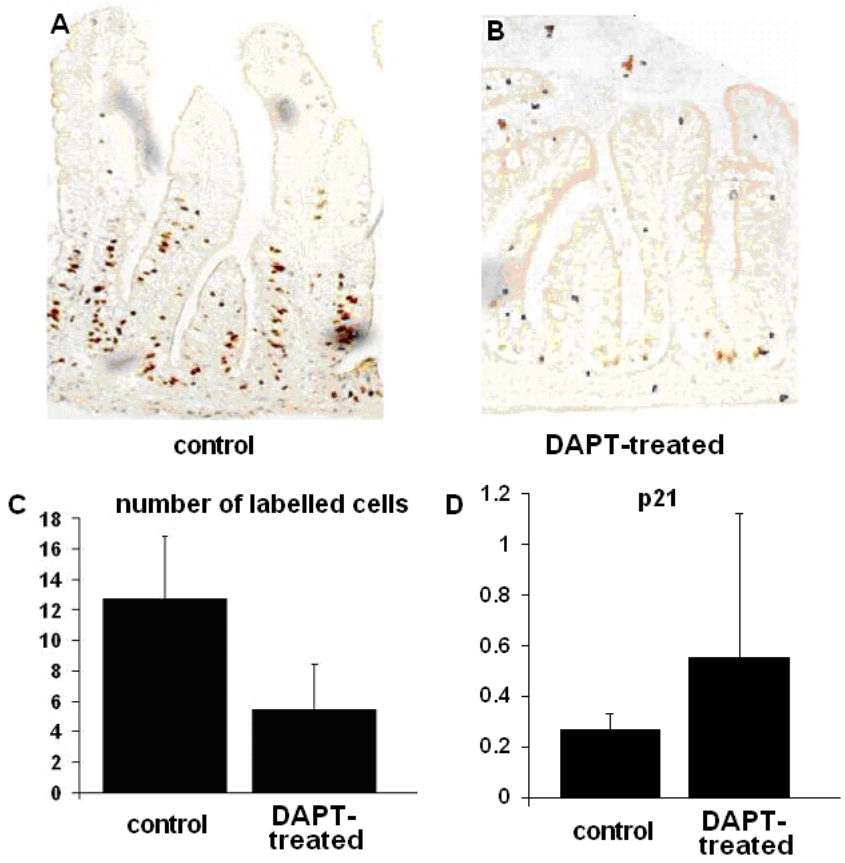

Figure 3.2: Changes in BrdU-labelled cells and expression of p21 upon inhibition of Notch
(A and B) BrdU assay on cross sections of adult fish intestines. BrdU-retaining cells are stained dark brown. There is an evident decrease in BrdU-retaining cells upon inhibition of Notch by DAPT treatment (B) when compared with control (A). (C) Counting of BrdU-labelled cells per villus on cross sections of adult intestines. A decrease in the cell number is observed after DAPT-treatment. (D) Changes in the expression of *p21* by qRT-PCR with mRNA extracted from adult intestines. Expression of this gene is up-regulated upon DAPT-treatment.

3.3.4 Increase of secretory lineages after inhibition of Notch signaling

Quantitative RT-PCR and histological examinations were conducted to evaluate the changes in epithelial cell differentiation toward different lineages. Expression of *zath1*, a known bHLH transcription factors favoring pan-secretory lineage differentiation in intestinal epithelium of larval zebrafish [79], was up-regulated in adult intestine upon inhibition of Notch signaling (Fig.3.1C).

Potential changes in goblet cells were investigated by histology. After inhibition of Notch signaling, there was an increase in the population of goblet cells as well as a more frequent presence of mature goblet cells in the inter-villi pockets, where precursor cells normally reside (Fig.3.3A and B). The number of mature goblet cells was further counted on each histological section after staining of both acidic and neutral mucopolysaccharides richly present in goblet cells with alcian blue and periodic acid/schiff's reagent. It was found that the population of mature goblet cells increased about two folds due to inhibition of Notch signaling (Fig.3.3C). In the mean time, generation of another secretory lineage, the enteroendocrine cells, was also up-regulated as indicated by expression of the marker gene, *ngn3*, which functions downstream of the *zath1*-initiated enteroendocrine lineage differentiation cascade [135] (Fig.3.3D).

While the increased differentiation along the secretory lineages was evidenced by up-regulation of *zath1* and *ngn3* (Fig.3.1C and Fig.3.3D), differentiation of enterocytes was found to decrease as shown by *in situ* hybridization of *fabp2* gene (Fig.3.3E and F), which was a marker for differentiated enterocytes. As shown in Fig.3.3E, in the intestines of control fish, *fabp2* was abundantly expressed in enterocytes along the villus axis except the inter-villi pocket, where most proliferative and undifferentiated progenitor cells resided. In the intestines of DAPT-treated fish, *fabp2* was expressed along the villus axis at a lower level and had less number of differentiated enterocytes. This suggests that more progenitors differentiated toward the secretory lineage at the cost of the absorptive lineage.

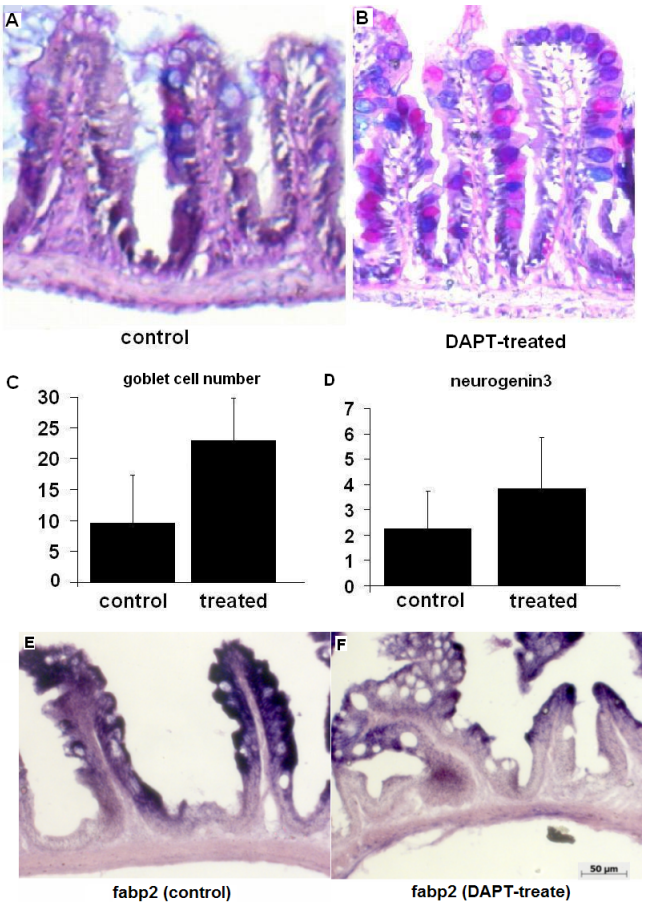

Figure 3.3: Changes in different cell lineages in zebrafish intestinal epithelia upon inhibition of Notch
(A and B) Alcian blue and Periodic Acid/Schiff's staining of goblet cells in a cross-section of the adult zebrafish intestines in control (A) and DAPT-treated (B) fish. Increase in goblet cell maturation is observed after inhibition of Notch signaling (B). Precocious differentiation of goblet cells are often seen in the basal regions of inter-villi pockets where precursor cells normally reside. (C) Changes in the number of goblet cells upon inhibition of Notch signaling. (D) Changes in expression of *ngn3* by qRT-PCR upon inhibition of Notch signaling. (E and F) *fabp2* expression in zebrafish intestine as detected by *in situ* hybridization on cross sections of intestine in control (E) and DAPT-treated zebrafish (F).

3.3.5 Enhanced expression of *gata6* upon inhibition of Notch in the intestine

gata6 is one of the major GATA transcription factors, along with gata-4 and gata-5, in the maintenance of the endodermal gene expression from the early developmental stages to adulthood [108] and *gata6* has been suggested as a suppressor gene of brain tumor [136, 137, 138]. *In situ* hybridization showed a moderate increase in the expression of *gata6* along the villus after the DAPT treatment (Fig.3.4A and B). In accordance, quantitative RT-PCR also detected an increased expression of *gata6* in the intestines of adult zebrafish upon treatment with DAPT (Fig.3.4C). The expression of *gata6* was seen in the differentiated epithelial cells lining the middle-to-upper part of villi (Fig.3.4A). Toward the inter-villi pocket, where most proliferating cells were residing, its expression appeared to be absent in the control fish (Fig.3.4A), but present in the DAPT-treated fish (Fig.3.4B, arrow heads). The complementary localization of *gata6*+ differentiated epithelium and proliferating progenitors shows existence of the compartment of cell differentiation (Fig.3.4A, region 1) and the compartments of cell proliferation (Fig.3.4A, region 2), similar to that in mammalian intestines where cells proliferate in crypts and differentiate along the villi [42].

3.3.6 Enhanced activity of BMP signaling due to inhibition of Notch signaling

The BMP signal has been known to be crucial for mediating epithelium-mesenchyme interaction in the intestine [42, 139] and *BMP4* is transcriptionally activated by *GATA6* [140]. In order to examine whether BMP signaling is enhanced upon inhibition of Notch, quantitative RT-PCR and *in situ* hybridization were conducted for zebrafish intestine. There was an induced up-regulation in the expression of *smad1* and *smad4*, the down-stream effectors of BMP signaling, as determined by quantitative RT-PCR (Fig.3.5A and B). These results supported an enhanced activity of BMP signaling together with *gata6*. To identify the link between BMP signaling and *gata6* activity in the intestine, we examined the promoter sequences of some relevant genes in search of the conserved GATA-binding motifs, (A/T)GATA(A/G) [141]. For example, *bmp4* and *bmp7* are known ligands that may initiate the BMP signaling cascade [142, 143]. As we have found, there are several conserved GATA binding sites in the promoter regions of *bmp4* and *bmp7* (Fig.3.5). In addition, the same binding motifs have also been found in the promoter regions of another two ligands, *tgfb2* and *tgfb3*, which are members of the transforming growth factor beta subfamily that mediate the signaling cascade through smad2/3/4

(Fig.3.5). Thus GATA transcription factors appear to positively regulate the activities of BMP signaling through their ligand expression in the intestine and we expect to see enhanced BMP signaling after DAPT-treatment.

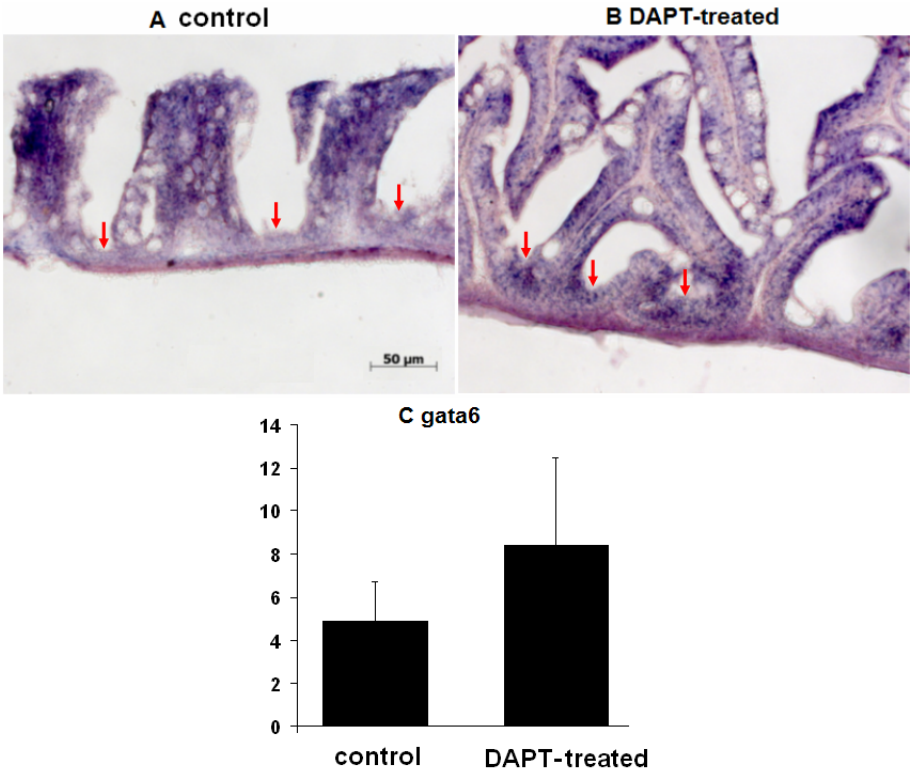

Figure 3.4: Up-regulation of *gata6* expression upon inhibition of Notch (A and B) *In situ* hybridization for *gata6* gene on cross sections of adult intestines. Transcripts of *gata6* are present along the villus of both control intestine (A) and DAPT-treated intestine (B). This gene is abundantly expressed in the differentiated epithelia along the villi, though its expression level is higher in the upper part of villi. In the inter-villi pockets, the transcripts are largely absent in the control intestine (A) but detected at a higher level in DAPT-treated intestine (B),as indicated by arrows. (C) qRT-PCR results for *gata6* expression. mRNAs were extracted in the intestines of control fish or DAPT-treated fish. Expression level of *gata6* is moderately higher upon inhibition of Notch by DAPT.

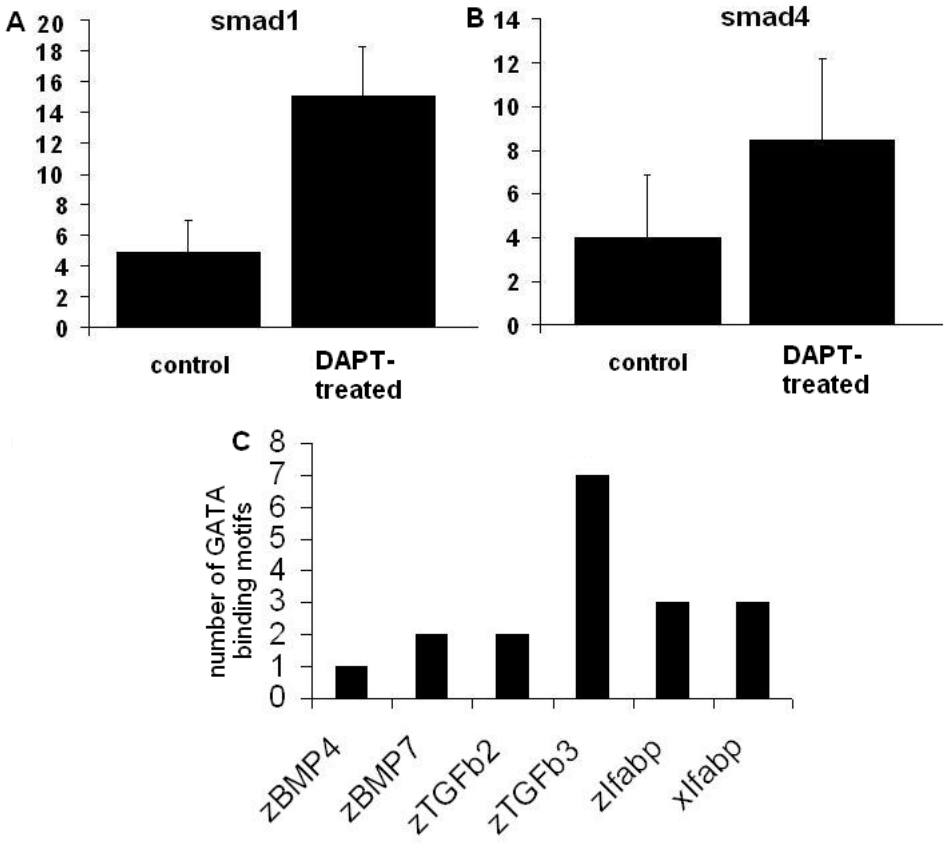

Figure 3.5: BMP signaling and GATA regulation
(A) qRT-PCR for *smad1*. mRNAs were extracted from adult intestines of control and DAPT-treated fish, respectively. The expression of *smad1* is up-regulated upon inhibition of Notch by DAPT treatment. (B) qRT-PCR for *smad4*. mRNAs were extracted from adult intestines of control and DAPT-treated fish, respectively. The expression of *smad4* is also up-regulated upon inhibition of Notch by DAPT treatment. (C) Identification of GATA binding motifs. The GATA binding motifs were analysed in the promoter regions of several genes (about 3kb upstream of trasncription start sites) and the number of their occurrences are shown.

3.3.7 Suppression of glycogen-rich intestinal subepithelial myofibroblasts (ISEMFs) along the villus axis due to inhibition of Notch signaling

Periodic acid/Schiffs reagent staining of paraffin-embedded, paraformaldehyde fixed sections showed that the glycogen-rich intestinal subepithelial myofibroblasts (ISEMFs) were present along the whole villus axis in the intestines of control fish (Fig.3.6A). These cells were located closely beneath the epithelial cells and they were featured by presence of abundant glycogen in the cytoplasm. Inhibition of Notch signaling caused a decrease in the number of these cells and their localization were restricted only to the basal region of the villus axis (Fig.3.6B). The goblet cells were stained blue (acidic mucopolysaccharides by alcian blue) or magenta (neutral mucopolysaccharides by periodic acid/schiff's). Glycogen-rich ISEMFs were also stained magenta, but these cells were distinguished by their localization beneath the single-celled epithelial layer and their glycogen-rich granules (Fig.3.6A and B, arrows in insets), which were smaller in size than the huge secretory vesicles in goblet cells - those vesicles were typically residing near the apical membranes of cells and identifiable by openings toward the intestinal lumen. In the mean time, it was observed that the glycogen-rich ISEMFs were mainly restricted to the lower

half of the villus axis after inhibition of Notch signaling (Fig.3.6C). The induced reduction in the population of glycogen-rich ISEMFs may imply the involvement of this population in mediating differentiation of progenitor cells toward the secretory lineage, in view of the multitude of secreted signaling molecules by the ISEMFs such as hepatocyte growth factor [144], cytokines (especially interleukins), stem cell factor, vascular endothelial growth factor [145] and so on.

The role of glycogen+ ISEMFs in the whole picture of intestinal epithelium homeostasis is sketched in Fig.3.7. Yet so far it is not clear what secreted molecules are important for the secretory lineage development and whether they act upstream or downstream of, or even in parallel to *zath1*.

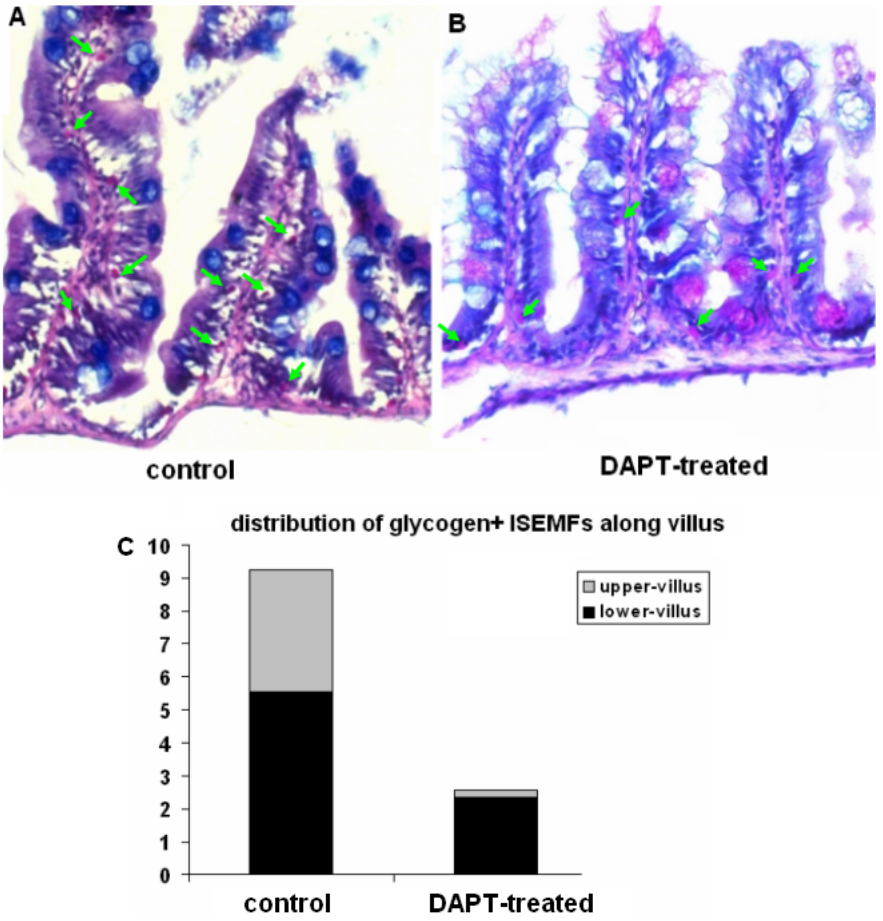

Figure 3.6: Reduction in glycogen-rich ISEMFs with increased goblet population
(A and B) Alcian blue and Periodic Acid/Schiff's staining on cross sections of adult intestine. Acidic mucin-secreting goblet cells are stained blue and neutral mucin-secreting goblet cells are stained purple. Granules of glycogen are stained purple. The glycogen+ ISEMFs are distributed along the whole villous axis in control intestine (A), but they are restricted to the lower half of villi in DAPT-treated intestine (B). (C) Counting of glycogen+ ISEMFs in over 100 villi on cross sections of adult intestines. Compared with control, there is a decrease in the number of glycogen+ ISEMFs, and majority of the cells are restricted in the lower half of villi after inhibition of Notch signaling.

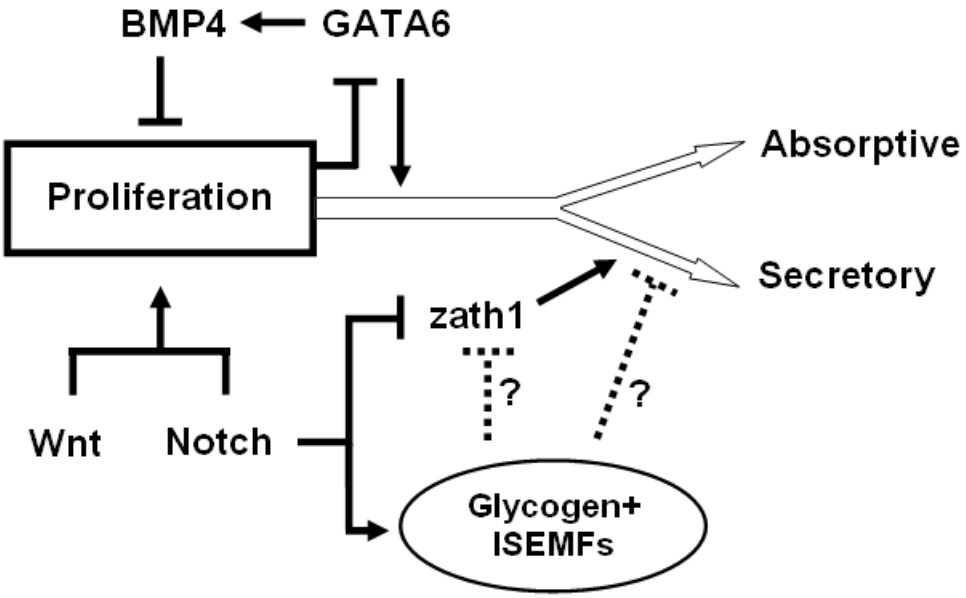

Figure 3.7: Potential role of the glycogen-rich ISEMFs in mediating the generation of goblet cells
In view of the negative correlation between glycogen-rich ISEMFs and goblet cell population, these cells potentially interact with the development of goblet cells through secreted molecules in a paracrine manner and it could be either zath1-dependent or zath1-independent. The potential signaling molecules secreted by the ISEMFs, however, remain unknown.

3.4 Discussion

3.4.1 Notch signaling and binary lineage allocation

The requirement of Notch signal in epithelial cell proliferation of mouse intestine [125] and its role in goblet cell differentiation [126] have been reported. Here, the effects of Notch signal on proliferation and secretory lineage differentiation are further confirmed in adult zebrafish intestine. Notch signaling has been shown to regulate a broad range of cellular events from early developmental stages till adulthood [146]. In the intestines, Notch has been shown to play a role in bipotential cell fate decisions between absorptive lineage and secretory lineage [79, 125]. Inhibition of Notch by DAPT could influence the cell fate decisions in favor of the secretory lineage by producing more goblet and enteroendocrine cells in the intestines. In consistence with previous studies [125, 126], our work showed increased goblet cell differentiation caused by inhibition of Notch signal in zebrafish intestine. Pan-secretory lineage differentiation was increased by inhibition of Notch as evident from increased expression of *zath1* (Fig.3.1); Enteroendocrine lineage differentiation was also enhanced as indicated by the increased *ngn3* expression (Fig.3.3). The increased population of goblet cells was confirmed with alcian blue staining of

histological sections (Fig.3.3).

As the intestinal epithelium is constantly renewed, changes in lineage allocation process will be manifested by changes in the cellular composition of the differentiated epithelial tissue. Appropriate lineage allocation is thus pivotal to the maintenance of tissue homeostasis. By inhibiting Notch signaling, one of the most important signals involved in this process, we were able to show that the reduction in the pool of the multipotent progenitor cells incurred a shift in the lineage allocation process, where the secretory lineage took a higher priority over the absorptive cells (Fig.3.2, Fig.3.3). In another study where beta-catenin was knocked out in mouse intestine, the proliferative crypt progenitor cells were almost depleted, but the population of goblet cells remained almost intact despite the impaired generation of absorptive cells and shrinking in villus size [121]. These results suggest a potentially important concept: a higher priority for generation of secretory cells may be used as a countermeasure when the pool of multipotent progenitors was reduced. In contrast, studies that allowed an increase in the pool of progenitors by knockout of the BMP signaling receptor, *Bmpr1a*, revealed a significant increase in the absorptive population (as manifested by the villus size), whereas the secretory population remained largely unchanged [147]. Together, these results reveal

the prioritizing nature of the lineage allocation process where the secretory lineage often takes higher priority.

Based on the evidence above, together with our own results, we would like to hypothesize the existence of a prioritized lineage allocation mechanism in the intestinal epithelium. Upon perturbations that may disrupt the homeostatic cell type composition, the secretory lineage would tend to take higher priority over that of the absorptive lineage, in terms of cell production.

3.4.2 Involvement of a distinct cohort of glycogen-rich ISEMFs in cell lineage allocation

As our BrdU assay showed, the size of the proliferative compartment was significantly reduced upon inhibition of Notch signaling (Fig.3.2). This may force the immature progenitors to leave this compartment earlier than usual. The prioritizing lineage allocation mechanism thus probably extends beyond the proliferative compartment and allows other signals to gain a chance to influence this allocation procedure. As discussed below, a distinct cohort of glycogen-rich ISEMFs appear to be specifically involved in this process.

The epithelium-mesenchyme interaction has been known to be essential for maintaining homeostasis of epithelial tissues in the intestine [6]. The BMP4

pathway represents one of the major communicating channels between the two tiers of cells with the ligands expressed in epithelia while the receptors expressed in the underlying mesenchyme [42, 6]. Here we showed that the activity of BMP signaling was enhanced after inhibition of Notch signal and this was accompanied by a reduction in cell number and retractive redistribution of glycogen-rich ISEMFs (Fig.3.6). ISEMFs are important for the organogenesis of the intestine, and a collection of growth factors and cytokines secreted by these cells promote epithelial restitution and proliferation [148]. BMP signaling, however, presents a reversed gradient against Notch and Wnt signaling along the villus axis (Fig.3.1 panel E) and suppression of it also inhibited the epithelial cell differentiation [127, 139, 149]. The induced changes in the number and distribution of the glycogen-rich ISEMFs by inhibition of Notch (Fig.3.6) indicate that they may mediate the equilibrium between proliferation and differentiation of the epithelia by bridging the cross-talk signals between the epithelia and the mesenchyme. The retraction in the distribution of the glycogen-rich ISEMFs along the villus axis may cause a redistribution of signals for the prioritizing lineage allocation procedure and shift in favor of the secretory cells.

3.4.3 Preferable targeting of secretory cells in cancer

The prioritizing nature of the lineage allocation mechanism thus appears to maintain the secretory cells with higher priority. During hyper-proliferation, the secretory population was best maintained whereas the absorptive population was over generated [147]; During hypo-proliferation when the pool of progenitor cells were reduced, the secretory population would be generated at the cost of absorptive cells, as documented in this study and other studies [125, 126].

Is there a situation where homeostasis of the secretory population is disrupted with higher priority even in the presence of a sufficiently large pool of progenitor cells? The positive answer comes from cancer studies. It has been well documented that there is a significant reduction in mucin-secreting goblet cells during development of colorectal cancer as only very few goblet cells are present in colorectal carcinoma specimens [150, 151, 152, 153, 154]. As discussed earlier, the Notch and Wnt/beta-catenin signaling pathways are positively cooperating with each other under normal physiology. During development of colorectal cancer where Wnt/beta-catenin signaling is frequently over-activated [155, 156], one might anticipate that the secretory population would increase. This is, however, not true. The lineage allocation process, in the case

of cancer, is distorted in such a way that the absorptive cells are overwhelmingly generated, whereas the secretory cells are greatly reduced [157, 151], probably through down-regulation of HATH1 (or Math1 in mouse).

3.4.4 Cooperative BMP and gata6 activities in epithelial differentiation

It has been previously shown that inhibition of Notch is potent to induce differentiation of proliferating cells both in normal intestinal tissue and adenomas [125, 126], but the downstream events are not well understood. Here we have shown that the glycogen-rich ISEMFs may be involved in this process (Fig.3.6). As noticed, the increased differentiation toward secretory lineage was accompanied by a reduction in epithelium proliferation and an increased expression of *gata6*, the master GATA factor mediating endodermal gene expressions. This suggests a suppressive role of *gata6* against epithelium proliferation in the intestine, in agreement with its role as a tumor suppressor in astrocytoma, where *gata6* expression was turned off during development of astrocytoma [136]. In the intestine, however, *gata6* suppresses epithelium proliferation by turning on cell differentiation allowing expression of a group of endodermal genes.

One of the suggested *gata6* target genes, *fabp2*, is highly expressed in enterocytes [108]. The zebrafish *fabp2* gene is located on chromosome 1 consisting of 4 exons. Our analysis shows that the conserved GATA binding sites (A/T)GATA(A/G)(ref. [141]) are present in the promoter region of *fabp2* gene in zebrafish (Ensembl genome database Zv7 data not shown). Notably, the GATA binding sites are also present in the promoter region of *fabp2* gene in other species, including mouse (3 GATA binding sites, data not shown) and Xenopus (3 GATA binding sites, Ref. [108]) among others, implying that this regulatory mechanism is well conserved across species.

The link between GATA transcription and BMP signaling is known. For example, transcriptional activation of BMP4 by GATA6 has been reported during mammalian organogenesis [140] and cardiomyocyte maturation [158]. In the adult intestine, BMP signals appear to cooperate with *gata6* mediating proliferation and differentiation of the epithelium, as suggested by our results (Fig.3.5, Fig.3.4). BMP signals are known to be an important channel for epithelium-mesenchyme crosstalk [159] and their activities are usually suppressed toward the basal crypts [127]. But BMP signaling is active in differentiated epithelium, where removal of BMP signaling would impair the differentiation of the intestinal secretory lineage [147]. This agrees with our

finding that BMP signaling becomes more active when secretory lineage differentiation is enhanced. In addition, our analysis identified GATA binding sites in the promoter regions of BMP4, BMP7, TGFb2 and TGFb3 (based on Ensembl genome database Zv7, Fig.3.4). This may explain the enhanced BMP signaling accompanying the increased *gata6* expression level in the intestine.

3.5 Conclusion

This study has shown that inhibition of Notch signal reduces epithelium proliferation and in the mean time, shifts the lineage allocation in favor of the secretory lineage. The Notch-mediated secretory lineage allocation procedure correlates the decrease of glycogen-rich ISEMFs. The secretory lineage is maintained with priority during normal physiology, but these cells will be reduced during cancer development.

Chapter 4

Regeneration of zebrafish intestine following whole body gamma-radiation

4.1 Introduction

The small intestine has been a nice model for the study of epithelium renewal, stem cell function and tissue regeneration. The mammalian intestinal epithelium is organized into hierarchical cell lineages derived from a small number of stem cells, which are located near the bottom of the crypts (about four or five cell position from the very bottom) [160]. Stem cells produce progenitor cells that undergo rapid clonal expansion, migrate out of the crypt and differentiate into absorptive cells, goblet cells, Paneth cells and enteroendocrine cells [18, 6]. The only exception is the Paneth cell population, which remain in the crypt during its whole life span.

Due to the persistent presence of stem cells, potential gene mutations or chromosomal aberrations to the stem cell genome may yield a long term effect on the epithelium renewal process, while a second or third mutation will significantly increase the frequency of carcinogenesis in the intestinal tract [161]. This explains one of the common scenarios where colorectal cancer occurs, with transformed cells proliferating in a uncontrolled manner, disrupting the normal epithelium renewal mechanism that is maintained during normal physiology. In addition, it is worth mentioning that the intestinal stem cells are very sensitive to radiation [80], which raises concerns over radiotherapy appli-

cations.

Current clinical management of colorectal cancers includes three major components: surgery, radiotherapy and chemotherapy. The effectiveness of these three components has been recognized during the past three to four decades, though wide variations in clinical outcomes still exist around the world [162, 163]. Part of the variations come from our limited understanding about the effects of radiation on tissue renewal and regeneration, such as the responsive nature of the regeneration process.

To understand the stem cell function, epithelium regeneration and radiation response, mammalian models have been used during the past few decades [9, 6, 26, 80]. But in recent years, zebrafish has been rising as a convenient model for the same purposes. In terms of intestine, this cryptless vertebrate shares several levels of similarity with the traditional mammalian models. At tissue level, zebrafish intestine features ridge-like in-foldings, which produce villus structures on two dimensional sections that appear similar to those of mammalian intestines. At cell level, absorptive cells, goblet cells and enteroendocrine cells are all present. At molecular level, the well known intestinal marker genes like intestine specific fatty acid binding proteins, villin and apolipoproteins are all conserved in zebrafish. Metabolic pathways of fatty

acids, lipids and vitamins that are active in mammalian intestines are similarly active in zebrafish intestine (refer to Chapter 2).

In comparison with mammalian models, which have a more limited threshold to whole body radiation [164, 165], zebrafish represents a vertebrate model that shows better tolerance to whole body radiation (to be shown below). This feature of zebrafish will allow us to study the effects of radiation on the whole intestinal tract from low dose to high dose radiation. By investigating the regeneration process over a widened range of radiation doses, knowledge may be gained to understand how the zebrafish intestine manages to survive the high dose radiation where mammalian intestines can not. To illustrate such potential applications, we have characterized the regeneration process in predefined regions of zebrafish intestine following high dose whole body radiation (16 gray). Some interesting observations are made, which have not been reported before.

4.2 Methods

4.2.1 Experiment setup for radiation

Adult zebrafish were subject to 16 gray whole body radiation (WBR) in a Gamma Chamber 2000 system at a rate of 2.2 gray per minute, with energy setting at 13.3 MeV using Co^{60} source. Detailed experiment setup is shown in Fig.4.1. Some concerns regarding this setup are to be addressed in the Discussion section.

4.2.2 Sampling schedule

These fish were then cultured in the aquarium under standard conditions and sacrificed at 3 hours, 1, 3, 5, 7, 9, 11 and 13 days after radiation (dpR), respectively, for RNA analysis and histological analysis. The time of sacrifice was scheduled in a manner that the fish were sampled on the same time of the day, that is, always at 3 pm of the day, except the first time point (6 pm or 3 hpR: hours post radiation). The sampling schedule is summarized in Table 4.1.

4.2.3 RNA extraction and real-time PCR

RNA was extracted using Trizol as described in Section 2.2 of Chapter 2. Real-time polymerase chain reaction was performed as described in previous chapters. The results were normalized against actin beta 2 level within each sample to minimize the internal error, as before.

4.2.4 Paraffin embedding and AB-PAS staining

Samples were fixed in 4% paraformaldehyde, embedded in paraffin and sectioned at 7 μm thickness. Details are described in previous chapters. Alcian blue and periodic acid in Schiffs reagent (AB-PAS) staining was performed according to the manufacturer's protocol. Details are described in previous chapters.

4.2.5 Alkaline phosphatase staining

PFA-fixed paraffin sections were dewaxed, rehydrated as described above. Intestinal expression of alkaline phosphatase was visualized by incubation in NBT/ BCIP substrates (4.5 μl NBT and 3.5 μl BCIP dissolved in freshly prepared buffer 9.5) for 30 min. The sections were then washed by PBST for 5 min twice, dehydrated as described above, cleared in histoclear, mounted in

DePex mounting medium (Gurr, England) and sealed by cover slips for image acquisition on an Zeiss Axiovert system (ZEISS, Germany).

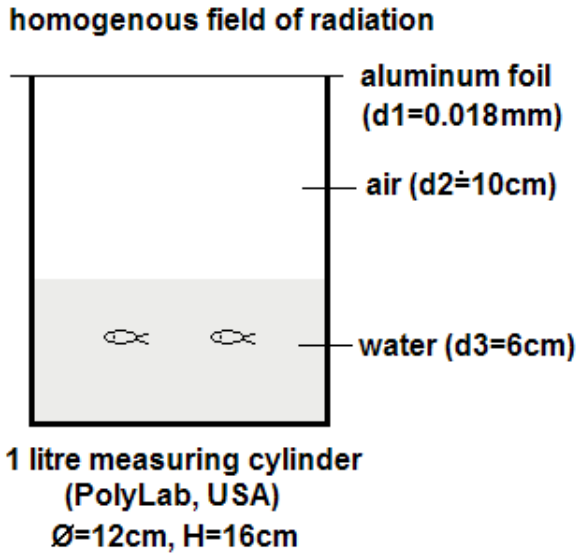

Figure 4.1: Experiment setup for radiation using a Gamma Chamber 2000 system.
Adult zebrafish were subject to a homogenous field of radiation at a rate of 2.2 gray per minute with total exposure of 16 gray. A measuring cylinder with a nominal volume of 1 litre was used (PolyLab, USA), covered with aluminum foil (Richmond, USA).

Table 4.1: Sampling schedule of radiated zebrafish

Time point	for RNA	for histology	time
ctrl	5	3	3 pm
3 hrs	5	3	6 pm
1 day	5	3	3 pm
3 day	5	3	3 pm
5 day	5	3	3 pm
7 day	5	3	3 pm
9 day	5	3	3 pm
11 day	5	3	3 pm
13 day	5	3	3 pm

4.3 Results

4.3.1 Survival of zebrafish after whole body gamma radiation

The zebrafish appeared much stressed immediately after radiation, swam around at a lower-than-normal speed and showed a slow response to disturbances. There was occasional, light bleeding in the dorsal region of a couple of fishes. They still had a reasonable appetite for artemia, though responding in a less active manner. They were able to expel feces that looked normal. Their general behaviors became apparently normal again within three days. They were monitored for at least two weeks and all of them successfully survived the radiation till the time of sacrifice [164].

4.3.2 Two rounds of elimination of intestinal villi

Histological analysis was performed to examine the architectural changes for the paraformaldehyde-fixed, paraffin-embedded intestinal sections.

Alcian blue-periodic acid in Schiff's reagent (AB-PAS) staining was performed for the intestines of zebrafish after whole body radiation. Three regions of zebrafish intestine, segments I, IV and V were analyzed. Degeneration of

villi was found since 3 hpR, but complete elimination of villous structures was first found by 24 hpR in segment I, resulting in vast regions along the intestinal circumferential wall covered by a flat sheet of epithelium (Fig.4.2). Following the first wave of proliferation, nascent villi were regenerated (from 3 days to 7 days). But the newly restituted tissue did not last long and the second round of villi elimination occurred by 9 dpR, again resulting in vast regions of flat epithelium lining. The two rounds of villi elimination did not annihilate the regenerative potential of zebrafish intestine, and the regeneration robustly ensued after the second round of villi elimination (Fig.4.2).

Though degeneration of villous structures took place along the intestine, these events in segment IV and segment V were not as evident as in segment I (Fig.4.2). Comparing the three regions of zebrafish intestine, whole body radiation was best manifested in segment I through complete elimination and regeneration of nascent villi before the tissue homeostasis was reestablished.

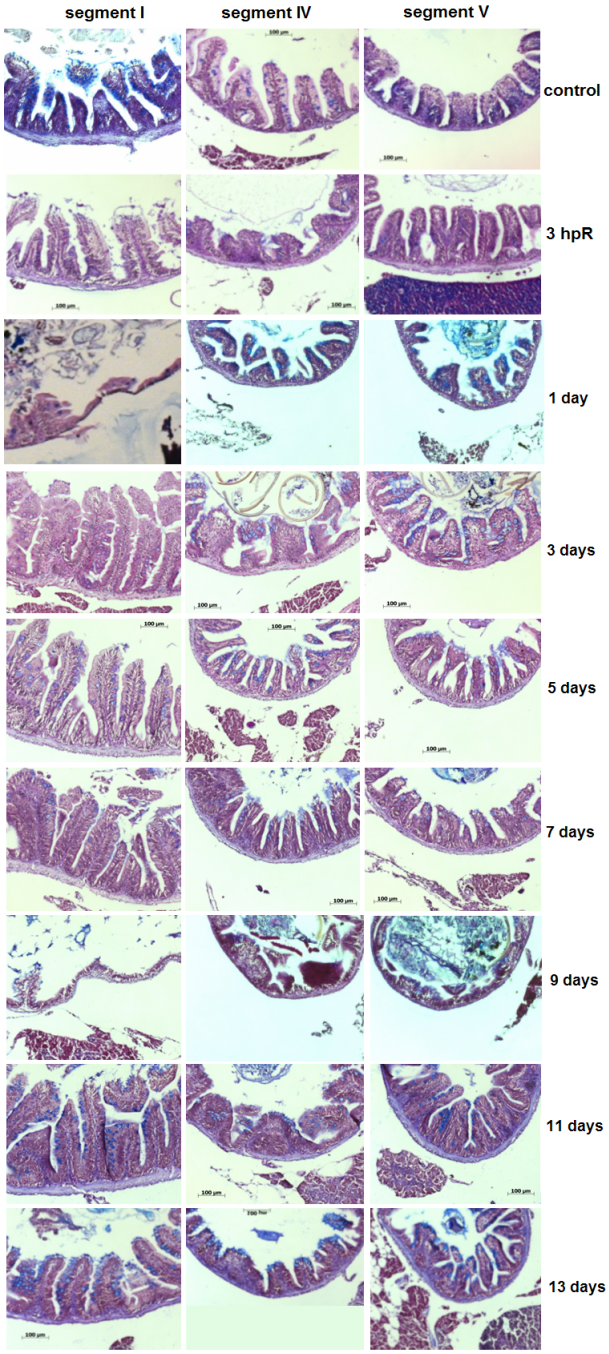

Figure 4.2: AB-PAS staining of paraffin sections of zebrafish intestine after total body radiation.
The fish were sacrificed at different time points following whole body radiation, as indicated by the numbers. Complete elimination of villi is first found by 124 hpR, and the second wave come by 216 hpR. hpR: hours post radiation. Scale bar: 100 μm

4.3.3 Two waves of Wnt/beta-catenin signaling: a driver of proliferation

To investigate the effect of radiation on zebrafish intestine, the total RNA of intestine was extracted and subjected to quantitative RT-PCR on a Roche LC480 system (Roche Applied Sciences, Swiss). As Wnt/beta-catenin is a major signaling pathway driving epithelial proliferation in the intestine [39, 42, 121, 78], expression level of *ctnnb1* (encoding beta-catenin in zebrafish) was measured at different time points following the exposure to radiation. As shown in Fig.4.3 panel A, the expression of *ctnnb1* was increased immediately after radiation (3 hpR), and this higher level of expression was maintained till 24 hpR. After that, there was a temporary drop in its expression to around the basal level. A second peak of *ctnnb1* expression was observed around 7 dpR, probably because of a second wave of cell proliferation. It did not return to basal level until around 11 dpR.

Interestingly, the *ezh2* gene (enhancer of zeste homolog 2), encoding a member of the Polycomb group (PcG) family that is involved in cell proliferation through regulating the activity of the Prc2/Eed-Ezh2 complex for histone modification [166, 167, 168, 169], also showed two waves of enhanced activities following the radiation (Fig.4.3 panel B), similar to *ctnnb1*. The two peaks

occurred at 24 hpR and 9 dpR, respectively. The two genes seemed to share similar cycling profiles, but the expression of *ezh2* temporally lagged a little behind that of *ctnnb1*. Expression of the house-keeping gene *bact2* is shown in Fig.4.3 panel C for reference purpose.

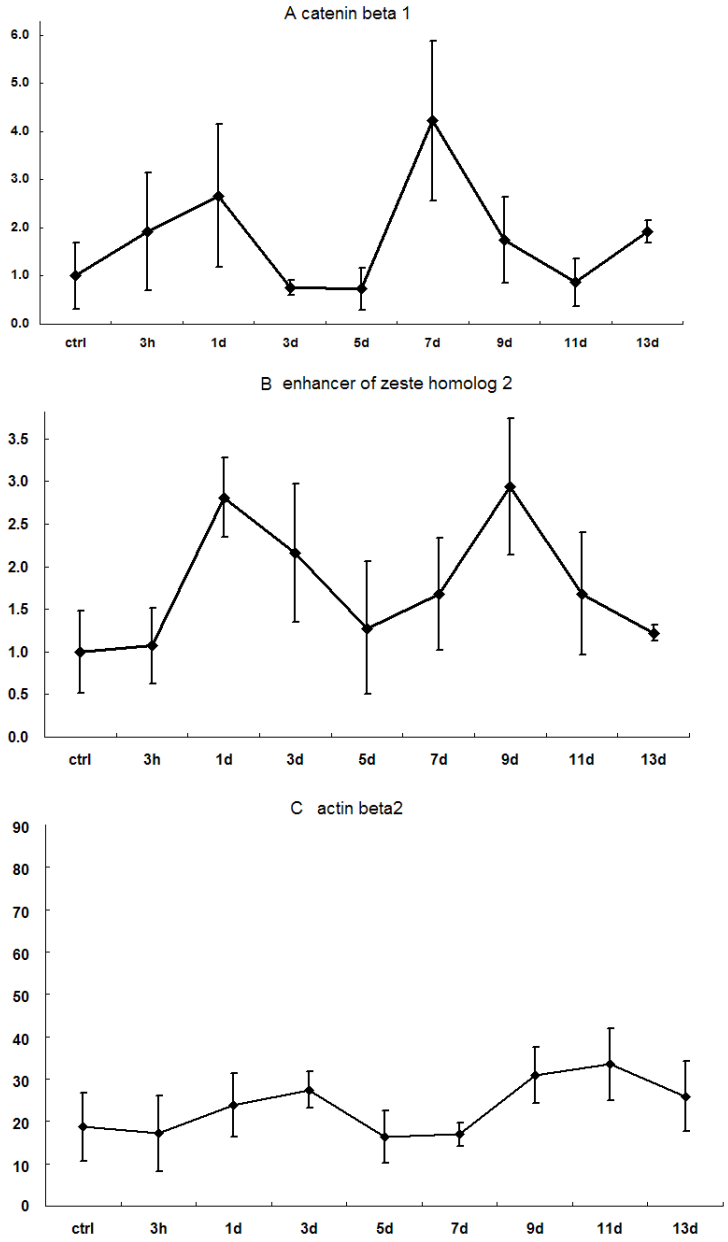

Figure 4.3: Two waves of proliferation in the intestine after whole body radiation.
(A) Expression of beta catenin (*ctnnb1*) in zebrafish intestine by quantitative RT-PCR. (B) Expression of enhancer of zeste homolog2 (*ezh2*) in zebrafish intestine by quantitative RT-PCR. (C) Expression of actin beta 2 (*actb2*) in zebrafish intestine by quantitative RT-PCR.

4.3.4 Cell proliferation as measured by *pcna* staining

As Wnt/beta-catenin signaling mediates the expression of a wide range of potential target genes [122], its effects may not be exclusively limited to proliferation. To further investigate the effects of radiation on cell proliferation, immunohistochemistry of *pcna* staining was carried out and results are shown in Fig.4.4. The number of cells expressing *pcna* was evidently increased by 3 hpR. But this increase did not last very long and by 24 hpR, *pcna* staining only identified a few cells in the inter-villi region. This was the time point when villi structures were undergoing degeneration and they shrunk significantly in size. The level of proliferation remained low till 5 dpR, and then suddenly increased by 7 dpR, driving fast repopulation of the epithelial tissue and growth of the villi. The level of proliferation, however, went down again at 9 dpR, when the villi structures underwent second round of degeneration. It did not return to normal level until $11 \sim 13$ dpR.

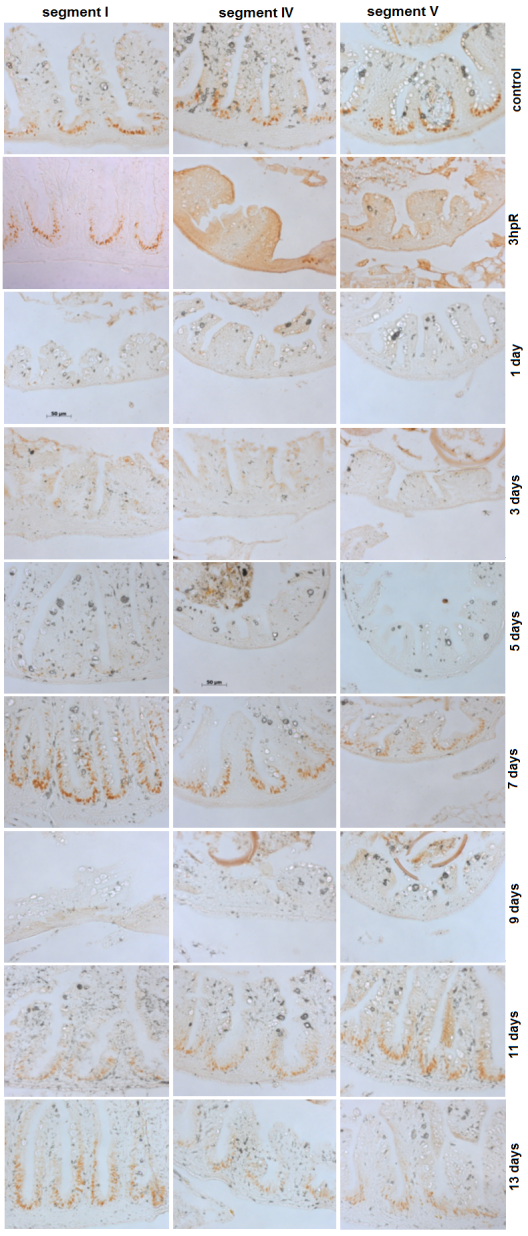

Figure 4.4: Cell proliferation as measured by *pcna* staining.
There is an increase in the population of PCNA positive cells by 3 hpR. The second increase is seen by 7 dpR. By 13 dpR, the number of cells expressing *pcna* becomes close to normal level. Scale bar: 100 μm

4.3.5 Radiation induced cell apoptosis

Radiation-induced cell death occurred virtually along the whole intestine following the whole body radiation. Some examples are shown in Fig.4.5 panel A. Typically, radiation induced some specific cell death in the inter-villi region, where stem and progenitor cells were known to reside, while in normal intestine, cell death in this region is a rare event. This agrees with previous studies that intestinal stem cells are sensitive to radiation [170, 171].

To understand whether radiation-induced cell death involves DNA fragmentation, quantitative RT-PCR was performed and result is shown in Fig.4.5 panel B. During the 24 hours post radiation, *dnase1* (deoxyribonuclease I) was expressed at a high level. But its expression seemed to have decreased after 24 hours.

On the other hand, apoptosis routinely occurs at the tips of villi in zebrafish intestine. Compared with radiation effects on stem cells, the effects of radiation on cell apoptosis at the tips of villi is less studied. Here a TUNEL assay was carried out to investigate the changes in apoptosis induced by radiation at the tips of villi. 16 gray whole body radiation immediately increased the level of apoptosis both at the tips and at the inter-villi regions (Fig.4.6) . This higher level of apoptosis was observed during the first 24 hours post radiation, till

the first round of villi elimination took place. A second high level of apoptosis was seen on 7 dpR (both at tips of villi and in the inter-villi region), preceding the second round of villi elimination. But in between, there was a temporary decrease in apoptosis around 5 dpR.

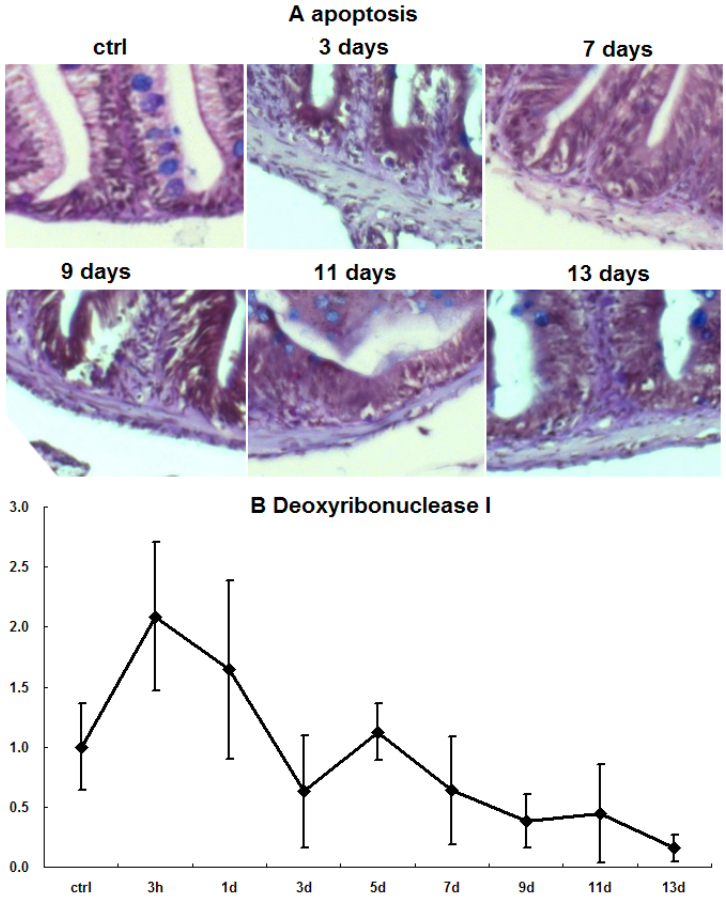

Figure 4.5: Gamma-radiation induced cell death through DNA fragmentation in the intestine.
(A) The chromosomes are often condensed and fragmented, with cellular organelles degenerated by neighbouring cells, leaving certain cavity behind after cell death. The inter-villi bottom region, where stem/progenitor cells reside, is the most frequent site for epithelial cell death. Scale bar: 100 μm (B) Elevated expression of DNaseI indicates a DNA fragmentation-dependent cell death.

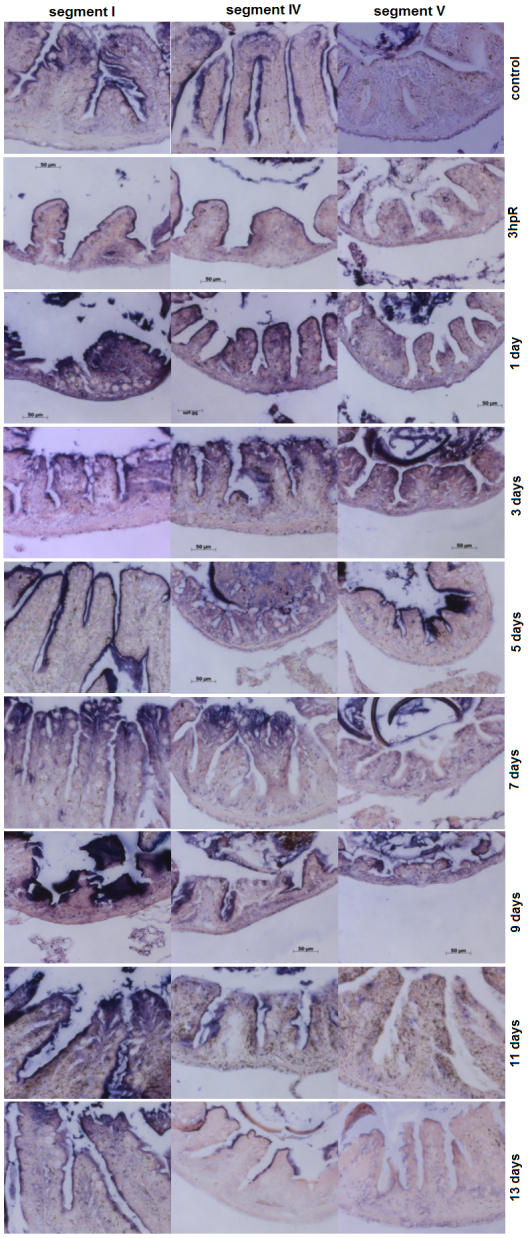

Figure 4.6: TUNEL assay for gamma-radiation induced cell apoptosis in zebrafish intestine.
A larger number of cells are going through apoptosis in zebrafish intestine immediately after the exposure, including specific cells in the inter-villi region. Note the high level of apoptosis at 3 dpR and 7 dpR. Scale bar: 100 μm

4.3.6 Changes in the intestinal epithelium renewal

Intestinal epithelium renewal is primarily determined by cell proliferation and cell apoptosis. Combining the results of proliferation assay and TUNEL assay shown earlier, it is obvious to see the changes in epithelium renewal. This is summarized and illustrated in Fig.4.7. Changes in proliferation and apoptosis are tabulated in the upper panel and sketched in the lower panel. There was an immediate increase in both proliferation and apoptosis, resulting in fast epithelium renewal at 3 hpR. Later on, a second orchestrated increase in both proliferation and apoptosis resulted in another fast renewal of epithelium around 7 dpR, before tissue homeostasis was reestablished by 13 dpR.

	ctrl	3h	1d	3d	5d	7d	9d	11d	13d
apoptosis	c	+	+	-	-	+	-	~	~
proliferation	c	+	--	--	--	+	-	~	~
renewal-rate	c	++	-	--	--	++	--	~	~

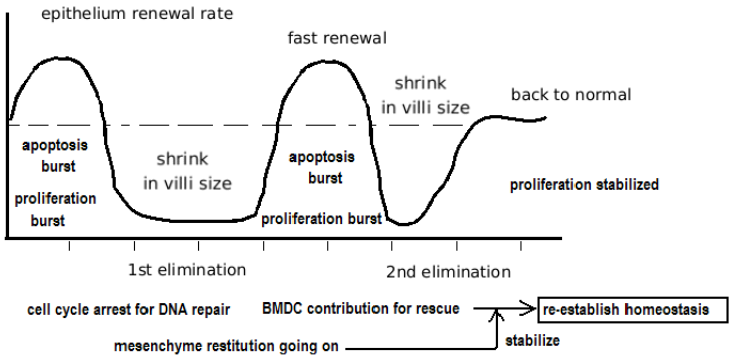

Figure 4.7: Changes in epithelium renewal as estimated from proliferation and apoptosis.
Changes in proliferation and apotosis are tabulated in the uper panel. c for control; + for increase; - for decrease; $\sim$ for little change. The resulting changes in epithelium renewal is sketched in the lower panel. There is a decrease both in epithelium renewal and villi size till the first round of villi elimination takes place. Later, a wave of fast epithelium renewal is seen preceding the second round of villi elimination, featuring high levels of proliferation and apoptosis.

4.3.7 Regeneration of the secretory epithelial cells

The secretory cells include the goblet cells and the enteroendocrine cells in the zebrafish intestine (where the Paneth cells are absent). As the goblet cells play an important role in maintaining the intestinal mucosal integrity and the enteroendocrine cells serve as a major regulator of intestinal peristalsis, it is necessary to examine their changes in order to understand how the zebrafish survived the strong radiation.

Quantitative RT-PCR analysis was performed for two key factors, the zinc-finger Kruppel-like transcription factor *klf4* and the bHLH transcription factor neurogenin 3, responsible for generation of the goblet cells and the enteroendocrine cells, respectively [172, 173, 174, 175, 16, 176]. Expression of *klf4* was elevated immediately following radiation (Fig.4.8 panel A). Its expression peaked at 24 hpR when the first round of villi elimination occurred and the higher level of expression was maintained throughout the whole recovery process of the intestine, indicating an active and prolonged process of regenerating goblet cells during tissue restitution. The expression of neurogenin 3, however, did not show an immediate response to radiation. The elevated expression of neurogenin 3 was seen by 3 dpR and it peaked by 7 dpR (Fig.4.8 panel B), preceding the occurrence of the second round of villi elimination.

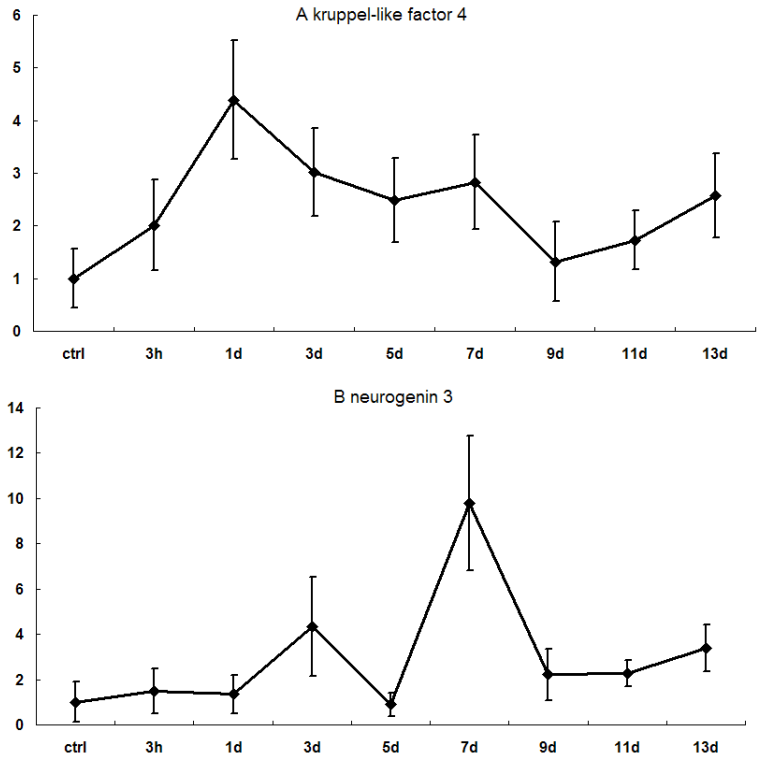

Figure 4.8: Quantitative RT-PCR results for response of *klf4* and *ngn3* genes to radiation.
(A) Expression of *klf4* was increased since 3 hpR and the higher level of expression was seen during the whole recovery process. (B) Expression of *ngn3* did not show an immediate response to radiation. But an increase was seen by 72 hpR and reached to a peak when the second round of villi elimination occurred.

4.3.8 Maintenance of basic intestinal functions following radiation

As 16 gray whole body radiation may cause extensive damages, it is interesting that all the fish survived the radiation. To understand how the fish managed to survive the radiation, we were interested to know whether the basic functions of the intestine were maintained. Thus expression of some basic genes like intestine specific fatty acid-binding protein 2 (*fabp2*) and alkaline phosphatase was examined by *in situ* hybridization. In the mean time, expression of smooth muscle-specific gene, actin a2, was also examined.

Expression of *fabp2* was robustly maintained during the 72 hours following radiation (Fig.4.9), though the strong radiation later caused a decrease in its expression. By 13 dpR, expression of *fabp2* was largely restored around its normal level in segment IV, but its expression in segment I was still lower than control level, indicating an incomplete recovery in this region of intestine. As sustained expression of *fabp2* gene ensured basic intestinal metabolic processes to go on before complete tissue recovery, this partially explains the survival of fish after radiation. In the mean time, intestinal smooth muscle was also affected by the radiation and expression of actin a2 gene was generally lower after the radiation (Fig.4.9).

Endogenous alkaline phosphatase was highly expressed at the apical membranes of mature intestinal epithelial cells during normal physiology. To further confirm the results of sustained intetsinal functions following radiation, expression of alkaline phosphatase was examined. Consistent to the expression of *fbap2*, expression of alkaline phosphatase was constantly maintained along the intestine, despite exposure to strong radiation (Fig.4.10). This further illustrated the presence of functional enterocytes that were maintained during the tissue recovery process, allowing the fish to survive the strong radiation.

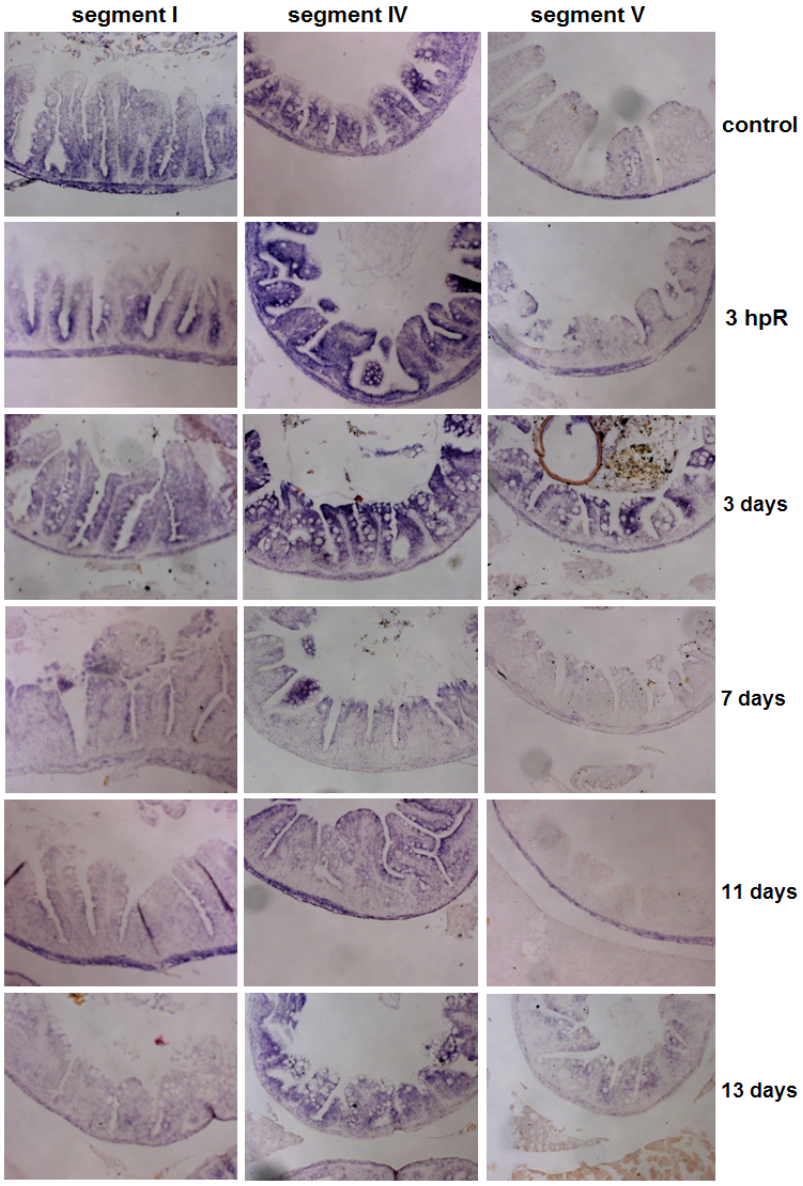

Figure 4.9: *In situ* hybridization for intestinal specific fatty acid binding protein 2 (*fabp2*) and smooth muscle specific actin a2 genes in zebrafish intestine, following exposure to whole body gamma radiation.
Expression of *fabp2* was maintained at a high level during the first 72 hours following radiation. It was decreased from 3 days but largely recovered by 13 days. Expression of *actb2* was present during most of the time. Note that *fabp2* is exclusively expressed in the epithelium and *actb2* is exclusively expressed in the intestinal smooth muscle. Scale bar: 100 μm

Figure 4.10: *In situ* hybridization for alkaline phosphatase in zebrafish intestine, following exposure to whole body gamma radiation.
Endogenous alkaline phosphatase was highly expressed in the apical membranes of epithelial cells in control. Its expression was continually maintained during the recovery process. Scale bar: 100 μm

4.3.9 Active involvement of intestinal stem cells during tissue restitution

Intestinal stem cells have been known to be capable of maintaining tissue homeostasis during normal physiology by producing all the epithelial cell types in the intestine [31, 33, 39, 45]. Recently, several marker genes have been proposed to identify the intestinal stem cells, including *Lgr5*, *Bmi1*, *Dcamkl1*, *Msh-1* and several others [28, 48, 41, 43, 44, 177]. To investigate the role of intestinal stem cells during tissue recovery after exposure to radiation, expression of the candidate stem cell marker gene, *bmi1* and *dcamkl1*, was examined by quantitative RT-PCR.

Consistent to our results of Wnt/beta-catenin mediated epithelial proliferation, expression of *bmi1* was also elevated immediately after radiation (Fig.4.11 panel A). Expression of both *bmi1* and *ctnnb1* reached their highest levels around 1 dpR and 7 dpR. The elevation in their expression was seen throughout the whole regenerating procedure.

The other putative intestinal stem cell marker, *dcamkl1*, showed some difference in its expression. A moderate elevation in expression was also seen immediately following radiation (Fig.4.11 panel B). Then its expression level steadily scaled up after 3 dpR and reached its highest level by 9 dpR, when the

second round of villi elimination occurred. From 11 dpR to 13 dpR, however, its expression returned to the normal level.

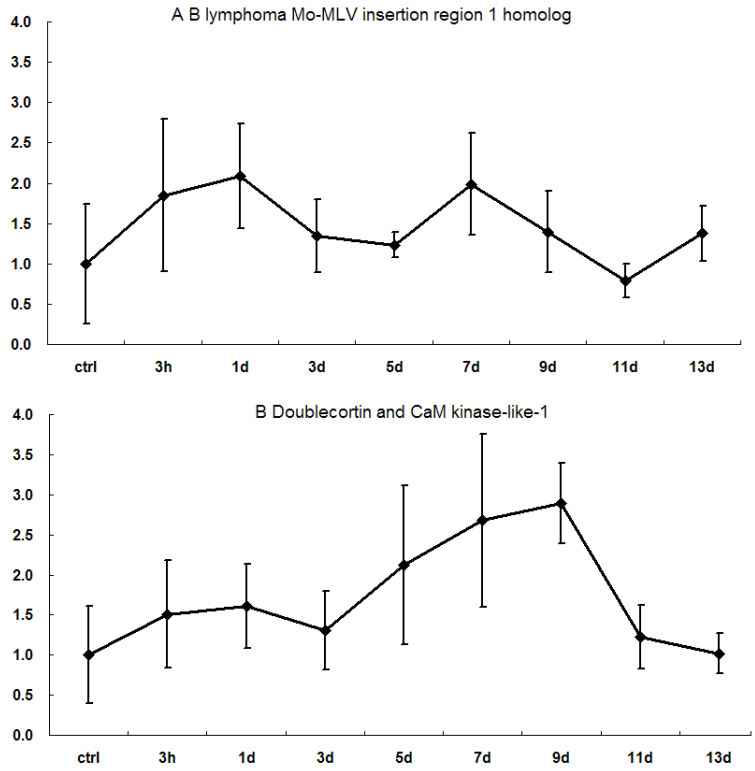

Figure 4.11: (A)Quantitative RT-PCR results for expression of *bmi1* in zebrafish intestine after whole body radiation. (B)Quantitative RT-PCR results for expression of *dcamkl1* in zebrafish intestine after whole body radiation. There was an elevation in expression of both genes after radiation.

4.3.10 Elevated mesenchymal activities

Epithelium-mesenchyme cross-talk has been important for maintainenance of tissue homeostasis during normal physiology. In case of radiation, the signaling of the fibroblast growth factor (FGF) family members has been suggested to have the potential to protect the intestine against the side effects of radiation therapy [178, 179]. Quantitative RT-PCR was performed to investigate the response of one of the major receptors of FGF signaling, *fgfr1*, in zebrafish intestine. The *fgfr1* receptor showed an immediate response to radiation (Fig.4.12). Its expression was elevated at 3 hpR and maintained at a high level throughout the whole recovery period of the intestine. Such a quick and prolonged response supported its significant role during intestinal tissue repair following whole body radiation.

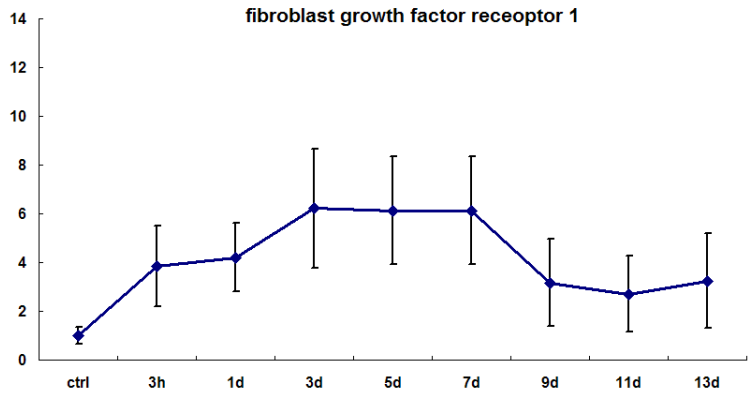

Figure 4.12: Quantitative RT-PCR results for expression of *fgfr1* in zebrafish intestine after whole body radiation.
Constant elevation in the expression of *fgfr1* in zebrafish intestine is seen after radiation.

4.4 Discussion

4.4.1 Concerns regarding the radiation setup

Some concerns have been raised regarding the radiation setup as indicated in Fig.4.1, especially the effects of the covering foil and water. To address the potential absorptive effects on radiation, we need to examine the traveling path of radiation in the chamber: air → aluminum foil → water → fish. Linear attenuation coefficients of the materials are listed in Table 4.2. These coefficients, however, may vary depending on the energy settings. So we need to estimate the numbers according to the energy level used in our experiment, which is 1.33 meV. Both polynomial and exponential curve fitting had been tried, and it was found that the exponential curve fitting worked much better. The fitted attenuation functions appear in the following form:

$$y = c_0 e^{-ax} \tag{4.1}$$

where c_0 and a are parameters to be fitted based on known values shown in Table 4.2. Fitting results are shown here.

For air:

$$y = 0.0002162 e^{-0.0013x} \tag{4.2}$$

For aluminum:

$$y = 0.4767e^{-0.0015x} \tag{4.3}$$

For water:

$$y = 0.1843e^{-0.0013x} \tag{4.4}$$

The attenuation coefficients at 1.33 meV as determined by these formulae are indicated in Table 4.2. Based on these coefficients and the distance traveled in each material, the effects of absorption can be easily calculated. Results are shown in Table 4.3.

Table 4.2: Attenuation coefficients of radiation (unit: cm^{-1})

	material	100 keV	200 keV	500 kev	...	1.33 meV
known	aluminum	0.435	0.324	0.227		?
predicted	aluminum	0.410	0.353	0.225		0.0648
known	water	0.167	0.136	0.097		?
predicted	water	0.162	0.142	0.096		0.0327
known	air	0.195e-3	0.159e-3	0.112e-3		?
predicted	air	0.190e-3	0.167e-3	0.113e-3		0.384e-4

Table 4.3: Absorption effects by different materials travelled by gamma radiation

material	distance	absorption (portion)	absorption (gray)	remaining (gray)
air	∼10 cm	0.00040	0.0064	15.994
foil	0.0018 cm	0.00002	0.0003	15.993
water	at 3cm	0.00012	0.0019	15.991
water	at 6 cm	0.00023	0.0040	15.987

4.4.2 Impressive regenerative capacity of zebrafish intestine

People normally think that the regenerative capacity of most vertebrate animals including zebrafish is very limited [180, 181]. In terms of radiation, whole body radiation has been a challenge for mammalian models like mice or rats, where medium-to-high range doses tend to kill the animals. For instance, whole body radiation at 10.4 gray will kill all mice by 14 days, while whole body radiation at 16 gray will kill all mice by 9 days [165]. In contrast, all zebrafish we tested (more than 50 fish in total) successfully survived the 16 gray whole body radiation within 14 days and a few spared fish survived pretty well even after one month. Though there is some difference in the practical experimental settings (for instance, mice are exposed to radiation in air, whereas zebrafish are in water), the absorption effects by foil and water, as we have shown above, are minimal. So we believe the difference in biology plays a significant role here.

Such an advantage of the zebrafish model had allowed us to monitor the intestinal responses to radiation over 14 days interval and for the first time, we reported the featured two waves of intestinal proliferation and correspondingly, two rounds of villi elimination during tissue restitution, though details of the

molecular mechanism behind largely remain unclear today.

4.4.3 Differential sensitivity of intestine to radiation and cancer rate

Upon exposure to radiation, the small intestine of zebrafish responds differentially to the large intestine (Previously, we have characterized the features of small and large intestine in zebrafish through analysis of genome-wide gene expressions). Radiation-induced apoptosis in the inter-villi region is more frequently observed in the small intestine than in the large intestine. In terms of villi elimination, it is most evident in segment I and segment IV (the small intestine), but less evident in segment V (the proximal large intestine). As altruistic cell apoptosis and elimination of villi serve as part of the mechanism to remove damaged cells and protect the intestine from potential development of cancer, the higher sensitivity to radiation and thorough elimination of damaged villi in the small intestine suggests an inherently better protection against environmental insults to its genome integrity, supporting the hypothesis that presence of such a mechanism explains, at least in part, the difference of cancer incidence in the small intestine and the large intestine [182].

4.4.4 Implications for colorectal cancer therapy

Over the past three decades, radiation therapy and chemotherapy have been introduced and improved in the treatment of patients with localized gastrointestinal malignancies. For patients with advanced stages of gastrointestinal cancer, radiation therapy and chemotherapy are often applied and sometimes integrated as adjuvant therapy, in a pre-operative or post-operative manner, to enhance local control resulting in improved survival and outcome of the patients [162, 183, 184, 185].

The protocol for delivery of radiation, however, is still actively evolving today. For instance, in many European cancer centers, the radiation schedule of 25 gray in 5 gray fractions for rectal cancer is being adopted. But in many rectal cancer centers in the USA, radiation therapy treatment approaches usually deliver 45 gray to the tumor and pelvic lymphatics, followed by additional radiation to gross tumor to a total dose of 50.4 to 54 gray in 28 to 30 fractions over 5.5 to 6 weeks [162]. Other protocols also exist in other parts of the world. While acute or late toxicity has been a concern, researchers are still taking effort to investigate the responses and outcomes in patients. Here, our study in zebrafish intestine has shed new light on these clinical applications by illustrating the presence of at least two waves of cell proliferation together

with two rounds of villi elimination. The temporal features of proliferation or villi elimination, once tested in patients, may be taken advantage to target the optimal time window for the best killing effects on radiation-sensitive cancer cells, thorough elimination of the transformed tissue and finally, regeneration of normal tissue. Therefore, characterization of the responsive features of the intestine to radiation will be of value for medicinal professionals to optimize the radiation delivery protocols to achieve minimal toxicity and better prognostic outcomes in patients.

4.4.5 Future directions

Our results on multiple rounds of cell proliferation and villi elimination appear interesting as this has not been reported in the current literature. Future work in this field may continue to explore whether there are third or more rounds of proliferation and villi elimination in zebrafish intestine following radiation. In the mean time, potential drugs or compounds that may have a protective effect from radiation should be tested. Some work has already been done along this direction [165, 186]. But the rational research will require further knowledge about the major pathways involved in mediating the radiation-induced cell removal, many aspects of which still remain elusive today.

The cycling nature of the regenerating process, however, may represent a universal feature of the intestinal biology, in view of the cross-species analogy at tissue, anatomy and molecular levels. Thus it is also interesting to carry out similar studies in other species and characterize their responsive properties. Though the potential cycling frequency and duration may be different, the universal cycling property of the regenerating process, if present, may be taken advantage in order to thoroughly remove the damaged/ transformed cells or tissues, maximizing the therapeutic effects for human patients.

Chapter 5

STORM: A General Model to Investigate Stem Cell Number and Their Adaptive Changes

5.1 Background

The intestinal epithelium represents the most rapidly renewing tissue in mammals [187, 6]. The intestinal stem cells play a pivotal role in epithelium renewal [188] and their deregulation will often lead to development of cancer, where colorectal cancer is one of the leading cancers in modern societies [13, 189]. Estimation of the number of stem cells and their adaptive changes in cell number or dividing frequency during physiopathological conditions would thus be helpful in diagnostics. To date, however, there is no tool available for this purpose. In this work, we aim to develop such a tool to facilitate the analysis of stem cells in the intestinal tracts of different species.

Current literature includes various reports studying the epithelium renewal process [190, 191, 192, 193, 194, 195, 196] by using either a grid model [197], lattice-free model [191] or multi-compartmental model [193]. For example, a hypothetical growth factor has been introduced to study the dynamics of epithelium proliferation and differentiation [190]; An age-structured model and a continuous model have been employed to study epithelium homeostasis and initiation of colon cancer [195]. None of the models in current literature, however, has been designed to directly address the number of intestinal stem cells and their adaptive changes. The progenies of intestinal stem cells are known

to migrate along the villous axis in a linear fashion, rendering linear strips of genetically marked cells along the villi [28, 8, 198, 199]. The intestinal epithelium renewal process, therefore, simplifies into a two-dimensional process that may be described by a two-dimensional mathematical model. In this work, a two-dimensional model has been developed to examine the number of intestinal stem cells present in each histological section of crypt in mammalian intestines, or equivalently, inter-villus pocket in zebrafish. It is named as STORM model ($\underline{ST}emcellmediated\underline{O}ptimal\underline{R}enewalofepithelium\underline{M}odel$). As an illustration, the model was applied to zebrafish, murine and human intestines, though it may also be applied to gastrointestinal tracts of other species. As the results suggest, the stem cell number is largely conserved across species during normal physiology. In the mean time, the results supports zebrafish as a valid model for study of intestinal stem cells [86, 7, 71, 79].

5.2 Materials and Methods

5.2.1 Development of the STORM model

Assumptions of the model

The model is developed based on two major assumptions: (1) Epithelial tissue is renewed in a *stem cell - transit amplification - differentiation - apoptosis* paradigm (Fig.5.1A); (2) The renewal rate of epithelial tissue has been evolutionarily optimized for efficient renewal of epithelium with requirement of minimal number of active stem cells.

Take zebrafish as an example. Incorporation of bromodeoxyuridine assay showed that the labeled cells were restricted in the lower part of the villi (Fig.5.1B). The cells were differentiated while they migrated upward. Once they reached the tips of villi, they underwent apoptosis (Fig.5.1C) and then were exfoliated. Thus four compartments can be defined along the villus axis: stem cell compartment, proliferation compartment, differentiation compartment and apoptosis compartment (Fig.5.1D). In mouse and human, the intestinal epithelium is organized and renewed in essentially the same manner [200]. Thus, the model we develop here will be applicable to both teleost and mammalian intestinal tracts. Coordination between epithelium renewal rate

and maintenance of genome integrity is pivotal to the rapidly renewing intestinal epithelium. Daily abrasion may wear out the differentiated epithelium and new cells need to be generated, but maintenance of genome integrity remains a high priority. This is especially important for an organism with a long lifespan like human as gastrointestinal cancers are becoming popular in modern societies [13, 189]. These two opposing requirements serve as the major driving forces for achieving an optimal epithelium renewal rate with minimal risk of carcinogenic transformations. Based on this, we have developed the model as follows.

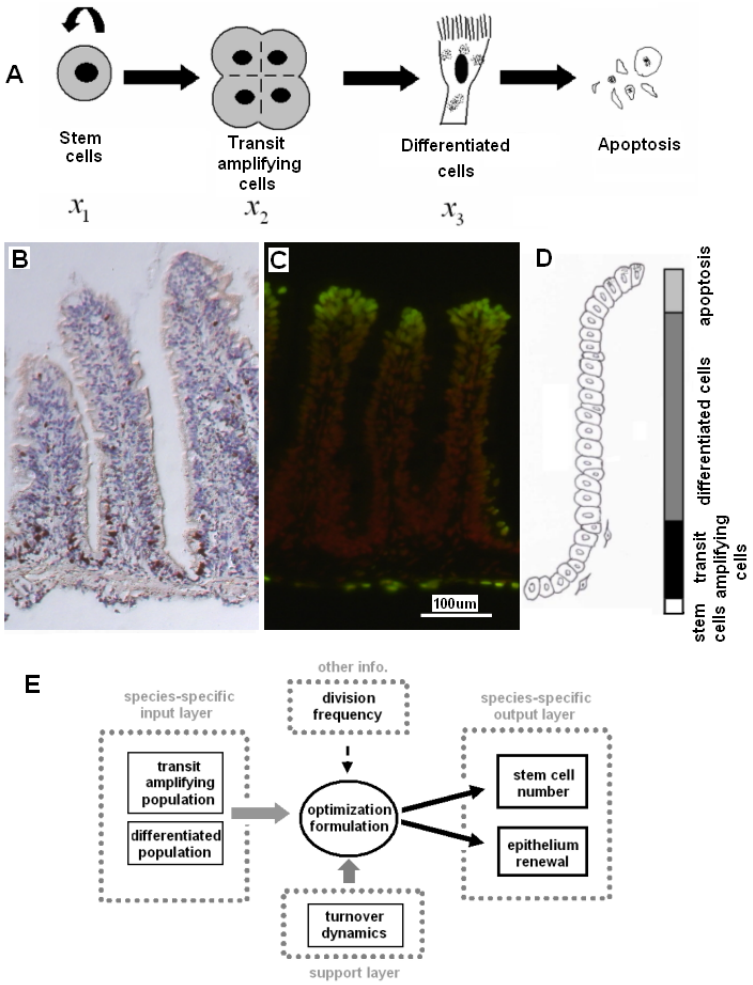

Figure 5.1: Paradigm of intestinal epithelium renewal and construction of the STORM model

(A) Paradigm of epithelium renewal. The intestinal epithelium is compartmentalized into four components while constructing the model, based on the analogous paradigm of epithelium renewal across teleost, murine and human species. x_1: population of stem cells; x_2: population of transit amplifying cells; x_3: population of differentiated epithelial cells. Note that all populations will be normalized against their homeostatic populations to produce a dimensionless model. (B) Cell proliferation assay with incorporation of BrdU, where S-phase cells are stained in dark brown color by the anti-BrdU antibody (see Materials and Methods for detail). (C) TUNEL assay for cell apoptosis. The apoptotic cells are stained in green color (see Materials and Methods for detail). (D) Compartmentalization of epithelium into stem cells, transit amplifying cells, differentiated cells and apoptotic cells along a villus. (E) Flowchart of the STORM model.

General workflow of the model

The overall workflow of the model is illustrated in Fig.5.1E. Based on the assumptions above and using measured populations of transit amplifying cells and differentiated cells, the optimization formulation will determine the number of active stem cell as well as their adaptive changes. Species-specific outcome of the model will require species-specific input information about the populations of cells.

A starting model for epithelium homeostasis

The process of epithelium turnover in the intestine is sketched in Fig.5.1A. This model consists of three major components: the stem cells, the transit amplifying cells and the differentiated epithelial cells. The population of stem cells is maintained through self-renewal and production of progenies. The population of transit amplifying cells is maintained through supply from stem cells and expense to cell commitment. The population of post-mitotic, differentiated epithelial cells is maintained through supply from transit amplifying progenitors and expense to apoptosis. All the populations are normalized against their homeostatic populations, respectively. It has been known that epithelium lining of one villus is constantly renewed by cells generated from

multiple crypts [8]. It has also been known that newly generated epithelial cells migrate along the villous axis in a linear fashion, rendering linear strips of genetically marked cells along the villi [8, 28, 198]. The intestinal epithelium renewal process, therefore, simplifies into a two-dimensional process that may be described by a two-dimensional mathematical model. Based on Fig.5.1A, a simple two-dimensional mathematical model can be derived assuming that fluxes of cells move only in a one-way manner. Transit amplifying progenitors do not reversely dedifferentiate to stem cells, which has been suggested to be a possibility under some special circumstances [200], as we are studying the normal tissue turnover. Using denotations shown in Fig.5.1A, a simple model reads as follows:

$$\frac{dx_1}{dt} = c_1 x_1 - c_0 x_1 \tag{5.1}$$

$$\frac{dx_2}{dt} = c_0 x_1 - k_1 x_2 \tag{5.2}$$

$$\frac{dx_3}{dt} = k_1 x_2 - k_2 x_3 \tag{5.3}$$

where c_0, c_1, k_1 and k_2 denotes the rates of cell flux for the population of stem cells, transit amplifying cells, differentiated cells and apoptosis, respectively. A non-trivial steady state may occur only if $c_1 = c_0$. If $c_1 > c_0$, the

model exhibits exponential growth(unbounded growth of stem cells); whereas if $c_1 < c_0$, the model exhibits exponential decay(extinction of stem cells and finally, of all cell populations). Thus the stability of this system depends on whether the relation $c_1 = c_0$ holds and thus the system is structurally unstable. Biological disturbances either caused by genome duplication-induced mutations or epigenetic deregulations may lead to unbounded growth of cells. In order for the system to maintain tissue homeostasis in a robust manner, as observed in reality, it is necessary to incorporate a feedback mechanism into the model.

The feedback mechanism in epithelium homeostasis

Equation (5.1) may be modified based on the assumption that stem cell differentiation is related to the second order of stem cell population (equivalent to a linear function of stem cell population for the differentiation coefficient c_0). Thus equation (5.1) becomes:

$$\frac{dx_1}{dt} = c_1 x_1 - c_0 x_1^2 \tag{5.4}$$

Now the stem cell population can be maintained in a more robust way, but this model still yields limited information about dynamics of the epithelium

turnover process. Then a term $\frac{k_5-x_3}{k_4+x_3}$ is incorporated into equation (5.2) and (5.3) introducing a saturable feedback regulation of stem cell self-renewal and transit amplifying cell division [201, 202, 203, 204, 205, 148, 206, 207, 208, 209]. In the mean time, a factor α, denoting the ratio of transit amplifying population over stem cell population, and a factor β, denoting the ratio of differentiated population over transit amplifying population, were incorporated into the model, respectively. To reflect the amplifying nature of the transit population, a factor is incorporated. Accordingly, the two modified equations of (5.2) and (5.3) now read as follows:

$$\frac{dx_2}{dt} = \frac{c_0}{\alpha}x_1 + \frac{k_5 - x_3}{k_4 + x_3}x_2 - k_1x_2 \tag{5.5}$$

$$\frac{dx_3}{dt} = \frac{\gamma k_1}{\beta}x_2 + \frac{k_5 - x_3}{k4 + x_3}x_3 - k_2x_3 \tag{5.6}$$

The modified model consists of equations (5.4), (5.5) and (5.6). As all cell populations are normalized against their homeostatic values, they are to be 1.0 when the system achieves tissue homeostasis. Thus we have:

$$c_0 = c_1 = \alpha k_1 = \alpha\beta k_2/\gamma \tag{5.7}$$

$$k_5 = 1.0 \tag{5.8}$$

for the homeostatic state. This information will be utilized in the following sections.

Dynamics of the intestinal epithelium turnover process

The steady state of the system is (1.0, 1.0, 1.0), normalized against respective cell populations. It represents the homeostatic state of the tissue. Equations (5.5) and (5.6) are of special interest as they contain the information on dynamics of epithelium turnover. By setting their gradients to zero, only one non-trivial steady state was found, which is $\{\hat{x}_2 = 1.0, \hat{x}_3 = 1.0\}$, just as we expected. The Jacobian matrix of for equation (5.5) and (5.6) is given as follows:

$$J_{(x_2,x_3)} = \begin{bmatrix} -\frac{c_0}{\alpha} + \frac{1-x_3}{k_4+x_3} & -\frac{x_2(1-x_3)}{(k_4+x_3)^2} - \frac{x_2}{k_4+x_3} \\ \frac{\gamma c_0}{\alpha\beta} & -\frac{\gamma c_0}{\alpha\beta} - \frac{(1-x_3)x_3}{(k_4+x_3)^2} + \frac{1-2x_3}{k_4+x_3} \end{bmatrix} \tag{5.9}$$

At steady state of $\{\hat{x}_2 = 1.0, \hat{x}_3 = 1.0\}$, the Jacobian matrix simplifies as:

$$J_{(\hat{x}_2=1.0,\hat{x}_3=1.0,)} = \begin{bmatrix} -\frac{c_0}{\alpha} & -\frac{1}{1+k_4} \\ \frac{\gamma c_0}{\alpha\beta} & -\frac{\gamma c_0}{\alpha\beta} - \frac{1}{1+k_4} \end{bmatrix} \tag{5.10}$$

Its eigenvalues are given in two parts, respectively. The first part is given by:

$$P1_{eig(J^*)} = -\frac{s(\beta+\gamma)}{2\beta} - \frac{1}{2(1+k_4)} \tag{5.11}$$

The second part is given by:

$$P2_{eig(J^*)} = \pm\frac{1}{2\beta(1+k_4)}\sqrt{(s(1+k_4)(\beta+\gamma)+\beta)^2 - 4s\beta\gamma(1+k_4)(1+\frac{\beta}{\gamma}+s+sk_4)} \tag{5.12}$$

where $s = c_0/\alpha$. So the two eigenvalues are P1+P2. When the determinant under the squared root sign is non-negative, the two eigenvalues are purely real and negative; when this determinant is negative, the two eigenvalues will assume the complex form yielding an oscillatory component of the system. Thus this steady state will be stable for all non-negative values of β, γ, s and k_4. Such information on dynamics of epithelium turnover will allow us to estimate the number of stem cells contained in each section of crypt.

The two-dimensional STORM formulation to estimate the number of epithelial stem cells on a histological section

The number of intestinal stem cells contained in a section of the mammalian crypt (or inter-villi pocket for zebrafish) will be determined by solving the

following formulation:

$$
\begin{aligned}
& argmin_{s,k_4|c_0,\beta,\gamma} -\tfrac{s(\beta+\gamma)}{2\beta} - \tfrac{1}{2(1+K_4)} \\
& +\tfrac{1}{2\beta(1+k_4)}\sqrt{(s(1+k_4)(\beta+\gamma)+\beta)^2 - 4s\beta\gamma(1+k_4)(1+\tfrac{\beta}{\gamma}+s+sk_4)} \\
& s.t.(s(1+k_4)(\beta+\gamma)+\beta)^2 - 4s\beta\gamma(1+k_4)(1+\tfrac{\beta}{\gamma}+s+sk_4) \geq 0; \\
& s \geq 0; \\
& k_4 \geq 0.
\end{aligned}
\tag{5.13}
$$

This is a multivariate optimization problem with non-linear objective function and non-linear constraints. γ is directly related to the *in vivo* division frequency of the transit amplifying cells. Given the species-specific value of α, β and γ, we are able to find out the stem cell number by solving the above formulation. This is a generalized model that may be applied to the intestinal tracts of teleost, murine and human where the same epithelium renewal paradigm holds (illustrated in Fig.5.1A). For adaptive changes to stem cells upon perturbation, we like to introduce the term of the capacity of stemness, which refers to the capacity of stem cells producing non-stem cell descendants, either through adaptation in stem cell number or through adaptation in dividing frequency.

5.2.2 Maintenance of zebrafish

Zebrafish (*Danio rerio*) were obtained from local aquarium and maintained in a controlled environment according to standard condition with a 14/10 hour light-dark cycle at 28^oC [129].

5.2.3 Tissue sectioning

Intestines were isolated from euthanized adult zebrafish, washed in ice-cold phosphate-buffered saline (PBS), fixed overnight in a 4% paraformaldehyde solution in PBS at room temperature. Fixed tissue was dehydrated in ethanol with increasing gradients (75%, 90%, 95%, 100% twice), cleared in histoClearII twice and embedded overnight in paraffin that was melted at 58^oC. Samples were then sectioned at 7 μm using a Reichert-Jung 2030 machine.

5.2.4 Immunohistochemistry

25mM Bromodeoxyuridine (Sigma-aldrich, St Louis, United States) was orally administered $50\mu L$ per fish 20 minutes before they were euthanized. Immunohistochemistry was performed according to the manufacturer's protocol (cat #2760, Chemicon International, United States). Briefly, the paraformaldehyde-fixed, paraffin-embedded slides were dewaxed in histoClear II, rehydrated and

quenched in 3% hydrogen peroxide, incubated in 0.2% trypsin solution for 10 minutes, denatured for 30 minutes. Slides were blocked for 10 minutes before incubation with detector (anti-BrdU) antibody for 60 minutes at room temperature. Then streptavidin-horse radish peroxidase conjugate was applied for 10 minutes and slides were subjected to a mixture of diaminobenzidine and substrate reaction buffer until color developed. The slides were covered by cover slips and sealed by DePex mounting medium and later, images were taken using a Zeiss Axiovert imaging system. Immunofluorescent TUNEL assay was carried out according to the manufacturer's protocol (cat #S7111, Chemicon International, United States). Briefly, slides were dewaxed in histoClear II, rehydrated and incubated in proteinase K ($20\mu g$/ml) for 15 minutes at room temperature. Equilibration buffer was applied before incubation in terminal deoxyribonucleic transferase enzyme in a humidified chamber at 37^oC for 60 minutes. Then stop buffer was applied before slides were incubated in anti-digoxigenin conjugate solution in a humidified chamber for 30 minutes at room temperature in dark. The slides were incubated in $0.5\mu g$/ml propidium iodide for 10 minutes as a fluorescent counterstaining of nuclei. Finally the slides were covered by cover slips, sealed by DePex mounting medium and images were taken using a Zeiss Axiovert imaging system.

5.3 Results

Formulation of the two-dimensional STORM model as we have developed is indicated by equation (5.13) in the Materials and Methods section.

5.3.1 General characteristics of the crypt-villus system

There are some general characteristics of the crypt-villus system independent of model details. First, as an adaptation to the villus size (varying value of β), the ratio of stem cells over transit amplifying cells may vary in response to different values of β (Fig.5.2A). Second, the renewal cycle of epithelium is correlated to the value of β. The epithelium will be renewed slowly for big values of β, but quickly for small values of β (Fig.5.2B). To tailor the model to be species-specific, information about the populations of transit amplifying cells, differentiated cells and *in vivo* dividing frequency of stem cells will be needed. The *in vivo* division frequency of intestinal stem cells is not well characterized in current literature, but it has been speculated to be once or twice every day [123, 39, 210]. For the transit amplifying cells, each round of cell division will double the cell number, so the amplifying factor γ has been introduced, which takes the value of 2.0.

5.3.2 Determination of the number of epithelial stem cells in a 2D section of the inter-villi pocket of zebrafish (Danio rerio) intestine

Cell counting over 200 villi in zebrafish based on our own specimens shows the population of proliferating cells (including transit amplifying cells and stem cells) to be 12.5 ± 3.2 cells (mean±std) and the population of differentiated cells with 100 ± 24 cells (mean±std). Representative histological sections are shown in Fig.5.1B. Based on these data, a prior β assumes the value of 8.0 for zebrafish. The STORM formulation may be solved with these inputs. After obtaining the stem cell number, the population of transit amplifying cells needs to be corrected in order to produce a posterior β with correction. This process is repeated several times until the solution converges. The final solution is as follows:

$$\beta = 10.3; s = \frac{c_0}{\alpha} = 0.508 \tag{5.14}$$

As the population of transit amplifying cells is known from the BrdU labeling assays, the number of stem cells may be calculated given the ratio between transit amplifying cells and stem cells:

$$number.of.active.stem.cells = \{ \begin{matrix} 4.1, \forall c_1 = 1 \\ \\ 2.0, \forall c_1 = 2 \end{matrix} \tag{5.15}$$

The actual number of active stem cells is dependent on their *in vivo* division frequency. If they divide once per day, then 4.1 stem cells need to be present in each section of the inter-villi pocket; If they divide twice per day, then only 2.0 stem cells need to be present. The results are shown in Table 5.1 with those of other species.

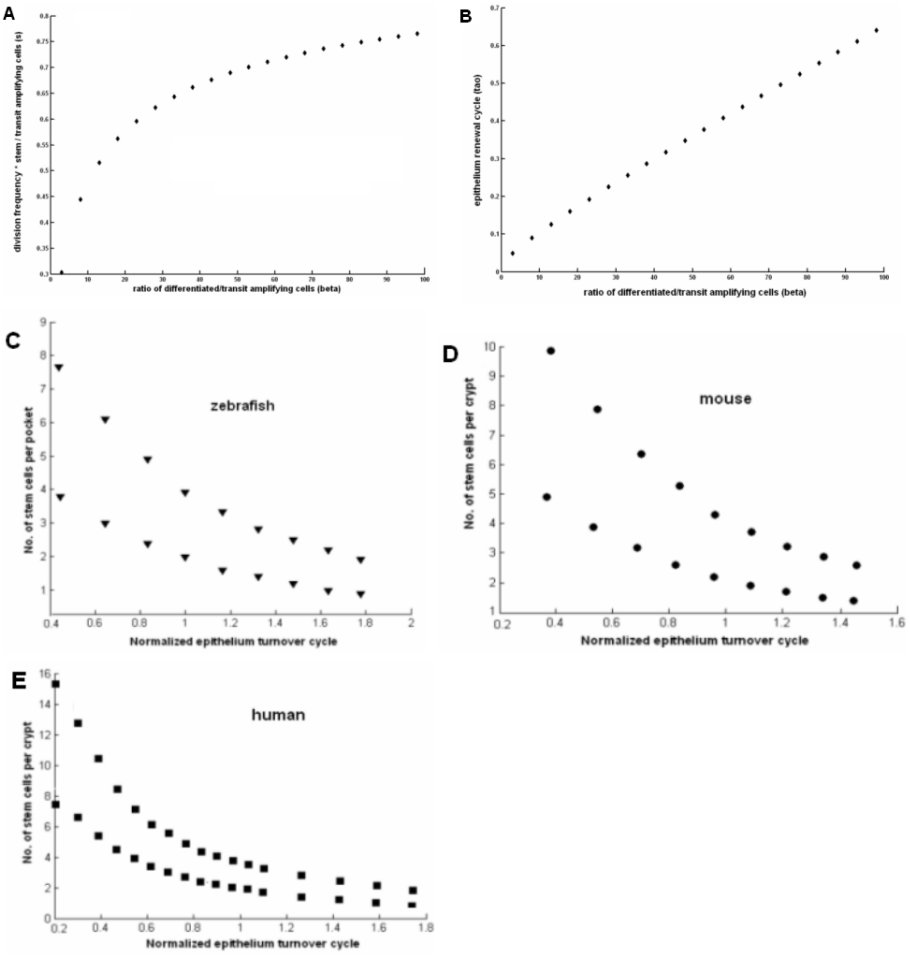

Figure 5.2: Results from the STORM model
(A) General relationship between ratio β and ratio s. (B) General relationship between ratio β and renewal cycle τ. (C) Adaptive changes of stem cell number versus epithelium renewal cycle in zebrafish intestine. (D) Adaptive changes of stem cell number versus epithelium renewal cycle in mouse intestine. (E) Adaptive changes of stem cell number versus epithelium renewal cycle in human intestine.

Table 5.1: The number of intestinal stem cells per section of mammalian crypt (or teleost inter-villi pocket) of the small intestine as suggested by the STORM model

in vivo division frequency	once per day	twice per day	species
stem cell number	4.1	2.0	zebrafish
stem cell number	4.1	2.0	mouse
stem cell number	3.5	1.8	human

To examine the adaptive changes in the capacity of stemness, the epithelium homeostasis was reduced by 50%, simulating damage caused to the epithelium. The system responds by initiating tissue restitution process. In the beginning stage, the value of β starts at 4.0 and by referring to the results in Fig.5.2B, the epithelium renewal cycle is 36% faster than the normal cycle and this will trigger an increase in the capacity of stemness (either the number of active stem cells or their dividing frequency) by 1.95-fold (Fig.5.2A). The increase in the capacity of stemness supports a transient expansion of transit amplifying population up to 14.5% (equivalent to one to two cells; Fig.5.3C). As new epithelium are being generated, the ratio of β gradually grows back to normal value; The transit amplifying and stem cell population will also return to their respective homeostatic states upon completion of epithelium restitution. The general correlation between the capacity of stemness and epithelium turnover cycle in zebrafish is plotted in Fig.5.2C.

5.3.3 Determination of the stem cell number in each crypt of mouse small intestine

In the small intestine of mouse, the population of differentiated epithelial cells is 96 ± 18; the crypt population is 38 ± 8; the population of labeled cells is

11.5 ± 2.5 (the numbers estimated based on references [39, 201, 147, 121, 211, 212, 126]). So the prior β assumes the value of 10.7 for mouse small intestine. The STORM formulation may be solved with these inputs. After posterior-correction as mentioned earlier, the model yields the final solution as follows:

$$\beta = 16.3; s = \frac{c_0}{\alpha} = 0.548 \tag{5.16}$$

Accordingly, the number of stem cells may be calculated as follows:

$$number.of.active.stem.cells = \{ \begin{matrix} 4.1, \forall c_1 = 1 \\ \\ 2.0, \forall c_1 = 2 \end{matrix} \tag{5.17}$$

If the stem cells divide once per day, then 4.1 active stem cells need to be present per section of crypt; If they divide twice per day, then only 2.0 stem cells need to be present per section of crypt. Results are displayed in Table 1 with those of other species. The result here generally agrees with previous estimations about the number of intestinal stem cells in the literature [200, 27, 31] as well as recent results with newly identified stem cell markers, which showed about 2-4 stem cells on each histological section of a crypt [198, 213]. Similar perturbation to the system has been conducted to examine the adaptive changes in the capacity of stemness. Briefly, 50% loss of the epithelium renders

β to be 5.3 and by referring to Fig.5.2B, the epithelium renewal cycle is 35% faster than the normal. The capacity of stemness grows by 1.9-fold (Fig.5.2D), supporting a transient expansion of transit amplifying population up to 14.7% (equivalent to one to two cells; Fig.5.3C). The system later may return to its homeostatic state. The general correlation between the capacity of stemness (in terms of stem cell number with fixed dividing frequency) and epithelium turnover cycle in mouse is shown in Fig.5.2D.

5.3.4 Determination of the stem cell number in each crypt of human duodenum

In human duodenum, the population of differentiated epithelial cells in the villus is 120 $\pm$ 33; the population of total cells in a crypt is 92 $\pm$ 12; the population of labeled cells is 8.8$\pm$2.1 (compiled from refs. [214, 215, 216, 217]). So the prior β assumes the value of 23.1 for human duodenum. The STORM formulation may be solved with these values. After posterior-correction, the final solution is as follows:

$$\beta = 39.0; s = \frac{c_0}{\alpha} = 0.665 \tag{5.18}$$

Accordingly, the number of stem cells may be calculated as follows:

$$number.of.active.stem.cells = \begin{cases} 3.5, \forall c_1 = 1 \\ 1.8, \forall c_1 = 2 \end{cases} \tag{5.19}$$

If stem cells divide once per day, then 3.5 stem cells need to be present per section of crypt; If they divide twice per day, then only 1.8 stem cells need to be present per section of crypt. The results are displayed in Table 1 together with those of other species. Similar perturbation has been conducted to examine the adaptive changes in the capacity of stemness in human. Briefly, 50% loss of epithelium renders the value of β to be 12.0 and by referring to Fig.5.2B, the epithelium renewal rate is 40% faster than the normal. The capacity of stemness grows by 2.5-fold (Fig.5.2E), supporting a transient expansion of transit amplifying population up to 11% (equivalent to one cell; Fig.5.3C). The system later may return to its homeostatic state. The general correlation between stem cell number and epithelium turnover cycle in human is shown in Fig.5.2E.

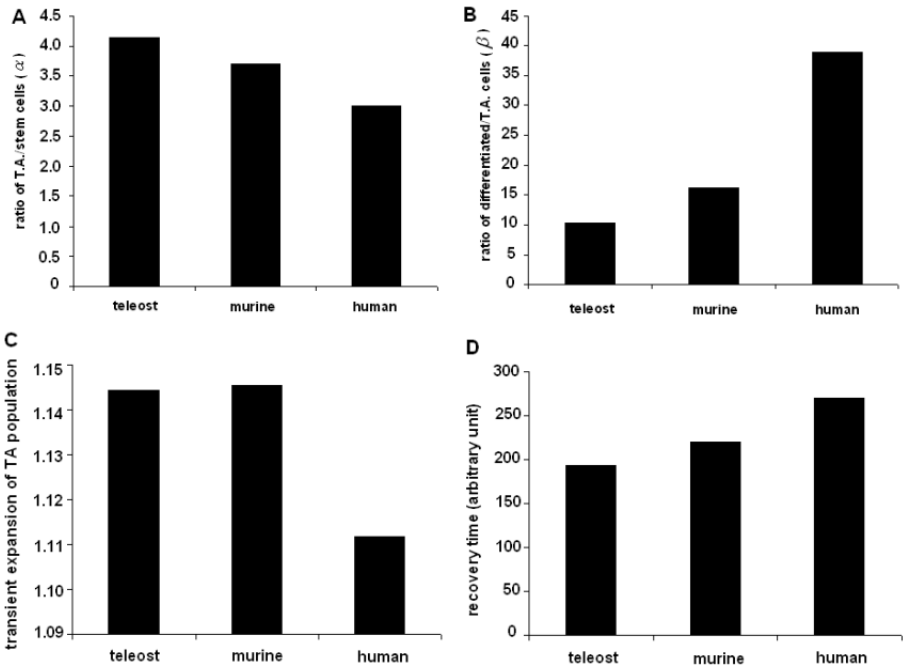

Figure 5.3: Comparing the transient response of the intestines of three different species
(A) The ratios of TA over stem cells. (B) The ratio of differentiated over TA cells (ratio of β) (C) Transient expansion of TA population in response to villus damge. (D) Recovery time in arbitrary unit after villus damage.

5.3.5 Comparison of the intestines of different species

To compare the epithelium renewal among three different species, the ratios between stem cells, transit amplifying cells and differentiated epithelial cells are shown in Fig.5.3A and B. There is a higher transit amplifying-to-stem cells ratio in teleost. This ratio is the lowest in human and it is accompanied by a higher differentiated-to-transit amplifying cells ratio in human. This probably reflects two different strategies in the epithelium renewal mechanism: Rapid repair and quick restitution of epithelium take higher priority in the teleost system, whereas slower tissue repair and restitution is allowed in human, with achievement of high fidelity in genomic duplication and reduction in susceptibility of carcinogenic transformations. The process of tissue restitution takes relatively longer time in human, but the transit amplifying population is better restrained from expansion compared with murine and teleost models (Fig.5.3C and D). This is important as unrestrained expansion of transit amplifying population is often seen before initiation of cancer. As the model reveals, unrestrained expansion of transit amplifying population tend to occur in extreme situations for the teleost and murine models, but it is not easily seen in human (Fig.5.4A). This may be partially explained by the feedback mechanism of the crypt-villus system. When the feedback signal is weakened

(with bigger k_4 value), the system tends to become unstable (Fig.5.4A). This is in consistence with the experimental finding that deficiency of Muc2 gene, the most abundantly secreted gastrointestinal mucin in mammals, would lead to formation of intestinal tumors in mouse [154].

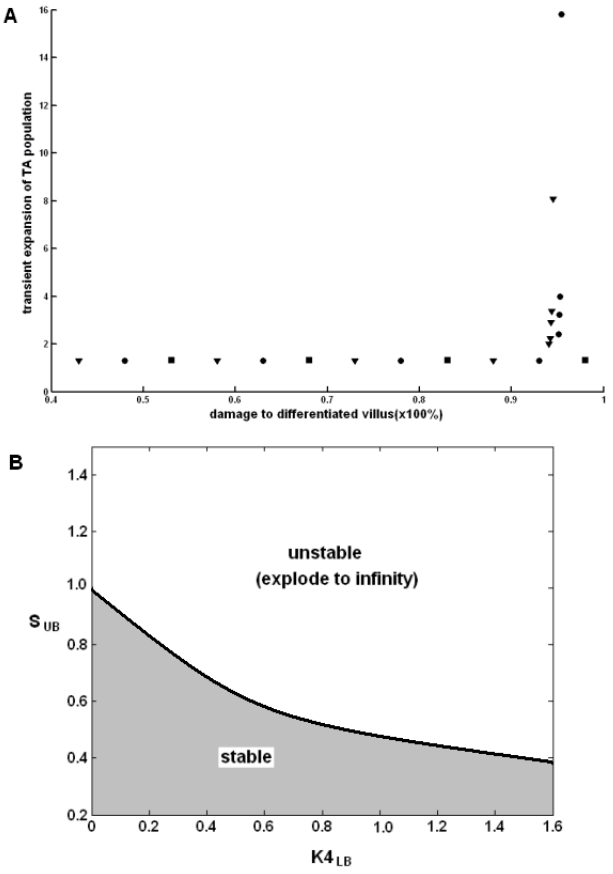

Figure 5.4: Analysis of the stability of the villus system in three species (A) Transient expansion of TA population. Uncontrolled expansion of TA population in response to extremely severe villus damage is possible in zebrafish and mouse, but less likely in human. The result shows the inbuilt robustness of the human crypt-villus system. Inverted triangle: zebrafish; circle: mouse; square: human. (B) Analysis of the stability of the system. When the strength of the feedback mechanism is forced to be weakened (k_4 goes toward bigger values), the villus system is prone to higher risk of uncontrolled stem cell expansion (expansion of the unstable region). In other words, the stem:TA ratio has to be kept small in order for the system to remain stable. A slight increase in the stem:TA ratio will likely initiate tissue hyperplasia, frequently seen before tumor develops, in the case of impaired feedback control.

5.3.6 Uncontrolled expansion of the capacity of stemness upon impaired feedback mechanism

As an important finding, the capacity of stemness will quickly explode when the feedback mechanism is impaired (i.e. force k_4 to grow), accompanied by faster epithelium renewal. Thus the STORM model highlights the pivotal role of the feedback mechanism, which relays signals from the differentiated population to the immature population. A major source of the feedback signals likely lies with the secretory cells, including goblet cells and enteroendocrine cells. This finding is further signified by the frequent observation of abnormal biogenesis of secretory cells in case of colorectal cancer [157, 153]. Accordingly, genetic deletion of Muc2 gene in mouse intestine produced colorectal cancers with impaired biogenesis of goblet cells and faster epithelium renewal [154], just as the STORM model suggests. Based on these results, we like to propose the hypothesis that the homeostasis of intestinal secretory cells takes higher priority than that of absorptive cells, and the feedback mechanism that they represent serves a key brake on development of colorectal cancers.

5.3.7 Application of the model to help evaluate hyperplasia in human duodenitis and ulcer

Previously, Bransom *et al* reported of mucosal cell proliferation in the duodenum with duodenitis or ulcer in endoscopic biopsies of a group of patients [215]. They intended to examine the epithelial hyperplasia. That may be achieved by quantitative analysis using the model we developed here. Based on the histological results, the villi were shortened by 30-50% in duodenal ulcer and duodenitis. Epithelium proliferation, as indicated by the labeling index, is 15.6 ± 1.7 in duodenal ulcer and 17.8 ± 1.5 in duodenitis. Utilizing these data, the model yields that: (1) For duodenal ulcer, $s = 0.419$, $\tau/\tau_0 = 0.54$, average capacity of stemness = 8.0 (in normal human duodenum, the stem cell number is 1.8-3.5, averaged 2.65 as shown earlier). As the model suggests, there is an increase in the capacity of stemness and an accelerated epithelium renewal rate (about two-fold faster than normal), supporting duodenal hyperplasia. (2) For duodenitis, $s = 0.444$, $\tau/\tau_0 = 0.60$, stem cell = 7.5 on average. The model suggests a significant increase in the capacity of stemness and an accelerated epithelium renewal rate (about 1.7-fold faster), supporting duodenal hyperplasia. The actual presence of hyperplasia is evidenced by the histological results of biopsies from the patients, in consistence with analysis result of the current

model.

5.4 Discussion

5.4.1 Epithelium apoptosis is actively initiated in zebrafish intestine before mature cells get exfoliated at the tips of villi

In contrast with the mammalian intestines, the number of apoptotic cells is notably larger in zebrafish, typically around 15-20 cells per villus (Fig.5.1C). In mouse, only a few cells are going through apoptosis along each villus. For instance, about 7 apoptotic cells were observed per 100 villi in mouse intestine [121]. The vast difference in cell apoptosis indicates a different strategy employed in teleosts, where apoptosis is initiated before cells are exfoliated into the intestinal lumen. This contrasts with that of mammals, where cells are exfoliated often before apoptosis is initiated.

5.4.2 Achieving the optimal epithelium renewal rate might be a fundamental principle of the crypt-villus system design by nature

The renewal rate of the intestinal epithelium tissue is a concern when it comes to maintenance of tissue integrity, sustainable organ function and potential risk of carcinogenic transformation. A high turnover rate would allow quick restitution of the lost tissue upon damage, but on the other hand, high turnover rate would require the presence of more active stem cells and more cell divisions, increasing the susceptibility to genome duplication-induced mutations and carcinogenic transformation of the epithelium tissue. These two opposing requirements ultimately lead to existence of an optimal turnover rate, allowing best possible maintenance of genome integrity with minimal requirement on the number of stem cells or stem cell divisions. The optimization model based on this rationale successfully yields an estimation of the stem cell number on a histological section of crypt that generally agrees previous speculations [39, 27, 31] as well as recent advances [198, 213]. As no stem cell marker has been established in zebrafish intestine, verification of the model results still awaits future progress in this field.

5.4.3 The number of stem cells is largely conserved in the small intestines of teleost, murine and human

Despite the vast differences in villus size from teleost to mammals, the stem cell number appears more or less conserved across species. Maintenance of a large number of stem cells on a daily basis seems not preferable due to their sensitivity to DNA damage and carcinogenic potential [218, 80, 219]. In presence of an amplifying mechanism, tissue homeostasis and restitution may be achieved through a prompt and capable response offered by the transit amplifying population. Of all the species examined, the human duodenum seems to be designed in a very robust manner in terms of maintaining genome integrity and reducing carcinogenic risk. This feature of the crypt-villus system appears understandable when one considers the long life-span of humans compared with teleosts and murines.

5.4.4 A general model for analysis of stem cell number with equal applicability to teleost, murine and human intestinal tracts

For the first time, a general model is developed to analyze the number of stem cells in the intestinal tracts of teleost, murine and human with experimental input of cell proliferation and differentiation information (illustration in Fig.5.1E). In absence of a universal stem cell marker for all species, this model provides a useful tool for us to examine the adaptive changes in stem cell number and epithelium renewal dynamics during physiological and pathological states of the organ.

5.4.5 Homeostasis of intestinal secretory cells takes high priority to ensure the integrity of the feedback mechanism

Genetic perturbations to the homeostasis of intestinal tissue would help us understand this feature built in the natural design of the crypt-villus system. Knockout of Bmpr1a gene (BMP receptor 1a, almost ubiquitously expressed in the intestinal epithelium) in mouse intestine showed increased population of

BrdU labeled cells and increased villus size (dominantly absorptive cells), but there was no significant change in goblet cells and Paneth cells [147]. On the other hand, knockout of beta-catenin in mouse intestine led to quick decrease in proliferating cells and degeneration of villi within a couple of days, but the number of goblet cells remained the same during that time period [121]. These two examples clearly suggest the homeostasis of the secretory cells to be more robust than that of the absorptive cells in the intestine, underlying the significance of the feedback mechanism we mentioned, which probably serves as a *brake* against the development of colorectal cancer. Go one step further and it is conceivable that the feedback mechanism will be preferably targeted during the initiation of colorectal cancer. In line with this, frequent observation of abnormal biogenesis of secretory cells in colorectal cancers has been documented [157, 153, 220, 221].

5.4.6 Growing evidence for validity of the model

After the development of the STORM model in mid 2007, new evidence supporting the validity of this model keeps coming out. First, the intestinal stem cell marker of Lgr5 was published in late 2007 [198, 213], which identified the number of stem cells to be about 2 to 5 per section of crypt in mouse. In early

2009, the same group reported a more specific marker of Ascl2 [36], which showed the typical number of stem cells to be no more than 4 per section of crypt. Another suggested stem cell marker, Olfm4, shows similar results both in the small intestines of mouse and human (human ortholog, OLFM4). For the large intestine, our STORM model has suggested presence of one or two stem cells per section of crypt, less than the number of stem cells in the small intestine. Interestingly, the reported Lgr5 marker showed one or two stem cells per section of crypt in mouse colon [198]. In April 2009, report of a new marker for human colon, aldehyde dehydrogenase 1, also shows presence of only one or two stem cells per section of crypt [222]. These results all agree well with the prediction of our STORM model.

5.5 Conclusion

In conclusion, the STORM model we developed may serve as a useful tool to analyze the number of stem cells in the intestinal tracts across species. Taking input information that is easily measurable, our model is able to provide quick and informative knowledge about stem cell number, epithelium turnover as well as their adaptive changes, which are not readily measurable through experiments.

Chapter 6

Conclusion

6.1 Conclusion

Prior to this thesis, not much work has been performed regarding adult zebrafish intestine. There has been a growing need among the zebrafish community to understand the analogy between zebrafish intestine and mammalian intestines in order to establish the zebrafish model for human gastrointestinal diseases. The current work, for the first time, has investigated the morphological, histological and molecular characteristics of adult zebrafish intestine using a systems biology approach. Findings of this work should lay down some foundations that will facilitate future research work where adult zebrafish intestine is utilized as a model organ of research. Major findings of the current work include:

(1) Zebrafish intestine regionalizes into at least two functionally different parts that are molecularly analogous to the small intestine and the large intestine of human, respectively. The small intestine connects to the large intestine through a region of transitional small intestine. The large intestine may be further divided into proximal and distal parts.

(2) Zebrafish intestinal villi extend to form long ridge-like structures with bifurcations to increase the inner surface of the intestinal tract. These ridge-like structures shrink in length and density toward the posterior intestine and com-

pletely disappear in the distal large intestine (segment S7).

(3) Zebrafish esophagus directly connects to its intestine without a stomach. There is no cecum found either. The pepsin gene locus that is generally conserved across most vertebrates is absent in zebrafish genome, accompanying the absence of stomach.

(4) There are no crypts of Lieberkuhn in zebrafish intestine. Proliferation of intestinal epithelium is restricted in the inter-villi pockets, without presence of Paneth cells. Apoptosis occurs at the tips of intestinal villi.

(5) Zebrafish intestine has demonstrated an impressive capability of regeneration following high range whole body radiation, reshaping our current understanding on the regenerative capability of vertebrate organs. It shows multiple waves of epithelial proliferation and correspondingly, multiple rounds of villi elimination before homeostasis is re-established. Similar observations have not been reported in other species so far. Moreover, zebrafish small intestine is more sensitive to radiation than its large intestine, supporting the hypothesis that the radiation-sensitive epithelium elimination mechanism would reduce the cancer incidence in the small intestine.

(6) Compared to highly specialized segments of mammalian digestive tracts, zebrafish intestine is functionally more versatile and less specialized along the

anterior-posterior axis. This indicates that the fish intestine may represent a primitive feature in evolution.

(7) Notch signaling mediates the fate determination of the bipotent precursors toward either an absorptive or a secretory lineage in the zebrafish intestine with involvement of a group of glycogen-rich intestinal subepithelial myofibroblasts.

(8) Intestinal stem cells are presumably located in the bottom of the inter-villi pockets and our computational analysis suggests the number to be 2 to 4 cells per section of one crypt-villus.

(9) STORM is a computational model that addresses the number of intestinal stem cells as well as their adaptive changes. Apart from fish, this model also applies to mammalian intestines and helps us to evaluate the biological status of the intestine organ.

6.2 Future research directions

To date, some questions in this field still remain open and are worthy of further studies. Here are some suggested future research directions:

(1)Homeostasis of villous ridges. Zebrafish intestine has no crypts but instead, it has villous ridges. During the day-to-day renewal of the intestinal epithe-

lium, the ridges may also go through a remodeling process where their shape, size and surface area will adapt to the physiological state of the fish. Studies on villi structures normally focus on cell renewal along the base-to-tip villous axis (viewed from the cross section), but homeostasis of the ridge structures in a different dimension (roughly along the circular axis of the whole intestine, see Fig.2.1) are largely ignored. We have noticed that they may grow or shrink in length, may duplicate themselves through bifurcation and may grow from anew. But the genes and molecules regulating the rate of their growth and duplication is not known yet. Further studies may be done by micro-dissecting the cells sitting on the edge of ridges or cells located at the bifurcating point. Analysis of their gene expression may discover genes important for controlling the diameter of the intestinal tube or the inner surface area of the intestine, which will affect the efficiency of nutrient absorption.

(2)The mechanism of tissue restitution. Stem cells are known to be important for maintaining tissue integrity during normal physiology. Since they are very sensitive to radiation, high dose radiation may remove all of them. Then the question rises regarding the regeneration of intestine thereafter: Is there another source of stem cell supply, for instance, from bone marrow, coming for rescue? Lineage tracing studies where bone marrow cells are genetically

labeled may address this question and verify this concept. While annihilation of stem cells may be verified by using animals whose intestinal stem cells are labeled, for example, by Bmi1 or Ascl2.

(3)Cycling nature of intestinal regeneration. Though a lot of work has been done using low dose radiation to perturb the stem cells, the regenerating process of the whole intestine following exposure to high dose radiation has not been well characterized. Our results have indicated multiple waves of villi elimination, which is most evident in the small intestine. But whether this is a general phenomenon in other species, such as mouse and human, still remains to be studied. In the mean time, assays may be developed to measure the level of genomic DNA damage (both double strand break and point mutations), from where it is possible to tell the efficiency of DNA repair during regeneration: Is multiple waves of villi elimination a better way of removing radiation-damaged tissues (if it is not present in other species)?

(4)Protection of intestine from radiation damage. This is of interest when radiotherapy is applied to colorectal cancer patients. Several drugs have been tested to have some protective effect, for example, R-spondin1 [165]. Since zebrafish seems to have a much better tolerance to radiation, the molecular mechanism may be revealed by profiling the responsive genes in zebrafish in-

testine following radiation. Using high throughput approaches like microarray or massive RNA sequencing, a group of genes may be identified this way and they will provide a list of candidates for a rational research in this field.

Bibliography

[1] Stevens C, Hume I: *Comparative Physiology of the Vertebrate Digestive System*. Cambridge University Press, 2nd edition edition 2004.

[2] Chivers D, Langer P: *Digestive System (The Amazing Human Body)*. Gretchen Hoffman, 1st edition edition 2005.

[3] Danbury C: *Encyclopedia Americana*. Grolier 1999.

[4] inc WB: *The world book encyclopedia*. Chicago: World Book 2000.

[5] website E: *Human anatomy online*. http://www.innerbody.com/ image/dige08.html accessed June, 2009.

[6] Crosnier C, Stamataki D, Lewis J: **Organizing cell renewal in the intestine: stem cells, signals and combinatorial control.** *Nat Rev Genet* 2006, **7**(5):349–59.

[7] Wallace KN, Akhter S, Smith EM, Lorent K, Pack M: **Intestinal growth and differentiation in zebrafish**. *Mech Dev* 2005, **122**(2):157–73.

[8] Wright NA, Irwin M: **The kinetics of villus cell populations in the mouse small intestine. I. Normal villi: the steady state requirement**. *Cell Tissue Kinet* 1982, **15**(6):595–609.

[9] van der Flier LG, Clevers H: **Stem Cells, Self-Renewal, and Differentiation in the Intestinal Epithelium**. *Annu Rev Physiol* 2008, :ahead of print.

[10] Brittan M, Wright N: **Gastrointestinal stem cells**. *Journal of Pathology* 2002, **197**:492–509.

[11] Wright N: **Epithelial stem cell repertoire in the gut: clues to the origin of cell lineages, proliferative units and cancer.** *Int J Exp Pathol* 2000, **81**:117–143.

[12] Cliffe L, Humphreys N, Thomas E, Potten C, Booth C, Grencis R: **Accelerated Intestinal Epithelial Cell Turnover: A New Mechanism of Parasite Expulsion**. *Science* 2005, **308**:1463–5.

[13] Jemal A, Siegel R, Ward E, Hao Y, Xu J, Murray T, Thun MJ: **Cancer statistics, 2008**. *CA Cancer J Clin* 2008, **58**(2):71–96.

[14] Institute NC: **Surveillance Epidemiology and End Results: Cancer Statistics**. *http://seer.cancer.gov* accessed May 27, 2009.

[15] Goh hs: *Colorectal cancer*. http://www.colon.com.sg accessed May, 2009.

[16] Bjerknes M, Cheng H: **Intestinal epithelial stem cells and progenitors**. *Methods Enzymol* 2006, **419**:337–83.

[17] Barker N, van Es JH, Jaks V, Kasper M, Snippert H, Toftgard R, Clevers H: **Very Long-term Self-renewal of Small Intestine, Colon, and Hair Follicles from Cycling Lgr5+ve Stem Cells**. *Cold Spring Harb Symp Quant Biol* 2008, :ahead of print.

[18] Cheng H, Leblond CP: **Origin, differentiation and renewal of the four main epithelial cell types in the mouse small intestine. V. Unitarian Theory of the origin of the four epithelial cell types**. *Am J Anat* 1974, **141**(4):537–61.

[19] Bach SP, Renehan AG, Potten CS: **Stem cells: the intestinal stem cell as a paradigm**. *Carcinogenesis* 2000, **21**(3):469–76.

[20] Potten CS: **The epidermal proliferative unit: the possible role of the central basal cell**. *Cell Tissue Kinet* 1974, **7**:77–88.

[21] Potten CS: **Cell replacement in epidermis (keratopoiesis) via discrete units of proliferation**. *Int Rev Cytol* 1981, **69**:271–318.

[22] Morris RJ, Fischer SM, Slaga TJ: **Evidence that the centrally and peripherally located cells in the murine epidermal proliferative unit are two distinct cell populations**. *J Invest Dermatol* 1985, **84**(4):277–81.

[23] Cairns J: **Mutation selection and the natural history of cancer**. *Nature* 1975, **255**(5505):197–200.

[24] Potten CS, Hume WJ, Reid P, Cairns J: **The segregation of DNA in epithelial stem cells**. *Cell* 1978, **15**(3):899–906.

[25] Potten CS, Owen G, Booth D: **Intestinal stem cells protect their genome by selective segregation of template DNA strands**. *J Cell Sci* 2002, **115**(Pt 11):2381–8.

[26] Potten CS, Booth C, Pritchard DM: **The intestinal epithelial stem cell: the mucosal governor**. *Int J Exp Pathol* 1997, **78**(4):219–43.

[27] Potten C: **Stem cells in gastrointestinal epithelium: numbers, characteristics and death**. *Philos Trans R Soc Lond B Biol Sci* 1998, **353**(1370):821–30.

[28] Sangiorgi E, Capecchi MR: **Bmi1 is expressed in vivo in intestinal stem cells**. *Nat Genet* 2008, **40**(7):915–20.

[29] Bjerknes M, Cheng H: **The stem-cell zone of the small intestinal epithelium. I. Evidence from Paneth cells in the adult mouse**. *Am J Anat* 1981, **160**:51–63.

[30] Bjerknes M, Cheng H: **The stem-cell zone of the small intestinal epithelium. III. Evidence from columnar, enteroendocrine, and mucous cells in the adult mouse**. *Am J Anat* 1981, **160**:77–91.

[31] Bjerknes M, Cheng H: **Clonal analysis of mouse intestinal epithelial progenitors**. *Gastroenterology* 1999, **116**:7–14.

[32] Stappenbeck TS, Mills JC, Gordon JI: **Molecular features of adult mouse small intestinal epithelial progenitors**. *Proc Natl Acad Sci U S A* 2003, **100**(3):1004–9.

[33] Bjerknes M, Cheng H: **Gastrointestinal stem cells. II. Intestinal stem cells**. *Am J Physiol Gastrointest Liver Physiol* 2005, **289**(3):G381–7.

[34] Barker N, van Es JH, Kuipers J, Kujala P, van den Born M, Cozijnsen M, Haegebarth A, Korving J, Begthel H, Peters PJ, Clevers H: **Identification of stem cells in small intestine and colon by marker gene Lgr5**. *Nature* 2007, **449**(7165):1003–7.

[35] Barker N, Clevers H: **Tracking down the stem cells of the intestine: strategies to identify adult stem cells**. *Gastroenterology* 2007, **133**(6):1755–60.

[36] van der Flier LG, van Gijn ME, Hatzis P, Kujala P, Haegebarth A, Stange DE, Begthel H, van den Born M, Guryev V, Oving I, van Es JH, Barker N, Peters PJ, van de Wetering M, Clevers H: **Transcription factor achaete scute-like 2 controls intestinal stem cell fate**. *Cell* 2009, **136**(5):903–12.

[37] Sato T, Vries RG, Snippert HJ, van de Wetering M, Barker N, Stange DE, van Es JH, Abo A, Kujala P, Peters PJ, Clevers H: **Single Lgr5 stem cells build crypt-villus structures in vitro without a mesenchymal niche**. *Nature* 2009, **459**(7244):262–5.

[38] Marshman E, Booth C, Potten CS: **The intestinal epithelial stem cell**. *Bioessays* 2002, **24**:91–8.

[39] Pinto D, Clevers H: **Wnt control of stem cells and differentiation in the intestinal epithelium**. *Exp Cell Res* 2005, **306**(2):357–63.

[40] Sakakibara S, Okano H: **Expression of neural RNA-binding proteins in the postnatal CNS: implications of their roles in neuronal and glial cell development**. *J Neurosci* 1997, **17**(21):8300–12.

[41] Murata H, Tsuji S, Tsujii M, Nakamura T, Fu HY, Eguchi H, Asahi K, Okano H, Kawano S, Hayashi N: **Helicobacter pylori infection induces candidate stem cell marker Musashi-1 in the human gastric epithelium**. *Dig Dis Sci* 2008, **53**(2):363–9.

[42] He XC, Zhang J, Tong WG, Tawfik O, Ross J, Scoville DH, Tian Q, Zeng X, He X, Wiedemann LM, Mishina Y, Li L: **BMP signaling inhibits intestinal stem cell self-renewal through suppression of Wnt-beta-catenin signaling**. *Nat Genet* 2004, **36**(10):1117–21.

[43] May R, Riehl TE, Hunt C, Sureban SM, Anant S, Houchen CW: **Identification of a novel putative gastrointestinal stem cell and adenoma stem cell marker, doublecortin and CaM kinase-like-1, following radiation injury and in adenomatous polyposis coli/multiple intestinal neoplasia mice**. *Stem Cells* 2008, **26**(3):630–7.

[44] Montgomery RK, Breault DT: **Small intestinal stem cell markers**. *J Anat* 2008, **213**:52–8.

[45] Barker N, van de Wetering M, Clevers H: **The intestinal stem cell**. *Genes Dev* 2008, **22**(14):1856–64.

[46] Reinisch C, K S, utsch, Uthman A, Pammer J: **BMI-1: a protein expressed in stem cells, specialized cells and tumors of the gastrointestinal tract**. *Histol Histopathol* 2006, **21**(11):1143–9.

[47] Zhu L, Gibson P, Currle DS, Tong Y, Richardson RJ, Bayazitov IT, Poppleton H, Zakharenko S, Ellison DW, Gilbertson RJ: **Prominin 1 marks intestinal stem cells that are susceptible to neoplastic transformation**. *Nature* 2009, **457**(7229):603–7.

[48] Jaks V, Barker N, Kasper M, van Es JH, Snippert HJ, Clevers H, Toftgard R: **Lgr5 marks cycling, yet long-lived, hair follicle stem cells**. *Nat Genet* 2008, **40**(11):1291–9.

[49] Sbarbati R: **Morphogenesis of the intestinal villi of the mouse embryo: chance and spatial necessity**. *J Anat* 1982, **135**(3):477–499.

[50] Ponder BA, Schmidt GH, Wilkinson MM, Wood MJ, Monk M, Reid A: **Derivation of mouse intestinal crypts from single progenitor cells**. *Nature* 1985, **313**(6004):689–91.

[51] Schmidt GH, Winton DJ, Ponder BA: **Development of the pattern of cell renewal in the crypt-villus unit of chimaeric mouse small intestine**. *Development* 1988, **103**(4):785–90.

[52] Sancho E, Batlle E, Clevers H: **Live and let die in the intestinal epithelium**. *Curr Opin Cell Biol* 2003, **15**(6):763–70.

[53] Schmidt GH, Wilkinson MM, Ponder BA: **Cell migration pathway in the intestinal epithelium: an in situ marker system using mouse aggregation chimeras**. *Cell* 1985, **40**(2):425–9.

[54] Cohn SM, Roth KA, Birkenmeier EH, Gordon JI: **Temporal and spatial patterns of transgene expression in aging adult mice provide insights about the origins, organization, and differentiation of the intestinal epithelium**. *Proc Natl Acad Sci U S A* 1991, **88**(3):1034–8.

[55] Bradley O, rev Grahame T: *Structure of the Fowl, 4th Edition*. Oliver and Boyd: Edinburgh, Scotland. 1960.

[56] Neisham M, Austic R, Card L: *Poultry Production, 12th Edition*. Lea and Febiger: Philadelphia, USA. 1979.

[57] Dingle J: *Module 3: Metabolism: Nutrient Procurement and Processing*. Study Book: Poultry Husbandry 1, DEC, USQ, Toowoomba. 1990.

[58] Burgess D: **Morphogenesis of intestinal villi. II. Mechanism of formation of previllous ridges.** *J. Embryol. Exp. Morph.* 1975, **34**:723–740.

[59] Hilton W: **The morphology and development of intestinal folds and villi in vertebrates.** *American Journal of Anatomy* 1902, **1**:459–504.

[60] Uni Z, Platin R, Sklan D: **Cell proliferation in chicken intestinal epithelium occurs both in the crypt and along the villus.** *J Comp Physiol B* 1998, **168**:241–247.

[61] Takeuchi T, Kitagawa H, Imagawa T, Uehara M: **Proliferation and cellular kinetics of villous epithelial cells and M cells in the chicken caecum**. *J Anat* 1998, **193 (Pt 2)**:233–9.

[62] Beyer EC, Barondes SH: **Secretion of endogenous lectin by chicken intestinal goblet cells**. *J Cell Biol* 1982, **92**:28–33.

[63] Hiramatsu K, Yamasaki A, Karasawa Y: **Comparative Study on the Distribution of Glucagon-like Peptide-1 (GLP-1)-immunoreactive Cells in the Intestine of Chicken and Ostrich.** *J Poul Sci* 2003, **40**:39–44.

[64] Kitagawa H, Shiraishi S, Imagawa T, Uehara M: **Ultrastructural characteristics and lectin-binding properties of M cells in the follicle-associated epithelium of chicken caecal tonsils**. *J Anat* 2000, **197 Pt 4**:607–16.

[65] Kitagawa H, Hosokawa M, Takeuchi T, Yokoyama T, Imagawa T, Uehara M: **The cellular differentiation of M cells from crypt undifferentiated epithelial cells into microvillous epithelial cells in follicle-associated epithelia of chicken cecal tonsils**. *J Vet Med Sci* 2003, **65**(2):171–8.

[66] Nile CJ, Townes CL, Michailidis G, Hirst BH, Hall J: **Identification of chicken lysozyme g2 and its expression in the intestine**. *Cell Mol Life Sci* 2004, **61**(21):2760–6.

[67] Ishizuya-Oka A, Hasebe T, Buchholz D, Kajita M, Fu L, Shi Y: **Origin of the adult intestinal stem cells induced by thyroid hormone in Xenopus laevis**. *FASEB J* 2009, :epub ahead of print.

[68] Schreiber A, Cai L, Brown D: **Remodeling of the intestine during metamorphosis of Xenopus laevis.** *Proc Natl Acad Sci U S A.* 2005, **102**(10):3720–5.

[69] Citterio V: **Le cellule entero chromaffini in Xenopus laevis.** *Monitore zoologico italiano* 1935, **46**:28–31.

[70] McAvoy JW, Dixon KE: **Cell specialization in the small intestinal epithelium of adult Xenopus laevis: functional aspects**. *J Anat* 1978, **125**(Pt 2):237–45.

[71] Ng AN, de Jong-Curtain TA, Mawdsley DJ, White SJ, Shin J, Appel B, Dong PD, Stainier DY, Heath JK: **Formation of the digestive system in zebrafish: III. Intestinal epithelium morphogenesis**. *Dev Biol* 2005, **286**:114–35.

[72] et al K: **The alimentary canal and digestion in Teleosts.** *Advcances in Marine Biology* 1975, :109–239.

[73] Feitsma H, Cuppen E: **Zebrafish as a cancer model**. *Mol Cancer Res* 2008, **6**(5):685–94.

[74] Davison JM, Woo Park S, Rhee JM, Leach SD: **Characterization of Kras-mediated pancreatic tumorigenesis in zebrafish**. *Methods Enzymol* 2008, **438**:391–417.

[75] Andre M, Ando S, Ballagny C, Durliat M, Poupard G, Briancon C, Babin PJ: **Intestinal fatty acid binding protein gene expression reveals the cephalocaudal patterning during zebrafish gut morphogenesis**. *Int J Dev Biol* 2000, **44**(2):249–52.

[76] Flores MV, Hall CJ, Davidson AJ, Singh PP, Mahagaonkar AA, Zon LI, Crosier KE, Crosier PS: **Intestinal differentiation in zebrafish requires Cdx1b, a functional equivalent of mammalian Cdx2**. *Gastroenterology* 2008, **135**(5):1665–75.

[77] Faro A, Boj SF, Ambrosio R, van den Broek O, Korving J, Clevers H: **T-cell factor 4 (tcf7l2) is the main effector of Wnt signaling during zebrafish intestine organogenesis**. *Zebrafish* 2009, **6**:59–68.

[78] Muncan V, Faro A, Haramis AP, Hurlstone AF, Wienholds E, van Es J, Korving J, Begthel H, Zivkovic D, Clevers H: **T-cell factor 4 (Tcf7l2) maintains proliferative compartments in zebrafish intestine**. *EMBO Rep* 2007, **8**(10):966–73.

[79] Crosnier C, Vargesson N, Gschmeissner S, Ariza-McNaughton L, Morrison A, Lewis J: **Delta-Notch signalling controls commitment to a secretory fate in the zebrafish intestine**. *Development* 2005, **132**(5):1093–104.

[80] Potten C: **Extreme sensitivity of some intestinal crypt cells to X and gama irradiation.** *Nature* 1977, **269**:518–521.

[81] Jankowski JA, Goodlad RA, Wright NA: **Maintenance of normal intestinal mucosa: function, structure, and adaptation**. *Gut* 1994, **35**(1 Suppl):S1–4.

[82] Radtke F, Clevers H: **Self-renewal and cancer of the gut: two sides of a coin**. *Science* 2005, **307**(5717):1904–9.

[83] Lam S, Wu Y, Vega V, Miller L, Liu E, Gong Z: **Conservation of gene expression signatures between zebrafish and human liver tumors and tumor progression**. *Nature Biotechnology* 2006, **24**:73–75.

[84] Amsterdam A, Sadler KC, Lai K, Farrington S, Bronson RT, Lees JA, Hopkins N: **Many ribosomal protein genes are cancer genes in zebrafish**. *PLoS Biol* 2004, **2**(5):E139.

[85] Lai K, Amsterdam A, Farrington S, Bronson RT, Hopkins N, Lees JA: **Many ribosomal protein mutations are associated with growth impairment and tumor predisposition in zebrafish**. *Dev Dyn* 2009, **238**:76–85.

[86] Wallace KN, Pack M: **Unique and conserved aspects of gut development in zebrafish**. *Dev Biol* 2003, **255**:12–29.

[87] Warga RM, Nusslein-Volhard C: **Origin and development of the zebrafish endoderm**. *Development* 1999, **126**(4):827–38.

[88] Harder W: **Anatomy of Fishes**. *Epubmed-ahead of print* 1975, :ahead of print.

[89] Nusslein-Volhard C, Dahm R: **Zebrafish**. *Oxford University Press, UK* 2002.

[90] Mathavan S, Gong Z, Liu E, Lufkin T: **Transcriptome analysis of zebrafish embryogenesis using microarrays.** *PLOS Genetics* 2005, **1**(2):260–76.

[91] Saeed AI, Sharov V, White J, Li J, Liang W, Bhagabati N, Braisted J, Klapa M, Currier T, Thiagarajan M, Sturn A, Snuffin M, Rezantsev A, Popov D, Ryltsov A, Kostukovich E, Borisovsky I, Liu Z, Vinsavich A, Trush V, Quackenbush J: **TM4: a free, open-source system for microarray data management and analysis**. *Biotechniques* 2003, **34**(2):374–8.

[92] Zhang B, Schmoyer D, Kirov S, Snoddy J: **GOTree Machine (GOTM): a web-based platform for interpreting sets of interesting genes using Gene Ontology hierarchies**. *BMC Bioinformatics* 2004, **5**:16.

[93] Zhang B, Kirov S, Snoddy J: **WebGestalt: an integrated system for exploring gene sets in various biological contexts**. *Nucleic Acids Res* 2005, **33**(Web Server issue):W741–8.

[94] Subramanian A, Tamayo P, Mootha V, Mesirov J: **Gene set enrichment analysis: A knowledge-based approach for interpreting genome-wide expression profiles**. *Proc Nat Acad Sci* 2005, **102**(43):15545–50.

[95] Yonkos L, Kane A: **Development of a digital atlas of fathead minnow histology.** *Lab Animal.* 1999, **28**:39–42.

[96] Sprague J, Bayraktaroglu L, Clements Dea: **The Zebrafish Information Network: the zebrafish model organism database.** *Nucl Acids Res* 2006, **34**:D581–585.

[97] Sprague J, Bayraktaroglu L, Clements Dea: **Zebrafish Atlas. an online database from the Pennsylvania State University.** *http://zfatlas.psu.edu/Nucl Acids Res* 2008, **na**:na.

[98] O'Riordan BG, Vilor M, Herrera L: **Small bowel tumors: an overview**. *Dig Dis* 1996, **14**(4):245–57.

[99] Sweetser DA, Birkenmeier EH, Klisak IJ, Zollman S, Sparkes RS, Moh T, as, Lusis AJ, Gordon JI: **The human and rodent intestinal fatty acid binding protein genes. A comparative analysis of their structure, expression, and linkage relationships**. *J Biol Chem* 1987, **262**(33):16060–71.

[100] Bazari W, Matsudaira P, Wallek M, Smeal T, Jakes R, Ahmed Y: **Villin sequence and peptide map identify six homologous domains.** *Proc Natl Acad Sci U S A* 1988, **85**:4986–4990.

[101] Bretscher A, Weber K: **Villin: the major microfilament-associated protein of the intestinal microvillus**. *Proc Natl Acad Sci U S A* 1979, **76**(5):2321–5.

[102] Ezzell R, Chafel M: **Differential localization of villin and fimbrin during development of the mouse visceral endoderm and intestinal epithelium.** *Development* 1989, **106**:407–419.

[103] Le Beyec L, Chauffeton V, Kan H, Janvier P, Cywiner-Golenzer Cea: **The -700/-310 fragment of the apolipoprotein A-IV gene combined with the -890/-500 apolipoprotein C-III enhancer is sufficient to direct a pattern of gene expression similar to that for the endogenous apolipoprotein A-IV gene.** *J Biol Chem* 1999, **274**:4954–4961.

[104] Sauvaget D, Chauffeton V, Citadelle D, Chatelet FP, Cywiner-Golenzer C, Chambaz J, Pincon-Raymond M, Cardot P, Le Beyec J, Ribeiro A: **Restriction of apolipoprotein A-IV gene expression to the intestine villus depends on a hormone-responsive element and parallels differential expression of the hepatic nuclear factor 4alpha and gamma isoforms**. *J Biol Chem* 2002, **277**(37):34540–8.

[105] Elshourbagy NA, Boguski MS, Liao WS, Jefferson LS, Gordon JI, Taylor JM: **Expression of rat apolipoprotein A-IV and A-I genes:**

mRNA induction during development and in response to glucocorticoids and insulin. *Proc Natl Acad Sci U S A* 1985, **82**(23):8242–6.

[106] Tso P, Nauli A, Lo CM: **Enterocyte fatty acid uptake and intestinal fatty acid-binding protein**. *Biochem Soc Trans* 2004, **32**(Pt 1):75–8.

[107] Agellon LB, Toth MJ, Thomson AB: **Intracellular lipid binding proteins of the small intestine**. *Mol Cell Biochem* 2002, **239**(1-2):79–82.

[108] Gao X, Sedgwick T, Shi YB, Evans T: **Distinct functions are implicated for the GATA-4, -5, and -6 transcription factors in the regulation of intestine epithelial cell differentiation**. *Mol Cell Biol* 1998, **18**(5):2901–11.

[109] Her GM, Chiang CC, Wu JL: **Zebrafish intestinal fatty acid binding protein (I-FABP) gene promoter drives gut-specific expression in stable transgenic fish**. *Genesis* 2004, **38**:26–31.

[110] Kueh HY, Brieher WM, Mitchison TJ: **Dynamic stabilization of actin filaments**. *Proc Natl Acad Sci U S A* 2008, **105**(43):16531–6.

[111] Ramirez-Lorca R, Vizuete ML, Venero JL, Revuelta M, Cano J, Ilundain AA, Echevarria M: **Localization of aquaporin-3 mRNA and protein along the gastrointestinal tract of Wistar rats**. *Pflugers Arch* 1999, **438**:94–100.

[112] Cutler CP, Martinez AS, Cramb G: **The role of aquaporin 3 in teleost fish**. *Comp Biochem Physiol A Mol Integr Physiol* 2007, **148**:82–91.

[113] Kurokawa T, Uji S, Suzuki T: **Identification of pepsinogen gene in the genome of stomachless fish, Takifugu rubripes**. *Comp Biochem Physiol B Biochem Mol Biol* 2005, **140**:133–40.

[114] Foltmann B: **Gastric proteinases–structure, function, evolution and mechanism of action**. *Essays Biochem* 1981, **17**:52–84.

[115] Kageyama T: **Pepsinogens, progastricsins, and prochymosins: structure, function, evolution, and development**. *Cell Mol Life Sci* 2002, **59**(2):288–306.

[116] Altschul S, Madden T, Schaffer A, Zhang J, Zhang Z, Miller W, Lipman D: **Gapped BLAST and PSI-BLAST: a new generation of protein database search programs.** *Nucleic Acids Res* 1997, **25**(17):3389–3402.

[117] Schmidt H, Strimmer K, Vingron M, von Haeseler A: **TREE-PUZZLE: maximum likelihood phylogenetic analysis using quartets and parallel computing.** *Bioinformatics* 2002, **18**:502–504.

[118] Page RD: **Visualizing phylogenetic trees using TreeView**. *Curr Protoc Bioinformatics* 2002, **Chapter 6**:Unit 6 2.

[119] Menard D: **Functional development of the human gastrointestinal tract: hormone- and growth factor-mediated regulatory mechanisms**. *Can J Gastroenterol* 2004, **18**:39–44.

[120] Arm Ma: **Lipases and lipolysis in the human digestive tract: where do we stand?** *Curr Opin Clin Nutr Metab Care* 2007, **10**(2):156–64.

[121] Fevr T, Robine S, Louvard D, Huelsken J: **Wnt/beta-catenin is essential for intestinal homeostasis and maintenance of intestinal stem cells.** *Mol Cell Biol* 2007, **27**(21):7551–9.

[122] de Lau W, Barker N, Clevers H: **WNT signaling in the normal intestine and colorectal cancer.** *Front Biosci* 2007, **12**:471–91.

[123] Li Y, Roberts S, Paulus U, Loeffler M, Potten C: **The crypt cycle in mouse small intestinal epithelium.** *J Cell Sci* 1994, **107**:3271–9.

[124] Cheng W, Tam P: **Apoptosis in murine duodenum during embryonic development.** *Pediatr Surg Int* 2000, **16**:485–487.

[125] Fre S, Huyghe M, Mourikis P, Robine S, Louvard D, Artavanis-Tsakonas S: **Notch signals control the fate of immature progenitor cells in the intestine**. *Nature* 2005, **435**(7044):964–8.

[126] van Es J, van Gijn M, Riccio O, van den Born M, Vooijs M, Begthel H, Cozijnsen M, Robine S, Winton D, Radtke F, Clevers H: **Notch/gamma-secretase inhibition turns proliferative cell in intestinal crypts and adenomas into goblet cells**. *Nature* 2005, **435**(7044):959–63.

[127] Kosinski C, Li V, Chan A, Zhang J, Ho C, Tsui W, Chan T, Mifflin R, Powell D, Yuen S, Leung S, Chen X: **Gene expression patterns of human colon tops and basal crypts and BMP antagonists as intestinal stem cell niche factors.** *Proc Natl Acad Sci U S A* 2007, **104**(39):15418–23.

[128] Afouda B, Ciau-Uitz A, Patient R: **GATA4, 5 and 6 mediate TGF-beta maintenance of endodermal gene expression in Xenopus embryos.** *Development* 2005, **132**(4):763–74.

[129] Westerfield M: **The Zebrafish Book**. *Epubmed-ahead of print* 1995, :ahead of print.

[130] Korzh V, Sleptsova I, Liao J, He J, Gong Z: **Expression of zebrafish bHLH genes ngn1 and nrd defines distinct stages of neural differentiation**. *Dev Dyn* 1998, **213**:92–104.

[131] Geling A, Steiner H, Willem M, Bally-Cuif L, Haass C: **A gamma-secretase inhibitor blocks Notch signaling in vivo and causes a severe neurogenic phenotype in zebrafish.** *EMBO reports* 2002, **3**(7):688C694.

[132] McKay J, Douglas J, Ross V: **Analysis of key cell-cycle checkpoint proteins in colorectal tumours**. *J. Pathol.* 2002, **196**:386–393.

[133] Yang Q, Bermingham NA, Finegold MJ, Zoghbi HY: **Requirement of Math1 for secretory cell lineage commitment in the mouse intestine**. *Science* 2001, **294**(5549):2155–8.

[134] Riccio O, van Gijn ME, Bezdek AC, Pellegrinet L, van Es JH, Zimber-Strobl U, Strobl LJ, Honjo T, Clevers H, Radtke F: **Loss of intestinal crypt progenitor cells owing to inactivation of both Notch1 and Notch2 is accompanied by derepression of CDK inhibitors p27Kip1 and p57Kip2**. *EMBO Rep* 2008, **9**(4):377–83.

[135] Schonhoff SE, Giel-Moloney M, Leiter AB: **Minireview: Development and differentiation of gut endocrine cells**. *Endocrinology* 2004, **145**(6):2639–44.

[136] Kamnasaran D, Qian B, Hawkins C, Stanford W, Guha A: **GATA6 is an astrocytoma tumor suppressor gene identified by gene**

trapping of mouse glioma model. *Proc Natl Acad Sci U S A* 2007, **104**(19):8053–8.

[137] Kiiveri S, Liu J, Heikkil P, Arola J, Lehtonen E, Voutilainen R, Heikinheimo M: **Transcription factors GATA-4 and GATA-6 in human adrenocortical tumors.** *Endocr Res.* 2004, **30**(4):919–23.

[138] Hellebrekers DM, Lentjes MH, van den Bosch SM, Melotte V, Wouters KA, Daenen KL, Smits KM, Akiyama Y, Yuasa Y, S S, uleanu, Khalid-de Bakker CA, Jonkers D, Weijenberg MP, Louwagie J, van Criekinge W, Carvalho B, Meijer GA, Baylin SB, Herman JG, de Bruine AP, van Engel Ma: **GATA4 and GATA5 are potential tumor suppressors and biomarkers in colorectal cancer**. *Clin Cancer Res* 2009, **15**(12):3990–7.

[139] Haramis A, Begthel H, van den Born M, van Es J, Jonkheer S, Offerhaus G, Clevers H: **De novo crypt formation and juvenile polyposis on BMP inhibition in mouse intestine.** *Science* 2004, **303**(5664):1684–6.

[140] Nemer G, Nemer M: **Transcriptional activation of BMP-4 and regulation of mammalian organogenesis by GATA-4 and -6**. *Dev Biol* 2003, **254**:131–48.

[141] Ko L, Engel J: **DNA-binding specificities of the GATA transcription factor family.** *Mol Cell Biol* 1993, **13**(7):4011–22.

[142] Chen D, Zhao M, Mundy GR: **Bone morphogenetic proteins**. *Growth Factors* 2004, **22**(4):233–41.

[143] Macias-Silva M, Hoodless PA, Tang SJ, Buchwald M, Wrana JL: **Specific activation of Smad1 signaling pathways by the BMP7 type I receptor, ALK2**. *J Biol Chem* 1998, **273**(40):25628–36.

[144] Goke M, Kanai M, Podolsky DK: **Intestinal fibroblasts regulate intestinal epithelial cell proliferation via hepatocyte growth factor**. *Am J Physiol* 1998, **274**(5 Pt 1):G809–18.

[145] Andoh A, Bamba S, Brittan M, Fujiyama Y, Wright NA: **Role of intestinal subepithelial myofibroblasts in inflammation and regenerative response in the gut**. *Pharmacol Ther* 2007, **114**:94–106.

[146] Artavanis-Tsakonas S, R M, , Lake R: **Notch signaling: cell fate control and signal integration in development.** *Science* 1999, **284**(5415):770–6.

[147] Auclair BA, Benoit YD, Rivard N, Mishina Y, Perreault N: **Bone morphogenetic protein signaling is essential for terminal differentiation of the intestinal secretory cell lineage**. *Gastroenterology* 2007, **133**(3):887–96.

[148] Powell D, Mifflin R, Valentich J, Crowe S, Saada J, West A: **Myofibroblasts. II. Intestinal subepithelial myofibroblasts**. *Am J Physiol Cell Physiol* 1999, **277**:183–201.

[149] Bhattacharyya S, Borthakur A, Dudeja P, Tobacman J: **Carrageenan reduces bone morphogenetic protein-4 (BMP4) and activates the Wnt/beta-catenin pathway in normal human colonocytes.** *Dig Dis Sci* 2007, **52**(10):2766–74.

[150] Ho S, Shekels L, Toribara N, Kim Y, Lyftogt C, Cherwits D, Niehans G: **Mucin gene expression in normal, preneoplastic, and neoplastic human gastric epithelium.** *Cancer Res.* 1995, **55**(12):2681–90.

[151] Hanski C, Riede E, Gratchev A, Foss H, Bohm C, Klussmann E, Hummel M, Mann B, Buhr H, Stein H, Kim Y, Gum J, Riechen E: **MUC2 gene suppression in human colorectal carcinomas and their metastases: in vitro evidence of the modulatory role of DNA methylation**. *Lab. Invest.* 1997, **77**:685–95.

[152] Ho S, Niehans G, Lyftogt C, Yan P, Cherwits D, Gum E, Dahiya R, Kim Y: **Heterogeneity of mucin gene expression in normal and neoplastic tissues**. *Cancer Res.* 1993, **53**(3):641–51.

[153] Sylvester P, Myerscough N, Warren B, Garlstedt I, Corfield A, Durdey P, Thomas M: **Differential expression of the chromosome 11 mucin genes in colorectal cancer.** *J. Pathol.* 2001, **195**:327–335.

[154] Velcich A, Yang W, Heyer J, Fragale A, Nicholas C, Viani S, Kucherlapati R, Lipkin M, Yang K, Augenlicht L: **Colorectal cancer in mice genetically deficient in the mucin Muc2**. *Science* 2002, **295**(5560):1726–9.

[155] Van der Flier LG, Sabates-Bellver J, Oving I, Haegebarth A, De Palo M, Anti M, Van Gijn ME, Suijkerbuijk S, Van de Wetering M, Marra

G, Clevers H: **The Intestinal Wnt/TCF Signature**. *Gastroenterology* 2007, **132**(2):628–32.

[156] Reya T, Clevers H: **Wnt signalling in stem cells and cancer**. *Nature* 2005, **434**(7035):843–50.

[157] Leow CC, Polakis P, Gao WQ: **A role for Hath1, a bHLH transcription factor, in colon adenocarcinoma**. *Ann N Y Acad Sci* 2005, **1059**:174–83.

[158] Peterkin T, Gibson A, Patient R: **GATA-6 maintains BMP-4 and Nkx2 expression during cardiomyocyte precursor maturation.** *EMBO J.* 2003, **22**(16):4260–73.

[159] Shroyer NF, Wong MH: **BMP signaling in the intestine: cross-talk is key**. *Gastroenterology* 2007, **133**(3):1035–8.

[160] Potten CS, Kovacs L, Hamilton E: **Continuous labelling studies on mouse skin and intestine.** *Cell Tissue Kinet* 1974, **7**:271–283.

[161] Fearon E, Vogelstein B: **A genetic model for colorectal tumorigenesis**. *Cell* 1990, **61**:759–767.

[162] Willet C, Czito B: **Chemoradiotherapy in gastrointestinal malignancies**. *Clinical Oncology* 2009, **21**:543–556.

[163] Francois Y, Namoz C, Baulieux Jea: **Influence of the interval between preoperative radiation therapy and surgery on downstaging and on the rate of sphincter-sparing surgery for rectal cancer: the Lyon R90-01 randomized trial**. *J Clin Oncol* 1999, **17**:2396.

[164] Both N, Vermey M: **Epithelial regeneration of transposed intestine after high doses of X-irradiation.** *Int J Radiat Biol* 1976, **29**:17–26.

[165] Bhanja P, Saha S, Kabarriti R, Liu L, Roy-CHowdhury Nea: **Protective role od R-spondin1, an intestinal stem cell growth factor, against radiation-induced gastrointestinal symdrome in mice**. *PLoS one* 2009, **4**(11):1–10.

[166] Simon J, Lange C: **Roles of the EZH2 histone methyltransferase in cancer epigenetics.** *Mutat Res* 2008, **647**(1-2):21–9.

[167] Tonini T, D'Andrilli G, Fucito A, Gaspa L, Bagella L: **Importance of Ezh2 polycomb protein in tumorigenesis process interfering with the pathway of growth suppressive key elements.** *J Cell Physiol* 2008, **214**(2):295–300.

[168] Gil J, Bernard D, Peters G: **Role of polycomb group proteins in stem cell self-renewal and cancer.** *DNA Cell Biol* 2005, **24**(2):117–25.

[169] Cao R, Zhang Y: **The functions of E(Z)/EZH2-mediated methylation of lysine 27 in histone H3.** *Curr Opin Genet Dev* 2004, **14**(2):155–64.

[170] Potten C, Merritt A, Hickman J, Hall P, Far Aa: **Characterization of radiation-induced apoptosis in the small intestine and its biological implications.** *Int J Radiat Biol.* 1994, **65**:71–8.

[171] Potten C, Grant H: **The relationship between ionizing radiation-induced apoptosis and stem cells in the small and large intestine.** *Br J Cancer* 1998, **78**(8):993–1003.

[172] Katz J, Perreault N, Goldstein abd CS B, Labosky P, Yang V, Kaestner K: **The zinc-finger transcription factor Klf4 is required for terminal differentiation of goblet cells in the colon.** *Development.* 2002, **129**(11):2619–28.

[173] Swamynathan S, Katz J, Kaestner K, Ashery-Padan R, Crawford M, Piatigorsky J: **Conditional deletion of the mouse Klf4 gene results in corneal epithelial fragility, stromal edema, and loss of conjunctival goblet cells.** *Mol Cell Biol.* 2007, **27**:182–94.

[174] Zheng H, Pritchard D, Yang X, Bennett E, Liu G, Liu C, Ai W: **KLF4 gene expression is inhibited by the notch signaling pathway that controls goblet cell differentiation in mouse gastrointestinal tract.** *m J Physiol Gastrointest Liver Physiol* 2009, **296**(3):G490–8.

[175] Lopez-Diaz L, Jain R, Keeley T, VanDussen K, Brunkan C, Gumucio D, Samuelson L: **Intestinal Neurogenin 3 directs differentiation of a bipotential secretory progenitor to endocrine cell rather than goblet cell fate.** *Dev Biol.* 2007, **309**(2):298–305.

[176] Wang J, Cortina G, Wu SV, Tran R, Cho JH, Tsai MJ, Bailey TJ, Jamrich M, Ament ME, Treem WR, Hill ID, Vargas JH, Gershman G, Farmer DG, Reyen L, Martin MG: **Mutant neurogenin-3 in congenital malabsorptive diarrhea**. *N Engl J Med* 2006, **355**(3):270–80.

[177] Jin G, Ramanathan V, Quante Mea: **Inactivating cholecystokinin-2 receptor inhibits progastrin-dependent colonic crypt fission, proliferation, and colorectal cancer in mice.** *J Clin Invest.* 2009, **119**(9):2691–701.

[178] Hagiwara A, Nakayama F, Motomura K, Asada M, Suzuki M, Imamura T, Akashi M: **Comparison of expression profiles of several fibroblast growth factor receptors in the mouse jejunum: suggestive evidence for a differential radioprotective effect among major FGF family members and the potency of FGF1.** *Radiat Res.* 2009, **172**:58–65.

[179] Okunieff P, Mester M, Wang J, Maddox T, Gong X, Tang D, Coffee M, Ding I: **In vivo radioprotective effects of angiogenic growth factors on the small bowel of C3H mice.** *Radiat Res.* 1998, **150**(2):204–11.

[180] Sanchez Alvarado A, Tsonis P: **Bridging the regeneration gap: genetic insights from diverse animal models.** *Nature Reviws Genetics* 2006, **7**(11):873–884.

[181] Ortiz-Pineda P, Ramirez-Gomez F, Perez-Ortiz Jea: **Gene expression profiling of intestinal regeneration in the sea cucumber.** *BMC Genomics* 2009, **10**(262):1–21.

[182] Potten C, Li Y, O'Connor P, Winton D: **A possible explanation for the differential cancer incidence in the intestine, based on distribution of the cytotoxic effects of carcinogens in the murine large bowel.** *PLoS one* 1992, **13**(12):2305–12.

[183] Macdonald J, Smalley S, Benedetti Jea: **Chemoradiotherapy after surgery compared with surgery alone for adenocarcinoma of the stomach or gastroesphageal junction**. *New Eng J Med* 2001, **345**:725–730.

[184] Bosset J, Gignoux M, Triboulet Jea: **Chemoradiotherapy followed by suegery comapred with suegery alone in squamous-cell caner of the esophagus.** *New Eng J Med* 1997, **337**:161–7.

[185] Herskovic A, al Sarraf Mea: **Combined chemotherapy and radiotherapy compared with radiotherapy alone on patients with cancer of the esophagus.** *New Eng J Med* 1992, **326**:1593–8.

[186] Valuckaite V, Zaborina O, Long J, Hauer-Jensen M, Wang J, Holbrook C, Zaborin A, Drabik K, Matthews J, Alverdy J: **Oral PEG 15C20 protects the intestine against radiation: role of lipid rafts**. *Am J Physiol Gastrointest Liver Physiol* 2009, **297**:G1041CG1052.

[187] Potten C, Wilson J: **Apoptosis: The life and death of cells**. *Epubmed-ahead of print* 2004, :136–183.

[188] Potten CS: **Clonogenic, stem and carcinogen-target cells in small intestine**. *Scand J Gastroenterol Suppl* 1984, **104**:3–14.

[189] Jemal A, Siegel R, Ward E, Murray T, Xu J, Thun MJ: **Cancer statistics, 2007**. *CA Cancer J Clin* 2007, **57**:43–66.

[190] Gerike T, Paulus U, Potten C, Loeffler M: **A dynamic model of proliferation and differentiation in the intestinal crypt based on a hypothetical intraepithelial growth factor.** *Cell Prolif.* 1998, **31**(2):93–110.

[191] Meineke F, Potten C, Loeffler M: **Cell migration and organization in the intestinal crypt using a lattice-free model.** *Cell Prolif.* 2001, **34**(4):253–66.

[192] Paulus U, Loeffler M, Zeidler J, Owen G, Potten C: **The differentiation and lineage development of goblet cells in the murine small intestinal crypt: experimental and modelling studies.** *J Cell Sci.* 1993, **106**:473–83.

[193] Paulus U, Potten C, Loeffler M: **A model of the control of cellular regeneration in the intestinal crypt after perturbation based solely on local stem cell regulation.** *Cell Prolif.* 1992, **25**(6):559–78.

[194] Tomlinson I, Bodmer W: **Failure of programmed cell death and differentiation as causes of tumors: some simple mathematical models.** *Proc Natl Acad Sci USA* 1995, **92**(24):11130–4.

[195] Johnston M, Edwards C, Bodmer W, Maini P, Chapman J: **Mathematical modeling of cell population dynamics in the colonic crypt and in colorectal cancer**. *Proc Natl Acad Sci USA* 2007, **104**:4008–4013.

[196] Boman B, Fields J, Bonham-Carter O, Runquist O: **Computer modeling implicates stem cell overproduction in colon cancer initiation.** *Cancer Res.* 2001, **61**(23):8408–11.

[197] Loeffler M, Potten C, Paulus U, Glatzer J, Chwalinski S: **Intestinal crypt proliferation. II. Computer modelling of mitotic index data provides further evidence for lateral and vertical cell migration in the absence of mitotic activity.** *Cell Tissue Kinet* 1988, **21**:247–58.

[198] Barker N, van Es JH, Kuipers J, Kujala P, van den Born M, Cozijnsen M, Haegebarth A, Korving J, Begthel H, Peters PJ, Clevers H: **Identification of stem cells in small intestine and colon by marker gene Lgr5**. *Nature* 2007, **449**(7165):1003–7.

[199] Hermiston ML, Gordon JI: **Organization of the crypt-villus axis and evolution of its stem cell hierarchy during intestinal development**. *Am J Physiol* 1995, **268**(5 Pt 1):G813–22.

[200] Booth C, Potten C: **Gut instincts: thoughts on intestinal epithelial stem cells**. *The Joutnal of Clinical Investigation* 2000, **105**(11):1493–1499.

[201] Bjerknes M, Cheng H: **Modulation of specific intestinal epithelial progenitors by enteric neurons**. *Proc Natl Acad Sci U S A* 2001, **98**(22):12497–502.

[202] Rubin D: **Intestinal morphogenesis**. *Curr Opin gastroenterol.* 2007, **23**(2):111–4.

[203] He X, Zhang J, Li L: **Cellular and molecular regulation of hematopoietic and intestinal stem cell behavior.** *Ann N Y Acad Sci* 2005, **1049**:28–38.

[204] Rijke RP, Hanson WR, Plaisier HM, Osborne JW: **The effect of ischemic villus cell damage on crypt cell proliferation in the small**

intestine: evidence for a feedback control mechanism. *Gastroenterology* 1976, **71**(5):786–92.

[205] Galhaard H, Van Der Meer-Fieggen W, Giesen J: **Feedback control by functioning villus cells on cell proliferation and maturation in intestinal epithelium**. *Exp Cell Res* 1972, **72**:197–207.

[206] Li X, Madison B, Zacharias W, Kolterud A, States D, Gumucio D: **Deconvoluting the intestine: molecular evidence for a major role of the mesenchyme in the modulation of signaling cross talk.** *Physiol Genomics* 2007, **29**(3):290–301.

[207] Ahuja V, Dieckqraefe B, Anant S: **Molecular biology of the small intestine.** *Curr Opin Gastroenterol.* 2006, **22**(2):90–4.

[208] Ishizuya-Oka A: **Regeneration of the amphibian intestinal epithelium under the control of stem cell niche.** *Dev Growth Differ.* 2007, **49**(2):99–107.

[209] Walters J: **Cell and molecular biology of the small intestine: new insights into differentiation, growth and repair.** *Curr Opin Gastroenterol.* 2004, **20**(2):70–6.

[210] Potten C, Loeffler M: **Stem cells: attributes, cycles, spirals, pitfalls and uncertainties. Lessons for and from the crypt.** *Development* 1990, **110**(4):1001–20.

[211] McGarvey MA, O'Kelly F, Ettarh RR: **Nimesulide inhibits crypt epithelial cell proliferation at 6 hours in the small intestine in CD-1 mice**. *Dig Dis Sci* 2007, **52**(9):2087–94.

[212] Mills J, Gordon J: **The intestinl stem cell niche: There grows the neighborhood**. *Proc Natl Acad Sci USA* 2001, **98**:12334–12336.

[213] Barker N, Clevers H: **Tracking down the stem cells of the intestine: strategies to identify adult stem cells**. *Gastroenterology* 2007, **133**(6):1755–60.

[214] Biasco G, Cenacchi G, Nobili E, Pantaleo MA, Calabrese C, Di Febo G, Morselli Labate A, Miglioli M, Br G, i: **Cell proliferation and ultrastructural changes of the duodenal mucosa of patients affected by familial adenomatous polyposis**. *Hum Pathol* 2004, **35**(5):622–6.

[215] Bransom CJ, Boxer ME, Palmer KR, Clark JC, Underwood JC, Duthie HL: **Mucosal cell proliferation in duodenal ulcer and duodenitis**. *Gut* 1981, **22**(4):277–82.

[216] Gorelick F, Sheahan D, DeLuca V: **In Vitro 3H-thymidine uptake in duodenal mucosa from patients with duodenal ulcer or duodenitis**. *Gastroenterlogy* 1979, **76**:1141.

[217] Macdonald WC, Trier JS, Everett NB: **Cell Proliferation and Migration in the Stomach, Duodenum, and Rectum of Man: Radioautographic Studies**. *Gastroenterology* 1964, **46**:405–17.

[218] Booth C, Booth D, Williamson S, Demchyshyn L, Potten CS: **Teduglutide ([Gly2]GLP-2) protects small intestinal stem cells from radiation damage.** *Cell Prolif.* 2004, **37**(6):385–400.

[219] Potten C: **Radiation, the ideal cytotoxic agent for studying the cell biology of tissues such as the small intestine.** *Radiat Res.* 2004, **161**(2):123–36.

[220] Hanski C, Riede E, Gratchev A, Foss HD, Bohm C, Klussmann E, Hummel M, Mann B, Buhr HJ, Stein H, Kim YS, Gum J, Riecken EO: **MUC2 gene suppression in human colorectal carcinomas and their metastases: in vitro evidence of the modulatory role of DNA methylation**. *Lab Invest* 1997, **77**(6):685–95.

[221] Hanski C, Hofmeier M, Schmitt-Graff A, Riede E, Hanski ML, Borchard F, Sieber E, Niedobitek F, Foss HD, Stein H, Riecken EO: **Overexpression or ectopic expression of MUC2 is the common property of mucinous carcinomas of the colon, pancreas, breast, and ovary**. *J Pathol* 1997, **182**(4):385–91.

[222] Huang E, Hynes M, Zhang T, Ginestier C, Dontu G, Appelman H, Fields J, Wicha M, Boman B: **Aldehyde Dehydrogenase 1 Is a Marker for Normal and Malignant Human Colonic Stem Cells (SC) and Tracks SC Overpopulation during Colon Tumorigenesis**. *Cancer Res* 2009, **69**(8):3382–9.

Appendix A

Table 1: Genes that are commonly enriched in S1 through S5

Unigene	GeneSym	Desc	Unigene	GeneSym	Desc
Dr.85699	ZGC:158130	Zgc:158130	Dr.42999	ZGC:110246	Zgc:110246
Dr.126001	PDSS2	Prenyl (decaprenyl) diphosphate synthase, subunit 2	Dr.132918		Transcribed locus
Dr.123192		Transcribed locus	Dr.75117	CKMA	Creatine kinase, muscle a
Dr.104972		Transcribed locus, strongly similar to NP 001001948.1 nucleoporin 54 [Danio rerio]	Dr.82571		Transcribed locus
Dr.83251		Transcribed locus	Dr.75902	ZGC:158387	Zgc:158387
Dr.122767		Transcribed locus	Dr.115973	ARNT2	Similar to Aryl hydrocarbon receptor nuclear translocator 2 (ARNT protein 2) (zfARNT2)
Dr.20961	CPLA2	Cytosolic phospholipase a2	Dr.84284	LOC572016	Hypothetical LOC572016
Dr.80069		Transcribed locus	Dr.82091		Transcribed locus
Dr.105241	SCD	Hypothetical protein LOC792020	Dr.122884		Transcribed locus
Dr.79463	SI:CH211-146M5.2	Si:ch211-146m5.2	Dr.124929	ZGC:113362	Zgc:113362
Dr.132314	ZGC:91794	Zgc:91794	Dr.78538	AGPAT4	1-acylglycerol-3-phosphate O-acyltransferase 4 (lysophosphatidic acid acyltransferase, delta)
Dr.12383	BCMO1	Beta-carotene 15,15'-monooxygenase 1	Dr.78859	KPNA3	Karyopherin (importin) alpha 3
Dr.105556		Transcribed locus, weakly similar to XP 392578.3 PREDICTED: similar to Ank2 CG7462-PB, isoform B [Apis mellifera]	Dr.108126	ZGC:65749	Zgc:65749
Dr.80070		Transcribed locus	Dr.80756	ZGC:77748	Zgc:77748
Dr.36543	AQP8	Aquaporin 8	Dr.76919	TIMM17A	Translocase of inner mitochondrial membrane 17 homolog A (yeast)
Dr.76148	ATP2B1A	ATPase, Ca++ transporting, plasma membrane 1a	Dr.85546	LOC562794	Hypothetical LOC562794
Dr.83800	DHCR7	7-dehydrocholesterol reductase	Dr.21333		Transcribed locus
Dr.123334		Transcribed locus	Dr.75197	ZGC:172243	Zgc:172243
Dr.133403		Transcribed locus	Dr.53929	SNF1LK2B	SNF1-like kinase 2b
Dr.107097	WU:FK81D02	Wu:fk81d02	Dr.3552	ZGC:136371	Zgc:136371
Dr.84413		Transcribed locus	Dr.113895	LOC793400	Hypothetical protein LOC793400
Dr.76999		Transcribed locus	Dr.14238		Transcribed locus
Dr.139852		Transcribed locus	Dr.89530	ZGC:77727	Zgc:77727
Dr.77210	ZGC:112368	Hypothetical protein LOC792169	Dr.77310	ANXA11A	Annexin A11a
Dr.143616	TPI1B	Triosephosphate isomerase 1b	Dr.4883	HSD17B4	Hydroxysteroid (17-beta) dehydrogenase 4
Dr.79004	ZGC:114137	Zgc:114137	Dr.76638	ZGC:77282	Zgc:77282
Dr.80443	ZGC:55398	Zgc:55398	Dr.76874	TEP1	Telomerase-associated protein 1
Dr.105907	LOC796793	Similar to LOC566928 protein	Dr.80057	ZGC:153984	Zgc:153984
Dr.5571		Transcribed locus	Dr.82013	ZGC:153411	Zgc:153411
Dr.78276	SI:DKEY-146N1.1	Si:dkey-146n1.1	Dr.78328	ZGC:91874	Zgc:91874
Dr.138552		Transcribed locus	Dr.81368	ENPP6	Sb:cb727
Dr.132866	ZGC:136551	Zgc:136551	Dr.77198	SERPINB1	Serpin peptidase inhibitor, clade B (ovalbumin), member 1
Dr.19519	ZGC:92440	Zgc:92440	Dr.82469	SCP2	Sterol carrier protein 2
Dr.76067	CNOT6L	CCR4-NOT transcription complex, subunit 6-like	Dr.80041	LOC407663	Hypothetical protein LOC407663
Dr.80025	LOC569162	Hypothetical LOC569162	Dr.41821	WU:FJ47D05	Wu:fj47d05
Dr.105704	CASZ1	Castor zinc finger 1	Dr.120048	LOC100003731	Hypothetical protein LOC100003731
Dr.82567	SI:CH211-284E13.2	Si:ch211-284e13.2	Dr.123008		Transcribed locus
Dr.105901	FAM60AL	Family with sequence similarity 60, member A, like	Dr.80071		Transcribed locus
Dr.78419	MGC162288	Hypothetical LOC562365	Dr.77771	SI:DKEY-252H13.6	Si:dkey-252h13.6
Dr.567	BMP4	Bone morphogenetic protein 4	Dr.81791		Transcribed locus
Dr.75837	STOM	Stomatin	Dr.52663	ZGC:153764	Hypothetical protein LOC791835
Dr.79464		Transcribed locus	Dr.32415		Transcribed locus

Dr.80430	TMEM184A	Transmembrane protein 184a	Dr.76985	CLDN10L	Claudin 10 like
Dr.75182	SDHB	Succinate dehydrogenase complex, subunit B, iron sulfur (Ip)	Dr.38006	CYP2V1	Hypothetical protein LOC792107
Dr.76987	ACE2	Angiotensin I converting enzyme (peptidyl-dipeptidase A) 2	Dr.81863	ZGC:112466	Zgc:112466
Dr.79871	DGAT1	Diacylglycerol O-acyltransferase homolog 1 (mouse)	Dr.115166		Transcribed locus, strongly similar to XP 001341527.1 PREDICTED: hypothetical protein isoform 1 [Danio rerio]
Dr.76365		Transcribed locus	Dr.76896	TMBIM4	Novel protein similar to vertebrate transmembrane BAX inhibitor motif containing 4 (TMBIM4, zgc:64112)
Dr.10050	ADIPOR2	Adiponectin receptor 2	Dr.79911		Transcribed locus
Dr.134285	DAO.2	D-amino-acid oxidase 2	Dr.10898	ZBTB8OS	Zinc finger and BTB domain containing 8 opposite strand
Dr.84719	LOC795901	Hypothetical protein LOC795901	Dr.105092	ZGC:136353	Zgc:136353
Dr.75974	PDZK1L	PDZ domain containing 1 like	Dr.75449		Transcribed locus
Dr.106173	MYO1BL2	Myosin 1b-like 2	Dr.78830	SI:DKEY-267I17.5	Si:dkey-267i17.5
Dr.77685	SLC1A4	Solute carrier family 1 (glutamate/neutral amino acid transporter), member 4	Dr.107471	ZGC:110742	Zgc:110742
Dr.132203	HOXC6A	Homeo box C6a	Dr.78217	ZGC:112992	Zgc:112992
Dr.75963	DAP1A	Death associated protein 1a	Dr.74624	WU:FJ21G01	Wu:fj21g01
Dr.84829	THRAP6	Thyroid hormone receptor associated protein 6	Dr.83284		Transcribed locus
Dr.132277		Transcribed locus	Dr.121549	LOC798137	Similar to Secretory carrier membrane protein 2
Dr.25699	ZGC:77082	Zgc:77082	Dr.107310	SI:CH211-241E15.2	Si:ch211-241e15.2
Dr.81910		Hypothetical LOC558964 (LOC558964), mRNA	Dr.85095		Transcribed locus
Dr.75440		Transcribed locus	Dr.76374	CASPA	Caspase a
Dr.107078	REVERBB1	Rev erb beta 1	Dr.123527		Transcribed locus
Dr.51340	ZGC:77739	Zgc:77739	Dr.4960	MDH1A	Malate dehydrogenase 1a, NAD (soluble)
Dr.77204	ZGC:136771	Zgc:136771	Dr.76507	FAAH2A	Fatty acid amide hydrolase 2a
Dr.12642		Transcribed locus	Dr.115707	PRKRI	Hypothetical protein LOC791666
Dr.78424	CD2APL	CD2-associated protein like	Dr.105991		Transcribed locus
Dr.31637	ZGC:92275	Zgc:92275	Dr.91756		Transcribed locus
Dr.8705	LOC794415	Hypothetical protein LOC794415	Dr.79907	NUCB2B	Nucleobindin 2b
Dr.79949	TM4SF5	Transmembrane 4 L six family member 5	Dr.77336	ZGC:113196	Zgc:113196
Dr.78050	ZGC:73324	Zgc:73324	Dr.78358	LOC100000526	Hypothetical protein LOC100000526
Dr.105434	ZGC:77177	Hypothetical protein LOC791497	Dr.75994	WU:FA56D06	Wu:fa56d06
Dr.76989	ABAT	4-aminobutyrate aminotransferase	Dr.21082	LOC791814	Hypothetical protein LOC791814
Dr.121917		Transcribed locus	Dr.79404		Transcribed locus
Dr.78126	PARP3	Poly (ADP-ribose) polymerase family, member 3	Dr.80699	SLC9A6A	Solute carrier family 9 (sodium/hydrogen exchanger), member 6a
Dr.75549	ZGC:55420	Hypothetical protein LOC792156	Dr.78188	ZGC:110540	Zgc:110540
Dr.42958	OSR2	Hypothetical protein LOC792005	Dr.105248		Transcribed locus, moderately similar to NP 001116831.1 hypothetical protein LOC733162 [Xenopus laevis]
Dr.119936	ZGC:92392	Zgc:92392	Dr.26261		Transcribed locus
Dr.37831	ZGC:103611	Zgc:103611	Dr.121965		Transcribed locus

Dr.124243		Transcribed locus, weakly similar to XP 001515003.1 PREDICTED: similar to sushi domain containing 2 [Ornithorhynchus anatinus]	Dr.132329	LOC100004607	Similar to Apoa4 protein
Dr.123269		Transcribed locus	Dr.110644	SI:DKEY-21K10.1	Si:dkey-21k10.1
Dr.83470	ZGC:123113	Zgc:123113	Dr.26496	GPSN2	Hypothetical protein LOC791459
Dr.107259	SEPP1A	Selenoprotein P, plasma, 1a	Dr.26560	ELOVL5	ELOVL family member 5, elongation of long chain fatty acids (yeast)
Dr.83076		CDNA clone IMAGE:7250984	Dr.78540	IM:7156396	Im:7156396
Dr.133115		Transcribed locus	Dr.80855		Transcribed locus, moderately similar to NP 001012948.1 B-cell CLL/lymphoma 6 (zinc finger protein 51) [Gallus gallus]
Dr.77083	ZGC:86714	Zgc:86714	Dr.132567	ZGC:136791	Zgc:136791
Dr.76671	HMGB3A	High-mobility group box 3a	Dr.5461	LOC402880	Hypothetical protein LOC402880
Dr.78673	LOC571547	Hypothetical LOC571547	Dr.116914	LOC100005579	Hypothetical protein LOC100005579
Dr.76905	ZGC:92744	Zgc:92744	Dr.683	FAM73A	Family with sequence similarity 73, member A
Dr.77157	ZGC:110064	Zgc:110064	Dr.75558	SLC4A2	Solute carrier family 4, anion exchanger, member 2
Dr.76014	CALM2B	Calmodulin 2b, (phosphorylase kinase, delta)	Dr.1301	PRKAG1	Hypothetical protein LOC791615
Dr.105771	LOC100007704	Similar to Slc7a8-prov protein	Dr.84404		Transcribed locus
Dr.117953	PR2Y4L	Pyrimidinergic receptor P2Y, G-protein coupled, 4-like	Dr.86860	ZGC:110017	Zgc:110017
Dr.36830	ZGC:101682	Zgc:101682	Dr.81478	SULT1ST3	Sulfotransferase family 1, cytosolic sulfotransferase 3
Dr.76994	CTH	Cystathionase (cystathionine gamma-lyase)	Dr.4854	LOC795881	Similar to Krt4 protein
Dr.79959		Transcribed locus, strongly similar to XP 001332873.1 PREDICTED: similar to Solute carrier family 15 (oligopeptide transporter), member 1 [Danio rerio]	Dr.6064	LOC100000433	Hypothetical protein LOC100000433
Dr.11921	NR5A5	Nuclear receptor subfamily 5, group A, member 5	Dr.107820	HNF4A	Hepatocyte nuclear factor 4, alpha
Dr.80184	ZGC:101071	Zgc:101071	Dr.85714		Transcribed locus
Dr.14492		Transcribed locus	Dr.77914		Transcribed locus
Dr.36558	EHD3L	EH-domain containing 3, like	Dr.86109	ZGC:100913	Hypothetical LOC554386
Dr.75475	MAFBA	V-maf musculoaponeurotic fibrosarcoma oncogene family, protein B (avian)	Dr.122418		Transcribed locus
Dr.84899	SSP2	Beta-3-galactosyltransferase	Dr.84935	FAM125BB	Family with sequence similarity 125, member B
Dr.16130	ADH8B	Alcohol dehydrogenase 8b	Dr.75118	ZGC:112098	Zgc:112098
Dr.79263	SLC3A2	Solute carrier family 3, member 2	Dr.13867		Transcribed locus
Dr.19659	EZRL	Ezrin like	Dr.80298	ZGC:111859	Zgc:111859
Dr.76395	ZGC:110340	Zgc:110340	Dr.839	LOC571955	Similar to hCG1987869
Dr.81221	C14ORF159	Chromosome 14 open reading frame 159	Dr.35566	ZGC:123283	Zgc:123283
Dr.77311	RBP2A	Retinol binding protein 2a, cellular	Dr.77810	UGT1AA	UDP glucuronosyltransferase 1 family a, a
Dr.81788	TBXAS1	Thromboxane A synthase 1 (platelet, cytochrome P450, family 5, subfamily A)	Dr.86203		Transcribed locus, strongly similar to XP 684040.1 PREDICTED: hypothetical protein [Danio rerio]
Dr.144128	ZGC:109868	Zgc:109868	Dr.81620	ZGC:113305	Hypothetical LOC554551
Dr.76268	CBR1L	Hypothetical protein LOC792137	Dr.72387	LOC557691	Hypothetical LOC557691
Dr.85726		Transcribed locus	Dr.76645		Transcribed locus

Dr.140543		Transcribed locus, moderately similar to NP 775564.1 solute carrier family 43, member 2 [Mus musculus]	Dr.37144		Transcribed locus
Dr.27215	ZGC:92770	Zgc:92770	Dr.4573	LGALS9L1	Hypothetical protein LOC791953
Dr.32551	CCDC124	Coiled-coil domain containing 124	Dr.43242		Transcribed locus, strongly similar to XP 001334092.1 PREDICTED: hypothetical protein [Danio rerio]
Dr.135374	ZGC:113336	Zgc:113336	Dr.21056	ZGC:77734	Zgc:77734
Dr.87549	ZGC:112418	Zgc:112418	Dr.77660	ZGC:100963	Zgc:100963
Dr.109065		Transcribed locus, weakly similar to NP 038841.1 erythrocyte protein band 4.1-like 3 [Mus musculus]	Dr.79916	NR1H4	Nuclear receptor subfamily 1, group H, member 4
Dr.84231	KITLGA	Kit ligand a	Dr.90271	ZGC:114175	Zgc:114175
Dr.76570	SI:CH211-219I10.1	Si:ch211-219i10.1	Dr.26719	ZDHHC16	Zinc finger, DHHC domain containing 16
Dr.77072		Transcribed locus	Dr.27189	LOC567259	Similar to ATP-binding cassette transporter 1
Dr.42009		Transcribed locus	Dr.84913	LOC100000643	Hypothetical protein LOC100000643
Dr.80802	ITPK1	Inositol 1,3,4-triphosphate 5/6 kinase	Dr.79390	ZGC:77868	Zgc:77868
Dr.75352	XPNPEP1	X-prolyl aminopeptidase (aminopeptidase P) 1, soluble	Dr.120392	ADA	Hypothetical protein LOC792200
Dr.81288	MAF	V-maf musculoaponeurotic fibrosarcoma (avian) oncogene homolog	Dr.25212		Transcribed locus
Dr.77103	WU:FB63A08	Wu:fb63a08	Dr.84486	LOC558790	Similar to novel sulfotransferase family protein
Dr.75520	GATM	Glycine amidinotransferase (L-arginine:glycine amidinotransferase)	Dr.77677	ZGC:85681	Zgc:85681
Dr.1574		Transcribed locus	Dr.76436		Transcribed locus
Dr.114529	LOC100003771	Similar to OTTHUMP00000028706	Dr.81614		Transcribed locus
Dr.79906	WU:FD59G01	Wu:fd59g01	Dr.48159		Transcribed locus, weakly similar to XP 001331394.1 PREDICTED: hypothetical protein [Danio rerio]
Dr.107944	ABP1	Amiloride binding protein 1 (amine oxidase (copper-containing))	Dr.121805		Transcribed locus
Dr.84019	ZGC:63614	Zgc:63614	Dr.104708	HIPK2	Homeodomain interacting protein kinase 2
Dr.84574	PCDH2AB2	Hypothetical protein LOC791897	Dr.131199		Transcribed locus
Dr.77107	SCCPDHA	Zgc:174379	Dr.76864	ZGC:65827	Wu:fb52e12
Dr.10429	ZGC:77067	Hypothetical LOC573178	Dr.23502	APOEB	Apolipoprotein Eb
Dr.76924	ZGC:110339	Zgc:110339	Dr.78758	GPD1	Hypothetical protein LOC792059
Dr.3394		Transcribed locus	Dr.79403		Transcribed locus
Dr.34264	GDPD1	Glycerophosphodiester phosphodiesterase domain containing 1	Dr.32530		Transcribed locus
Dr.82025	ZGC:112208	Zgc:112208	Dr.118399	LOC564350	Similar to cytochrome P450
Dr.77381	ZGC:92479	Zgc:92479	Dr.81832	LOC553407	Hypothetical protein LOC100006308
Dr.69146	LOC799188	Hypothetical protein LOC799188	Dr.114385	ZGC:163023	Zgc:163023
Dr.106780	ZGC:63486	Zgc:63486	Dr.86220	ETFA	Electron-transfer-flavoprotein, alpha polypeptide
Dr.76489	ZGC:92763	Zgc:92763	Dr.84970	ZGC:63602	Zgc:63602
Dr.52856	ABCG2A	ATP-binding cassette, sub-family G (WHITE), member 2a	Dr.75844	IDH1	Isocitrate dehydrogenase 1 (NADP+), soluble
Dr.77089	APOA4	Apolipoprotein A-IV	Dr.78000	LOC553341	Hypothetical protein LOC553341
Dr.45492	PTBP1	Polypyrimidine tract binding protein 1	Dr.122295		Transcribed locus

Dr.115882	LOC796920	Hypothetical protein LOC796920	Dr.80224	PSMB9B	Proteasome (prosome, macropain) subunit, beta type, 9b
Dr.23638		Transcribed locus	Dr.76547	ZGC:158323	Zgc:158323
Dr.3325		Transcribed locus	Dr.16380	ALDH8A1	Aldehyde dehydrogenase 8 family, member A1
Dr.83374	LGALS1L2	Lectin, galactoside-binding, soluble, 1 (galectin 1)-like 2	Dr.105242	ZGC:171763	Zgc:171763
Dr.80438	VIL1L	Villin 1 like	Dr.91373	DGAT2	Diacylglycerol O-acyltransferase 2
Dr.143630		Transcribed locus	Dr.24063	ABCC2	ATP-binding cassette, sub-family C (CFTR/MRP), member 2
Dr.105351		Transcribed locus	Dr.80312	GABPB2	Hypothetical LOC554849
Dr.82986		Transcribed locus	Dr.77668	HBL3	Hexose-binding lectin 3
Dr.32732	INVS	Inversin	Dr.11569	OSBPL2	Oxysterol binding protein-like 2
Dr.9564	ZGC:162874	Zgc:162874	Dr.75578	ZGC:92628	Zgc:92628
Dr.76174		Transcribed locus	Dr.13823		Transcribed locus
Dr.82465	ZGC:63528	Zgc:63528	Dr.140680	SHMT2	Serine hydroxymethyltransferase 2 (mitochondrial)
Dr.114249	HAGH	Hydroxyacylglutathione hydrolase	Dr.122973		Transcribed locus
Dr.83673	MET	Similar to c-Met receptor tyrosine kinase	Dr.77043	ZGC:85789	Zgc:85789
Dr.25239	SULT2ST1	Hypothetical protein LOC792298	Dr.122174		Transcribed locus
Dr.140575	CD164	CD164 molecule, sialomucin	Dr.2648	ARPP19	CAMP-regulated phosphoprotein 19
Dr.81250	CBLN1	Cerebellin 1 precursor	Dr.79904	SLC5A8L	Solute carrier family 5 (iodide transporter), member 8-like
Dr.78356	GATA6	GATA-binding protein 6	Dr.76346		Transcribed locus
Dr.78058	MYH11	Myosin, heavy polypeptide 11, smooth muscle	Dr.91916	HLXB9LA	Homeo box HB9 like a
Dr.82536	LOC556236	Hypothetical LOC556236	Dr.79778	OSTF1	Osteoclast stimulating factor 1
Dr.121957		Transcribed locus	Dr.74509	LAD1	Ladinin
Dr.80026		Transcribed locus	Dr.34109	SI:DKEY-91F15.6	Si:dkey-91f15.6
Dr.122838		Transcribed locus	Dr.37073	ZGC:101553	Zgc:101553
Dr.80003		Transcribed locus	Dr.40063	ACO1	Aconitase 1, soluble
Dr.129054		Transcribed locus	Dr.117581	ZGC:154087	Zgc:154087
Dr.1967		Transcribed locus	Dr.81328	SI:CH211-218C17.2	Si:ch211-218c17.2
Dr.76827		Transcribed locus	Dr.80063	RETSAT	Retinol saturase (all-trans-retinol 13,14-reductase)
Dr.82256	ZGC:153186	Zgc:153186	Dr.78118		Transcribed locus
Dr.113556	UGDH	UDP-glucose dehydrogenase	Dr.117819	LOC791911	Hypothetical protein LOC791911
Dr.79378	LOC561658	Hypothetical LOC561658	Dr.123223		Transcribed locus
Dr.133125		Transcribed locus	Dr.134550	ZGC:77906	Zgc:77906
Dr.77166	ZGC:85790	Zgc:85790	Dr.81599	SI:DKEY-98P3.7	Si:dkey-98p3.7
Dr.79900	CX28.9	Connexin 28.9	Dr.78731		Transcribed locus
Dr.2976	SI:CH211-200O3.4	Si:ch211-200o3.4	Dr.76097	ZGC:103594	Zgc:103594
Dr.75775	APOA1	Apolipoprotein A-I	Dr.81163	ZGC:85947	Hypothetical protein LOC791634
Dr.86683	LOC100002984	Hypothetical protein LOC100002984	Dr.77005	YWHAB1	Tyrosine 3-monooxygenase/tryptophan 5-monooxygenase activation protein, beta polypeptide 1
Dr.82554	LOC568302	Hypothetical LOC568302	Dr.77139	RH50	Rh50-like protein
Dr.78711	ACSL4	Acyl-CoA synthetase long-chain family member 4	Dr.83942		Transcribed locus
Dr.111542		Transcribed locus	Dr.14424	ZGC:112518	Zgc:112518
Dr.1479	BLMH	Bleomycin hydrolase	Dr.76783	PLA2G12B	Phospholipase A2, group XIIB
Dr.14156		Transcribed locus	Dr.82199		Transcribed locus
Dr.4955		Transcribed locus	Dr.21703	ZGC:110680	Zgc:110680
Dr.80059	ZGC:92732	Zgc:92732	Dr.107659	ABI1	Abl-interactor 1
Dr.26580	VAPA	VAMP (vesicle-associated membrane protein)-associated protein A	Dr.21094		Transcribed locus, weakly similar to XP 001333287.1 PREDICTED: similar to ENSANGP00000022061 isoform 1 [Danio rerio]
Dr.76256	DSC2L	Desmocollin 2 like	Dr.122419		Transcribed locus

Dr.139822		Transcribed locus	Dr.143586		Transcribed locus, strongly similar to NP 001002205.1 dehydrogenase/reductase (SDR family) member 1 [Danio rerio]
Dr.46547	ZGC:114067	Zgc:114067	Dr.122713		Transcribed locus
Dr.38064	ANXA2B	Hypothetical protein LOC791669	Dr.91379	ZGC:103433	Hypothetical protein LOC791921
Dr.83415		Transcribed locus	Dr.104435	SI:CH211-93F2.1	Si:ch211-93f2.1
Dr.85634	S100A10A	S100 calcium binding protein A10a	Dr.86025		Transcribed locus
Dr.123250		Transcribed locus	Dr.91549	ZGC:111958	Zgc:111958
Dr.105078	CYP1A	Cytochrome P450, family 1, subfamily A	Dr.75691	GORASP2	Golgi reassembly stacking protein 2
Dr.106940	RGL1	Ral guanine nucleotide dissociation stimulator-like 1	Dr.47557	WU:FA18F11	Wu:fa18f11
Dr.90487	ZGC:172295	Zgc:172295	Dr.19947	LMBR1L	Limb region 1 like
Dr.10826		Transcribed locus, weakly similar to XP 424539.2 PREDICTED: similar to PDNP1 [Gallus gallus]	Dr.28990	ZGC:136770	Zgc:136770
Dr.72371	WU:FB60G05	Wu:fb60g05	Dr.121770		Transcribed locus
Dr.140606		Transcribed locus	Dr.2478	TXNDC4	Thioredoxin domain containing 4 (endoplasmic reticulum)
Dr.111731	AQP10	Aquaporin 10	Dr.23314	WAS	Wiskott-Aldrich syndrome (eczema-thrombocytopenia)
Dr.81907	TMEM19	Transmembrane protein 19	Dr.78902		Transcribed locus
Dr.35698	LOC100003669	Hypothetical protein LOC100003669	Dr.117056	ZGC:101030	Hypothetical protein LOC791832
Dr.10893	SARA2	Hypothetical protein LOC792159	Dr.74237	ZGC:101555	Zgc:101555
Dr.78736	WU:FC28F08	Wu:fc28f08	Dr.17457	ZGC:63667	Hypothetical protein LOC100005281
Dr.12800	PTPLB	Protein tyrosine phosphatase-like (proline instead of catalytic arginine), member b	Dr.116678	ZGC:110200	Zgc:110200
Dr.106395		Transcribed locus	Dr.76544		Transcribed locus, strongly similar to NP 001007284.2 deiodinase, iodothyronine, type I [Danio rerio]
Dr.2625		Transcribed locus	Dr.110647	EPHX1	Epoxide hydrolase 1, microsomal (xenobiotic)
Dr.75392	AK3L1	Adenylate kinase 3-like 1	Dr.14176	CTSH	Cathepsin H
Dr.104230	LOC569770	Hypothetical LOC569770	Dr.61277	AK2	Adenylate kinase 2
Dr.23008		Transcribed locus	Dr.20705	ZGC:103537	Zgc:103537
Dr.88645	ZGC:86611	Zgc:86611	Dr.102843		Transcribed locus
Dr.14219	ZGC:64043	Hypothetical protein LOC791889	Dr.75825	NOTCH1B	Notch homolog 1b
Dr.77508	MAO	Monoamine oxidase	Dr.9528	PDK2	Pyruvate dehydrogenase kinase, isoenzyme 2
Dr.11244	GPIA	Glucose phosphate isomerase a	Dr.82585	LOC562304	Similar to cytochrome P450, family 2, subfamily J, polypeptide 2
Dr.87868	SLC5A1	Solute carrier family 5 (sodium/glucose cotransporter), member 1	Dr.76933	WU:FC31G06	Wu:fc31g06
Dr.122079		Transcribed locus	Dr.114476	ZGC:92161	Hypothetical protein LOC791539
Dr.122712	CLIC5	Chloride intracellular channel 5	Dr.88609	TH	Tyrosine hydroxylase
Dr.117328	LOC559563	Hypothetical LOC559563	Dr.75931	CKMT1	Creatine kinase, mitochondrial 1
Dr.105120		Transcribed locus	Dr.76083	DNAJC11	DnaJ (Hsp40) homolog, subfamily C, member 11
Dr.76046	ATP1B1A	ATPase, Na+/K+ transporting, beta 1a polypeptide	Dr.134327	ZGC:85816	Zgc:85816
Dr.75374		Transcribed locus	Dr.80219		Transcribed locus
Dr.82564	ESR2B	Estrogen receptor 2b	Dr.122977		Transcribed locus

Dr.133221		Transcribed locus, moderately similar to XP 001175895.1 PREDICTED: hypothetical protein, partial [Strongylocentrotus purpuratus]	Dr.75906	SLC25A3	Solute carrier family 25 (mitochondrial carrier, phosphate carrier), member 3
Dr.105084	RDHE2	Epidermal retinal dehydrogenase 2	Dr.133710	ZGC:63812	Zgc:174035
Dr.117302	ZGC:92083	Zgc:92083	Dr.76124	ZGC:153978	Zgc:153978
Dr.132305	ZGC:77439	Zgc:77439	Dr.82376	ZGC:63863	Hypothetical protein LOC797468
Dr.83273	ZGC:63960	Zgc:63960	Dr.133174		Transcribed locus, strongly similar to NP 991283.1 testis derived transcript [Danio rerio]
Dr.143409	RORAB	RAR-related orphan receptor A, paralog b	Dr.43950		Transcribed locus
Dr.80724	SULT1ST6	Sulfotransferase family, cytosolic sulfotransferase 6	Dr.120175	HSD11B3	Hydroxysteroid (11-beta) dehydrogenase 3
Dr.77306	UPB1	Ureidopropionase, beta	Dr.77502	ZGC:113301	Hypothetical LOC554606
Dr.122409		Transcribed locus	Dr.3583	ZGC:111843	Zgc:111843
Dr.28948	TWF1B	Twinfilin, actin-binding protein, homolog 1b	Dr.8749	WBP2	WW domain binding protein 2
Dr.77202	RDH1L	Retinol dehydrogenase 1, like	Dr.122701		Transcribed locus
Dr.77343		Transcribed locus	Dr.87576	ZGC:92205	Zgc:92205
Dr.121609		Transcribed locus	Dr.106816	ZGC:154090	Zgc:154090
Dr.21543		Transcribed locus	Dr.88598		Isolate G5197 T-cell receptor alpha variable region
Dr.37032	CYP2J30	Cytochrome P450, family 2, subfamily J, polypeptide 30	Dr.14609		Transcribed locus
Dr.75843	CHPT1	Choline phosphotransferase 1	Dr.108840	RDH12L	Retinol dehydrogenase 12, like
Dr.39606	ZGC:136891	Zgc:136891	Dr.75429	CPT2	Carnitine palmitoyltransferase II
Dr.40298	WU:FB58E08	Wu:fb58e08	Dr.72352	SI:CH211-286M4.4	Si:ch211-286m4.4
Dr.77610	ZGC:101667	Zgc:101667	Dr.79800	LOC569894	Hypothetical LOC569894
Dr.77295	PGD	Phosphogluconate hydrogenase	Dr.121806		Transcribed locus
Dr.132490	ZGC:77867	Zgc:77867	Dr.24921	GPX4B	Glutathione peroxidase 4b
Dr.87714	PKNOX1.2	Pbx/knotted 1 homeobox 1.2	Dr.113808	PLS1	Plastin 1 (I isoform)
Dr.132547		Transcribed locus	Dr.121757		Transcribed locus
Dr.86150		Transcribed locus	Dr.43919	ZGC:112954	Zgc:112954
Dr.87070	ZGC:85680	Zgc:85680	Dr.79889	ZGC:92254	Zgc:92254
Dr.80128	ZGC:158435	Similar to solute carrier family 26 meber 1	Dr.76793	GPX4A	Glutathione peroxidase 4a
Dr.12608	LASS2	LAG1 homolog, ceramide synthase 2 (S. cerevisiae)	Dr.18920	ZGC:136871	Zgc:136871
Dr.32573	RPL11	Ribosomal protein L11	Dr.8695	LOC793786	Hypothetical protein LOC793786
Dr.91521	ZGC:101575	Zgc:101575	Dr.77160	CYP3A65	Cytochrome P450, family 3, subfamily A, polypeptide 65
Dr.88778	GLI1	GLI-Kruppel family member 1	Dr.79664		Transcribed locus
Dr.82435	CH211-106H4.4	Similar to MAM domain containing 4	Dr.82727		Transcribed locus
Dr.122690		Transcribed locus	Dr.76802		Transcribed locus
Dr.115711	LOC567858	Hypothetical LOC567858	Dr.132259	PSMB10	Proteasome (prosome, macropain) subunit, beta type, 10
Dr.29092		Transcribed locus	Dr.82519	FECH	Ferrochelatase
Dr.75229		Transcribed locus	Dr.36376	TFB2M	Transcription factor B2, mitochondrial
Dr.82190	WU:FL05F04	Wu:fl05f04	Dr.42665		Transcribed locus, strongly similar to XP 001333791.1 PREDICTED: hypothetical protein [Danio rerio]
Dr.75372	STARD3NL	STARD3 N-terminal like	Dr.30709	ZGC:92630	Zgc:92630
Dr.131930		Transcribed locus	Dr.5040	CYB5A	Cytochrome b5 type A (microsomal)
Dr.81511	ZGC:113156	Zgc:113156	Dr.76235	ZGC:92631	Zgc:92631
Dr.77009	CA2	Similar to Carbonic anhydrase II	Dr.25277	AGR2	Anterior gradient homolog 2 (Xenopus laevis)
Dr.40624	LOC569148	Hypothetical LOC569148	Dr.81269	PAX2B	Paired box gene 2b

Dr.106515	LOC795458	Similar to ENSANGP00000022061	Dr.77140	RAB1A	RAB1A, member RAS oncogene family
Dr.133084	ZGC:110131	Zgc:110131	Dr.108245	ZGC:113169	Zgc:113169
Dr.143804	TBX18	T-box 18	Dr.82968	GCHFR	GTP cyclohydrolase I feedback regulator
Dr.80987	ZGC:153628	Zgc:153628	Dr.78105	ZGC:56518	Zgc:56518
Dr.76753		Transcribed locus	Dr.76749	CD63	Cd63 antigen
Dr.23444	SERPINB1L3	Serpin peptidase inhibitor, clade B (ovalbumin), member 1, like 3	Dr.85668	RGN	Regucalcin
Dr.15775	DKEY-151P17.3	Plasma membrane proteolipid	Dr.143602		Transcribed locus, strongly similar to XP 001336617.1 PREDICTED: similar to Adenylate kinase 3-like 1 [Danio rerio]
Dr.79965	CYP4V2	Cytochrome P450, family 4, subfamily V, polypeptide 2	Dr.80946		Transcribed locus
Dr.140737		Transcribed locus, moderately similar to NP 957035.1 cysteine dioxygenase, type I [Danio rerio]	Dr.97636		Transcribed locus
Dr.40732	CHCHD7	Coiled-coil-helix-coiled-coil-helix domain containing 7	Dr.114483	LOC799845	Hypothetical protein LOC799845
Dr.26481	EPS8L3	EPS8-like 3	Dr.78519	SPAG1	Sperm associated antigen 1
Dr.19030	ZGC:92360	Zgc:92360	Dr.76983	ZGC:110286	Hypothetical protein LOC791833
Dr.294		Transcribed locus	Dr.39467	ZGC:110312	Zgc:110312
Dr.13438	IM:7145298	Im:7145298	Dr.81276	NOG3	Noggin 3
Dr.118182	ZGC:103681	Zgc:103681	Dr.33603	GPT2	Glutamic pyruvate transaminase (alanine aminotransferase) 2
Dr.77462		Transcribed locus	Dr.43244		Transcribed locus, strongly similar to NP 001017717.1 gamma-butyrobetaine hydroxylase [Danio rerio]
Dr.132693	LOC798331	Hypothetical protein LOC798331	Dr.105736		Transcribed locus
Dr.492		Transcribed locus	Dr.75810	PDX1	Pancreatic and duodenal homeobox 1
Dr.90055	ZGC:112172	Zgc:112172	Dr.24982	ZGC:56585	Hypothetical protein LOC792146
Dr.47275	HNRPKL	Hypothetical protein LOC791602	Dr.75470	LOC563514	Hypothetical LOC563514
Dr.132653	ZGC:162095	Zgc:162095	Dr.133296	YAF2	YY1 associated factor 2
Dr.30247	ZGC:77118	Zgc:113969	Dr.132399	MTX2	Metaxin 2
Dr.77245	COPS4	COP9 constitutive photomorphogenic homolog subunit 4 (Arabidopsis)	Dr.105040	ZGC:162119	Zgc:162119
Dr.125451		Transcribed locus	Dr.77809		Transcribed locus
Dr.79183	ZGC:101040	Zgc:101040	Dr.80201		Transcribed locus
Dr.104488	MAPK12	Mitogen-activated protein kinase 12	Dr.47567	SI:DKEY-30H14.2	Si:dkey-30h14.2
Dr.87644	ZGC:113259	Zgc:113259	Dr.132384	SULT1ST1	Sulfotransferase family, cytosolic sulfotransferase 1
Dr.27131	CD9	CD9 antigen (p24)	Dr.81384	SLC35A5	Solute carrier family 35, member A5
Dr.72337		Transcribed locus, moderately similar to XP 001068011.1 PREDICTED: similar to eukaryotic translation initiation factor 4, gamma 1 isoform a [Rattus norvegicus]	Dr.107707		Transcribed locus
Dr.9584	LOC567688	Similar to hCG28765	Dr.6336	ZGC:77387	Hypothetical protein LOC792296
Dr.20850	FABP7A	Fatty acid binding protein 7, brain, a	Dr.39952	VPS33A	Vacuolar protein sorting 33A
Dr.32636	LOC558298	Similar to stress-activated protein kinase-3	Dr.132343	ZGC:86722	Wu:fb65d05
Dr.1304	ARHGDIA	Rho GDP dissociation inhibitor (GDI) alpha	Dr.79923	GPX1B	Glutathione peroxidase 1b

Dr.77407	SI:DKEY-190L1.1	Si:dkey-190l1.1	Dr.41512	GNG2	Guanine nucleotide binding protein (G protein), gamma 2
Dr.78484	ZGC:85843	Hypothetical protein LOC791495	Dr.123024		Transcribed locus
Dr.82649	ZGC:73259	Zgc:73259	Dr.10121	TFG	TRK-fused gene
Dr.79901		Transcribed locus	Dr.78805	ZGC:56517	Hypothetical protein LOC792074
Dr.144		Transcribed locus	Dr.116160	LOC792335	Hypothetical protein LOC792335
Dr.88724	ZGC:109902	Zgc:109902	Dr.83294	ZGC:92178	Zgc:92178
Dr.36001	LOC571420	Si:dkey-236e20.5	Dr.29419	PPP1CB	Protein phosphatase 1, catalytic subunit, beta isoform
Dr.89328		Transcribed locus	Dr.72357	ZGC:153136	Zgc:153136
Dr.132672	WU:FD46E10	Wu:fd46e10	Dr.86201		Transcribed locus
Dr.132916		Transcribed locus	Dr.118221	ZGC:92349	Zgc:92349
Dr.37828	ZGC:162025	Zgc:162025	Dr.26640	CYP46A1	Cytochrome P450, family 46, subfamily A, polypeptide 1
Dr.100029	ZGC:77732	Zgc:77732	Dr.122414		Transcribed locus
Dr.79847	ZGC:112279	Zgc:112279	Dr.118526	LOC556210	S100 calcium binding protein V1
Dr.23036	ZGC:112282	Zgc:112282	Dr.78399	ZGC:73292	Zgc:73292
Dr.69856	LOC562640	Similar to LOC495046 protein	Dr.76748	CALM3B	Calmodulin 3b (phosphorylase kinase, delta)
Dr.107002		Transcribed locus	Dr.36440	ABHD3	Abhydrolase domain containing 3
Dr.106921	ZGC:110586	Zgc:110586	Dr.80055		Transcribed locus
Dr.37659	BIN2	Bridging integrator 2	Dr.78702	ZGC:92326	Zgc:92326
Dr.83039	GCGA	Glucagon a	Dr.75522	GOT1	Glutamic-oxaloacetic transaminase 1, soluble
Dr.86937		Transcribed locus	Dr.79272	TTC4	Tetratricopeptide repeat domain 4
Dr.2710	TOM1	Similar to target of myb1 (chicken)	Dr.121673		Transcribed locus
Dr.33635	ZGC:110087	Zgc:110087	Dr.76110	COX5AB	Cytochrome c oxidase subunit Vab
Dr.132340		Transcribed locus	Dr.81902	LOC100004225	Hypothetical protein LOC100004225
Dr.80850	PTPN6	Protein tyrosine phosphatase, non-receptor type 6	Dr.12429	NITR4A	Novel immune-type receptor 4a
Dr.77358	ZGC:110411	Zgc:110411	Dr.77116	ZGC:101540	Zgc:101540
Dr.77172	ZGC:153968	Zgc:153968	Dr.86126		Transcribed locus
Dr.78256	IVNS1ABPA	Influenza virus NS1A binding protein a	Dr.77176	LOC571991	Hypothetical LOC571991
Dr.118073	ZGC:110641	Zgc:110641	Dr.76586	ZGC:65964	Zgc:65964
Dr.78765	ZGC:64130	Zgc:64130	Dr.45962	LOC792966	Similar to cathepsin A
Dr.88608	ZGC:92332	Zgc:92332	Dr.75473	LMNB2	Lamin B2
Dr.133388		Transcribed locus	Dr.48703	ZGC:92869	Zgc:113898
Dr.4243	CX32.3	Connexin 32.3	Dr.22246	LOC100008492	Hypothetical protein LOC100008492
Dr.36960	ZGC:91861	Zgc:91861	Dr.21044		Transcribed locus
Dr.75090	IHHB	Hypothetical protein LOC791618	Dr.83192	SI:DKEY-3N22.7	Si:dkey-3n22.7
Dr.52445	LOC553339	Hypothetical protein LOC553339	Dr.76945	S100U	S100 calcium binding protein U
Dr.104980	APOC2	Apolipoprotein C-II	Dr.76319	SRI	Hypothetical protein LOC791966
Dr.122443		Transcribed locus	Dr.78941	WU:FC47E12	Wu:fc47e12
Dr.94336	LOC100004795	Similar to lambda-recombinase-like protein	Dr.81537	ZGC:101021	Zgc:101021
Dr.79516	ZGC:92027	Zgc:92027	Dr.77631		Transcribed locus
Dr.75679		Transcribed locus	Dr.132239	ZGC:153440	Zgc:153440
Dr.97099	RDH1	Retinol dehydrogenase 1	Dr.47346		Transcribed locus
Dr.132874	CYP2J22	Cytochrome P450, family 2, subfamily J, polypeptide 23	Dr.86370	ZGC:77076	Zgc:173915
Dr.91454	ZGC:110410	Zgc:110410	Dr.36480	ZGC:103645	Zgc:103645
Dr.140625		Transcribed locus, moderately similar to NP 999857.1 membrane protein, palmitoylated 1 [Danio rerio]	Dr.77507	MALT1	Mucosa associated lymphoid tissue lymphoma translocation gene 1
Dr.90519	OLFM1A	Olfactomedin 1a	Dr.122020		Transcribed locus
Dr.123452		Transcribed locus	Dr.31094	RBKS	Hypothetical protein LOC792027

Dr.77432	LYRICL	Lyric-like	Dr.79892	KMO	Kynurenine 3-monooxygenase
Dr.79979		Transcribed locus	Dr.76266	PSME2	Proteasome activator subunit 2
Dr.122207		Transcribed locus	Dr.119008	LOC569427	Hypothetical LOC569427
Dr.132155	GATA5	GATA-binding protein 5	Dr.107323	ZGC:56005	Zgc:56005
Dr.80056	DHDDS	Dehydrodolichyl diphosphate synthase	Dr.81091		Transcribed locus
Dr.140798		Transcribed locus, strongly similar to NP 001014389.1 hypothetical protein LOC541554 [Danio rerio]	Dr.80189	LOC559610	Hypothetical LOC559610
Dr.76653	NET1	Neuroepithelial cell transforming gene 1	Dr.80066		Transcribed locus
Dr.121695		Transcribed locus, moderately similar to NP 001117721.1 glucokinase [Oncorhynchus mykiss]	Dr.82169	ZGC:123333	Zgc:123333
Dr.22212	CYP3C1L2	Cytochrome P450, family 3, subfamily c, polypeptide 1 like, 2	Dr.82172	PSMA6B	Proteasome (prosome, macropain) subunit, alpha type, 6b
Dr.38442	ZGC:101874	Zgc:101874	Dr.81866		Transcribed locus
Dr.114244		Transcribed locus, strongly similar to XP 001337510.1 PREDICTED: similar to Major vault protein isoform 1 [Danio rerio]	Dr.42866	MGST1	Microsomal glutathione S-transferase 1
Dr.89100	ALLC	Allantoicase	Dr.132777	ZGC:63493	Zgc:63493
Dr.13779		Transcribed locus	Dr.114908	ZGC:100952	Hypothetical protein LOC791585
Dr.78303		Transcribed locus	Dr.76855	ZGC:66117	Zgc:66117
Dr.82782		Transcribed locus	Dr.79051	ZGC:153507	Zgc:153507
Dr.20277	ACTA2	Actin, alpha 2, smooth muscle, aorta	Dr.105356	ZGC:92026	Zgc:92026
Dr.39930	UGT1AB	Zgc:123097	Dr.79547	IM:6895749	Im:6895749
Dr.85924	PURA	Purine-rich element binding protein A	Dr.81544		Transcribed locus
Dr.83720		Transcribed locus	Dr.27946		Transcribed locus
Dr.84183	LOC100005118	Hypothetical protein LOC100005118	Dr.80870		Transcribed locus
Dr.20376	CLIC4	Chloride intracellular channel 4	Dr.83166	ZGC:101630	Hypothetical LOC573613
Dr.86287	ZGC:63651	Zgc:63651			

Table 2: Genes that are enriched in S1 (in addition to those genes commonly enriched in S1-S5)

Unigene	GeneSym	Desc	Unigene	GeneSym	Desc
Dr.13660	ZGC:101744	Hypothetical protein LOC791489	Dr.122797		Transcribed locus
Dr.79969	LOC566714	Hypothetical LOC566714	Dr.86133	MPP2B	Membrane protein, palmitoylated 2b (MAGUK p55 subfamily member 2b)
Dr.108168	CSAD	Cysteine sulfinic acid decarboxylase	Dr.121301	NITR3A	Novel immune-type receptor 3a
Dr.74715	LOC571260	Zgc:162816	Dr.77866	SI:RP71-39B20.7	Si:rp71-39b20.7
Dr.79354		Transcribed locus	Dr.122503		Transcribed locus
Dr.89216		Transcribed locus	Dr.27305	ZGC:92111	Zgc:92111
Dr.83156		Transcribed locus	Dr.945	PGAM1	Phosphoglycerate mutase 1
Dr.75672	LOC796109	Similar to Eukaryotic translation initiation factor 3, subunit 8	Dr.3585	AGT	Angiotensinogen
Dr.78704	ZGC:66317	Zgc:66317	Dr.80701		Transcribed locus
Dr.80471	ZGC:110537	Hypothetical protein LOC791913	Dr.76457		Transcribed locus, strongly similar to NP 001039312.1 hypothetical protein LOC559391 [Danio rerio]
Dr.79021	ZGC:92903	Zgc:92903	Dr.80635		Transcribed locus
Dr.87802	ZGC:112146	Zgc:112146	Dr.78934	PCF11	Zgc:175013
Dr.82671	SI:CH211-51L3.4	Si:ch211-51l3.4	Dr.22286		Transcribed locus
Dr.75811	INS	Preproinsulin	Dr.29744	SP8L	Sp8 transcription factor-like
Dr.87101	ZGC:110143	Zgc:110143	Dr.85455	ZGC:112432	Zgc:112432
Dr.28449	SLC2A12	Solute carrier family 2 (facilitated glucose transporter), member 12	Dr.75226	KHDRBS1	KH domain containing, RNA binding, signal transduction associated 1
Dr.78375	3-Sep	Septin 3	Dr.78088	ZGC:101000	Zgc:101000
Dr.31849	ZGC:136380	Zgc:158165	Dr.3332	ANGPTL3	Angiopoietin-like 3
Dr.89368	ZGC:103506	Hypothetical protein LOC792269	Dr.82598	STAR	Steroidogenic acute regulatory protein
Dr.10723	TBR1	T-box 1, brain	Dr.17802	LOC796123	Hypothetical protein LOC796123
Dr.76732	GLDC	Glycine dehydrogenase (decarboxylating)	Dr.81274	SEMA3H	Semaphorin 3h
Dr.4621	PIP5K2	Phosphatidylinositol-4-phosphate 5-kinase, type II	Dr.75441	VTNA	Vitronectin a
Dr.77547	ZGC:100868	Zgc:100868	Dr.76353	TIAL1	TIA1 cytotoxic granule-associated RNA binding protein-like 1
Dr.113486	SLC34A2A	Solute carrier family 34 (sodium phosphate), member 2a	Dr.77434	ZGC:56326	Zgc:56326
Dr.122425		Transcribed locus	Dr.86306	LOC100002825	Hypothetical protein LOC100002825
Dr.84337		Transcribed locus	Dr.88913	TH2	Tyrosine hydroxylase 2
Dr.11111		Transcribed locus	Dr.78018	PDSS1	Prenyl (decaprenyl) diphosphate synthase, subunit 1
Dr.84618	ZGC:92762	Zgc:92762	Dr.48573	DISP1	Zgc:111866
Dr.12007	WU:FJ98A08	Wu:fj98a08	Dr.117029	ZGC:112265	Zgc:112265
Dr.84727	CHMP7	CHMP family, member 7	Dr.134435	ZGC:91876	Zgc:91876
Dr.83978	ZGC:110755	Zgc:110755	Dr.83965	ZGC:103754	Zgc:103754
Dr.83818	LOC563332	Similar to PHD finger protein 20 (Hepatocellular carcinoma-associated antigen 58 homolog)	Dr.96078	ZGC:100836	Zgc:100836
Dr.22087		Transcribed locus	Dr.120697	FADS2	Fatty acid desaturase 2
Dr.122080		Transcribed locus	Dr.33222	ZGC:56053	Zgc:56053
Dr.78320	ZGC:110281	Zgc:110281	Dr.79590	BARHL2	BarH-like 2
Dr.81191	LOC793458	Similar to Peptide Y	Dr.81898	ZGC:110741	Zgc:110741
Dr.89227	PPM1E	Protein phosphatase 1E (PP2C domain containing)	Dr.77181	CYP2J28	Ccytochrome P450, family 2, subfamily J, polypeptide 28
Dr.80398	ZGC:153079	Zgc:153079	Dr.77992	MEIS4.1A	Myeloid ecotropic viral integration site 4.1a
Dr.23725		Transcribed locus	Dr.114006	LRRC6L	Leucine-rich repeat-containing 6 like
Dr.54293		Transcribed locus	Dr.133139		Transcribed locus
Dr.76656	CAPN8	Calpain 8	Dr.22416		Transcribed locus

Dr.5169	WU:FC20C02	Wu:fc20c02	Dr.30454	NR5A1B	Nuclear receptor subfamily 5, group A, member 1b
Dr.78089	COX5AA	Cytochrome c oxidase subunit Vaa	Dr.30880	VKORC1L1	Vitamin K epoxide reductase complex, subunit 1-like 1
Dr.80282	ZGC:110141	Zgc:110141	Dr.41381	FAM20B	Family with sequence similarity 20, member B (H. sapiens)
Dr.123399		Transcribed locus, weakly similar to XP 682884.1 PREDICTED: hypothetical protein isoform 1 [Danio rerio]	Dr.115139	PMPCA	Peptidase (mitochondrial processing) alpha
Dr.84633	ABHD2B	Zgc:153750	Dr.83836	ZGC:109965	Zgc:109965
Dr.78779		Transcribed locus	Dr.91088	ZGC:113307	Zgc:113307
Dr.87130	ZGC:85888	Zgc:85888	Dr.74470	JAK1	Janus kinase 1
Dr.75609	BTF3	Basic transcription factor 3			

Table 3: Genes that are enriched in S2 (in addition to those genes commonly enriched in S1-S5)

Unigene	GeneSym	Desc	Unigene	GeneSym	Desc
Dr.13660	ZGC:101744	Hypothetical protein LOC791489	Dr.122797		Transcribed locus
Dr.79969	LOC566714	Hypothetical LOC566714	Dr.86133	MPP2B	Membrane protein, palmitoylated 2b (MAGUK p55 subfamily member 2b)
Dr.108168	CSAD	Cysteine sulfinic acid decarboxylase	Dr.121301	NITR3A	Novel immune-type receptor 3a
Dr.74715	LOC571260	Zgc:162816	Dr.77866	SI:RP71-39B20.7	Si:rp71-39b20.7
Dr.79354		Transcribed locus	Dr.122503		Transcribed locus
Dr.89216		Transcribed locus	Dr.27305	ZGC:92111	Zgc:92111
Dr.83156		Transcribed locus	Dr.945	PGAM1	Phosphoglycerate mutase 1
Dr.75672	LOC796109	Similar to Eukaryotic translation initiation factor 3, subunit 8	Dr.3585	AGT	Angiotensinogen
Dr.78704	ZGC:66317	Zgc:66317	Dr.80701		Transcribed locus
Dr.80471	ZGC:110537	Hypothetical protein LOC791913	Dr.76457		Transcribed locus, strongly similar to NP 001039312.1 hypothetical protein LOC559391 [Danio rerio]
Dr.79021	ZGC:92903	Zgc:92903	Dr.80635		Transcribed locus
Dr.87802	ZGC:112146	Zgc:112146	Dr.78934	PCF11	Zgc:175013
Dr.82671	SI:CH211-51L3.4	Si:ch211-51l3.4	Dr.22286		Transcribed locus
Dr.75811	INS	Preproinsulin	Dr.29744	SP8L	Sp8 transcription factor-like
Dr.87101	ZGC:110143	Zgc:110143	Dr.85455	ZGC:112432	Zgc:112432
Dr.28449	SLC2A12	Solute carrier family 2 (facilitated glucose transporter), member 12	Dr.75226	KHDRBS1	KH domain containing, RNA binding, signal transduction associated 1
Dr.78375	3-Sep	Septin 3	Dr.78088	ZGC:101000	Zgc:101000
Dr.31849	ZGC:136380	Zgc:158165	Dr.3332	ANGPTL3	Angiopoietin-like 3
Dr.89368	ZGC:103506	Hypothetical protein LOC792269	Dr.82598	STAR	Steroidogenic acute regulatory protein
Dr.10723	TBR1	T-box 1, brain	Dr.17802	LOC796123	Hypothetical protein LOC796123
Dr.76732	GLDC	Glycine dehydrogenase (decarboxylating)	Dr.81274	SEMA3H	Semaphorin 3h
Dr.4621	PIP5K2	Phosphatidylinositol-4-phosphate 5-kinase, type II	Dr.75441	VTNA	Vitronectin a
Dr.77547	ZGC:100868	Zgc:100868	Dr.76353	TIAL1	TIA1 cytotoxic granule-associated RNA binding protein-like 1
Dr.113486	SLC34A2A	Solute carrier family 34 (sodium phosphate), member 2a	Dr.77434	ZGC:56326	Zgc:56326
Dr.122425		Transcribed locus	Dr.86306	LOC100002825	Hypothetical protein LOC100002825
Dr.84337		Transcribed locus	Dr.88913	TH2	Tyrosine hydroxylase 2
Dr.11111		Transcribed locus	Dr.78018	PDSS1	Prenyl (decaprenyl) diphosphate synthase, subunit 1
Dr.84618	ZGC:92762	Zgc:92762	Dr.48573	DISP1	Zgc:111866
Dr.12007	WU:FJ98A08	Wu:fj98a08	Dr.117029	ZGC:112265	Zgc:112265
Dr.84727	CHMP7	CHMP family, member 7	Dr.134435	ZGC:91876	Zgc:91876
Dr.83978	ZGC:110755	Zgc:110755	Dr.83965	ZGC:103754	Zgc:103754
Dr.83818	LOC563332	Similar to PHD finger protein 20 (Hepatocellular carcinoma-associated antigen 58 homolog)	Dr.96078	ZGC:100836	Zgc:100836
Dr.22087		Transcribed locus	Dr.120697	FADS2	Fatty acid desaturase 2
Dr.122080		Transcribed locus	Dr.33222	ZGC:56053	Zgc:56053
Dr.78320	ZGC:110281	Zgc:110281	Dr.79590	BARHL2	BarH-like 2
Dr.81191	LOC793458	Similar to Peptide Y	Dr.81898	ZGC:110741	Zgc:110741
Dr.89227	PPM1E	Protein phosphatase 1E (PP2C domain containing)	Dr.77181	CYP2J28	Ccytochrome P450, family 2, subfamily J, polypeptide 28
Dr.80398	ZGC:153079	Zgc:153079	Dr.77992	MEIS4.1A	Myeloid ecotropic viral integration site 4.1a
Dr.23725		Transcribed locus	Dr.114006	LRRC6L	Leucine-rich repeat-containing 6 like
Dr.54293		Transcribed locus	Dr.133139		Transcribed locus
Dr.76656	CAPN8	Calpain 8	Dr.22416		Transcribed locus

Dr.5169	WU:FC20C02	Wu:fc20c02	Dr.30454	NR5A1B	Nuclear receptor subfamily 5, group A, member 1b
Dr.78089	COX5AA	Cytochrome c oxidase subunit Vaa	Dr.30880	VKORC1L1	Vitamin K epoxide reductase complex, subunit 1-like 1
Dr.80282	ZGC:110141	Zgc:110141	Dr.41381	FAM20B	Family with sequence similarity 20, member B (H. sapiens)
Dr.123399		Transcribed locus, weakly similar to XP 682884.1 PREDICTED: hypothetical protein isoform 1 [Danio rerio]	Dr.115139	PMPCA	Peptidase (mitochondrial processing) alpha
Dr.84633	ABHD2B	Zgc:153750	Dr.83836	ZGC:109965	Zgc:109965
Dr.78779		Transcribed locus	Dr.91088	ZGC:113307	Zgc:113307
Dr.87130	ZGC:85888	Zgc:85888	Dr.74470	JAK1	Janus kinase 1
Dr.75609	BTF3	Basic transcription factor 3			

Table 4: Genes that are enriched in S3 (in addition to those genes commonly enriched in S1-S5)

Unigene	GeneSym	Desc	Unigene	GeneSym	Desc
Dr.79635	ZGC:158316	Zgc:158316	Dr.23725		Transcribed locus
Dr.79887	SLC6A19	Solute carrier family 6 (neurotransmitter transporter), member 19	Dr.5169	WU:FC20C02	Wu:fc20c02
Dr.77138	CPA2	Hypothetical protein LOC792272	Dr.78089	COX5AA	Cytochrome c oxidase subunit Vaa
Dr.108168	CSAD	Cysteine sulfinic acid decarboxylase	Dr.80282	ZGC:110141	Zgc:110141
Dr.106275		Transcribed locus	Dr.84633	ABHD2B	Zgc:153750
Dr.79354		Transcribed locus	Dr.87130	ZGC:85888	Zgc:85888
Dr.77514	ELA3L	Elastase 3 like	Dr.84169	ZGC:175098	Zgc:175098
Dr.82353	ELA2	Similar to Ela2 protein	Dr.122797		Transcribed locus
Dr.77126	CTRB1	Chymotrypsinogen B1	Dr.86133	MPP2B	Membrane protein, palmitoylated 2b (MAGUK p55 subfamily member 2b)
Dr.77127	ZGC:66382	Zgc:66382	Dr.121301	NITR3A	Novel immune-type receptor 3a
Dr.80832		Transcribed locus	Dr.77866	SI:RP71-39B20.7	Si:rp71-39b20.7
Dr.83156		Transcribed locus	Dr.122503		Transcribed locus
Dr.47389	CEL.2	Hypothetical protein LOC792128	Dr.945	PGAM1	Phosphoglycerate mutase 1
Dr.75672	LOC796109	Similar to Eukaryotic translation initiation factor 3, subunit 8	Dr.80701		Transcribed locus
Dr.79021	ZGC:92903	Zgc:92903	Dr.80635		Transcribed locus
Dr.75811	INS	Preproinsulin	Dr.78934	PCF11	Zgc:175013
Dr.87101	ZGC:110143	Zgc:110143	Dr.22286		Transcribed locus
Dr.28449	SLC2A12	Solute carrier family 2 (facilitated glucose transporter), member 12	Dr.29744	SP8L	Sp8 transcription factor-like
Dr.78375	3-Sep	Septin 3	Dr.75226	KHDRBS1	KH domain containing, RNA binding, signal transduction associated 1
Dr.31849	ZGC:136380	Zgc:158165	Dr.104993	ZGC:158450	Similar to eukaryotic translation initiation factor 4 gamma, 1
Dr.89368	ZGC:103506	Hypothetical protein LOC792269	Dr.78088	ZGC:101000	Zgc:101000
Dr.10723	TBR1	T-box 1, brain	Dr.82598	STAR	Steroidogenic acute regulatory protein
Dr.76732	GLDC	Glycine dehydrogenase (decarboxylating)	Dr.76099	CDKN1C	Cyclin-dependent kinase inhibitor 1C (p57, Kip2)
Dr.47548	HOXD11A	Homeo box D11a	Dr.17802	LOC796123	Hypothetical protein LOC796123
Dr.77547	ZGC:100868	Zgc:100868	Dr.81274	SEMA3H	Semaphorin 3h
Dr.113486	SLC34A2A	Solute carrier family 34 (sodium phosphate), member 2a	Dr.86306	LOC100002825	Hypothetical protein LOC100002825
Dr.122425		Transcribed locus	Dr.88913	TH2	Tyrosine hydroxylase 2
Dr.77689	ZGC:153769	Zgc:153769	Dr.78018	PDSS1	Prenyl (decaprenyl) diphosphate synthase, subunit 1
Dr.75547	TRY	Trypsin	Dr.48573	DISP1	Zgc:111866
Dr.84337		Transcribed locus	Dr.134435	ZGC:91876	Zgc:91876
Dr.116102	ELA2L	Elastase 2 like	Dr.83965	ZGC:103754	Zgc:103754
Dr.11111		Transcribed locus	Dr.120697	FADS2	Fatty acid desaturase 2
Dr.84618	ZGC:92762	Zgc:92762	Dr.33222	ZGC:56053	Zgc:56053
Dr.12007	WU:FJ98A08	Wu:fj98a08	Dr.79590	BARHL2	BarH-like 2
Dr.84727	CHMP7	CHMP family, member 7	Dr.77181	CYP2J28	Ccytochrome P450, family 2, subfamily J, polypeptide 28
Dr.75138	NOLC1L	Nucleolar and coiled-body phosphoprotein 1-like	Dr.77992	MEIS4.1A	Myeloid ecotropic viral integration site 4.1a
Dr.83978	ZGC:110755	Zgc:110755	Dr.114006	LRRC6L	Leucine-rich repeat-containing 6 like
Dr.83818	LOC563332	Similar to PHD finger protein 20 (Hepatocellular carcinoma-associated antigen 58 homolog)	Dr.133139		Transcribed locus
Dr.22087		Transcribed locus	Dr.22416		Transcribed locus
Dr.76170	ZGC:55429	Zgc:55429	Dr.30454	NR5A1B	Nuclear receptor subfamily 5, group A, member 1b
Dr.89525	P2RX1	Purinergic receptor P2X, ligand-gated ion channel, 1	Dr.30880	VKORC1L1	Vitamin K epoxide reductase complex, subunit 1-like 1

Dr.81191	LOC793458	Similar to Peptide Y	Dr.115139	PMPCA	Peptidase (mitochondrial processing) alpha
Dr.89227	PPM1E	Protein phosphatase 1E (PP2C domain containing)	Dr.83836	ZGC:109965	Zgc:109965
Dr.80398	ZGC:153079	Zgc:153079	Dr.34348	LOC566646	Hypothetical LOC566646

Table 5: Genes that are enriched in S4 (in addition to those genes commonly enriched in S1-S5)

Unigene	GeneSym	Desc	Unigene	GeneSym	Desc
Dr.79635	ZGC:158316	Zgc:158316	Dr.81191	LOC793458	Similar to Peptide Y
Dr.79887	SLC6A19	Solute carrier family 6 (neurotransmitter transporter), member 19	Dr.89227	PPM1E	Protein phosphatase 1E (PP2C domain containing)
Dr.77138	CPA2	Hypothetical protein LOC792272	Dr.80398	ZGC:153079	Zgc:153079
Dr.108168	CSAD	Cysteine sulfinic acid decarboxylase	Dr.23725		Transcribed locus
Dr.106275		Transcribed locus	Dr.5169	WU:FC20C02	Wu:fc20c02
Dr.75792	HOXD9A	Homeo box D9a	Dr.80282	ZGC:110141	Zgc:110141
Dr.123166		Transcribed locus	Dr.84633	ABHD2B	Zgc:153750
Dr.77514	ELA3L	Elastase 3 like	Dr.78779		Transcribed locus
Dr.82353	ELA2	Similar to Ela2 protein	Dr.87130	ZGC:85888	Zgc:85888
Dr.77126	CTRB1	Chymotrypsinogen B1	Dr.84169	ZGC:175098	Zgc:175098
Dr.77127	ZGC:66382	Zgc:66382	Dr.122797		Transcribed locus
Dr.80832		Transcribed locus	Dr.86133	MPP2B	Membrane protein, palmitoylated 2b (MAGUK p55 subfamily member 2b)
Dr.10201	SEPW1	Selenoprotein W, 1	Dr.78888	ZGC:77415	Zgc:77415
Dr.6725		Transcribed locus	Dr.77866	SI:RP71-39B20.7	Si:rp71-39b20.7
Dr.47389	CEL.2	Hypothetical protein LOC792128	Dr.122503		Transcribed locus
Dr.32109	ZGC:91959	Zgc:91959	Dr.945	PGAM1	Phosphoglycerate mutase 1
Dr.77027	KNTC2L	Kinetochore associated 2-like	Dr.80635		Transcribed locus
Dr.75672	LOC796109	Similar to Eukaryotic translation initiation factor 3, subunit 8	Dr.22286		Transcribed locus
Dr.79047	ZGC:113480	Zgc:113480	Dr.29744	SP8L	Sp8 transcription factor-like
Dr.89368	ZGC:103506	Hypothetical protein LOC792269	Dr.78088	ZGC:101000	Zgc:101000
Dr.10723	TBR1	T-box 1, brain	Dr.3332	ANGPTL3	Angiopoietin-like 3
Dr.76732	GLDC	Glycine dehydrogenase (decarboxylating)	Dr.82598	STAR	Steroidogenic acute regulatory protein
Dr.4621	PIP5K2	Phosphatidylinositol-4-phosphate 5-kinase, type II	Dr.17802	LOC796123	Hypothetical protein LOC796123
Dr.47548	HOXD11A	Homeo box D11a	Dr.81274	SEMA3H	Semaphorin 3h
Dr.77547	ZGC:100868	Zgc:100868	Dr.77272	E2F4	E2F transcription factor 4
Dr.113486	SLC34A2A	Solute carrier family 34 (sodium phosphate), member 2a	Dr.76353	TIAL1	TIA1 cytotoxic granule-associated RNA binding protein-like 1
Dr.122425		Transcribed locus	Dr.86306	LOC100002825	Hypothetical protein LOC100002825
Dr.121990		Transcribed locus	Dr.78018	PDSS1	Prenyl (decaprenyl) diphosphate synthase, subunit 1
Dr.77689	ZGC:153769	Zgc:153769	Dr.48573	DISP1	Zgc:111866
Dr.75547	TRY	Trypsin	Dr.134435	ZGC:91876	Zgc:91876
Dr.84337		Transcribed locus	Dr.83965	ZGC:103754	Zgc:103754
Dr.116102	ELA2L	Elastase 2 like	Dr.96078	ZGC:100836	Zgc:100836
Dr.11111		Transcribed locus	Dr.120697	FADS2	Fatty acid desaturase 2
Dr.83578	LOC556669	Hypothetical LOC556669	Dr.33222	ZGC:56053	Zgc:56053
Dr.84618	ZGC:92762	Zgc:92762	Dr.79590	BARHL2	BarH-like 2
Dr.12007	WU:FJ98A08	Wu:fj98a08	Dr.77181	CYP2J28	Ccytochrome P450, family 2, subfamily J, polypeptide 28
Dr.84727	CHMP7	CHMP family, member 7	Dr.77992	MEIS4.1A	Myeloid ecotropic viral integration site 4.1a
Dr.83978	ZGC:110755	Zgc:110755	Dr.114006	LRRC6L	Leucine-rich repeat-containing 6 like
Dr.83818	LOC563332	Similar to PHD finger protein 20 (Hepatocellular carcinoma-associated antigen 58 homolog)	Dr.133139		Transcribed locus
Dr.121574		Transcribed locus	Dr.86192	LOC559127	Similar to AWKS9372
Dr.22087		Transcribed locus	Dr.30880	VKORC1L1	Vitamin K epoxide reductase complex, subunit 1-like 1
Dr.76170	ZGC:55429	Zgc:55429	Dr.115139	PMPCA	Peptidase (mitochondrial processing) alpha
Dr.89525	P2RX1	Purinergic receptor P2X, ligand-gated ion channel, 1	Dr.85728	LOC557582	Hypothetical LOC557582

Table 6: Genes that are enriched in S5 (in addition to those genes commonly enriched in S1-S5)

Unigene	GeneSym	Desc	Unigene	GeneSym	Desc
Dr.79635	ZGC:158316	Zgc:158316	Dr.76170	ZGC:55429	Zgc:55429
Dr.79887	SLC6A19	Solute carrier family 6 (neurotransmitter transporter), member 19	Dr.21244	UCP2	Uncoupling protein 2
Dr.77138	CPA2	Hypothetical protein LOC792272	Dr.132380	CPVL	Carboxypeptidase, vitellogenic-like
Dr.108168	CSAD	Cysteine sulfinic acid decarboxylase	Dr.32320	LGMN	Legumain
Dr.106275		Transcribed locus	Dr.76172	FUCA1	Fucosidase, alpha-L- 1, tissue
Dr.75792	HOXD9A	Homeo box D9a	Dr.5169	WU:FC20C02	Wu:fc20c02
Dr.77514	ELA3L	Elastase 3 like	Dr.80289		Transcribed locus
Dr.82353	ELA2	Similar to Ela2 protein	Dr.80282	ZGC:110141	Zgc:110141
Dr.77126	CTRB1	Chymotrypsinogen B1	Dr.84633	ABHD2B	Zgc:153750
Dr.77127	ZGC:66382	Zgc:66382	Dr.88326	SLC10A2	Solute carrier family 10 (sodium/bile acid cotransporter family), member 2
Dr.89216		Transcribed locus	Dr.78779		Transcribed locus
Dr.32560	ZGC:113564	Zgc:113564	Dr.132230	ZGC:101116	Zgc:101116
Dr.80832		Transcribed locus	Dr.111513	LOC100001879	Similar to Widely-interspaced zinc finger motifs
Dr.83156		Transcribed locus	Dr.87130	ZGC:85888	Zgc:85888
Dr.30882	ZGC:103420	Zgc:103420	Dr.84169	ZGC:175098	Zgc:175098
Dr.78850		Transcribed locus	Dr.86913	FABP6	Fatty acid binding protein 6, ileal (gastrotropin)
Dr.82756	LOC402976	Hypothetical protein LOC402976	Dr.122503		Transcribed locus
Dr.47389	CEL.2	Hypothetical protein LOC792128	Dr.27305	ZGC:92111	Zgc:92111
Dr.32109	ZGC:91959	Zgc:91959	Dr.122381		Transcribed locus
Dr.75672	LOC796109	Similar to Eukaryotic translation initiation factor 3, subunit 8	Dr.80840	LOC564852	Similar to 6-phosphofructo-2-kinase/fructose-2,6-biphosphatase 2
Dr.79021	ZGC:92903	Zgc:92903	Dr.80635		Transcribed locus
Dr.80589	SCPEP1	Serine carboxypeptidase 1	Dr.18814	WU:FI40C08	Wu:fi40c08
Dr.75811	INS	Preproinsulin	Dr.2918	SAFB	Scaffold attachment factor B
Dr.87101	ZGC:110143	Zgc:110143	Dr.132909	SNX14	Sorting nexin 14
Dr.81287	KRML2	Kreisler (mouse) maf-related leucine zipper homolog 2	Dr.75226	KHDRBS1	KH domain containing, RNA binding, signal transduction associated 1
Dr.31849	ZGC:136380	Zgc:158165	Dr.78088	ZGC:101000	Zgc:101000
Dr.10723	TBR1	T-box 1, brain	Dr.3332	ANGPTL3	Angiopoietin-like 3
Dr.85174	CTSL.1	Cathepsin L.1	Dr.83376	ST3GAL3	ST3 beta-galactoside alpha-2,3-sialyltransferase 3
Dr.47548	HOXD11A	Homeo box D11a	Dr.81274	SEMA3H	Semaphorin 3h
Dr.122425		Transcribed locus	Dr.28311	ZGC:152997	Hypothetical protein LOC791544
Dr.77689	ZGC:153769	Zgc:153769	Dr.77272	E2F4	E2F transcription factor 4
Dr.75547	TRY	Trypsin	Dr.76353	TIAL1	TIA1 cytotoxic granule-associated RNA binding protein-like 1
Dr.79066	ACSL1	Acyl-CoA synthetase long-chain family member 1	Dr.88583	FOXD1	Forkhead box D1
Dr.77961	ZGC:92765	Zgc:92765	Dr.88913	TH2	Tyrosine hydroxylase 2
Dr.84337		Transcribed locus	Dr.83965	ZGC:103754	Zgc:103754
Dr.116102	ELA2L	Elastase 2 like	Dr.96078	ZGC:100836	Zgc:100836
Dr.76001	RPS18	Ribosomal protein S18	Dr.91026	LOC100006536	Hypothetical protein LOC100006536
Dr.80969	LOC100004989	Hypothetical protein LOC100004989	Dr.77992	MEIS4.1A	Myeloid ecotropic viral integration site 4.1a
Dr.84618	ZGC:92762	Zgc:92762	Dr.133139		Transcribed locus
Dr.79471		CDNA clone IMAGE:7137180	Dr.86192	LOC559127	Similar to AWKS9372
Dr.84727	CHMP7	CHMP family, member 7	Dr.22416		Transcribed locus
Dr.7668	ZGC:158605	Zgc:158605	Dr.6703	CH211-106H4.12	Hypothetical LOC561742
Dr.88453	ZGC:77182	Zgc:77182	Dr.84960	GRTP1B	Hypothetical protein LOC791767
Dr.83978	ZGC:110755	Zgc:110755	Dr.74470	JAK1	Janus kinase 1

Dr.83818	LOC563332	Similar to PHD finger protein 20 (Hepatocellular carcinoma-associated antigen 58 homolog)	Dr.85728	LOC557582	Hypothetical LOC557582
Dr.121574		Transcribed locus	Dr.34348	LOC566646	Hypothetical LOC566646
Dr.32463	CTSC	Cathepsin C			

Table 7: Genes that are enriched in S6

Unigene	GeneSym	Desc	Unigene	GeneSym	Desc
Dr.83251		Transcribed locus	Dr.80057	ZGC:153984	Zgc:153984
Dr.122767		Transcribed locus	Dr.106493	SHCBP1	Hypothetical LOC554973
Dr.13660	ZGC:101744	Hypothetical protein LOC791489	Dr.80835	SI:CH73-13B6.3	Si:ch73-13b6.3
Dr.80773	RP2	Retinitis pigmentosa 2 (X-linked recessive)	Dr.15182	ZGC:56596	Zgc:56596
Dr.105241	SCD	Hypothetical protein LOC792020	Dr.78671	ZGC:55888	Zgc:55888
Dr.106275		Transcribed locus	Dr.47436	MCM7	Hypothetical LOC554619
Dr.123334		Transcribed locus	Dr.12263	LOC402824	Hypothetical protein LOC402824
Dr.79354		Transcribed locus	Dr.77198	SERPINB1	Serpin peptidase inhibitor, clade B (ovalbumin), member 1
Dr.75384	ZGC:66430	Zgc:66430	Dr.75383	ZGC:110687	Zgc:110687
Dr.75792	HOXD9A	Homeo box D9a	Dr.105413	TPM1	Tropomyosin 1 (alpha)
Dr.77210	ZGC:112368	Hypothetical protein LOC792169	Dr.75920	SMARCE1	SWI/SNF related, matrix associated, actin dependent regulator of chromatin, subfamily e, member 1
Dr.143616	TPI1B	Triosephosphate isomerase 1b	Dr.76710		Transcribed locus
Dr.123166		Transcribed locus	Dr.76848	LOC798717	Hypothetical protein LOC798717
Dr.132573	MT2	Metallothionein 2	Dr.105554	ZGC:173994	Zgc:173994
Dr.77514	ELA3L	Elastase 3 like	Dr.105858	ZGC:112971	Zgc:112971
Dr.78276	SI:DKEY-146N1.1	Si:dkey-146n1.1	Dr.45506	ZGC:112291	Zgc:112291
Dr.132866	ZGC:136551	Zgc:136551	Dr.75731	BTG4	B-cell translocation gene 4
Dr.82353	ELA2	Similar to Ela2 protein	Dr.81117	ZGC:153243	Zgc:153243
Dr.77126	CTRB1	Chymotrypsinogen B1	Dr.123008		Transcribed locus
Dr.105901	FAM60AL	Family with sequence similarity 60, member A, like	Dr.13694	ZGC:163003	Zgc:163003
Dr.78419	MGC162288	Hypothetical LOC562365	Dr.15633	LOC570432	Hypothetical LOC570432
Dr.82877	LOC571645	Similar to sperm associated antigen 9	Dr.77534	ZGC:55702	Zgc:55702
Dr.77127	ZGC:66382	Zgc:66382	Dr.78385	HIC2	Hypermethylated in cancer 2
Dr.89216		Transcribed locus	Dr.87643	ZGC:101827	Zgc:101827
Dr.32560	ZGC:113564	Zgc:113564	Dr.32320	LGMN	Legumain
Dr.79871	DGAT1	Diacylglycerol O-acyltransferase homolog 1 (mouse)	Dr.122870		Transcribed locus, moderately similar to NP 001103190.1 hypothetical protein LOC571939 [Danio rerio]
Dr.157	NFYC	Nuclear transcription factor Y, gamma	Dr.85513	WU:FC54A11	Wu:fc54a11
Dr.85873	EYA4	Eyes absent homolog 4 (Drosophila)	Dr.77771	SI:DKEY-252H13.6	Si:dkey-252h13.6
Dr.134285	DAO.2	D-amino-acid oxidase 2	Dr.114174	ZGC:63569	Hypothetical protein LOC100000446
Dr.117291	WU:FD10H03	Wu:fd10h03	Dr.20974	ZGC:55943	Zgc:55943
Dr.84719	LOC795901	Hypothetical protein LOC795901	Dr.81396	PPIL2	Peptidylprolyl isomerase (cyclophilin)-like 2
Dr.106173	MYO1BL2	Myosin 1b-like 2	Dr.74466	SI:DKEY-264G21.1	Si:dkey-264g21.1
Dr.132203	HOXC6A	Homeo box C6a	Dr.78587	TSC1B	Tuberous sclerosis 1b
Dr.31100	NUDT15	Hypothetical protein LOC791620	Dr.78346	ZGC:152925	Zgc:152925
Dr.10201	SEPW1	Selenoprotein W, 1	Dr.79423	ZGC:114119	Zgc:114119
Dr.76508	DIRC2	Disrupted in renal carcinoma 2	Dr.85158	ZGC:162611	Zgc:162611
Dr.81910		Hypothetical LOC558964 (LOC558964), mRNA	Dr.21063	NKX3.2	NK3 homeobox 2
Dr.75440		Transcribed locus	Dr.75618	ZGC:171444	Zgc:171444
Dr.108202	ZGC:103514	Zgc:103514	Dr.29173	KLF2A	Kruppel-like factor 2a
Dr.83156		Transcribed locus	Dr.78271	ZGC:158414	Zgc:158414
Dr.61171	ALDOAA	Aldolase a, fructose-bisphosphate, a	Dr.13175		Transcribed locus
Dr.2724	SIP1	Survival of motor neuron protein interacting protein 1	Dr.75449		Transcribed locus
Dr.105934		Transcribed locus, strongly similar to NP 001096603.1 hypothetical protein LOC798351 [Danio rerio]	Dr.84876	LOC555985	Hypothetical LOC555985

Dr.78850		Transcribed locus	Dr.78830	SI:DKEY-267I17.5	Si:dkey-267i17.5
Dr.44401	ZGC:153587	Zgc:153587	Dr.9520	NFATC2IP	Nuclear factor of activated T-cells, cytoplasmic, calcineurin-dependent 2 interacting protein
Dr.76387	LOC791684	Hypothetical protein LOC791684	Dr.74207	CH211-271J4.1	Apoptosis-stimulating protein of p53
Dr.78272	C20ORF149L	Chromosome 20 open reading frame 149, like	Dr.81839	ZGC:77563	Zgc:77563
Dr.6725		Transcribed locus	Dr.91044	LOC557719	Hypothetical LOC557719
Dr.8705	LOC794415	Hypothetical protein LOC794415	Dr.121549	LOC798137	Similar to Secretory carrier membrane protein 2
Dr.76646	ZGC:165381	Zgc:165381	Dr.121988		Transcribed locus
Dr.89589	ZGC:101650	Zgc:101650	Dr.79037	ZGC:110259	Zgc:110259
Dr.79949	TM4SF5	Transmembrane 4 L six family member 5	Dr.76979	ZGC:153225	Zgc:153225
Dr.76989	ABAT	4-aminobutyrate aminotransferase	Dr.54293		Transcribed locus
Dr.47389	CEL.2	Hypothetical protein LOC792128	Dr.14775	ZGC:91872	Zgc:91872
Dr.77027	KNTC2L	Kinetochore associated 2-like	Dr.105609	ZGC:110159	Zgc:110159
Dr.79878	DAB2	Disabled homolog 2 (Drosophila)	Dr.97360	ZGC:111826	Zgc:111826
Dr.105771	LOC100007704	Similar to Slc7a8-prov protein	Dr.22874	WU:FC21E07	Wu:fc21e07
Dr.75553	ZGC:112226	Zgc:112226	Dr.115707	PRKRI	Hypothetical protein LOC791666
Dr.78430		Transcribed locus, strongly similar to XP 698433.2 PREDICTED: hypothetical protein [Danio rerio]	Dr.89596	ZGC:103559	Zgc:103559
Dr.23685		Transcribed locus	Dr.75252	COL9A2	Procollagen, type IX, alpha 2
Dr.78704	ZGC:66317	Zgc:66317	Dr.76665	LOC566399	Hypothetical LOC566399
Dr.76994	CTH	Cystathionase (cystathionine gamma-lyase)	Dr.80663	ALG1	Asparagine-linked glycosylation 1 homolog (yeast, beta-1,4-mannosyltransferase)
Dr.31691	LOC562438	Similar to LDLR dan	Dr.83792	ZGC:158807	Zgc:158807
Dr.4044	ZGC:92139	Zgc:92139	Dr.76172	FUCA1	Fucosidase, alpha-L- 1, tissue
Dr.85767	ZGC:92705	Zgc:92705	Dr.132876	ZGC:113984	Zgc:113984
Dr.86277		Transcribed locus	Dr.117460	LOC792416	Hypothetical protein LOC792416
Dr.46022	TPTE	Transmembrane phosphatase with tensin homology	Dr.107744		Transcribed locus
Dr.7323	LOC571692	Hypothetical LOC571692	Dr.117593	LOC799087	Similar to Oip5 protein
Dr.76568	CLYBL	Zgc:136594	Dr.26261		Transcribed locus
Dr.80597	TAF1B	TATA box binding protein (Tbp)-associated factor, RNA polymerase I, B	Dr.80630	ZGC:73340	Zgc:73340
Dr.16130	ADH8B	Alcohol dehydrogenase 8b	Dr.22576	TNKS	Tankyrase, TRF1-interacting ankyrin-related ADP-ribose polymerase
Dr.80471	ZGC:110537	Hypothetical protein LOC791913	Dr.88420	ZGC:101803	Zgc:101803
Dr.12330	WDR33	WD repeat domain 33	Dr.76656	CAPN8	Calpain 8
Dr.78996	ZGC:55661	Zgc:55661	Dr.122289		Transcribed locus
Dr.122702		Transcribed locus	Dr.80332	MCRS1	Microspherule protein 1
Dr.24323	ZGC:56608	Zgc:56608	Dr.29919	METT10D	Methyltransferase 10 domain containing
Dr.81546	TRAPPC6BL	Trafficking protein particle complex 6b-like	Dr.3436	LOC100000870	Hypothetical protein LOC100000870
Dr.75320	HSPD1	Heat shock 60kD protein 1 (chaperonin)	Dr.6975	ZGC:66107	Zgc:66107
Dr.76739	WU:FC44A11	Wu:fc44a11	Dr.75913	MAPK3	Mitogen-activated protein kinase 3
Dr.144128	ZGC:109868	Zgc:109868	Dr.80454	WU:FI20G04	Wu:fi20g04
Dr.140543		Transcribed locus, moderately similar to NP 775564.1 solute carrier family 43, member 2 [Mus musculus]	Dr.5461	LOC402880	Hypothetical protein LOC402880
Dr.78624		Transcribed locus	Dr.23039		Transcribed locus

Dr.6635	SH3BP5LA	SH3-binding domain protein 5-like, a	Dr.80340	WU:FI04F09	Wu:fi04f09
Dr.17300	LOC559362	Hypothetical LOC559362	Dr.117507	ZGC:174575	Zgc:174575
Dr.80589	SCPEP1	Serine carboxypeptidase 1	Dr.79151	PXK	PX domain containing serine/threonine kinase
Dr.81772	SI:BUSM1-241H12.4	Si:busm1-241h12.4	Dr.9174	ZGC:55673	Zgc:55673
Dr.26675	ZGC:55492	Hypothetical LOC554468	Dr.133159		Transcribed locus
Dr.132878	LOC100002850	Similar to Secretory carrier membrane protein 2, like	Dr.77053	WU:FC18A08	Wu:fc18a08
Dr.76472	ZGC:110821	Zgc:110821	Dr.37018	ZGC:112003	Zgc:112003
Dr.82787	IM:7150662	Im:7150662	Dr.75558	SLC4A2	Solute carrier family 4, anion exchanger, member 2
Dr.121617		Transcribed locus	Dr.103297	LOC564151	Similar to Claspin
Dr.81288	MAF	V-maf musculoaponeurotic fibrosarcoma (avian) oncogene homolog	Dr.123677		Transcribed locus
Dr.75131	FBL	Fibrillarin	Dr.113787		Transcribed locus, strongly similar to NP 001070795.1 hypothetical protein LOC768184 [Danio rerio]
Dr.29762	EFNA2	Non-POU domain containing, octamer-binding	Dr.143610	WDR43L	WD repeat domain 43, like
Dr.76196	GSNB	Gelsolin b	Dr.82517	HMX3	Homeo box (H6 family) 3
Dr.107944	ABP1	Amiloride binding protein 1 (amine oxidase (copper-containing))	Dr.78005	MPZ	Sc:d0186
Dr.87101	ZGC:110143	Zgc:110143	Dr.132401	SENP3A	SUMO1/sentrin/SMT3 specific peptidase 3a
Dr.77107	SCCPDHA	Zgc:174379	Dr.80988	PAQR3	Progestin and adipoQ receptor family member III
Dr.79110	SUFU	Suppressor of fused homolog (Drosophila)	Dr.6651	PIAS4	Protein inhibitor of activated STAT, 4
Dr.76972	ZGC:110109	Zgc:110109	Dr.85714		Transcribed locus
Dr.9109	GLMNL	Glomulin, like	Dr.74197	ZGC:153452	Zgc:153452
Dr.81287	KRML2	Kreisler (mouse) maf-related leucine zipper homolog 2	Dr.143864	ZGC:113153	Zgc:113153
Dr.4587	WDR82	WD repeat domain containing 82	Dr.133028	ADIPOR1A	Adiponectin receptor 1a
Dr.34264	GDPD1	Glycerophosphodiester phosphodiesterase domain containing 1	Dr.2657	GATS	Opposite strand transcription unit to Stag3
Dr.84521	LOC560369	Hypothetical LOC560369	Dr.15041		Transcribed locus, strongly similar to XP 001343059.1 PREDICTED: similar to MGC64297 protein [Danio rerio]
Dr.106780	ZGC:63486	Zgc:63486	Dr.80282	ZGC:110141	Zgc:110141
Dr.75949		Transcribed locus	Dr.80187	ZGC:92035	Zgc:92035
Dr.81689	ZGC:55733	Zgc:55733	Dr.143654	ZGC:77183	Zgc:77183
Dr.81475	MMP13	Matrix metalloproteinase 13	Dr.91580	ZGC:171753	Zgc:171753
Dr.80438	VIL1L	Villin 1 like	Dr.82327	ZGC:153958	Zgc:153958
Dr.143630		Transcribed locus	Dr.83069		Transcribed locus
Dr.84463	ZGC:101524	Zgc:101524	Dr.75215	ERG	V-ets erythroblastosis virus E26 oncogene like (avian)
Dr.86029	LOC796017	Hypothetical protein LOC796017	Dr.122141		Transcribed locus, strongly similar to NP 955968.1 STIP1 homology and U-box containing protein 1 [Danio rerio]
Dr.82986		Transcribed locus	Dr.122501	API5	Apoptosis inhibitor 5
Dr.107618		Transcribed locus	Dr.77740	SETD2	SET domain containing 2
Dr.32732	INVS	Inversin	Dr.77595		Transcribed locus
Dr.20429	DLG7	Discs, large homolog 7 (Drosophila)	Dr.83417	BNIP2	BCL2/adenovirus E1B interacting protein 2
Dr.109638	ZGC:114129	Im:7136473	Dr.140596		Transcribed locus
Dr.31849	ZGC:136380	Zgc:158165	Dr.80631	ZDHHC24	Zinc finger, DHHC-type containing 24
Dr.82465	ZGC:63528	Zgc:63528	Dr.18206		Transcribed locus
Dr.5413		Transcribed locus, moderately similar to XP 520446.2 PREDICTED: similar to ANKRD15 protein [Pan troglodytes]	Dr.5549	ZGC:66286	Zgc:66286

Dr.132825	ZGC:64095	Hypothetical protein LOC792222	Dr.80871		Transcribed locus
Dr.114938	H2AFX	H2A histone family, member X	Dr.80632	ZGC:73124	Zgc:73124
Dr.114249	HAGH	Hydroxyacylglutathione hydrolase	Dr.77660	ZGC:100963	Zgc:100963
Dr.39143	ZGC:112982	Zgc:112982	Dr.75730	ZGC:114123	Zgc:114123
Dr.81250	CBLN1	Cerebellin 1 precursor	Dr.268	EPD	Ependymin
Dr.122161		Transcribed locus, strongly similar to NP 001104632.1 hypothetical protein LOC559922 [Danio rerio]	Dr.88635	SI:CH211-139A5.6	Si:ch211-139a5.6
Dr.90586	CAMK2G1	Calcium/calmodulin-dependent protein kinase (CaM kinase) II gamma 1	Dr.79523	ZGC:158289	Zgc:158289
Dr.76410	RAB20	RAB20, member RAS oncogene family	Dr.14396	LOC572175	Similar to Muc2 protein
Dr.122707		Transcribed locus	Dr.79193	MED12	Mediator of RNA polymerase II transcription, subunit 12 homolog
Dr.43915	ZGC:175195	Zgc:175195	Dr.79368	SF3A3	Splicing factor 3a, subunit 3
Dr.79864	LOC556561	Similar to polyhomeotic like 3 (Drosophila)	Dr.84914	ZGC:152928	Zgc:152928
Dr.82256	ZGC:153186	Zgc:153186	Dr.17244	ZGC:56533	Zgc:56533
Dr.84470	LOC797345	Zgc:163126	Dr.28305	HMMR	Hyaluronan mediated motility receptor
Dr.75521	TIMP2	Tissue inhibitor of metalloproteinase 2	Dr.79588	MAP4K5	Mitogen-activated protein kinase kinase kinase kinase 5
Dr.48567	SI:BUSM1-234G15.1	Si:busm1-234g15.1	Dr.118849	ZGC:63958	Zgc:63958
Dr.143593	PCM1	Pericentriolar material 1	Dr.16985	ZGC:162290	Zgc:162290
Dr.26118	ARRDC2	Arrestin domain containing 2	Dr.76745	ZGC:56361	Zgc:56361
Dr.107727	IM:7142942	Im:7142942	Dr.32351	LGALS3L	Lectin, galactoside-binding, soluble, 3 (galectin 3)-like
Dr.75344	HOMEZ	Homeodomain leucine zipper gene	Dr.105126	NPM3	Nucleophosmin/nucleoplasmin, 3
Dr.76317	ZGC:112050	Zgc:112050	Dr.109966		Transcribed locus
Dr.76512	SEPT7A	Septin 7a	Dr.79390	ZGC:77868	Zgc:77868
Dr.3955	LOC798142	Hypothetical protein LOC798142	Dr.120392	ADA	Hypothetical protein LOC792200
Dr.2976	SI:CH211-200O3.4	Si:ch211-200o3.4	Dr.39628	WU:FJ66B05	Wu:fj66b05
Dr.108624	ZGC:86716	Zgc:86716	Dr.133630	ZGC:110329	Zgc:110329
Dr.78373		Transcribed locus	Dr.17340	HNMT	Histamine N-methyltransferase
Dr.76159	APRT	Adenine phosphoribosyl transferase	Dr.13798		Transcribed locus
Dr.83419	ZGC:153301	Hypothetical protein LOC791996	Dr.26907	DND	Dead end
Dr.76296	ZGC:56419	Zgc:56419	Dr.114009		Transcribed locus
Dr.74196	SI:DKEYP-87E7.4	Si:dkeyp-87e7.4	Dr.78599	GTF2B	General transcription factor IIB
Dr.82468	TBC1D19	TBC1 domain family, member 19	Dr.76816	SCNM1	Sodium channel modifier 1
Dr.75224		Transcribed locus	Dr.83427	ZGC:91890	Zgc:91890
Dr.16810	LOC798400	Similar to N-acetylgalactosaminyltransferase	Dr.132230	ZGC:101116	Zgc:101116
Dr.4955		Transcribed locus	Dr.29995	WU:FI27C05	Wu:fi27c05
Dr.80059	ZGC:92732	Zgc:92732	Dr.75243	ZGC:113447	Zgc:113447
Dr.76732	GLDC	Glycine dehydrogenase (decarboxylating)	Dr.96932	ZGC:174234	Zgc:174234
Dr.84109	LOC796103	Similar to Chromosome condensation protein G	Dr.107611	ZGC:110182	Zgc:110182
Dr.84250	LOC563634	Hypothetical LOC563634	Dr.116322	LOC795399	Hypothetical protein LOC795399
Dr.81385	SI:DKEY-24P1.5	Si:dkey-24p1.5	Dr.31566		Transcribed locus
Dr.82345	ASZ1	Ankyrin repeat, SAM and basic leucine zipper domain containing 1	Dr.83494	ZGC:110788	Zgc:110788
Dr.6973	WTAP	Wilms tumor 1 associated protein	Dr.79403		Transcribed locus
Dr.121668		Transcribed locus	Dr.75369	DUS1L	Dihydrouridine synthase 1-like (S. cerevisiae)
Dr.79634	LOC561231	Hypothetical LOC561231	Dr.111513	LOC100001879	Similar to Widely-interspaced zinc finger motifs

Dr.85634	S100A10A	S100 calcium binding protein A10a	Dr.76427		Transcribed locus, moderately similar to NP 071918.1 zinc finger protein 106 homolog [Homo sapiens]
Dr.144133	LOC565165	Hypothetical LOC565165	Dr.76152	LOC560112	Hypothetical LOC560112
Dr.80441	ZGC:171298	Zgc:171298	Dr.78498	ZGC:77560	Zgc:77560
Dr.14153	ZGC:153434	Zgc:153434	Dr.80336	CYP11A1	Cytochrome P450, subfamily XIA, polypeptide 1
Dr.80580	CCNB2	Cyclin B2	Dr.24755	PPP2R2D	Protein phosphatase 2, regulatory subunit B, delta isoform
Dr.81345	LOC798299	Hypothetical protein LOC798299	Dr.82334	ZGC:153929	Zgc:153929
Dr.85174	CTSL.1	Cathepsin L.1	Dr.84169	ZGC:175098	Zgc:175098
Dr.47548	HOXD11A	Homeo box D11a	Dr.3155	LOC100007780	Similar to putative RNA methylase
Dr.132594		Transcribed locus	Dr.122543		Transcribed locus
Dr.88756	ZGC:110238	Hypothetical protein LOC791572	Dr.18504	NSMCE1	Non-SMC element 1 homolog (S. cerevisiae)
Dr.36953	ASAH1	N-acylsphingosine amidohydrolase (acid ceramidase) 1	Dr.75844	IDH1	Isocitrate dehydrogenase 1 (NADP+), soluble
Dr.32947	NUPL1	Nucleoporin like 1	Dr.84313	ELP3	Elongation protein 3 homolog (S. cerevisiae)
Dr.39108	ZGC:154168	Zgc:154168	Dr.80338	ZGC:66432	Zgc:66432
Dr.76852	ZGC:92643	Zgc:92643	Dr.122295		Transcribed locus
Dr.33734	ZGC:110008	Zgc:110008	Dr.67796	ICN	Ictacalcin
Dr.76790	RPA1	Replication protein A1	Dr.75608	ESCO2	Establishment of cohesion 1 homolog 2 (S. cerevisiae)
Dr.6471	ZGC:172228	Zgc:172228	Dr.24234	SMC2	Structural maintenance of chromosomes 2
Dr.117314	ZGC:101843	Zgc:101843	Dr.77600	SRL	Sarcalumenin
Dr.52310	ZGC:123190	Zgc:123190	Dr.33521	KRCP	Kelch repeat-containing protein
Dr.111731	AQP10	Aquaporin 10	Dr.42971	ZGC:112455	Zgc:112455
Dr.76190	CFL1	Cofilin 1 (non-muscle)	Dr.133660		Transcribed locus
Dr.75987	RPP40L	Ribonuclease P 40 subunit like	Dr.16380	ALDH8A1	Aldehyde dehydrogenase 8 family, member A1
Dr.85554	ZGC:112322	Zgc:112322	Dr.76784	SEPT8A	Septin 8a
Dr.35904	ZGC:85729	Zgc:85729	Dr.106681	LOC569952	Hypothetical LOC569952
Dr.1499	TAF9	TAF9 RNA polymerase II, TATA box binding protein (TBP)-associated factor	Dr.79344	ZGC:56407	Zgc:56407
Dr.2713	CD82	Hypothetical protein LOC792047	Dr.78676	SI:CH211-225P5.3	Si:ch211-225p5.3
Dr.35698	LOC100003669	Hypothetical protein LOC100003669	Dr.80428	ZGC:66477	Zgc:66477
Dr.119277	ZGC:101026	Zgc:101026	Dr.77987	ZGC:113026	Zgc:113026
Dr.78736	WU:FC28F08	Wu:fc28f08	Dr.15534	LOC571197	Similar to Thrap4 protein
Dr.76207	AQP3	Aquaporin 3	Dr.132353	RNF14	Ring finger protein 14
Dr.80393	ZGC:66450	Zgc:66450	Dr.31086	RNF2	Ring finger protein 2
Dr.13965		Transcribed locus	Dr.91373	DGAT2	Diacylglycerol O-acyltransferase 2
Dr.122910		Transcribed locus, moderately similar to NP 956523.1 COP9 signalosome subunit 8 [Danio rerio]	Dr.77448	WDR21	WD repeat domain 21
Dr.84502	ZGC:103761	Zgc:103761	Dr.20969	FOXI1	Forkhead box I1
Dr.75392	AK3L1	Adenylate kinase 3-like 1	Dr.85037	CHRNE	Cholinergic receptor, nicotinic, epsilon
Dr.81243	ZGC:86850	Wu:fj61b08	Dr.1823	SI:CH211-150C22.2	Si:ch211-150c22.2
Dr.75265		Transcribed locus	Dr.77976	BYSL	Bystin-like
Dr.88645	ZGC:86611	Zgc:86611	Dr.96184	ZGC:101095	Zgc:101095
Dr.118834	LOC566639	Similar to AHNAK nucleoprotein	Dr.79271	ZGC:77294	Zgc:77294
Dr.104726	ZGC:114097	Zgc:114097	Dr.84790	UNG	Uracil-DNA glycosylase
Dr.34097	PMP22B	Peripheral myelin protein 22b	Dr.28227	IM:7148063	Im:7148063
Dr.77817	ZGC:77086	Hypothetical protein LOC791995	Dr.7461	SI:DKEY-114G7.4	Si:dkey-114g7.4
Dr.83194	CYP1C1	Cytochrome P450, family 1, subfamily C, polypeptide 1	Dr.27090	DOCK8	Similar to dedicator of cytokinesis 8
Dr.80192	ZGC:162158	Zgc:162158	Dr.84534	LOC100007999	Hypothetical protein LOC100007999

Dr.82140	LOC100005813	Similar to sno, strawberry notch homolog 1 (Drosophila)	Dr.78222	ZGC:77529	Zgc:77529
Dr.114277	LOC794653	Similar to MGC84009 protein	Dr.122973		Transcribed locus
Dr.89720	LOC556114	Hypothetical LOC556114	Dr.32210	SEPM	Selenoprotein M
Dr.39753		Transcribed locus, strongly similar to XP 001346081.1 PREDICTED: hypothetical protein [Danio rerio]	Dr.83681	LYZ	Lysozyme
Dr.730	THOC7	THO complex 7	Dr.78487	SI:CH211-191I18.1	Si:ch211-191i18.1
Dr.77508	MAO	Monoamine oxidase	Dr.33564	IPO9	Importin 9
Dr.77582	LOC560453	Similar to KIAA1794	Dr.133114	LOC100000528	Hypothetical protein LOC100000528
Dr.76907	PCBP2	Poly(rC) binding protein 2	Dr.84342	ZGC:92085	Zgc:92085
Dr.28430	SETX	Senataxin	Dr.77007	HIAT1A	Hippocampus abundant transcript 1a
Dr.83081	ZGC:153696	Zgc:153696	Dr.81733	RBBP5	Retinoblastoma binding protein 5
Dr.123669		Transcribed locus, strongly similar to NP 001017864.1 hypothetical protein LOC550562 [Danio rerio]	Dr.28300	ZGC:66024	Zgc:66024
Dr.32093	RAB30	RAB30, member RAS oncogene family	Dr.32244	HSPB1	Heat shock protein, alpha-crystallin-related, 1
Dr.75193	FAM76B	Family with sequence similarity 76, member B	Dr.34109	SI:DKEY-91F15.6	Si:dkey-91f15.6
Dr.52862	LIN7C	Lin-7 homolog C (C. elegans)	Dr.83993	NCBP2	Nuclear cap binding protein subunit 2
Dr.1956		Transcribed locus, strongly similar to XP 702446.2 PREDICTED: hypothetical protein [Danio rerio]	Dr.78113	ZGC:77390	Zgc:77390
Dr.104406	ADRM1B	Adhesion regulating molecule 1b	Dr.37073	ZGC:101553	Zgc:101553
Dr.80692	UBE2Q1	Ubiquitin-conjugating enzyme E2Q (putative) 1	Dr.75129	ARGLU1A	Arginine and glutamate rich 1a
Dr.75468	ZGC:77304	Zgc:77304	Dr.117581	ZGC:154087	Zgc:154087
Dr.75753	NOTCH1A	Notch homolog 1a	Dr.86913	FABP6	Fatty acid binding protein 6, ileal (gastrotropin)
Dr.31752	HDAC1	Histone deacetylase 1	Dr.82719	DAP3	Death associated protein 3
Dr.75451		Transcribed locus	Dr.106771	SI:DKEY-15J16.2	Si:dkey-15j16.2
Dr.77619	RUVBL1	RuvB-like 1 (E. coli)	Dr.76650	ING4	Inhibitor of growth family, member 4
Dr.1489	ZGC:136963	Zgc:136963	Dr.80063	RETSAT	Retinol saturase (all-trans-retinol 13,14-reductase)
Dr.114062	STAP2A	Signal transducing adaptor family member 2a	Dr.80000	SLC25A26	Solute carrier family 25, member 26
Dr.117302	ZGC:92083	Zgc:92083	Dr.80524	WU:FI34B01	Wu:fi34b01
Dr.78703	RTKN2	Rhotekin 2	Dr.119738	SETB	SET translocation (myeloid leukemia-associated) B
Dr.132305	ZGC:77439	Zgc:77439	Dr.78731		Transcribed locus
Dr.83273	ZGC:63960	Zgc:63960	Dr.78888	ZGC:77415	Zgc:77415
Dr.77306	UPB1	Ureidopropionase, beta	Dr.43277	RAD21	RAD21 homolog (S. pombe)
Dr.28948	TWF1B	Twinfilin, actin-binding protein, homolog 1b	Dr.80713	FSHR	Follicle stimulating hormone receptor
Dr.31639	ZGC:112095	Zgc:112095	Dr.140573		Transcribed locus, weakly similar to NP 081830.2 ubiquitin specific peptidase 38 [Mus musculus]
Dr.106380	PRDM8	PR domain containing 8	Dr.104286		Transcribed locus, strongly similar to NP 001071010.2 mitochondrial methionyl-tRNA formyltransferase [Danio rerio]
Dr.4479	SI:CH211-244O22.2	Si:ch211-244o22.2	Dr.37970	SI:RP71-1C10.3	Si:rp71-1c10.3
Dr.75141	ZGC:153228	DNA polymerase nu	Dr.115188	SERINC5	Serine incorporator 5
Dr.100463	SMPD4	Sphingomyelin phosphodiesterase 4	Dr.82751	SSX2IP	Synovial sarcoma, X breakpoint 2 interacting protein
Dr.77454	ZGC:73265	Zgc:73265	Dr.106021	SLC43A1	Solute carrier family 43, member 1

Dr.121609		Transcribed locus	Dr.132611	LOC793280	Hypothetical protein LOC793280
Dr.75547	TRY	Trypsin	Dr.120800	ZGC:92512	Zgc:92512
Dr.105427		Transcribed locus	Dr.41494	WU:FI46G11	Wu:fi46g11
Dr.95737	CCNH	Cyclin H	Dr.74211	TAKRP	T-cell activation kelch repeat protein
Dr.79066	ACSL1	Acyl-CoA synthetase long-chain family member 1	Dr.114283	WU:FD16E03	Wu:fd16e03
Dr.77961	ZGC:92765	Zgc:92765	Dr.75195	BTBD10B	BTB (POZ) domain containing 10b
Dr.82355	ZGC:171819	Zgc:171819	Dr.27305	ZGC:92111	Zgc:92111
Dr.80572	ZGC:103530	Zgc:103530	Dr.76783	PLA2G12B	Phospholipase A2, group XIIB
Dr.37643	ZGC:103509	Zgc:103509	Dr.78545		Transcribed locus
Dr.1786	ZGC:55292	Zgc:55292	Dr.78401	AATF	Apoptosis antagonizing transcription factor
Dr.79972	GOLGA5	Golgi autoantigen, golgin subfamily a, 5	Dr.77471		Transcribed locus
Dr.75202	HDGFRP2	Hepatoma-derived growth factor, related protein 2	Dr.80820	ZGC:85615	Zgc:85615
Dr.75603	H3F3A	H3 histone, family 3A	Dr.107659	ABI1	Abl-interactor 1
Dr.81899	ZGC:56699	Zgc:56699	Dr.31063	ZGC:86895	Zgc:86895
Dr.79720	ZGC:86839	Zgc:86839	Dr.84049	LOC556705	Hypothetical LOC556705
Dr.133457		CDNA clone IMAGE:7053246	Dr.132378	PLS3	Plastin 3 (T isoform)
Dr.116102	ELA2L	Elastase 2 like	Dr.81955		Transcribed locus
Dr.84043	ZGC:86635	Zgc:86635	Dr.81616	LOC569587	Similar to transcription factor-like nuclear regulator
Dr.5696	PRC1	Protein regulator of cytokinesis 1	Dr.106367	PRPSAP2	Phosphoribosyl pyrophosphate synthetase-associated protein 2
Dr.14855	RAB35	RAB35, member RAS oncogene family	Dr.78235	STK38L	Serine/threonine kinase 38 like
Dr.75324	POLA1	Polymerase (DNA directed), alpha 1	Dr.3508	ZGC:101819	Zgc:101819
Dr.142263		Transcribed locus, strongly similar to XP 001332593.1 PREDICTED: similar to L(3)mbt-like 2 (Drosophila) isoform 1 [Danio rerio]	Dr.14066	LOC565592	Similar to hCG32806
Dr.77649	MYST2	MYST histone acetyltransferase 2	Dr.78602	WU:FD14A01	Wu:fd14a01
Dr.106465	LOC799140	Hypothetical protein LOC799140	Dr.122142	ATP1A3B	ATPase, Na+/K+ transporting, alpha 3b polypeptide
Dr.3839		Transcribed locus, strongly similar to XP 001341031.1 PREDICTED: hypothetical protein [Danio rerio]	Dr.118088	HNRNPL	Heterogeneous nuclear ribonucleoprotein L
Dr.75741	ZGC:100869	Zgc:100869	Dr.77174	C3A	Similar to complement C3-H1
Dr.83301	FOXC1B	Forkhead box C1b	Dr.82744	ZGC:92689	Zgc:92689
Dr.15573	RCOR2	REST corepressor 2	Dr.3585	AGT	Angiotensinogen
Dr.82008		CDNA clone IMAGE:8128378	Dr.1291	SUMO3	SMT3 suppressor of mif two 3 homolog 3 (yeast)
Dr.85085	PDLIM7	PDZ and LIM domain 7	Dr.122381		Transcribed locus
Dr.80637	ITGA5	Integrin, alpha 5 (fibronectin receptor, alpha polypeptide)	Dr.91549	ZGC:111958	Zgc:111958
Dr.82521	ZGC:73144	Hypothetical protein LOC792240	Dr.81780	PANE1	Proliferation associated nuclear element
Dr.80659	WU:FI33G05	Wu:fi33g05	Dr.19947	LMBR1L	Limb region 1 like
Dr.115711	LOC567858	Hypothetical LOC567858	Dr.15095	ZGC:113968	Hypothetical protein LOC100001511
Dr.29092		Transcribed locus	Dr.14778	ZGC:103752	Zgc:103752
Dr.75229		Transcribed locus	Dr.76520	ST13	Suppression of tumorigenicity 13 (colon carcinoma) (Hsp70 interacting protein)
Dr.1047	TYMS	Thymidylate synthase	Dr.76187	KRT15	Hypothetical protein LOC791817
Dr.77760	PUS1	Hypothetical protein LOC792133	Dr.132927	RAVER1	Hypothetical protein LOC791538

Dr.88329	HIF1AL2	Hypoxia-inducible factor 1, alpha subunit, like 2	Dr.75458	ARNTL1A	Aryl hydrocarbon receptor nuclear translocator-like 1a
Dr.50843	CD9L	CD9 antigen, like	Dr.78902		Transcribed locus
Dr.84307	ZGC:86870	Zgc:86870	Dr.132373		Transcribed locus
Dr.75748	ORC6L	Origin recognition complex, subunit 6 homolog-like (yeast)	Dr.117056	ZGC:101030	Hypothetical protein LOC791832
Dr.80266	ITM2C	Integral membrane protein 2C	Dr.80821	SPAG6	Sperm associated antigen 6
Dr.114001	ZGC:110183	Zgc:110183	Dr.774	VDAC1	Voltage-dependent anion channel 1
Dr.81511	ZGC:113156	Zgc:113156	Dr.67263	LOC561668	Hypothetical LOC561668
Dr.76676	LOC793260	Hypothetical protein LOC793260	Dr.77751		Transcribed locus
Dr.79544	ING5B	Inhibitor of growth family, member 5b	Dr.91511	LCK	Zgc:136695
Dr.81958	GNAT2	Guanine nucleotide binding protein (G protein), alpha transducing activity polypeptide 2	Dr.82260	LOC565205	Hypothetical LOC565205
Dr.75255		Transcribed locus	Dr.79519	ATP5S	ATP synthase, H+ transporting, mitochondrial F0 complex, subunit s
Dr.105341	RACGAP1	Rac GTPase-activating protein 1	Dr.119419	LOC572149	Similar to Dihydropyrimidine dehydrogenase
Dr.23593	ZGC:56412	Zgc:56412	Dr.20705	ZGC:103537	Zgc:103537
Dr.106684	LOC799913	Similar to cell surface flocculin	Dr.13909		Transcribed locus
Dr.75152	CDK2	Cyclin-dependent kinase 2	Dr.5991	ZGC:101708	Zgc:101708
Dr.77280		Transcribed locus	Dr.9528	PDK2	Pyruvate dehydrogenase kinase, isoenzyme 2
Dr.7036	G3BP1	GTPase activating protein (SH3 domain) binding protein 1	Dr.42600	LOC553397	Hypothetical protein LOC553397
Dr.106515	LOC795458	Similar to ENSANGP00000022061	Dr.20155	SS18	Synovial sarcoma translocation, chromosome 18 (H. sapiens)
Dr.143647	POLD2	Polymerase (DNA directed), delta 2, regulatory subunit	Dr.84971	ZGC:153462	Zgc:153462
Dr.79840	ZGC:92006	Zgc:92006	Dr.82585	LOC562304	Similar to cytochrome P450, family 2, subfamily J, polypeptide 2
Dr.143804	TBX18	T-box 18	Dr.79823	ZGC:91926	Zgc:91926
Dr.79258	LOC100000846	Similar to PHD finger protein 12	Dr.16483	SLC39A6	Solute carrier family 39 (zinc transporter), member 6
Dr.67738	ZGC:153795	Zgc:153795	Dr.76933	WU:FC31G06	Wu:fc31g06
Dr.84500	ZGC:92287	Zgc:92287	Dr.15227		Transcribed locus
Dr.85969	NDUFAF2	NADH dehydrogenase (ubiquinone) 1 alpha subcomplex, assembly factor 2	Dr.80564	RBM38	RNA binding motif protein 38
Dr.81062	PPM1D	Protein phosphatase 1D magnesium-dependent, delta isoform	Dr.113485	LOC100002387	Hypothetical protein LOC100002387
Dr.41866	CRYBB3	Crystallin, beta B3	Dr.75931	CKMT1	Creatine kinase, mitochondrial 1
Dr.36004	ZGC:153454	Zgc:153454	Dr.4757	WU:FB08G06	Wu:fb08g06
Dr.140737		Transcribed locus, moderately similar to NP 957035.1 cysteine dioxygenase, type I [Danio rerio]	Dr.78296	SI:CH211-147A11.3	Si:ch211-147a11.3
Dr.26481	EPS8L3	EPS8-like 3	Dr.83007	ZGC:110677	Zgc:110677
Dr.83578	LOC556669	Hypothetical LOC556669	Dr.121634		Transcribed locus
Dr.52170		Transcribed locus, strongly similar to NP 001002726.1 WD repeat and HMG-box DNA binding protein 1 [Danio rerio]	Dr.79728	LOC564287	Similar to MGC69156 protein
Dr.78694	UTP15	Utp15, U3 small nucleolar ribonucleoprotein, homolog	Dr.106024	WU:FC46H12	Wu:fc46h12
Dr.80609	KIF23	Kinesin family member 23	Dr.121431	LOC563410	Hypothetical LOC563410
Dr.118684	LOC100002310	Hypothetical protein LOC100002310	Dr.80157	ZGC:56161	Zgc:56161

Dr.77945	DNMT5	DNA (cytosine-5-)-methyltransferase 5	Dr.79711	ZGC:158802	Zgc:158802
Dr.109592	ZGC:92151	Zgc:92151	Dr.99488	ZGC:171912	Zgc:171912
Dr.86190	ZGC:86715	Zgc:86715	Dr.39528	LOC100001396	Hypothetical protein LOC100001396
Dr.82476	ZGC:112072	Zgc:112072	Dr.82458	DDX26B	DEAD/H (Asp-Glu-Ala-Asp/His) box polypeptide 26B
Dr.33507	ZGC:123170	Zgc:123170	Dr.86027	LOC100006639	Hypothetical protein LOC100006639
Dr.67664	SI:DKEY-8L13.4	Si:dkey-8l13.4	Dr.2885	FTSJ1	FtsJ homolog 1 (E. coli)
Dr.78239	DDI2	DNA-damage inducible protein 2	Dr.76280	ZGC:152779	Zgc:152779
Dr.119089	TOP2A	Topoisomerase (DNA) II alpha	Dr.75477	RTF1	Rtf1, Paf1/RNA polymerase II complex component, homolog (S. cerevisiae)
Dr.118182	ZGC:103681	Zgc:103681	Dr.18870	ZGC:86619	Zgc:86619
Dr.29859	IM:7142837	Im:7142837	Dr.40661		Transcribed locus
Dr.105784	NASP	Nuclear autoantigenic sperm protein (histone-binding)	Dr.8916	ZGC:110734	Zgc:110734
Dr.394		Transcribed locus, strongly similar to XP 700078.2 PREDICTED: similar to D13S106E-like [Danio rerio]	Dr.81229		Transcribed locus, strongly similar to XP 001332444.1 PREDICTED: similar to sreb2 isoform 1 [Danio rerio]
Dr.78166	PVALB7	Parvalbumin	Dr.132872	ANKRD12	Ankyrin repeat domain 12
Dr.79083	TMEM57	Transmembrane protein 57	Dr.108840	RDH12L	Retinol dehydrogenase 12, like
Dr.4660	LOC100006592	Hypothetical protein LOC100006592	Dr.9441	UTXL1	Ubiquitously transcribed tetratricopeptide repeat, X chromosome like 1
Dr.32436	ZGC:101883	Hypothetical protein LOC792171	Dr.39103	ZGC:101646	Zgc:101646
Dr.75610	BHMT	Betaine-homocysteine methyltransferase	Dr.89166		Transcribed locus
Dr.75815	FOXA	Forkhead box A sequence	Dr.80967	ZGC:112254	Zgc:112254
Dr.86116	ZGC:56589	Novel protein similar to vertebrate phosphatidylinositol glycan anchor biosynthesis, class A (paroxysmal nocturnal hemoglobinuria) (PIGA, zgc:56589)	Dr.84741	ZGC:113085	Zgc:113085
Dr.361	SEPH	Selenoprotein H	Dr.114161	ZGC:112397	Zgc:112397
Dr.87644	ZGC:113259	Zgc:113259	Dr.106470	ZGC:165536	Zgc:165536
Dr.132727	ALDH18A1	Aldehyde dehydrogenase 18 family, member A1	Dr.77969	LOC796797	Hypothetical protein LOC796797
Dr.75779	PL10	Pl10	Dr.50820	LOC565671	Similar to MGC89155 protein
Dr.18376	ZGC:56538	Zgc:56538	Dr.89787	ZGC:113334	Zgc:113334
Dr.114177	DNAJA3A	DnaJ (Hsp40) homolog, subfamily A, member 3A	Dr.123739		Transcribed locus
Dr.9584	LOC567688	Similar to hCG28765	Dr.80660	PLK4	Polo-like kinase 4 (Drosophila)
Dr.77921	LOC564669	Similar to ARVCF	Dr.83896	LOC100005060	Hypothetical protein LOC100005060
Dr.83148	LOC556113	Similar to FLJ00281 protein	Dr.113808	PLS1	Plastin 1 (I isoform)
Dr.104975	ZGC:56513	Zgc:56513	Dr.77001	CDC42EP4	CDC42 effector protein (Rho GTPase binding) 4
Dr.77407	SI:DKEY-190L1.1	Si:dkey-190l1.1	Dr.43919	ZGC:112954	Zgc:112954
Dr.78484	ZGC:85843	Hypothetical protein LOC791495	Dr.82697		Transcribed locus, moderately similar to XP 001345745.1 PREDICTED: hypothetical protein [Danio rerio]
Dr.18312	U2AF1	U2(RNU2) small nuclear RNA auxiliary factor 1	Dr.80478	ZGC:55308	Zgc:55308
Dr.27758	ZGC:85914	Zgc:85914	Dr.79117	SI:DKEY-97O5.1	Si:dkey-97o5.1
Dr.89328		Transcribed locus	Dr.79876	LOC100002142	Hypothetical protein LOC100002142
Dr.33530	SLC38A7	Solute carrier family 38, member 7	Dr.88552	PNX	Hypothetical protein LOC791806
Dr.6442	ZGC:92875	Zgc:92875	Dr.18920	ZGC:136871	Zgc:136871
Dr.82342	DKEY-57A22.11	Similar to CG14692-PA	Dr.8695	LOC793786	Hypothetical protein LOC793786

Dr.67167	SIAH2L	Seven in absentia homolog 2 (Drosophila)-like	Dr.4322	DKEYP-94H10.2	Novel protein similar to vertebrate PAS domain containing serine/threonine kinase (PASK)
Dr.37828	ZGC:162025	Zgc:162025	Dr.105744	ZGC:175186	Zgc:175186
Dr.80456		Transcribed locus, strongly similar to XP 691447.2 PREDICTED: hypothetical protein [Danio rerio]	Dr.134087	C6ORF83	Hypothetical protein LOC100004524
Dr.76462	RBB4	Retinoblastoma binding protein 4	Dr.105605	WU:FJ98G07	Wu:fj98g07
Dr.81636	ZBTB2A	Zinc finger and BTB domain containing 2a	Dr.143375		Transcribed locus
Dr.23036	ZGC:112282	Zgc:112282	Dr.82434	SLA/LPL	Soluble liver antigen/liver pancreas antigen (Homo sapiens), like
Dr.67809	LOC558178	Similar to 19.9kD myosin light chain	Dr.116962	LOC558028	Similar to exosome component 10
Dr.115906	LOC799556	Similar to LOC553285 protein	Dr.120811	ZGC:65845	Zgc:65845
Dr.133627	ZGC:123209	Zgc:123209	Dr.36307	LOC562529	Hypothetical LOC562529
Dr.104586	LOC557328	Similar to XTimeless1	Dr.14549	ZGC:92307	Zgc:92307
Dr.120542	ZGC:63920	Zgc:63920	Dr.83661	GLE1L	GLE1 RNA export mediator-like
Dr.113957	LOC100007887	Similar to LOC559853 protein	Dr.42665		Transcribed locus, strongly similar to XP 001333791.1 PREDICTED: hypothetical protein [Danio rerio]
Dr.37659	BIN2	Bridging integrator 2	Dr.5040	CYB5A	Cytochrome b5 type A (microsomal)
Dr.70549	ARL8	ADP-ribosylation factor-like 8	Dr.25277	AGR2	Anterior gradient homolog 2 (Xenopus laevis)
Dr.4206	ZGC:76977	Hypothetical protein LOC792029	Dr.83536	ZGC:103540	Zgc:103540
Dr.77026		Transcribed locus	Dr.120243	SI:CH211-197I12.2	Si:ch211-197i12.2
Dr.11520	SI:CH211-51E12.7	Si:ch211-51e12.7	Dr.15263	ZGC:73231	Zgc:73231
Dr.75704	PTGDS	Prostaglandin D2 synthase	Dr.140985	ZGC:112365	Zgc:112365
Dr.83502	ZGC:56310	Zgc:56310	Dr.16383	LOC564722	Similar to receptor associated protein 80
Dr.7668	ZGC:158605	Zgc:158605	Dr.79098	MBD1	Methyl-CpG binding domain protein 1
Dr.132734	LOC556271	Hypothetical LOC556271	Dr.133834	ZGC:66359	Zgc:66359
Dr.143646	ZGC:101616	Zgc:101616	Dr.33603	GPT2	Glutamic pyruvate transaminase (alanine aminotransferase) 2
Dr.77484	ZGC:110417	Zgc:110417	Dr.105736		Transcribed locus
Dr.75662	ZGC:114087	Zgc:114087	Dr.77272	E2F4	E2F transcription factor 4
Dr.110716		Transcribed locus	Dr.76937	LOC570063	Similar to MGC115669 protein
Dr.88453	ZGC:77182	Zgc:77182	Dr.132634	HERPUD1	Homocysteine-inducible, endoplasmic reticulum stress-inducible, ubiquitin-like domain member 1
Dr.83525	ZGC:162268	Zgc:162268	Dr.76353	TIAL1	TIA1 cytotoxic granule-associated RNA binding protein-like 1
Dr.75732		Transcribed locus, strongly similar to NP 008855.1 splicing factor, arginine/serine-rich 1 isoform 1 [Homo sapiens]	Dr.5024	PHF16	PHD finger protein 16
Dr.77985	ZGC:92279	Zgc:92279	Dr.113781	ZGC:85851	Zgc:85851
Dr.78765	ZGC:64130	Zgc:64130	Dr.14734	PUS7	Pseudouridylate synthase 7 homolog (S. cerevisiae)
Dr.36931	ZGC:103747	Zgc:103747	Dr.105040	ZGC:162119	Zgc:162119
Dr.90996	SNX33	Sorting nexin 33	Dr.80201		Transcribed locus
Dr.133388		Transcribed locus	Dr.76675	ALDH3D1	Aldehyde dehydrogenase 3 family, member D1
Dr.4243	CX32.3	Connexin 32.3	Dr.77434	ZGC:56326	Zgc:56326
Dr.78916	ARHGEF7B	Rho guanine nucleotide exchange factor (GEF) 7b	Dr.32820	ZGC:56597	Zgc:56597
Dr.86053	TBCCL	Tubulin-specific chaperone c-like	Dr.75970	FLNA	Filamin A, alpha
Dr.36960	ZGC:91861	Zgc:91861	Dr.85904	IM:7143992	Im:7143992

Dr.25142	WDR8	WD repeat domain 8	Dr.80627	B3GAT3	Beta3-glucuronyltransferase
Dr.28229	BCL7A	B-cell CLL/lymphoma 7A	Dr.79578	EXT1A	Exostoses (multiple) 1a
Dr.78604	ZGC:66488	Hypothetical LOC555138	Dr.30395	IRX3B	Iroquois homeobox protein 3b
Dr.133796	ZGC:162319	Zgc:162319	Dr.83245	SKP1	S-phase kinase-associated protein 1
Dr.30339	ZGC:85911	Zgc:85911	Dr.132343	ZGC:86722	Wu:fb65d05
Dr.75170	ACVR1B	Activin A receptor, type IB	Dr.123024		Transcribed locus
Dr.77853	SRPK1	Serine/arginine-rich protein specific kinase 1	Dr.83159	IM:7140357	Im:7140357
Dr.122443		Transcribed locus	Dr.256	SEC61B	SEC61, beta subunit
Dr.106626	LOC559414	Hypothetical LOC559414	Dr.84846		Transcribed locus, strongly similar to XP 690639.2 PREDICTED: similar to alpha-2,3-sialyltransferase ST3Gal I-r2 [Danio rerio]
Dr.117303	CRYGMX	Crystallin, gamma MX	Dr.36499	ZGC:101635	Zgc:101635
Dr.109645	ZGC:152986	Zgc:152986	Dr.75231	CHERP	Calcium homeostasis endoplasmic reticulum protein
Dr.80703	ATXN7L2	Ataxin 7-like 2	Dr.31536	RCL1	RNA terminal phosphate cyclase-like 1
Dr.81503	ZGC:112063	Zgc:112063	Dr.87304	ZGC:77234	Zgc:77234
Dr.75159	WU:FB25B09	Wu:fb25b09	Dr.81961	LOC100002864	Hypothetical protein LOC100002864
Dr.33969	TNNI2B.2	Troponin I, skeletal, fast 2b.2	Dr.96078	ZGC:100836	Zgc:100836
Dr.140625		Transcribed locus, moderately similar to NP 999857.1 membrane protein, palmitoylated 1 [Danio rerio]	Dr.122815		Transcribed locus
Dr.11480	RAP2IP	Rap2 interacting protein	Dr.36440	ABHD3	Abhydrolase domain containing 3
Dr.79148	LOC565706	Similar to cyclic AMP specific phosphodiesterase	Dr.80055		Transcribed locus
Dr.140317	ZGC:110333	Zgc:110333	Dr.105425	ZGC:92164	Zgc:92164
Dr.83943	ZGC:113100	Zgc:113100	Dr.78702	ZGC:92326	Zgc:92326
Dr.75346		Transcribed locus	Dr.76110	COX5AB	Cytochrome c oxidase subunit Vab
Dr.123514		Transcribed locus	Dr.84795	ZGC:113293	Zgc:113293
Dr.79747	MYCL1A	V-myc myelocytomatosis viral oncogene homolog 1, lung carcinoma derived (avian) a	Dr.77870	RNGTT	RNA guanylyltransferase and 5'-phosphatase
Dr.28823		Transcribed locus	Dr.143376	ZGC:86753	Zgc:86753
Dr.13985	ZGC:152948	Hypothetical protein LOC792228	Dr.115125	ZGC:77336	Zgc:77336
Dr.75596	DKEY-79C1.2	Novel protein similar to vertebrate praja family protein	Dr.77116	ZGC:101540	Zgc:101540
Dr.122845		Transcribed locus	Dr.86126		Transcribed locus
Dr.76653	NET1	Neuroepithelial cell transforming gene 1	Dr.77176	LOC571991	Hypothetical LOC571991
Dr.83945	BXDC5	Brix domain containing 5	Dr.45332		Transcribed locus
Dr.123021		Transcribed locus	Dr.82411	SPTLC2	Serine palmitoyltransferase, long chain base subunit 2
Dr.140590		CDNA clone MGC:173911 IMAGE:5915517	Dr.21044		Transcribed locus
Dr.132325	SOX19B	SRY-box containing gene 19b	Dr.72465	ZGC:153103	Zgc:153103
Dr.22945	LOC795535	Hypothetical protein LOC795535	Dr.91026	LOC100006536	Hypothetical protein LOC100006536
Dr.31447	MBTPS2	Membrane-bound transcription factor protease, site 2	Dr.80532	DCP1A	Decapping enzyme
Dr.7577		Transcribed locus, strongly similar to XP 691993.2 PREDICTED: similar to pogo transposable element with ZNF domain [Danio rerio]	Dr.104703	U2AF2A	U2 small nuclear RNA auxiliary factor 2a
Dr.143410		Transcribed locus	Dr.38382	NBEA	Neurobeachin
Dr.89100	ALLC	Allantoicase	Dr.85608	TBPL2	TATA box binding protein like 2

Dr.24325	ZGC:65780	Zgc:65780	Dr.77631		Transcribed locus
Dr.39930	UGT1AB	Zgc:123097	Dr.81898	ZGC:110741	Zgc:110741
Dr.32463	CTSC	Cathepsin C	Dr.24546	ZGC:66327	Hypothetical protein LOC791777
Dr.74638	LOC100007461	Hypothetical protein LOC100007461	Dr.108054	SUPT3H	Suppressor of Ty 3 homolog (S. cerevisiae)
Dr.104982	WU:FB55E05	Wu:fb55e05	Dr.76556	ZGC:110112	Hypothetical protein LOC792281
Dr.80745		Oogenesis-related protein	Dr.80679	ZGC:112364	Zgc:112364
Dr.89609	LOC558120	Hypothetical LOC558120	Dr.86370	ZGC:77076	Zgc:173915
Dr.74222	SI:CH211-81I17.1	Si:ch211-81i17.1	Dr.83002	ZGC:101657	Zgc:101657
Dr.75117	CKMA	Creatine kinase, muscle a	Dr.85461	ZGC:56706	Zgc:56706
Dr.74031	SI:DKEY-202B22.2	Si:dkey-202b22.2	Dr.119008	LOC569427	Hypothetical LOC569427
Dr.82571		Transcribed locus	Dr.16782		Transcribed locus
Dr.80488	PPP1R10	Protein phosphatase 1, regulatory subunit 10	Dr.85829	CETN2	Centrin, EF-hand protein, 2
Dr.91347	ZGC:113381	Zgc:113381	Dr.132294	NOL14	Hypothetical protein LOC792320
Dr.32625	STKA	Wu:fa09g06	Dr.110726	LOC572168	Hypothetical LOC572168
Dr.82091		Transcribed locus	Dr.86192	LOC559127	Similar to AWKS9372
Dr.7724	ZGC:154063	Zgc:154063	Dr.107641	LOC569277	Similar to ubiquitously transcribed tetratricopeptide repeat, X chromosome
Dr.45587	ZGC:110611	Zgc:110611	Dr.80066		Transcribed locus
Dr.33127	IFRD2	Interferon-related developmental regulator 2	Dr.82169	ZGC:123333	Zgc:123333
Dr.79190	ZGC:158607	Zgc:158607	Dr.82451	CDC42EP2	CDC42 effector protein (Rho GTPase binding) 2
Dr.132448		Transcribed locus	Dr.143590	ZGC:85948	Zgc:85948
Dr.29131	ZGC:56476	Zgc:56476	Dr.132789		Transcribed locus, strongly similar to XP 001333536.1 PREDICTED: hypothetical protein [Danio rerio]
Dr.105269	SUPT16H	Suppressor of Ty 16 homolog	Dr.6703	CH211-106H4.12	Hypothetical LOC561742
Dr.85496	FANCL	Fanconi anemia, complementation group L	Dr.84866	LOC100005159	Hypothetical protein LOC100005159
Dr.21244	UCP2	Uncoupling protein 2	Dr.2877	WU:FB08E07	Wu:fb08e07
Dr.82168		Transcribed locus, strongly similar to NP 001004652.1 COX17 cytochrome c oxidase assembly homolog [Danio rerio]	Dr.81115		Transcribed locus
Dr.84467	ZGC:56388	Zgc:56388	Dr.42866	MGST1	Microsomal glutathione S-transferase 1
Dr.79437	ZGC:110299	Hypothetical LOC557968	Dr.123167		Transcribed locus
Dr.41980	ARID3B	AT rich interactive domain 3B (Bright like)	Dr.76453	ARL4D	ADP-ribosylation factor-like 4D
Dr.80756	ZGC:77748	Zgc:77748	Dr.7628	ZGC:158611	Zgc:158611
Dr.115569	ATXN3	Ataxin 3	Dr.77441	ZGC:64148	Zgc:64148
Dr.81807	LOC100002531	Hypothetical protein LOC100002531	Dr.82147	SI:DKEY-274C14.3	Si:dkey-274c14.3
Dr.9860	MDH1B	Malate dehydrogenase 1b, NAD (soluble)	Dr.78511	LOC559941	Similar to Rho-guanine nucleotide exchange factor
Dr.75940	DEF	Digestive-organ expansion factor	Dr.43999	CGNL1	Cingulin-like 1
Dr.124001		Transcribed locus	Dr.10250	TDH	L-threonine dehydrogenase
Dr.3552	ZGC:136371	Zgc:136371	Dr.133306	CHM	Choroideremia
Dr.122080		Transcribed locus	Dr.16206	ZGC:153334	Zgc:153334
Dr.80074	POP4	Hypothetical LOC554559	Dr.105356	ZGC:92026	Zgc:92026
Dr.121869		Transcribed locus, moderately similar to NP 001035095.1 transcription elongation regulator 1 isoform 2 [Homo sapiens]	Dr.77776	SI:CH211-59D15.5	Si:ch211-59d15.5
Dr.14064	ZGC:55418	Zgc:55418	Dr.81544		Transcribed locus
Dr.51681	LOC799717	Hypothetical protein LOC799717	Dr.116711	LOC561733	Hypothetical LOC561733
Dr.78991	LOC100006201	Hypothetical protein LOC100006201	Dr.75239	WU:FB74B10	Wu:fb74b10
Dr.115855	TK2	Hypothetical protein LOC791677	Dr.85728	LOC557582	Hypothetical LOC557582
Dr.114689	FAM116B	Family with sequence similarity 116, member B	Dr.28581	OPHN1	Oligophrenin 1
Dr.13689	ZGC:66449	Zgc:66449	Dr.121941		Transcribed locus

Dr.4883	HSD17B4	Hydroxysteroid (17-beta) dehydrogenase 4	Dr.76567	RGS7	Regulator of G-protein signalling 7
Dr.18318	SNRPC	Small nuclear ribonucleoprotein polypeptide C	Dr.76198	IM:7150932	Im:7150932
Dr.36457	PPP2R1B	Protein phosphatase 2 (formerly 2A), regulatory subunit A, beta isoform	Dr.75142	SI:CH211-197G15.1	Si:ch211-197g15.1
Dr.78320	ZGC:110281	Zgc:110281			

Table 8: Genes that are enriched in S7

Unigene	GeneSym	Desc	Unigene	GeneSym	Desc
Dr.85699	ZGC:158130	Zgc:158130	Dr.76238	SC:D0144	Sc:d0144
Dr.104972		Transcribed locus, strongly similar to NP 001001948.1 nucleoporin 54 [Danio rerio]	Dr.79262	FBXO5	F-box protein 5
Dr.83251		Transcribed locus	Dr.121869		Transcribed locus, moderately similar to NP 001035095.1 transcription elongation regulator 1 isoform 2 [Homo sapiens]
Dr.122767		Transcribed locus	Dr.51681	LOC799717	Hypothetical protein LOC799717
Dr.13660	ZGC:101744	Hypothetical protein LOC791489	Dr.78991	LOC100006201	Hypothetical protein LOC100006201
Dr.77138	CPA2	Hypothetical protein LOC792272	Dr.77310	ANXA11A	Annexin A11a
Dr.80069		Transcribed locus	Dr.76874	TEP1	Telomerase-associated protein 1
Dr.105241	SCD	Hypothetical protein LOC792020	Dr.78320	ZGC:110281	Zgc:110281
Dr.132314	ZGC:91794	Zgc:91794	Dr.80638	WU:FE05B03	Wu:fe05b03
Dr.76148	ATP2B1A	ATPase, Ca++ transporting, plasma membrane 1a	Dr.106493	SHCBP1	Hypothetical LOC554973
Dr.83800	DHCR7	7-dehydrocholesterol reductase	Dr.81476	SI:DKEY-171O17.7	Si:dkey-171o17.7
Dr.106275		Transcribed locus	Dr.80835	SI:CH73-13B6.3	Si:ch73-13b6.3
Dr.123334		Transcribed locus	Dr.76339	UBE4B	Ubiquitination factor E4B, UFD2 homolog (S. cerevisiae)
Dr.133403		Transcribed locus	Dr.47436	MCM7	Hypothetical LOC554619
Dr.107097	WU:FK81D02	Wu:fk81d02	Dr.77198	SERPINB1	Serpin peptidase inhibitor, clade B (ovalbumin), member 1
Dr.75792	HOXD9A	Homeo box D9a	Dr.84455	ZGC:92240	Zgc:92240
Dr.123166		Transcribed locus	Dr.75383	ZGC:110687	Zgc:110687
Dr.77514	ELA3L	Elastase 3 like	Dr.105413	TPM1	Tropomyosin 1 (alpha)
Dr.82353	ELA2	Similar to Ela2 protein	Dr.75920	SMARCE1	SWI/SNF related, matrix associated, actin dependent regulator of chromatin, subfamily e, member 1
Dr.77126	CTRB1	Chymotrypsinogen B1	Dr.122296		Transcribed locus
Dr.77127	ZGC:66382	Zgc:66382	Dr.105858	ZGC:112971	Zgc:112971
Dr.89216		Transcribed locus	Dr.45506	ZGC:112291	Zgc:112291
Dr.115420	TH1L	TH1-like (Drosophila)	Dr.81117	ZGC:153243	Zgc:153243
Dr.32560	ZGC:113564	Zgc:113564	Dr.134857	ZGC:113294	Zgc:113294
Dr.85873	EYA4	Eyes absent homolog 4 (Drosophila)	Dr.13694	ZGC:163003	Zgc:163003
Dr.10050	ADIPOR2	Adiponectin receptor 2	Dr.80584	LOC560382	Hypothetical LOC560382
Dr.134285	DAO.2	D-amino-acid oxidase 2	Dr.15633	LOC570432	Hypothetical LOC570432
Dr.117291	WU:FD10H03	Wu:fd10h03	Dr.80071		Transcribed locus
Dr.75974	PDZK1L	PDZ domain containing 1 like	Dr.77534	ZGC:55702	Zgc:55702
Dr.77685	SLC1A4	Solute carrier family 1 (glutamate/neutral amino acid transporter), member 4	Dr.82867	ZGC:65875	Zgc:65875
Dr.31100	NUDT15	Hypothetical protein LOC791620	Dr.80398	ZGC:153079	Zgc:153079
Dr.10201	SEPW1	Selenoprotein W, 1	Dr.87643	ZGC:101827	Zgc:101827
Dr.79165	SB:CB14	Sb:cb14	Dr.81341	CAPRIN2	Caprin family member 2
Dr.76508	DIRC2	Disrupted in renal carcinoma 2	Dr.32320	LGMN	Legumain
Dr.1214	ARL6IP1	ADP-ribosylation factor-like 6 interacting protein 1	Dr.85513	WU:FC54A11	Wu:fc54a11
Dr.21233	ZGC:103515	Zgc:103515	Dr.77771	SI:DKEY-252H13.6	Si:dkey-252h13.6
Dr.25699	ZGC:77082	Zgc:77082	Dr.114174	ZGC:63569	Hypothetical protein LOC100000446
Dr.81910		Hypothetical LOC558964 (LOC558964), mRNA	Dr.20974	ZGC:55943	Zgc:55943
Dr.75440		Transcribed locus	Dr.32415		Transcribed locus
Dr.83156		Transcribed locus	Dr.6360	WU:FD16G01	Wu:fd16g01
Dr.78850		Transcribed locus	Dr.78587	TSC1B	Tuberous sclerosis 1b
Dr.44401	ZGC:153587	Zgc:153587	Dr.76985	CLDN10L	Claudin 10 like
Dr.76387	LOC791684	Hypothetical protein LOC791684	Dr.80419	ZGC:153999	Zgc:153999

Dr.39134	SLC27A1	Solute carrier family 27 (fatty acid transporter), member 1	Dr.76762	IHPK2	Inositol hexaphosphate kinase 2
Dr.6725		Transcribed locus	Dr.81863	ZGC:112466	Zgc:112466
Dr.76646	ZGC:165381	Zgc:165381	Dr.79423	ZGC:114119	Zgc:114119
Dr.82756	LOC402976	Hypothetical protein LOC402976	Dr.113263	LOC793284	Similar to beta-microseminoprotein
Dr.89589	ZGC:101650	Zgc:101650	Dr.21063	NKX3.2	NK3 homeobox 2
Dr.78050	ZGC:73324	Zgc:73324	Dr.133000		Transcribed locus
Dr.75549	ZGC:55420	Hypothetical protein LOC792156	Dr.75618	ZGC:171444	Zgc:171444
Dr.47389	CEL.2	Hypothetical protein LOC792128	Dr.78271	ZGC:158414	Zgc:158414
Dr.84591		Transcribed locus, strongly similar to NP 001018198.1 spermatogenesis associated 18 [Danio rerio]	Dr.13175		Transcribed locus
Dr.119936	ZGC:92392	Zgc:92392	Dr.75449		Transcribed locus
Dr.83470	ZGC:123113	Zgc:123113	Dr.84876	LOC555985	Hypothetical LOC555985
Dr.107259	SEPP1A	Selenoprotein P, plasma, 1a	Dr.74207	CH211-271J4.1	Apoptosis-stimulating protein of p53
Dr.32109	ZGC:91959	Zgc:91959	Dr.81839	ZGC:77563	Zgc:77563
Dr.77027	KNTC2L	Kinetochore associated 2-like	Dr.91044	LOC557719	Hypothetical LOC557719
Dr.31694	ZGC:56304	Zgc:56304	Dr.1692	ZBTB2B	Zinc finger and BTB domain containing 2b
Dr.79878	DAB2	Disabled homolog 2 (Drosophila)	Dr.23725		Transcribed locus
Dr.77083	ZGC:86714	Zgc:86714	Dr.83279	ZGC:113070	Zgc:113070
Dr.78673	LOC571547	Hypothetical LOC571547	Dr.86083		Transcribed locus
Dr.105771	LOC100007704	Similar to Slc7a8-prov protein	Dr.85095		Transcribed locus
Dr.78430		Transcribed locus, strongly similar to XP 698433.2 PREDICTED: hypothetical protein [Danio rerio]	Dr.121988		Transcribed locus
Dr.74013	WU:FJ63D08	Wu:fj63d08	Dr.79037	ZGC:110259	Zgc:110259
Dr.23685		Transcribed locus	Dr.76979	ZGC:153225	Zgc:153225
Dr.78704	ZGC:66317	Zgc:66317	Dr.54293		Transcribed locus
Dr.79959		Transcribed locus, strongly similar to XP 001332873.1 PREDICTED: similar to Solute carrier family 15 (oligopeptide transporter), member 1 [Danio rerio]	Dr.105609	ZGC:110159	Zgc:110159
Dr.31691	LOC562438	Similar to LDLR dan	Dr.97360	ZGC:111826	Zgc:111826
Dr.4044	ZGC:92139	Zgc:92139	Dr.22874	WU:FC21E07	Wu:fc21e07
Dr.85767	ZGC:92705	Zgc:92705	Dr.12595	HSF2	Heat shock factor 2
Dr.86277		Transcribed locus	Dr.89596	ZGC:103559	Zgc:103559
Dr.11921	NR5A5	Nuclear receptor subfamily 5, group A, member 5	Dr.75252	COL9A2	Procollagen, type IX, alpha 2
Dr.80597	TAF1B	TATA box binding protein (Tbp)-associated factor, RNA polymerase I, B	Dr.77336	ZGC:113196	Zgc:113196
Dr.133716	ZGC:101841	Zgc:101841	Dr.10637	LOC797698	Similar to 5-3 exoribonuclease 2
Dr.19659	EZRL	Ezrin like	Dr.78358	LOC100000526	Hypothetical protein LOC100000526
Dr.80471	ZGC:110537	Hypothetical protein LOC791913	Dr.76665	LOC566399	Hypothetical LOC566399
Dr.78996	ZGC:55661	Zgc:55661	Dr.80663	ALG1	Asparagine-linked glycosylation 1 homolog (yeast, beta-1,4-mannosyltransferase)
Dr.122702		Transcribed locus	Dr.76172	FUCA1	Fucosidase, alpha-L- 1, tissue
Dr.24323	ZGC:56608	Zgc:56608	Dr.117460	LOC792416	Hypothetical protein LOC792416
Dr.75320	HSPD1	Heat shock 60kD protein 1 (chaperonin)	Dr.85731	ZGC:162509	Zgc:162509
Dr.76739	WU:FC44A11	Wu:fc44a11	Dr.11991	CXXC1	CXXC finger 1 (PHD domain)
Dr.144128	ZGC:109868	Zgc:109868	Dr.81010	LOC795788	Similar to CC chemokine SCYA103

Dr.78624		Transcribed locus	Dr.24983	POLR3F	Polymerase (RNA) III (DNA directed) polypeptide F
Dr.6635	SH3BP5LA	SH3-binding domain protein 5-like, a	Dr.107744		Transcribed locus
Dr.87549	ZGC:112418	Zgc:112418	Dr.117593	LOC799087	Similar to Oip5 protein
Dr.17300	LOC559362	Hypothetical LOC559362	Dr.26261		Transcribed locus
Dr.80589	SCPEP1	Serine carboxypeptidase 1	Dr.80630	ZGC:73340	Zgc:73340
Dr.33597	LOC562370	Hypothetical LOC562370	Dr.132329	LOC100004607	Similar to Apoa4 protein
Dr.81772	SI:BUSM1-241H12.4	Si:busm1-241h12.4	Dr.110644	SI:DKEY-21K10.1	Si:dkey-21k10.1
Dr.79047	ZGC:113480	Zgc:113480	Dr.88420	ZGC:101803	Zgc:101803
Dr.132878	LOC100002850	Similar to Secretory carrier membrane protein 2, like	Dr.45899	ZGC:113183	Zgc:113183
Dr.76472	ZGC:110821	Zgc:110821	Dr.26560	ELOVL5	ELOVL family member 5, elongation of long chain fatty acids (yeast)
Dr.82787	IM:7150662	Im:7150662	Dr.76656	CAPN8	Calpain 8
Dr.117801	SMAD5	MAD homolog 5 (Drosophila)	Dr.122289		Transcribed locus
Dr.121617		Transcribed locus	Dr.80332	MCRS1	Microspherule protein 1
Dr.81288	MAF	V-maf musculoaponeurotic fibrosarcoma (avian) oncogene homolog	Dr.3436	LOC100000870	Hypothetical protein LOC100000870
Dr.75131	FBL	Fibrillarin	Dr.14806	PPP2R3C	Protein phosphatase 2, regulatory subunit B", gamma
Dr.29762	EFNA2	Non-POU domain containing, octamer-binding	Dr.6975	ZGC:66107	Zgc:66107
Dr.75520	GATM	Glycine amidinotransferase (L-arginine:glycine amidinotransferase)	Dr.75913	MAPK3	Mitogen-activated protein kinase 3
Dr.82671	SI:CH211-51L3.4	Si:ch211-51l3.4	Dr.5461	LOC402880	Hypothetical protein LOC402880
Dr.85217	FLJ32675	Flj32675	Dr.23039		Transcribed locus
Dr.114529	LOC100003771	Similar to OTTHUMP00000028706	Dr.116914	LOC100005579	Hypothetical protein LOC100005579
Dr.78031	WHSC1	Wolf-Hirschhorn syndrome candidate 1 protein	Dr.79733	SI:CH211-67E16.9	Si:ch211-67e16.9
Dr.75811	INS	Preproinsulin	Dr.117507	ZGC:174575	Zgc:174575
Dr.107944	ABP1	Amiloride binding protein 1 (amine oxidase (copper-containing))	Dr.79151	PXK	PX domain containing serine/threonine kinase
Dr.87101	ZGC:110143	Zgc:110143	Dr.9174	ZGC:55673	Zgc:55673
Dr.84019	ZGC:63614	Zgc:63614	Dr.133159		Transcribed locus
Dr.28449	SLC2A12	Solute carrier family 2 (facilitated glucose transporter), member 12	Dr.37018	ZGC:112003	Zgc:112003
Dr.79110	SUFU	Suppressor of fused homolog (Drosophila)	Dr.75863	ZGC:77488	Zgc:77488
Dr.76972	ZGC:110109	Zgc:110109	Dr.75558	SLC4A2	Solute carrier family 4, anion exchanger, member 2
Dr.9109	GLMNL	Glomulin, like	Dr.122732		Transcribed locus
Dr.121650		Transcribed locus	Dr.1301	PRKAG1	Hypothetical protein LOC791615
Dr.34301	ITGB5	Integrin, beta 5	Dr.105135	PPRC1	Peroxisome proliferator-activated receptor gamma, coactivator-related 1
Dr.38076	ZGC:158780	Zgc:158780	Dr.103297	LOC564151	Similar to Claspin
Dr.81287	KRML2	Kreisler (mouse) maf-related leucine zipper homolog 2	Dr.123677		Transcribed locus
Dr.31250	ZGC:92808	Zgc:92808	Dr.143610	WDR43L	WD repeat domain 43, like
Dr.34264	GDPD1	Glycerophosphodiester phosphodiesterase domain containing 1	Dr.81478	SULT1ST3	Sulfotransferase family 1, cytosolic sulfotransferase 3
Dr.82025	ZGC:112208	Zgc:112208	Dr.78005	MPZ	Sc:d0186
Dr.77381	ZGC:92479	Zgc:92479	Dr.132401	SENP3A	SUMO1/sentrin/SMT3 specific peptidase 3a
Dr.84521	LOC560369	Hypothetical LOC560369	Dr.132665	ZGC:153695	Zgc:153695
Dr.76489	ZGC:92763	Zgc:92763	Dr.80988	PAQR3	Progestin and adipoQ receptor family member III
Dr.104263	ZGC:92057	Zgc:92057	Dr.6651	PIAS4	Protein inhibitor of activated STAT, 4
Dr.78421	ZGC:163008	Zgc:163008	Dr.85714		Transcribed locus
Dr.75949		Transcribed locus	Dr.6944	ZGC:100860	Zgc:100860
Dr.4742	ZGC:101121	Zgc:101121	Dr.133028	ADIPOR1A	Adiponectin receptor 1a

Dr.115882	LOC796920	Hypothetical protein LOC796920	Dr.15041		Transcribed locus, strongly similar to XP 001343059.1 PREDICTED: similar to MGC64297 protein [Danio rerio]
Dr.81689	ZGC:55733	Zgc:55733	Dr.80282	ZGC:110141	Zgc:110141
Dr.80558	ZGC:111879	Zgc:111879	Dr.80187	ZGC:92035	Zgc:92035
Dr.76364	ZGC:158773	Zgc:158773	Dr.75118	ZGC:112098	Zgc:112098
Dr.107618		Transcribed locus	Dr.78675	CCNA1	Zgc:173602
Dr.20429	DLG7	Discs, large homolog 7 (Drosophila)	Dr.143654	ZGC:77183	Zgc:77183
Dr.109638	ZGC:114129	Im:7136473	Dr.46626	LOC100002480	Similar to A kinase (PRKA) anchor protein 1
Dr.31849	ZGC:136380	Zgc:158165	Dr.91580	ZGC:171753	Zgc:171753
Dr.143234		Transcribed locus	Dr.82327	ZGC:153958	Zgc:153958
Dr.82465	ZGC:63528	Zgc:63528	Dr.77563	WU:FB82H05	Wu:fb82h05
Dr.5413		Transcribed locus, moderately similar to XP 520446.2 PREDICTED: similar to ANKRD15 protein [Pan troglodytes]	Dr.83069		Transcribed locus
Dr.84939	ST6GAL1	ST6 beta-galactosamide alpha-2,6-sialyltranferase 1	Dr.75215	ERG	V-ets erythroblastosis virus E26 oncogene like (avian)
Dr.132825	ZGC:64095	Hypothetical protein LOC792222	Dr.76888	WU:FB37G07	Wu:fb37g07
Dr.114938	H2AFX	H2A histone family, member X	Dr.78720	ZGC:63810	Zgc:63810
Dr.114249	HAGH	Hydroxyacylglutathione hydrolase	Dr.76645		Transcribed locus
Dr.80461	GNAI2	Guanine nucleotide binding protein (G protein), alpha inhibiting activity polypeptide 2	Dr.77740	SETD2	SET domain containing 2
Dr.39143	ZGC:112982	Zgc:112982	Dr.77595		Transcribed locus
Dr.76444	ZGC:172180	Zgc:172180	Dr.83417	BNIP2	BCL2/adenovirus E1B interacting protein 2
Dr.78356	GATA6	GATA-binding protein 6	Dr.140596		Transcribed locus
Dr.122161		Transcribed locus, strongly similar to NP 001104632.1 hypothetical protein LOC559922 [Danio rerio]	Dr.80631	ZDHHC24	Zinc finger, DHHC-type containing 24
Dr.90586	CAMK2G1	Calcium/calmodulin-dependent protein kinase (CaM kinase) II gamma 1	Dr.18206		Transcribed locus
Dr.76410	RAB20	RAB20, member RAS oncogene family	Dr.5549	ZGC:66286	Zgc:66286
Dr.75714	WU:FD20A04	Wu:fd20a04	Dr.4573	LGALS9L1	Hypothetical protein LOC791953
Dr.76827		Transcribed locus	Dr.80871		Transcribed locus
Dr.79864	LOC556561	Similar to polyhomeotic like 3 (Drosophila)	Dr.121558		Transcribed locus
Dr.105962	WU:FC50C06	Wu:fc50c06	Dr.80632	ZGC:73124	Zgc:73124
Dr.84470	LOC797345	Zgc:163126	Dr.77660	ZGC:100963	Zgc:100963
Dr.143593	PCM1	Pericentriolar material 1	Dr.75730	ZGC:114123	Zgc:114123
Dr.78701	ZGC:110212	Zgc:110212	Dr.268	EPD	Ependymin
Dr.119225	LOC797428	Similar to Tubulin folding cofactor B	Dr.14396	LOC572175	Similar to Muc2 protein
Dr.113556	UGDH	UDP-glucose dehydrogenase	Dr.105738	WU:FI38H09	Wu:fi38h09
Dr.32211	ACIN1A	Similar to Apoptotic chromatin condensation inducer in the nucleus (Acinus)	Dr.79193	MED12	Mediator of RNA polymerase II transcription, subunit 12 homolog
Dr.76240	FUBP1	Far upstream element (FUSE) binding protein 1	Dr.106542	SLC25A25	Solute carrier family 25 (mitochondrial carrier, phosphate carrier), member 25
Dr.79378	LOC561658	Hypothetical LOC561658	Dr.84914	ZGC:152928	Zgc:152928
Dr.76512	SEPT7A	Septin 7a	Dr.114873	GBGT1L3	Globoside alpha-1,3-N-acetylgalactosaminyltransferase 1, like 3
Dr.79900	CX28.9	Connexin 28.9	Dr.118849	ZGC:63958	Zgc:63958
Dr.2976	SI:CH211-200O3.4	Si:ch211-200o3.4	Dr.16985	ZGC:162290	Zgc:162290
Dr.108624	ZGC:86716	Zgc:86716	Dr.132934	ZGC:63617	Zgc:63617
Dr.78373		Transcribed locus	Dr.76745	ZGC:56361	Zgc:56361

Dr.76296	ZGC:56419	Zgc:56419	Dr.32351	LGALS3L	Lectin, galactoside-binding, soluble, 3 (galectin 3)-like
Dr.82468	TBC1D19	TBC1 domain family, member 19	Dr.120392	ADA	Hypothetical protein LOC792200
Dr.78711	ACSL4	Acyl-CoA synthetase long-chain family member 4	Dr.133630	ZGC:110329	Zgc:110329
Dr.78921	ZGC:153420	Zgc:153420	Dr.13798		Transcribed locus
Dr.75224		Transcribed locus	Dr.26907	DND	Dead end
Dr.11428	LOC100001855	Similar to supervillin	Dr.114009		Transcribed locus
Dr.80222	CASC3	Cancer susceptibility candidate 3	Dr.78779		Transcribed locus
Dr.16810	LOC798400	Similar to N-acetylgalactosaminyltransferase	Dr.94519	ZGC:112296	Zgc:112296
Dr.9166	BLZF1	Hypothetical protein LOC791432	Dr.83427	ZGC:91890	Zgc:91890
Dr.143598	CLDNI	Claudin i	Dr.75901	SI:DKEYP-117H8.4	Si:dkeyp-117h8.4
Dr.4955		Transcribed locus	Dr.132230	ZGC:101116	Zgc:101116
Dr.76732	GLDC	Glycine dehydrogenase (decarboxylating)	Dr.29995	WU:FI27C05	Wu:fi27c05
Dr.84109	LOC796103	Similar to Chromosome condensation protein G	Dr.75243	ZGC:113447	Zgc:113447
Dr.23391	SLC16A3	Hypothetical LOC554697	Dr.96932	ZGC:174234	Zgc:174234
Dr.81385	SI:DKEY-24P1.5	Si:dkey-24p1.5	Dr.31566		Transcribed locus
Dr.140471		Transcribed locus	Dr.78758	GPD1	Hypothetical protein LOC792059
Dr.4451	ZGC:55363	Zgc:55363	Dr.10580	NEK2	Hypothetical LOC554896
Dr.6973	WTAP	Wilms tumor 1 associated protein	Dr.83494	ZGC:110788	Zgc:110788
Dr.121668		Transcribed locus	Dr.6833	SI:CH211-238N5.5	Si:ch211-238n5.5
Dr.83415		Transcribed locus	Dr.25733	RDBP	RD RNA binding protein
Dr.79634	LOC561231	Hypothetical LOC561231	Dr.75369	DUS1L	Dihydrouridine synthase 1-like (S. cerevisiae)
Dr.132880		Transcribed locus	Dr.135199	IL12A	Interleukin 12a
Dr.85634	S100A10A	S100 calcium binding protein A10a	Dr.87908	LIFRA	Leukemia inhibitory factor receptor alpha
Dr.144133	LOC565165	Hypothetical LOC565165	Dr.81832	LOC553407	Hypothetical protein LOC100006308
Dr.123250		Transcribed locus	Dr.76427		Transcribed locus, moderately similar to NP 071918.1 zinc finger protein 106 homolog [Homo sapiens]
Dr.80441	ZGC:171298	Zgc:171298	Dr.76152	LOC560112	Hypothetical LOC560112
Dr.14153	ZGC:153434	Zgc:153434	Dr.78498	ZGC:77560	Zgc:77560
Dr.81345	LOC798299	Hypothetical protein LOC798299	Dr.80336	CYP11A1	Cytochrome P450, subfamily XIA, polypeptide 1
Dr.90487	ZGC:172295	Zgc:172295	Dr.114385	ZGC:163023	Zgc:163023
Dr.85174	CTSL.1	Cathepsin L.1	Dr.77591	SI:DKEY-175G20.1	Si:dkey-175g20.1
Dr.77065	HMHA1	Histocompatibility (minor) HA-1	Dr.24755	PPP2R2D	Protein phosphatase 2, regulatory subunit B, delta isoform
Dr.47548	HOXD11A	Homeo box D11a	Dr.82334	ZGC:153929	Zgc:153929
Dr.132594		Transcribed locus	Dr.122543		Transcribed locus
Dr.88756	ZGC:110238	Hypothetical protein LOC791572	Dr.18504	NSMCE1	Non-SMC element 1 homolog (S. cerevisiae)
Dr.72371	WU:FB60G05	Wu:fb60g05	Dr.75844	IDH1	Isocitrate dehydrogenase 1 (NADP+), soluble
Dr.77547	ZGC:100868	Zgc:100868	Dr.84313	ELP3	Elongation protein 3 homolog (S. cerevisiae)
Dr.36953	ASAH1	N-acylsphingosine amidohydrolase (acid ceramidase) 1	Dr.67796	ICN	Ictacalcin
Dr.118663	ZGC:64050	Hypothetical protein LOC794885	Dr.75608	ESCO2	Establishment of cohesion 1 homolog 2 (S. cerevisiae)
Dr.32947	NUPL1	Nucleoporin like 1	Dr.24234	SMC2	Structural maintenance of chromosomes 2
Dr.76852	ZGC:92643	Zgc:92643	Dr.77600	SRL	Sarcalumenin
Dr.33734	ZGC:110008	Zgc:110008	Dr.42971	ZGC:112455	Zgc:112455
Dr.55498	WU:FO94F09	Wu:fo94f09	Dr.76547	ZGC:158323	Zgc:158323
Dr.76790	RPA1	Replication protein A1	Dr.133660		Transcribed locus
Dr.6471	ZGC:172228	Zgc:172228	Dr.16380	ALDH8A1	Aldehyde dehydrogenase 8 family, member A1
Dr.117314	ZGC:101843	Zgc:101843	Dr.76784	SEPT8A	Septin 8a
Dr.111731	AQP10	Aquaporin 10	Dr.106681	LOC569952	Hypothetical LOC569952
Dr.76190	CFL1	Cofilin 1 (non-muscle)	Dr.79287	ZGC:110077	Zgc:110077
Dr.2636	IMPDH2	IMP (inosine monophosphate) dehydrogenase 2	Dr.6291		Transcribed locus
Dr.85554	ZGC:112322	Zgc:112322	Dr.15534	LOC571197	Similar to Thrap4 protein

Dr.19939	LOC555164	Hypothetical LOC555164	Dr.132353	RNF14	Ring finger protein 14
Dr.9988	WU:FD44F11	Wu:fd44f11	Dr.31086	RNF2	Ring finger protein 2
Dr.35904	ZGC:85729	Zgc:85729	Dr.91373	DGAT2	Diacylglycerol O-acyltransferase 2
Dr.79955	ATL3	Atlastin 3	Dr.77448	WDR21	WD repeat domain 21
Dr.2713	CD82	Hypothetical protein LOC792047	Dr.20969	FOXI1	Forkhead box I1
Dr.10893	SARA2	Hypothetical protein LOC792159	Dr.85037	CHRNE	Cholinergic receptor, nicotinic, epsilon
Dr.119277	ZGC:101026	Zgc:101026	Dr.1823	SI:CH211-150C22.2	Si:ch211-150c22.2
Dr.78736	WU:FC28F08	Wu:fc28f08	Dr.77932	SI:CH211-173P18.3	Si:ch211-173p18.3
Dr.76207	AQP3	Aquaporin 3	Dr.8200	SI:CH211-45M15.2	Si:ch211-45m15.2
Dr.80393	ZGC:66450	Zgc:66450	Dr.77976	BYSL	Bystin-like
Dr.122910		Transcribed locus, moderately similar to NP 956523.1 COP9 signalosome subunit 8 [Danio rerio]	Dr.81932	GNB3	Guanine nucleotide binding protein (G protein), beta polypeptide 3
Dr.84502	ZGC:103761	Zgc:103761	Dr.96184	ZGC:101095	Zgc:101095
Dr.39081	ZGC:110239	Zgc:110239	Dr.11569	OSBPL2	Oxysterol binding protein-like 2
Dr.75392	AK3L1	Adenylate kinase 3-like 1	Dr.79271	ZGC:77294	Zgc:77294
Dr.75265		Transcribed locus	Dr.84790	UNG	Uracil-DNA glycosylase
Dr.117538	ZGC:77785	Zgc:77785	Dr.28227	IM:7148063	Im:7148063
Dr.88645	ZGC:86611	Zgc:86611	Dr.7461	SI:DKEY-114G7.4	Si:dkey-114g7.4
Dr.118834	LOC566639	Similar to AHNAK nucleoprotein	Dr.27090	DOCK8	Similar to dedicator of cytokinesis 8
Dr.34097	PMP22B	Peripheral myelin protein 22b	Dr.84534	LOC100007999	Hypothetical protein LOC100007999
Dr.83194	CYP1C1	Cytochrome P450, family 1, subfamily C, polypeptide 1	Dr.3168	SNUPN	Snurportin 1
Dr.2532	PRKCI	Protein kinase C, iota	Dr.80082	LOC559441	Similar to E3 ubiquitin ligase
Dr.114279	LOC555064	Hypothetical LOC555064	Dr.122973		Transcribed locus
Dr.80192	ZGC:162158	Zgc:162158	Dr.84465	ZGC:110718	Hypothetical protein LOC791932
Dr.82140	LOC100005813	Similar to sno, strawberry notch homolog 1 (Drosophila)	Dr.76346		Transcribed locus
Dr.89720	LOC556114	Hypothetical LOC556114	Dr.116845		Transcribed locus, strongly similar to NP 001073523.1 hypothetical protein LOC571403 [Danio rerio]
Dr.77508	MAO	Monoamine oxidase	Dr.33564	IPO9	Importin 9
Dr.76643	HIBADHA	3-hydroxyisobutyrate dehydrogenase a	Dr.133114	LOC100000528	Hypothetical protein LOC100000528
Dr.79774	CCDC98	Coiled-coil domain containing 98	Dr.14824		Transcribed locus
Dr.78811	RNASEH2B	Ribonuclease H2, subunit B	Dr.84342	ZGC:92085	Zgc:92085
Dr.77582	LOC560453	Similar to KIAA1794	Dr.8058	GBAS	Glioblastoma amplified sequence
Dr.76907	PCBP2	Poly(rC) binding protein 2	Dr.81733	RBBP5	Retinoblastoma binding protein 5
Dr.77012	RCC1	Regulator of chromosome condensation 1	Dr.141683		Transcribed locus, weakly similar to XP 001341760.1 PREDICTED: similar to Si:ch211-14a17.6 [Danio rerio]
Dr.107710	LOC561086	Similar to putative adenylate cyclase	Dr.28300	ZGC:66024	Zgc:66024
Dr.84504	TRAIP	TRAF-interacting protein	Dr.82354	VLDLR	Very low density lipoprotein receptor
Dr.121990		Transcribed locus	Dr.79957	TMEM9B	TMEM9 domain family, member B
Dr.123669		Transcribed locus, strongly similar to NP 001017864.1 hypothetical protein LOC550562 [Danio rerio]	Dr.32244	HSPB1	Heat shock protein, alpha-crystallin-related, 1
Dr.32093	RAB30	RAB30, member RAS oncogene family	Dr.78113	ZGC:77390	Zgc:77390
Dr.52862	LIN7C	Lin-7 homolog C (C. elegans)	Dr.37073	ZGC:101553	Zgc:101553

Dr.1956		Transcribed locus, strongly similar to XP 702446.2 PREDICTED: hypothetical protein [Danio rerio]	Dr.117581	ZGC:154087	Zgc:154087
Dr.32749	ZGC:91847	Zgc:91847	Dr.86913	FABP6	Fatty acid binding protein 6, ileal (gastrotropin)
Dr.104406	ADRM1B	Adhesion regulating molecule 1b	Dr.82719	DAP3	Death associated protein 3
Dr.75753	NOTCH1A	Notch homolog 1a	Dr.77391	UTP6	UTP6, small subunit (SSU) processome component, homolog (yeast)
Dr.31752	HDAC1	Histone deacetylase 1	Dr.76650	ING4	Inhibitor of growth family, member 4
Dr.77619	RUVBL1	RuvB-like 1 (E. coli)	Dr.77926	ZGC:63774	Zgc:109744
Dr.1489	ZGC:136963	Zgc:136963	Dr.80524	WU:FI34B01	Wu:fi34b01
Dr.78703	RTKN2	Rhotekin 2	Dr.119738	SETB	SET translocation (myeloid leukemia-associated) B
Dr.132305	ZGC:77439	Zgc:77439	Dr.80032	ZGC:162976	Zgc:162976
Dr.80724	SULT1ST6	Sulfotransferase family, cytosolic sulfotransferase 6	Dr.104887	LOC572121	Similar to XL-INCENP
Dr.122409		Transcribed locus	Dr.134550	ZGC:77906	Zgc:77906
Dr.17174	ANKRD28	Ankyrin repeat domain 28	Dr.78888	ZGC:77415	Zgc:77415
Dr.31639	ZGC:112095	Zgc:112095	Dr.80713	FSHR	Follicle stimulating hormone receptor
Dr.77202	RDH1L	Retinol dehydrogenase 1, like	Dr.106217	C20ORF20	Chromosome 20 open reading frame 20 (H. sapiens)
Dr.106380	PRDM8	PR domain containing 8	Dr.86476	LOC100001302	Similar to ubiquitin-activating enzyme E1
Dr.116756	RIPK4	Receptor-interacting serine-threonine kinase 4	Dr.140573		Transcribed locus, weakly similar to NP 081830.2 ubiquitin specific peptidase 38 [Mus musculus]
Dr.77343		Transcribed locus	Dr.104286		Transcribed locus, strongly similar to NP 001071010.2 mitochondrial methionyl-tRNA formyltransferase [Danio rerio]
Dr.75547	TRY	Trypsin	Dr.37970	SI:RP71-1C10.3	Si:rp71-1c10.3
Dr.140810		Transcribed locus, weakly similar to XP 690938.2 PREDICTED: hypothetical protein [Danio rerio]	Dr.79014		Transcribed locus
Dr.105427		Transcribed locus	Dr.115188	SERINC5	Serine incorporator 5
Dr.37032	CYP2J30	Cytochrome P450, family 2, subfamily J, polypeptide 30	Dr.82751	SSX2IP	Synovial sarcoma, X breakpoint 2 interacting protein
Dr.75843	CHPT1	Choline phosphotransferase 1	Dr.106021	SLC43A1	Solute carrier family 43, member 1
Dr.79066	ACSL1	Acyl-CoA synthetase long-chain family member 1	Dr.85700	NUP43	Nucleoporin 43
Dr.77961	ZGC:92765	Zgc:92765	Dr.132611	LOC793280	Hypothetical protein LOC793280
Dr.40298	WU:FB58E08	Wu:fb58e08	Dr.120800	ZGC:92512	Zgc:92512
Dr.77610	ZGC:101667	Zgc:101667	Dr.41494	WU:FI46G11	Wu:fi46g11
Dr.80572	ZGC:103530	Zgc:103530	Dr.74211	TAKRP	T-cell activation kelch repeat protein
Dr.37643	ZGC:103509	Zgc:103509	Dr.114283	WU:FD16E03	Wu:fd16e03
Dr.2274	STARD3	START domain containing 3	Dr.21958	LBR	Lamin B receptor
Dr.1786	ZGC:55292	Zgc:55292	Dr.78401	AATF	Apoptosis antagonizing transcription factor
Dr.79972	GOLGA5	Golgi autoantigen, golgin subfamily a, 5	Dr.77471		Transcribed locus
Dr.75202	HDGFRP2	Hepatoma-derived growth factor, related protein 2	Dr.93960		Transcribed locus, strongly similar to NP 998703.1 v-crk sarcoma virus CT10 oncogene-like [Danio rerio]
Dr.75603	H3F3A	H3 histone, family 3A	Dr.83735	HPRT1L	Hypoxanthine phosphoribosyltransferase 1, like
Dr.76761	ZGC:91996	Zgc:91996	Dr.31063	ZGC:86895	Zgc:86895
Dr.2143	PRPF38B	PRP38 pre-mRNA processing factor 38 (yeast) domain containing B	Dr.132378	PLS3	Plastin 3 (T isoform)

Dr.132490	ZGC:77867	Zgc:77867	Dr.21094		Transcribed locus, weakly similar to XP 001333287.1 PREDICTED: similar to ENSANGP00000022061 isoform 1 [Danio rerio]
Dr.79720	ZGC:86839	Zgc:86839	Dr.81955		Transcribed locus
Dr.133457		CDNA clone IMAGE:7053246	Dr.81616	LOC569587	Similar to transcription factor-like nuclear regulator
Dr.24235	DDX18	DEAD (Asp-Glu-Ala-Asp) box polypeptide 18	Dr.106367	PRPSAP2	Phosphoribosyl pyrophosphate synthetase-associated protein 2
Dr.7003	BMP15	Bone morphogenetic protein 15	Dr.78235	STK38L	Serine/threonine kinase 38 like
Dr.116102	ELA2L	Elastase 2 like	Dr.4705	NOL10	Nucleolar protein 10
Dr.77703	UHRF1	Ubiquitin-like, containing PHD and RING finger domains, 1	Dr.119787	LOC554474	Similar to Protein phosphatase 1, regulatory (inhibitor) subunit 3B
Dr.84043	ZGC:86635	Zgc:86635	Dr.78602	WU:FD14A01	Wu:fd14a01
Dr.5696	PRC1	Protein regulator of cytokinesis 1	Dr.122142	ATP1A3B	ATPase, Na+/K+ transporting, alpha 3b polypeptide
Dr.32573	RPL11	Ribosomal protein L11	Dr.135679		Transcribed locus, moderately similar to NP 001107527.1 hypothetical protein LOC100135392 [Xenopus tropicalis]
Dr.82263	LOC796453	Hypothetical protein LOC796453	Dr.118088	HNRNPL	Heterogeneous nuclear ribonucleoprotein L
Dr.75324	POLA1	Polymerase (DNA directed), alpha 1	Dr.82744	ZGC:92689	Zgc:92689
Dr.140642		Transcribed locus, strongly similar to NP 956291.1 TAR (HIV) RNA binding protein 2 [Danio rerio]	Dr.80840	LOC564852	Similar to 6-phosphofructo-2-kinase/fructose-2,6-biphosphatase 2
Dr.142263		Transcribed locus, strongly similar to XP 001332593.1 PREDICTED: similar to L(3)mbt-like 2 (Drosophila) isoform 1 [Danio rerio]	Dr.81780	PANE1	Proliferation associated nuclear element
Dr.77649	MYST2	MYST histone acetyltransferase 2	Dr.120681	ZGC:171428	Zgc:171428
Dr.106465	LOC799140	Hypothetical protein LOC799140	Dr.106432	ZGC:171537	Zgc:171537
Dr.3839		Transcribed locus, strongly similar to XP 001341031.1 PREDICTED: hypothetical protein [Danio rerio]	Dr.14778	ZGC:103752	Zgc:103752
Dr.75741	ZGC:100869	Zgc:100869	Dr.76520	ST13	Suppression of tumorigenicity 13 (colon carcinoma) (Hsp70 interacting protein)
Dr.83301	FOXC1B	Forkhead box C1b	Dr.80701		Transcribed locus
Dr.75260	C2ORF24	Chromosome 2 open reading frame 24	Dr.12565	VAT1	Vesicle amine transport protein 1 homolog (T californica)
Dr.85085	PDLIM7	PDZ and LIM domain 7	Dr.121512	LOC100004500	Hypothetical protein LOC100004500
Dr.80637	ITGA5	Integrin, alpha 5 (fibronectin receptor, alpha polypeptide)	Dr.75458	ARNTL1A	Aryl hydrocarbon receptor nuclear translocator-like 1a
Dr.81184	ZGC:92818	Zgc:92818	Dr.78902		Transcribed locus
Dr.82521	ZGC:73144	Hypothetical protein LOC792240	Dr.82999	INTS6	Integrator complex subunit 6
Dr.80659	WU:FI33G05	Wu:fi33g05	Dr.132373		Transcribed locus
Dr.75229		Transcribed locus	Dr.80821	SPAG6	Sperm associated antigen 6
Dr.77760	PUS1	Hypothetical protein LOC792133	Dr.17457	ZGC:63667	Hypothetical protein LOC100005281
Dr.88329	HIF1AL2	Hypoxia-inducible factor 1, alpha subunit, like 2	Dr.75286	CKAP5	Cytoskeleton associated protein 5
Dr.75372	STARD3NL	STARD3 N-terminal like	Dr.116678	ZGC:110200	Zgc:110200
Dr.75748	ORC6L	Origin recognition complex, subunit 6 homolog-like (yeast)	Dr.67263	LOC561668	Hypothetical LOC561668

Dr.80266	ITM2C	Integral membrane protein 2C	Dr.77751		Transcribed locus
Dr.85627	ANXA3A	Hypothetical protein LOC791593	Dr.82056	LHX8	LIM homeobox 8
Dr.118555	LOC567390	Hypothetical LOC567390	Dr.79519	ATP5S	ATP synthase, H+ transporting, mitochondrial F0 complex, subunit s
Dr.114001	ZGC:110183	Zgc:110183	Dr.119419	LOC572149	Similar to Dihydropyrimidine dehydrogenase
Dr.79757	ZGC:77112	Zgc:77112	Dr.13909		Transcribed locus
Dr.81511	ZGC:113156	Zgc:113156	Dr.59	ANXA1A	Annexin A1a
Dr.76676	LOC793260	Hypothetical protein LOC793260	Dr.75602	TRIM71	Tripartite motif-containing 71
Dr.133005	LOC100001846	Hypothetical protein LOC100001846	Dr.42600	LOC553397	Hypothetical protein LOC553397
Dr.79544	ING5B	Inhibitor of growth family, member 5b	Dr.20155	SS18	Synovial sarcoma translocation, chromosome 18 (H. sapiens)
Dr.75255		Transcribed locus	Dr.82585	LOC562304	Similar to cytochrome P450, family 2, subfamily J, polypeptide 2
Dr.79169	PAPOLG	Poly(A) polymerase gamma	Dr.79823	ZGC:91926	Zgc:91926
Dr.105341	RACGAP1	Rac GTPase-activating protein 1	Dr.16483	SLC39A6	Solute carrier family 39 (zinc transporter), member 6
Dr.23593	ZGC:56412	Zgc:56412	Dr.15227		Transcribed locus
Dr.106684	LOC799913	Similar to cell surface flocculin	Dr.80564	RBM38	RNA binding motif protein 38
Dr.74227	ANLN-LIKE	Anillin, actin binding protein-like	Dr.114476	ZGC:92161	Hypothetical protein LOC791539
Dr.40624	LOC569148	Hypothetical LOC569148	Dr.80447	ZGC:55983	Zgc:55983
Dr.75152	CDK2	Cyclin-dependent kinase 2	Dr.75906	SLC25A3	Solute carrier family 25 (mitochondrial carrier, phosphate carrier), member 3
Dr.7036	G3BP1	GTPase activating protein (SH3 domain) binding protein 1	Dr.121634		Transcribed locus
Dr.106515	LOC795458	Similar to ENSANGP00000022061	Dr.79728	LOC564287	Similar to MGC69156 protein
Dr.79840	ZGC:92006	Zgc:92006	Dr.106024	WU:FC46H12	Wu:fc46h12
Dr.79258	LOC100000846	Similar to PHD finger protein 12	Dr.17275	WU:FI75F03	Wu:fi75f03
Dr.67738	ZGC:153795	Zgc:153795	Dr.80157	ZGC:56161	Zgc:56161
Dr.41866	CRYBB3	Crystallin, beta B3	Dr.79711	ZGC:158802	Zgc:158802
Dr.15775	DKEY-151P17.3	Plasma membrane proteolipid	Dr.82376	ZGC:63863	Hypothetical protein LOC797468
Dr.75966	THOC1	THO complex 1	Dr.99488	ZGC:171912	Zgc:171912
Dr.83578	LOC556669	Hypothetical LOC556669	Dr.39528	LOC100001396	Hypothetical protein LOC100001396
Dr.52170		Transcribed locus, strongly similar to NP 001002726.1 WD repeat and HMG-box DNA binding protein 1 [Danio rerio]	Dr.7489		Transcribed locus, weakly similar to NP 001034277.1 ras responsive element binding protein 1 isoform 2 [Mus musculus]
Dr.78694	UTP15	Utp15, U3 small nucleolar ribonucleoprotein, homolog	Dr.2195	TNPO3	Transportin 3
Dr.13960	S100A1	S100 calcium binding protein A1	Dr.120175	HSD11B3	Hydroxysteroid (11-beta) dehydrogenase 3
Dr.118684	LOC100002310	Hypothetical protein LOC100002310	Dr.82458	DDX26B	DEAD/H (Asp-Glu-Ala-Asp/His) box polypeptide 26B
Dr.77945	DNMT5	DNA (cytosine-5-)-methyltransferase 5	Dr.74706		Transcribed locus, moderately similar to NP 775564.1 solute carrier family 43, member 2 [Mus musculus]
Dr.109592	ZGC:92151	Zgc:92151	Dr.116738	LOC794025	Hypothetical protein LOC794025
Dr.86190	ZGC:86715	Zgc:86715	Dr.8749	WBP2	WW domain binding protein 2
Dr.80969	LOC100004989	Hypothetical protein LOC100004989	Dr.117431	SI:CH211-51N14.2	Si:ch211-51n14.2
Dr.80848	ZGC:100856	Zgc:100856	Dr.86027	LOC100006639	Hypothetical protein LOC100006639

Dr.77864	PHC2	Polyhomeotic-like 2 (Drosophila)	Dr.2885	FTSJ1	FtsJ homolog 1 (E. coli)
Dr.82476	ZGC:112072	Zgc:112072	Dr.76280	ZGC:152779	Zgc:152779
Dr.33507	ZGC:123170	Zgc:123170	Dr.87817	DNAJC5	DnaJ (Hsp40) homolog, subfamily C, member 5
Dr.67664	SI:DKEY-8L13.4	Si:dkey-8l13.4	Dr.25529	PHEX	Phosphate regulating gene with homologues to endopeptidases on the X chromosome
Dr.78239	DDI2	DNA-damage inducible protein 2	Dr.132507	ZGC:85696	Zgc:85696
Dr.47041	ZGC:92126	Zgc:92126	Dr.75477	RTF1	Rtf1, Paf1/RNA polymerase II complex component, homolog (S. cerevisiae)
Dr.67618	USP25	Ubiquitin specific protease 25	Dr.29744	SP8L	Sp8 transcription factor-like
Dr.29859	IM:7142837	Im:7142837	Dr.40661		Transcribed locus
Dr.80409	IVNS1ABPB	Influenza virus NS1A binding protein b	Dr.8916	ZGC:110734	Zgc:110734
Dr.394		Transcribed locus, strongly similar to XP 700078.2 PREDICTED: similar to D13S106E-like [Danio rerio]	Dr.32297	CAHZ	Carbonic anhydrase
Dr.78166	PVALB7	Parvalbumin	Dr.81229		Transcribed locus, strongly similar to XP 001332444.1 PREDICTED: similar to sreb2 isoform 1 [Danio rerio]
Dr.79083	TMEM57	Transmembrane protein 57	Dr.132872	ANKRD12	Ankyrin repeat domain 12
Dr.4660	LOC100006592	Hypothetical protein LOC100006592	Dr.9441	UTXL1	Ubiquitously transcribed tetratricopeptide repeat, X chromosome like 1
Dr.32436	ZGC:101883	Hypothetical protein LOC792171	Dr.89166		Transcribed locus
Dr.32150	DJ383J4.3L	DJ383J4.3-like	Dr.80967	ZGC:112254	Zgc:112254
Dr.119791		Transcribed locus, strongly similar to XP 001332437.1 PREDICTED: hypothetical protein [Danio rerio]	Dr.84741	ZGC:113085	Zgc:113085
Dr.75610	BHMT	Betaine-homocysteine methyltransferase	Dr.114161	ZGC:112397	Zgc:112397
Dr.86041	ZGC:92277	Zgc:92277	Dr.77969	LOC796797	Hypothetical protein LOC796797
Dr.75815	FOXA	Forkhead box A sequence	Dr.50820	LOC565671	Similar to MGC89155 protein
Dr.78299	PHF17	PHD finger protein 17	Dr.89787	ZGC:113334	Zgc:113334
Dr.80537	ZGC:55621	Zgc:55621	Dr.123739		Transcribed locus
Dr.30247	ZGC:77118	Zgc:113969	Dr.80660	PLK4	Polo-like kinase 4 (Drosophila)
Dr.86116	ZGC:56589	Novel protein similar to vertebrate phosphatidylinositol glycan anchor biosynthesis, class A (paroxysmal nocturnal hemoglobinuria) (PIGA, zgc:56589)	Dr.83896	LOC100005060	Hypothetical protein LOC100005060
Dr.81259	DAZL	Daz-like gene	Dr.121806		Transcribed locus
Dr.82958	MCEE	Methylmalonyl CoA epimerase	Dr.113808	PLS1	Plastin 1 (I isoform)
Dr.76154	ZGC:77241	Zgc:77241	Dr.77001	CDC42EP4	CDC42 effector protein (Rho GTPase binding) 4
Dr.87644	ZGC:113259	Zgc:113259	Dr.82697		Transcribed locus, moderately similar to XP 001345745.1 PREDICTED: hypothetical protein [Danio rerio]
Dr.84074	SB:CB157	Sb:cb157	Dr.115947	LOC563252	Similar to MTG16a
Dr.36081	KIF11	Kinesin family member 11	Dr.80478	ZGC:55308	Zgc:55308
Dr.78997		Transcribed locus	Dr.79117	SI:DKEY-97O5.1	Si:dkey-97o5.1
Dr.75779	PL10	Pl10	Dr.37370	ZGC:103562	Zgc:103562
Dr.15518	ZGC:113343	Zgc:113343	Dr.4322	DKEYP-94H10.2	Novel protein similar to vertebrate PAS domain containing serine/threonine kinase (PASK)

Dr.114177	DNAJA3A	DnaJ (Hsp40) homolog, subfamily A, member 3A	Dr.105744	ZGC:175186	Zgc:175186
Dr.47266	SNIP1	Smad nuclear interacting protein	Dr.143375		Transcribed locus
Dr.52195	SI:CH211-152C12.2	Si:ch211-152c12.2	Dr.82434	SLA/LPL	Soluble liver antigen/liver pancreas antigen (Homo sapiens), like
Dr.77921	LOC564669	Similar to ARVCF	Dr.77353	ZGC:101663	Hypothetical protein LOC792193
Dr.83148	LOC556113	Similar to FLJ00281 protein	Dr.116962	LOC558028	Similar to exosome component 10
Dr.76348	ZGC:63504	Zgc:63504	Dr.133285	ZGC:153878	Hypothetical protein LOC795094
Dr.104975	ZGC:56513	Zgc:56513	Dr.83484	EED	Embryonic ectoderm development
Dr.18312	U2AF1	U2(RNU2) small nuclear RNA auxiliary factor 1	Dr.120811	ZGC:65845	Zgc:65845
Dr.6442	ZGC:92875	Zgc:92875	Dr.36307	LOC562529	Hypothetical LOC562529
Dr.82342	DKEY-57A22.11	Similar to CG14692-PA	Dr.14549	ZGC:92307	Zgc:92307
Dr.80456		Transcribed locus, strongly similar to XP 691447.2 PREDICTED: hypothetical protein [Danio rerio]	Dr.25277	AGR2	Anterior gradient homolog 2 (Xenopus laevis)
Dr.76462	RBB4	Retinoblastoma binding protein 4	Dr.83536	ZGC:103540	Zgc:103540
Dr.107002		Transcribed locus	Dr.120243	SI:CH211-197I12.2	Si:ch211-197i12.2
Dr.106921	ZGC:110586	Zgc:110586	Dr.114355		Transcribed locus, strongly similar to NP 999931.1 mediator of RNA polymerase II transcription, subunit 25 [Danio rerio]
Dr.35596	TPP1	Tripeptidyl peptidase I	Dr.78105	ZGC:56518	Zgc:56518
Dr.115906	LOC799556	Similar to LOC553285 protein	Dr.15263	ZGC:73231	Zgc:73231
Dr.75192	ZGC:109901	Zgc:109901	Dr.140985	ZGC:112365	Zgc:112365
Dr.120542	ZGC:63920	Zgc:63920	Dr.16383	LOC564722	Similar to receptor associated protein 80
Dr.113957	LOC100007887	Similar to LOC559853 protein	Dr.79098	MBD1	Methyl-CpG binding domain protein 1
Dr.37659	BIN2	Bridging integrator 2	Dr.6354	CNOT3	CCR4-NOT transcription complex, subunit 3
Dr.70549	ARL8	ADP-ribosylation factor-like 8	Dr.143602		Transcribed locus, strongly similar to XP 001336617.1 PREDICTED: similar to Adenylate kinase 3-like 1 [Danio rerio]
Dr.4206	ZGC:76977	Hypothetical protein LOC792029	Dr.133834	ZGC:66359	Zgc:66359
Dr.29879		Transcribed locus	Dr.78519	SPAG1	Sperm associated antigen 1
Dr.77026		Transcribed locus	Dr.77928	SCYL3	SCY1-like 3 (S. cerevisiae)
Dr.11520	SI:CH211-51E12.7	Si:ch211-51e12.7	Dr.6680	MKNK2A	MAP kinase-interacting serine/threonine kinase 2a
Dr.75704	PTGDS	Prostaglandin D2 synthase	Dr.76983	ZGC:110286	Hypothetical protein LOC791833
Dr.83502	ZGC:56310	Zgc:56310	Dr.80737	ZGC:110307	Hypothetical protein LOC791571
Dr.23244		Transcribed locus	Dr.43244		Transcribed locus, strongly similar to NP 001017717.1 gamma-butyrobetaine hydroxylase [Danio rerio]
Dr.132340		Transcribed locus	Dr.77272	E2F4	E2F transcription factor 4
Dr.77971	LOC798926	Hypothetical protein LOC798926	Dr.24982	ZGC:56585	Hypothetical protein LOC792146
Dr.78423	LOC571567	Hypothetical LOC571567	Dr.132634	HERPUD1	Homocysteine-inducible, endoplasmic reticulum stress-inducible, ubiquitin-like domain member 1
Dr.77484	ZGC:110417	Zgc:110417	Dr.76573	SPNS1	Spinster homolog 1 (Drosophila)
Dr.75662	ZGC:114087	Zgc:114087	Dr.76353	TIAL1	TIA1 cytotoxic granule-associated RNA binding protein-like 1
Dr.77172	ZGC:153968	Zgc:153968	Dr.5024	PHF16	PHD finger protein 16

Dr.83525	ZGC:162268	Zgc:162268	Dr.14734	PUS7	Pseudouridylate synthase 7 homolog (S. cerevisiae)
Dr.78256	IVNS1ABPA	Influenza virus NS1A binding protein a	Dr.90256	DSCC1	Zgc:103507
Dr.105855	ZGC:171818	Zgc:171818	Dr.80201		Transcribed locus
Dr.77985	ZGC:92279	Zgc:92279	Dr.76675	ALDH3D1	Aldehyde dehydrogenase 3 family, member D1
Dr.78765	ZGC:64130	Zgc:64130	Dr.47567	SI:DKEY-30H14.2	Si:dkey-30h14.2
Dr.36931	ZGC:103747	Zgc:103747	Dr.132384	SULT1ST1	Sulfotransferase family, cytosolic sulfotransferase 1
Dr.90996	SNX33	Sorting nexin 33	Dr.81681	ZGC:55557	Zgc:55557
Dr.133388		Transcribed locus	Dr.122970		Transcribed locus
Dr.78823	LOC572451	Similar to zona pellucida glycoprotein ZPB	Dr.77434	ZGC:56326	Zgc:56326
Dr.116371	ZGC:171776	Zgc:171776	Dr.32820	ZGC:56597	Zgc:56597
Dr.75241	PCID2	Hypothetical protein LOC791435	Dr.75970	FLNA	Filamin A, alpha
Dr.116223	ZGC:55879	Zgc:55879	Dr.85904	IM:7143992	Im:7143992
Dr.78916	ARHGEF7B	Rho guanine nucleotide exchange factor (GEF) 7b	Dr.39952	VPS33A	Vacuolar protein sorting 33A
Dr.28229	BCL7A	B-cell CLL/lymphoma 7A	Dr.79340	ZGC:56653	Zgc:56653
Dr.78604	ZGC:66488	Hypothetical LOC555138	Dr.80627	B3GAT3	Beta3-glucuronyltransferase
Dr.133796	ZGC:162319	Zgc:162319	Dr.35822	ZGC:92425	Zgc:92425
Dr.30339	ZGC:85911	Zgc:85911	Dr.83245	SKP1	S-phase kinase-associated protein 1
Dr.77853	SRPK1	Serine/arginine-rich protein specific kinase 1	Dr.80551	ZGC:110655	Zgc:110655
Dr.104630	MBD3A	Methyl-CpG binding domain protein 3a	Dr.83159	IM:7140357	Im:7140357
Dr.88388	NEDD8L	Neural precursor cell expressed, developmentally down-regulated 8, like	Dr.256	SEC61B	SEC61, beta subunit
Dr.117303	CRYGMX	Crystallin, gamma MX	Dr.75185	ZGC:110767	Zgc:110767
Dr.109645	ZGC:152986	Zgc:152986	Dr.36499	ZGC:101635	Zgc:101635
Dr.80703	ATXN7L2	Ataxin 7-like 2	Dr.75231	CHERP	Calcium homeostasis endoplasmic reticulum protein
Dr.81104	LOC568795	Similar to Anaphase promoting complex subunit 1	Dr.31536	RCL1	RNA terminal phosphate cyclase-like 1
Dr.79516	ZGC:92027	Zgc:92027	Dr.87304	ZGC:77234	Zgc:77234
Dr.106451	ZGC:113828	Hypothetical protein LOC797940	Dr.81961	LOC100002864	Hypothetical protein LOC100002864
Dr.78406	ZGC:66448	Zgc:66448	Dr.72357	ZGC:153136	Zgc:153136
Dr.117779	ZGC:110128	Hypothetical protein LOC791907	Dr.117029	ZGC:112265	Zgc:112265
Dr.75159	WU:FB25B09	Wu:fb25b09	Dr.122414		Transcribed locus
Dr.11480	RAP2IP	Rap2 interacting protein	Dr.118526	LOC556210	S100 calcium binding protein V1
Dr.78825	ELOVL1	Hypothetical protein LOC791805	Dr.96078	ZGC:100836	Zgc:100836
Dr.13043	TPST1L	Tyrosylprotein sulfotransferase 1, like	Dr.122815		Transcribed locus
Dr.140317	ZGC:110333	Zgc:110333	Dr.77086	ZGC:92664	Zgc:92664
Dr.83943	ZGC:113100	Zgc:113100	Dr.105425	ZGC:92164	Zgc:92164
Dr.79979		Transcribed locus	Dr.12491	LOC562579	Similar to complement C4-2
Dr.75346		Transcribed locus	Dr.77870	RNGTT	RNA guanylyltransferase and 5'-phosphatase
Dr.123514		Transcribed locus	Dr.118097	LOC566888	Hypothetical LOC566888
Dr.80056	DHDDS	Dehydrodolichyl diphosphate synthase	Dr.143376	ZGC:86753	Zgc:86753
Dr.51813		CDNA clone IMAGE:7897837	Dr.115125	ZGC:77336	Zgc:77336
Dr.119113	SUV420H1	Suppressor of variegation 4-20 homolog 1 (Drosophila)	Dr.77116	ZGC:101540	Zgc:101540
Dr.114210	LOC794370	Similar to DNA polymerase delta1 catalytic subunit	Dr.86126		Transcribed locus
Dr.85121	ZGC:56259	Zgc:56259	Dr.45962	LOC792966	Similar to cathepsin A
Dr.122845		Transcribed locus	Dr.45332		Transcribed locus
Dr.83945	BXDC5	Brix domain containing 5	Dr.82411	SPTLC2	Serine palmitoyltransferase, long chain base subunit 2
Dr.78482	IM:7158730	Im:7158730	Dr.72465	ZGC:153103	Zgc:153103

Dr.121695		Transcribed locus, moderately similar to NP 001117721.1 glucokinase [Oncorhynchus mykiss]	Dr.91026	LOC100006536	Hypothetical protein LOC100006536
Dr.123021		Transcribed locus	Dr.80532	DCP1A	Decapping enzyme
Dr.140590		CDNA clone MGC:173911 IMAGE:5915517	Dr.85930	ZGC:66419	Hypothetical protein LOC791547
Dr.22945	LOC795535	Hypothetical protein LOC795535	Dr.104703	U2AF2A	U2 small nuclear RNA auxiliary factor 2a
Dr.31447	MBTPS2	Membrane-bound transcription factor protease, site 2	Dr.38382	NBEA	Neurobeachin
Dr.29035	CTNNB2	Catenin, beta 2	Dr.85608	TBPL2	TATA box binding protein like 2
Dr.7577		Transcribed locus, strongly similar to XP 691993.2 PREDICTED: similar to pogo transposable element with ZNF domain [Danio rerio]	Dr.81537	ZGC:101021	Zgc:101021
Dr.77837	LOC100005775	Similar to MGC53357 protein	Dr.81898	ZGC:110741	Zgc:110741
Dr.20277	ACTA2	Actin, alpha 2, smooth muscle, aorta	Dr.24546	ZGC:66327	Hypothetical protein LOC791777
Dr.133827	ZGC:63676	Zgc:63676	Dr.87085	ZGC:92113	Zgc:92113
Dr.24325	ZGC:65780	Zgc:65780	Dr.108054	SUPT3H	Suppressor of Ty 3 homolog (S. cerevisiae)
Dr.32463	CTSC	Cathepsin C	Dr.80679	ZGC:112364	Zgc:112364
Dr.115301	LOC567840	Similar to KIAA1573 protein	Dr.84245	CUL4A	Cullin 4A
Dr.80745		Oogenesis-related protein	Dr.31762	WU:FI12A09	Wu:fi12a09
Dr.143767	ZGC:152922	Zgc:152922	Dr.86370	ZGC:77076	Zgc:173915
Dr.14063	EML2	Echinoderm microtubule associated protein like 2	Dr.36480	ZGC:103645	Zgc:103645
Dr.74222	SI:CH211-81I17.1	Si:ch211-81i17.1	Dr.77910	FAM46C	Family with sequence similarity 46, member C
Dr.82571		Transcribed locus	Dr.31094	RBKS	Hypothetical protein LOC792027
Dr.76341	LOC100002247	Hypothetical protein LOC100002247	Dr.119008	LOC569427	Hypothetical LOC569427
Dr.80488	PPP1R10	Protein phosphatase 1, regulatory subunit 10	Dr.531	DCPS	MRNA decapping enzyme
Dr.75902	ZGC:158387	Zgc:158387	Dr.16782		Transcribed locus
Dr.91347	ZGC:113381	Zgc:113381	Dr.85829	CETN2	Centrin, EF-hand protein, 2
Dr.32625	STKA	Wu:fa09g06	Dr.132294	NOL14	Hypothetical protein LOC792320
Dr.82091		Transcribed locus	Dr.13677	ZGC:55317	Zgc:55317
Dr.45587	ZGC:110611	Zgc:110611	Dr.110726	LOC572168	Hypothetical LOC572168
Dr.85340	MRPL14	Mitochondrial ribosomal protein L14	Dr.86192	LOC559127	Similar to AWKS9372
Dr.33127	IFRD2	Interferon-related developmental regulator 2	Dr.107641	LOC569277	Similar to ubiquitously transcribed tetratricopeptide repeat, X chromosome
Dr.83423	LOC569187	Similar to PHD finger protein 6	Dr.82169	ZGC:123333	Zgc:123333
Dr.1220	ZGC:64155	Zgc:64155	Dr.82451	CDC42EP2	CDC42 effector protein (Rho GTPase binding) 2
Dr.122884		Transcribed locus	Dr.143590	ZGC:85948	Zgc:85948
Dr.75665	MYLIP	Myosin regulatory light chain interacting protein	Dr.84866	LOC100005159	Hypothetical protein LOC100005159
Dr.85496	FANCL	Fanconi anemia, complementation group L	Dr.123167		Transcribed locus
Dr.21244	UCP2	Uncoupling protein 2	Dr.76453	ARL4D	ADP-ribosylation factor-like 4D
Dr.82168		Transcribed locus, strongly similar to NP 001004652.1 COX17 cytochrome c oxidase assembly homolog [Danio rerio]	Dr.119324	ZGC:110245	Zgc:110245
Dr.79437	ZGC:110299	Hypothetical LOC557968	Dr.7628	ZGC:158611	Zgc:158611
Dr.3855	PRMT7	Protein arginine N-methyltransferase 7	Dr.77441	ZGC:64148	Zgc:64148
Dr.41980	ARID3B	AT rich interactive domain 3B (Bright like)	Dr.82147	SI:DKEY-274C14.3	Si:dkey-274c14.3
Dr.80756	ZGC:77748	Zgc:77748	Dr.78511	LOC559941	Similar to Rho-guanine nucleotide exchange factor

Dr.27180	PPARB2	Peroxisome proliferator activated receptor beta 2	Dr.43999	CGNL1	Cingulin-like 1
Dr.86792	DT1P1A10L	Hypothetical protein DT1P1A10 (human) - like	Dr.84960	GRTP1B	Hypothetical protein LOC791767
Dr.115569	ATXN3	Ataxin 3	Dr.133306	CHM	Choroideremia
Dr.81807	LOC100002531	Hypothetical protein LOC100002531	Dr.81558	SI:DKEY-98F17.2	Si:dkey-98f17.2
Dr.53929	SNF1LK2B	SNF1-like kinase 2b	Dr.27946		Transcribed locus
Dr.75940	DEF	Digestive-organ expansion factor	Dr.28581	OPHN1	Oligophrenin 1
Dr.124001		Transcribed locus	Dr.14931	ZGC:153327	Zgc:153327
Dr.122080		Transcribed locus	Dr.81311	DRL	Hypothetical protein LOC791603
Dr.80074	POP4	Hypothetical LOC554559	Dr.76198	IM:7150932	Im:7150932
Dr.132767	ZGC:77051	Zgc:77051	Dr.75142	SI:CH211-197G15.1	Si:ch211-197g15.1
Dr.33631	SI:CH211-124K10.2	Si:ch211-124k10.2	Dr.86287	ZGC:63651	Zgc:63651